SYNERGY BETWEEN JAK INHIBITOR RUXOLITINIB AND TYROSINE KINASE INHIBITORS TO OVERCOME DRUG RESISTANCE RELATED TO BONE MARROW STROMA MICROENVIRONMENT IN CHRONIC MYELOID LEUKEMIA

BIAGIO DE ANGELIS

Dottorato in Scienze Biotecnologiche – XXV ciclo
Indirizzo Biotecnologie Mediche
Università di Napoli Federico II

Dottorato in Scienze Biotecnologiche – XXV ciclo
Indirizzo Biotecnologie Mediche
Università di Napoli Federico II

SYNERGY BETWEEN JAK INHIBITOR RUXOLITINIB AND TYROSINE KINASE INHIBITORS TO OVERCOME DRUG RESISTANCE RELATED TO BONE MARROW STROMA MICROENVIRONMENT IN CHRONIC MYELOID LEUKEMIA

Biagio De Angelis

Dottorando:	Dott. Biagio De Angelis
Relatore:	Prof. Fabrizio Pane
Coordinatore:	Prof. Giovanni Sannia

Alla mia famiglia

INDICE

Riassunto
Le patologie ematologiche sono disordini clonali generati dalla trasformazione neoplastica di cellule progenitrici ematopoietiche. La progressione leucemica delle cellule tumorali è indotta da eventi intrinseci come l'attivazione di oncogeni e la perdita di geni soppressori. Sebbene i difetti cellulari intrinseci causativi della trasformazione neoplastica siano stati studiati estensivamente nel campo delle leucemie, i fattori del microambiente midollare coinvolti negli eventi della tumorigenesi non sono stati ancora chiaramente definiti. In particolare, le cellule staminali ematopoietiche risiedono nel midollo osseo ed interagiscono con un microambiente altamente organizzato composto da diverse sotto-popolazioni di cellule stromali e una matrice extracellulare ricca di fibronectina, collagene e vari proteoglicani. L'interazione tra le cellule staminali e il microambiente midollare è critica nella regolazione dei processi di migrazione, "self-renewal", proliferazione e differenziazione cellulare. Similmente alla loro controparte normale, i progenitori cellulari ematopoietici leucemici restano dipendenti dai segnali provenienti dal microambiente per sopravvivere e proliferare durante la progressione neoplastica. In particolare, la cellula staminale ematopoietica normale o tumorale, risiede all'interno di aree del midollo osseo altamente specializzate, definite nicchie del microambiente midollare: la nicchia endosteale (o osteoblastica) e la nicchia vascolare. La nicchia osteoblastica, localizzata nella superficie interna della cavità dell'osso, fornisce stimoli di quiescenza per le cellule staminali long-term (cosi definite poiché cellule indifferenziate con elevata capacità di generare cellule a loro volta immature e toti/multi potenti a lungo termine) coinvolte nell'emopoiesi. Invece, le nicchie vascolari, che consistono in cellule sinusoidali endoteliali ricoprenti il vaso sanguigno, promuovono la proliferazione e la differenziazione di cellule ematopoietiche staminali short-term (ovvero cellule staminali più differenziate con capacità di generare cellule a loro volta immature a breve termine). L'interazione delle cellule stromali e della matrice extracellulare con i blasti leucemici controlla anche i segnali anti-apoptotici che contribuiscono alla progressione neoplastica e alla persistenza del clone neoplastico residuo dopo trattamento.
La LMC è una neoplasia mieloproliferativa che colpisce le cellule staminali del midollo emopoietico da cui derivano i globuli bianchi (leucociti), le piastrine ed i globuli rossi. Alla base della malattia c'è un evento genetico che porta alla formazione del cromosoma Philadelphia (Ph)**,** così chiamato dal nome della città in cui è stato scoperto nel 1960.
La malattia rappresenta circa il 15% di tutti i casi di leucemia e la prevalenza è stimata intorno a uno-due casi ogni 100.000 persone/anno. L'età media alla diagnosi è circa 60 anni e raramente inferiore a 20 anni.
Un ruolo centrale nella patogenesi della CML è la formzione del gene di fusione tra il gene "Abelson murine leukemia" (ABL) sul cromosoma 9 e il gene "breakpoint cluster region" (BCR) sul cromosoma 22. Il gene di fusione BCR-ABL codifica per l'oncoproteina BCR-ABL.
Il gene ABL appartiene alla categoria delle tirosino-chinasi (TK), enzimi che fosforilano i substrati a livello di residui di tirosina. mediante la sua attività TKI, abl è in grado di attivare una "cascata" di altre proteine intracellulari che innescano i meccanismi della proliferazione cellulare.
Nella t(9;22) il gene ABL viene pressoché interamente traslocato sul cromosoma 22 e la proteina ibrida derivata dal gene ibrido BCR-ABL mantiene una attività TK aumentata e non più sottoposta a normali meccanismi di controllo. Da ciò deriva il potenziale leucemogenico della proteina ibrida, per le conseguenti interferenze a

livello dell'attività proliferativa della cellula neoplastica, dei meccanismi di adesione e della responsività ai fattori regolanti la proliferazione, e dei meccanismi di morte cellulare (apoptosi). Quindi la proteina ibrida BCR-ABL è una TK costitutivamente attiva che promuove la crescita e la replicazione cellulare attivando una serie di cascate a valle come RAS, RAF, la JUN chinasi, MYC e STAT.
Nella storia naturale della LMC si distinguono tre fasi successive:

1. Fase cronica, durante la quale i leucociti vengono prodotti in eccesso per cui è caratterizzata da aumento dei leucociti nel sangue periferico associato a volte ad anemia e/o piastrinopenia oppure piastrinosi e spesso a splenomegalia; raramente epatomegalia.
2. Fase accelerata (AP) di transizione. La fase accelerata è caratterizzata abitualmente dalla comparsa di sintomi quali febbre, sudorazione notturna, perdita di peso e dolore alle ossa, uniti alla perdita di efficacia delle terapie convenzionali, all'aumento del numero di cellule immature nel midollo osseo e nel sangue periferico e all'evidenza di alterazioni cromosomiche.
   L'Organizzazione Mondiale della Sanità (OMS) definisce questo stadio della LMC in base alla presenza di uno o più dei seguenti condizioni:
   a) percentuale di blasti (cellule immature) nel midollo osseo o nel sangue periferico pari al 10-19%;
   b) percentuale di basofili nel sangue periferico pari o superiore al 20%;
   c) conta piastrinica persistentemente inferiore a 100 x 10^9/l o superiore a >1000 x 10^9/l, indipendentemente dalla terapia;
   d) aumento di dimensioni della milza e aumento del numero dei globuli bianchi nel sangue periferico, indipendentemente dalla terapia;
   e) segni di evoluzione clonale (cioè comparsa di un'anomalia genetica aggiuntiva che non era presente al momento della diagnosi). Le alterazioni citogenetiche associate più frequentemente all'evoluzione della malattia sono un cromosoma Philadelphia aggiuntivo, la trisomia 8 (presenza di tre copie del cromosoma 8 invece di due), l'isocromosoma 17q (cromosoma anomalo formato dalla duplicazione di uno dei due bracci del cromosoma, che sostituisce l'altro) e la trisomia 19.
3. Fase blastica (BC) caratterizzata dalla perdita della capacità maturativa delle cellule leucemiche per cui il quadro clinico risulta simile a quello di una leucemia acuta. L'OMS definisce la BC in base alla presenza di uno o più dei seguenti condizioni:
   a. percentuale di blasti nel midollo osseo o nel sangue periferico pari o superiore al 20%;
   b. presenza di ampi aggregati o gruppi di blasti alla biopsia del midollo osseo;
   c. sviluppo di blasti al di fuori del midollo osseo. In circa un terzo dei pazienti i blasti hanno un aspetto linfoide (cioè somigliante a quello dei progenitori dei linfociti), mentre nei due terzi rimanenti hanno un aspetto mieloide (cioè somigliante a quello dei progenitori di tutti gli altri globuli bianchi) o indifferenziato (cioè senza caratteristiche distintive particolari). Le sedi extramidollari più frequentemente interessate dalla BC sono la pelle, i linfonodi, la milza, le ossa e il sistema nervoso centrale, ma la fase blastica può coinvolgere qualunque altro distretto corporeo.

La malattia viene generalmente diagnosticata in fase cronica, spesso in occasione di esami di routine quando il paziente è asintomatico. Molto raramente alla diagnosi il paziente si presenta in fase accelerata o blastica.
Fino a poco più di dieci anni fa, la terapia per la LMC era limitata ad alcuni agenti terapeutici non specifici come l'agente alchilante ciclo cellulare non-specifico busulfan, idrossiurea ed interferone alfa.
L'inibitore della sintesi del DNA I idrossiurea fu introdotto negli anni '70 e sostituì il busulfan per la sua maggior maneggevolezza nel controllo della soppressione midollare e per la mancanza di tossicità polmonare. Negli anni '80 fu sperimentato nei pazienti affetti da LMC l'uso dell'INF-α. Questo farmaco induce una risposta ematologica completa nell' 50-70% dei pazienti ed una risposta citogenetica (definita come percentuale di cellule midollari Ph+ inferiore al 35%) nel 10-20% dei casi. Purtroppo la terapia con INF-α induce alcuni effetti collaterali importanti: sintomi simil influenzali, calo ponderale e, meno frequentemente, diarrea e neurotossicità che si presenta con depressione e deficit anamnestici, cioè disturbi della memoria. L'unico intervento curativo è il trapianto allogenico di cellule staminali (AlloSCT); una scelta terapeutica associata ad un elevato rischio di morbidità e mortalità.
La terapia della LMC è stata profondamente modificata negli ultimi dieci anni dalla introduzione di una classe di farmaci noti come "inibitori delle tirosino-chinasi" (TKI). Il primo di questi farmaci ad affermarsi nel trattamento della LMC è stato l'Imatinib mesilato, cui hanno fatto seguito il Nilotinib e il Dasatinib. I farmaci TKI sono una classe di antineoplastici che appartengono ad una categoria di nuovi farmaci detti "a bersaglio molecolare (target) " o "biologici " o ancora "intelligenti ". Caratteristiche peculiari e vantaggiose di questi nuovi farmaci sono:

1. l'azione selettiva su definiti substrati delle cellule tumorali,
2. la modesta insorgenza di effetti indesiderati,
3. la possibilità di essere somministrati, in alcuni casi (come nel caso dell'Imatinib), per via orale,
4. la possibilità di utilizzo in associazione con terapie tradizionali.

L'introduzione di una terapia "a bersaglio molecolare" nella pratica clinica ha migliorato drammaticamente la storia naturale della malattia, incrementando la sopravvivenza globale dei pazienti con LMC a dieci anni dal 20% all' 80-90%.
Con l'uso dei TKI, primo fra tutti l'Imatinib, è sorta l'esigenza di monitorare la risposta molecolare, utilizzando tecniche di biologia molecolare caratterizzate da una elevata sensibilità e specificità, ovvero la PCR (reazione a catena polimerasica) di tipo qualitativo o quantitativo. Una riduzione precoce dei livelli di trascritto ibrido BCR-ABL sono predittivi di una risposta terapeutica (cioè una diminuzione del clone leucemico caratterizzato dal cromosoma Ph) e di un decorso clinico favorevole. Il monitoraggio della Malattia Minima Residua consente di stratificare i pazienti in classi prognostiche ad elevato impatto clinico. Per tanto è possibile definire che un paziente è in risposta molecolare maggiore, quando con tecnica quantitativa il rapporto tra quantità di trascritto (BCR-ABL) e del gene di controllo (ABL) è inferiore a 0,1; mentre il paziente si definisce in risposta molecolare completa quando il trascritto BCR-ABL non è più determinabile, in presenza di un numero di copie del gene di controllo ABL non inferiore a 10.000 copie. In particolare, una risposta molecolare maggiore a 12 mesi di terapia è predittiva di una lunga sopravvivenza con un rischio di progressione di malattia molto basso.
L'obiettivo della terapia con i TKI è di raggiungere inizialmente la remissione completa ematologica, cioè la normalizzazione dei parametri dell'emocromo e del midollo e quanto prima, ottenere anche la remissione citogenetica, cioè la completa e

definitiva scomparsa del cromosoma Ph, presupposto fondamentale per una remissione duratura stabile nel tempo. Il mancato riscontro dell'anomalia cromosomica, specie se confermata nel tempo, indica che con buona probabilità il clone neoplastico è stato ridotto e bloccato, con ripristino della normale emopoiesi. Vari studi clinici hanno dimostrato chiaramente che la stragrande maggioranza dei pazienti in remissione citogenetica completa (CCyR) ottengono anche la remissione molecolare maggiore definita con livelli di trascritto BCR-ABL ≤ 0.1% espressi su scala internazionale.
Un team di ricerca europeo ha costituito con il "The European Leukemia Net" una rete europea di medici che lavora insieme con l'obiettivo di implementare le linee guida per i trattamenti delle varie forme leucemiche, compiendo notevoli progressi nella standardizzazione delle tecniche di monitoraggio.
Questo team ha definito le linee guida per monitorare la risposta terapeutica dei pazienti con LMC, definendo una risposta ottimale come:
risposta ematologica completa (CHR) a 3 mesi, una risposta citogenetica parziale (PCyR) a 6 mesi, cioè con metafasi Ph+ < 35%, una CCyR a 12 mesi, e un risposta molecolare completa (MMR) a 18 mesi.
Nelle linee guida si definisce invece fallimento terapeutico una qualunque delle seguenti condizioni nei pazienti in trattamento con imatinib: assenza di risposta ematologica e di una risposta citogenetica almeno minore (cioè metafasi Ph+ < 65%) a 3 mesi; assenza di una risposta citogenetica almeno parziale (cioè metafasi Ph+ < 35%) a 6 mesi; assenza di una risposta citogenetica completa a 12 mesi; assenza di risposta molecolare maggiore a 18 mesi. La perdita della riposta precedentemente ottenuta, invece, è definita in base alla presenza di uno dei seguenti criteri: perdita della risposta ematologica; perdita della risposta citogenetica, con aumento superiore al 10% delle cellule Ph+; aumento della trascrizione di BCR-ABL pari ad almeno 5-10 volte in due determinazioni distinte o ad almeno 10 volte in una sola determinazione (sebbene su questo punto non vi sia un accordo unanime). I criteri di valutazione per i pazienti in trattamento di seconda linea con gli inibitori di seconda generazione (cioè nilotinib o dasatinib) sono simili, ma richiedono risposte più rapide, trattandosi di farmaci più potenti.
Sono stati riportati fenomeni di resistenza all'imatinib, più frequenti in fase avanzata di malattia e tale fenomeno è associato a diversi meccanismi.
La resistenza primaria è soprattutto dovuta a scarsa inibizione di BCR/ABL.
Le cause di una scarsa inibizione di BCR/ABL sono varie; ne ricordiamo alcune:
una concentrazione plasmatica insufficiente di imatinib per una scarsa compliance del paziente (adesione cioè del paziente alla terapia), un malassorbimento intestinale ed il rapido metabolismo del farmaco,ecc.
La resistenza secondaria è un evento multifattoriale: le mutazioni puntiformi (modificazioni di un singolo aminoacido) nel sito di legame della proteina BCR-ABL sono le cause più frequenti, ma possono entrare in gioco anche l'amplificazione genomica con iperespressione di BCR/ABL, iperespressione di molecole per resistenza ai farmaci, evoluzioni clonali con presenza di alterazioni citogenetiche aggiuntive, attivazione del segnale di traduzione per vie alternative. Sono note più di 73 mutazioni, riconoscibili con metodiche cromatografiche quali il DHPLC (Denaturant High Performance Liquid Chromatography) o il sequenziamento genico e diversi sono gli approcci terapeutici per superare tali meccanismi di resistenza, come aumentare il dosaggio del farmaco a 600-800 mg al giorno, combinare il Glivec con altri farmaci, o utilizzare altri inibitori di seconda generazione. Si possono poi

sviluppare durante il trattamento con questi farmaci delle mutazioni nel clone neoplastico che lo rendono resistente a tutti e tre i TKI, come ad esempio la T315I.
Bosutinib (SKY-606) è un inibitore delle tirosin chinasi di terza generazione con un duplice bersaglio. A differenza di imatinib, infatti, inibisce l'autofosforilazione di due chinasi, Abl ed Src, portando a un'inibizione della crescita cellulare e ad apoptosi. È proprio in virtù di questo doppio meccanismo d'azione che il farmaco può essere attivo nella LMC in fase blastica, resistenti o intolleranti ad altre terapie, tra cui imatinib.
Nonostante i notevoli progressi ottenuti nella terapia della LMC con i TKI, numerose evidenze sperimentali hanno dimostrato chiaramente che inibire l'attività chinasica BCR-ABL non è sufficiente ad eliminare la malattia minima residua, la cui persistenza è dovuta ad una mancata eliminazione delle cellule staminali leucemiche nel tessuto midollare. Pertanto una strategia curativa, necessariamente deve prevedere la combinazione di un farmaco TKI con agenti che specificamente agiscono sulla cellula staminale leucemica all'interno della nicchia midollare.
Il progetto sviluppato ha inizialmente valutato il ruolo del microambiente tumorale nella determinazione degli eventi di leucemogenesi, di progressione e di induzione della resistenza al trattamento sia su cellule neoplastiche isolate da pazienti affetti da LMC in trattamento con TKI (Farmaci inibitori della tirosin chinasi: Imatinib, Dasatinib o Nilotinib) sia su linee cellulari Ph+ immortalizzate.
A tale scopo le cellule leucemiche derivate dai pazienti in trattamento con i TKI, sono state testate per le loro proprietà di adesione e interazione con il mocroambiente midollare, con il fine di identificare gli eventuali fattori peculiari che li legano alla nicchia osteoblastica midollare. In particolare sono state raccolte le cellule Ph+ isolate dai campioni di BM (sangue midollare) e dal PB (sangue periferico) di paziente affetti da LMC in pretrattamento e/o durante il trattamento con TKI (in particolare al terzo e sesto mese di trattamento).
In particolare abbiamo ricevuto 41 campioni midollari e 41 campioni periferici in pre-trattamento (Visita 1) e 40 campioni (sia midollari che periferici per ogni singolo paziente) alla Visita 2 (alla fine del terzo mese) e alla Visita 3 (fine del sesto mese). Dai 41campioni midollari e/o periferici in pre-trattamento abbiamo selezionato la popolazione cellulare CD34+ e 14 popolazioni di cellule stromali MSCA+ . Dai 40 campioni biologici arrivati alla visita successiva non abbiamo ricavato un numero sufficiente di cellule da poter selezionare le cellule CD34+ o MSCA+.
L'antigene CD34 si ritrova sulle cellule progenitrici ematopoietiche di tutte le linee così come la maggior parte delle cellule staminali primitive totipotenti. L'antigene CD34 ha la sua massima espressione sulla maggior parte delle cellule staminali primitive e viene gradualmente perso quando le cellule progenitrici predestinate della linea si differenziano. L'antigene CD34 é anche presente sulle cellule endoteliali capillari e sulle cellule stromali del midollo osseo. L'antigene CD34 é espresso in circa il 60% dei casi di leucemia acuta, sia linfoide che mieloide.
Nelle CML, l'aumento del numero di CD34+ può essere un indice rilevante della progressione a fase accelerata o blastica.
Le cellule CD34+ sono state selezionate dalle cellule mononucleate totali dopo separazione immunomagnetica usando il kit MiniMACS per le cellule CD34 (Miltenyi Biotec), secondo le istruzioni della ditta produttrice.
Le cellule staminali si distinguono in totipotenti, capaci di trasformarsi in qualsiasi tipo di tessuto; pluripotenti, che si trasformano solo in alcuni tipi di tessuti; unipotenti, che possono dar luogo soltanto ad un tipo cellulare. Le cellule staminali mesenchimali sono una popolazione cellulare pluripotente.

Le “cellule staminali mesenchimali” (MSCs), dotate di capacità di automantenimento e differenziativa in senso osteoblastico, condrocitario, adipocitario, mioblastico e fibroblastico. Sono anche denominate “cellule stromali midollari”, data la loro capacità di generare le cellule del microambiente midollare. Infatti, le cellule staminali mesenchimali sono contenute all'interno dello stroma midollare.
L’ anti-MSCA (W8B2) è un anticorpo sviluppato per l’isolamento delle cellule stromali mesenchimali (MSC) dall’aspirato midollare. L’espressione dell’antigene MSCA-1 è ristretto, nella popolazione cellulare midollare, alla frazione $CD271^{bright}$. Le cellule MSC $CD271^{bright}CD45^{dim}$ hanno un’altissima capacità clonogenica comparata alla frazione midollare $CD271^{+}CD45^{+}$.
Le cellule MSCA+ sono state selezionate dalle cellule mononucleate totali dopo separazione immunomagnetica, secondo le istruzioni della ditta produttrice.
Nella prima parte del lavoro scientifico abbiamo osservato sperimentalmente che sia le linee Ph+ (K562, KT1 o BV173) che cellule staminali CD34+Ph+ sono significativamente protette dalla mortalità cellulare TKI-dipendente (Imatinib, Nilotinib o Dasatinib) quando incubate in presenza (direttamente o separate da una membrana che lascia passare solo i fattori solubili) della linea cellulare stromale HS5 o di linee stromali MSCA+ ottenute ex-vivo da campioni midollari isolati da pazienti affetti da LMC alla diagnosi.
Inoltre, ho osservato nel mio studio sperimentale che la resistenza è BCR-ABL indipendente, mediata presumibilmente dalla attivazione della cascata JAK-STAT3. Infatti, il co-trattamento delle linee tumorali Ph+ con uno dei TKI e un inibitore specifico della tirosin chinasi non recettoriale JAK2 è in grado di superare questa resistenza. Inoltre le due categorie di farmaci hanno mostrato un significativo effetto sinergico nell’azione terapeutica.
Nella parte finale del progetto, con il fine di determinare il ruolo esatto dei differenti fattori di crescita e delle citochine nella sopravvivenza delle cellule leucemiche, abbiamo determinato mediante il saggio ELISA assay BioPlex il livello di espressione contemporaneamente di 20 differenti citochine prodotte dalle cellule stromali isolate da pazienti affetti da LMC alla diagnosi o dalla linea immortalizzata HS5. I fattori solubili valutati sono stati: IL1a, IL1b, IL3, IL6, IL7, IL8, IL10, IL12, IL15, G-CSF, M-CSF, SCF, SDF1, TRAIL, HGF, PDGFbb, GM-CSF, MIP-1a, TNFa e VEGF. Questi fattori sono noti avere un ruolo chiave nell’interazione delle cellule staminali Ph+ con il microambiente midollare.
Quindi, tutte le citochine espresse sia dalle cellule HS5 che dalle cellule stromali ottenute dai pazienti affetti da LMC, sono state poi testate in vitro per verificare se e come andassero a modulare la risposta farmacologica delle cellule Ph+ ai TKI. Il saggio ELISA assay BioPlex è stato effettuato sul mezzo di 24 ore di coltura della linea stromale HS5 (HS5/SCM) e sui mezzi condizionati derivanti dalla coltura delle cellule stromali ottenute da 8 differenti pazienti affetti da CML (CML/SCM). Nel nostro saggio abbiamo identificato una serie di fattori altamente espressi in entrambe le linee cellulari, quali il fattore G-CSF, IL-6, IL-8 e VEGF, conosciuti avere un ruolo fondamentale nell’attivazione di STAT3 e quindi della via JAK/STAT3.
G-CSF (Granulocyte Colony-Stimulating Factor), è un fattore di crescita che stimola la differenziazione, la sopravvivenza e la migrazione dei granulociti. Il G-CSF è una glicoproteina prodotta da vari tipi cellulari, tra cui macrofagi e cellule endoteliali. Agisce nel midollo osseo in risposta a segnali infiammatori stimolando la differenziazione dei precursori dei granulociti neutrofili ed è attivo nella mobilitazione delle cellule staminali.
IL-6 è un potente attivatore di STAT3.

IL-8, anche noto come fattore chemiotattico neutrofilico, induce chemiotassi in cellule bersaglio, sopratutto dei neutrofoli ma anche altri granulociti, facendoli migrare verso il sito di infezione. Un incremento di espressione di IL-8 e/o dei suoi recettori è stata ben caratterizzata nelle cellule tumorali, cellule endoteliali, neutrofili infiltranti, e macrofagi associati al tumore, suggerendo che IL-8 funziona come un fattore regolatore nel microambiente tumorale. IL-8 tramite i suoi recettori è in grado di attivare la cascata JAK-STAT3 e la beta-catenina, promuovendone la traslocazione nucleare. Recentemente utilizzando topi knock-out per STAT3 si è dimostrato il suo ruolo fondamentale nel dare origine alla malattia, ma non nel mantenimento della stessa. Nel contesto del microambiente midollare, STAT3 è attivato in maniera BCR-ABL indipendente dalle citochine presenti nel mezzo di coltura dello stroma midollare. Quindi l'attivazione della via JAK/STAT3 contribuisce alla sopravvivenza del clone staminale leucemico anche in presenza dei TKI. I nostri dati suggeriscono che la via JAK/STAT3 è un bersaglio terapeutico interessante nell'ottica di una terapia combinatoria con i TKI, e rappresenta una strategia vitale nell'eliminare o almeno ridurre la malattia minima residua dei pazienti affetti da LMC.

Summary
Inhibition of the constitutively active kinase BCR-ABL1 with tyrosine kinase inhibitors (TKIs) contributed to a remarkable progress in the treatment of Chronic myeloid leukemia (CML) and Philadelphia chromosome positive (Ph+) Acute Lymphoblastic Leukemia (ALL) with 87% of complete cytogenetic response at 5 years among CML patients receiving the TKI Imatinib. Nevertheless, although the comprehension of the molecular mechanisms of neoplastic transformation in Ph+ cells has greatly improved in the TKI era, less clear are the mechanisms that underlie the variable degree of response to TKI treatment in patients with chronic phase (CP) CML versus patients with advanced phase CML or Ph+ ALL. The importance of tumor microenvironment for cancer progression and drug resistance is becoming widely recognized in recent years. Interaction of cancer cells with their stromal microenvironment overcoming the physiological barrier function of stromal cells synergizes growth, angiogenesis and initiation of an invasive and metastatic phenotype of the cancer cell. Bone Marrow (BM) is loosely composed of hematopoietic cells set within a milieu surrounded by a mesenchymal landscape. There have been various attempts to define bone microenvironments that nurture and determine stem cell fate. Two such stem cell 'niches' are well described: the vascular and the endosteal niche.
The BM is a dynamic microenvironment with high concentration of growth factors and cytokines regulating haematopoiesis, enhancing leukemia blast survival and modulating their resistant to treatment. Thus, here I demonstrated that the half maximal inhibitory concentration (IC50) of three clinical relevant TKIs (Imatinib, Nilotinib and Dasatinib) is significantly increased when Ph+ cell lines are treated in the presence of soluble factors produced by BM mesenchymal stroma cells (stroma conditioned media or SCM). In addition, I observed that the higher cell viability, noticed in Ph+ cell lines cells treated with TKI in the presence of SCM respect to control cell culture condition (RM), is not related to cytokine cell cycle regulation but to a significant reduction in apoptosis induction. Moreover, the observed TKI resistance is associated to a BCR-ABL independent STAT-3 activation leading to a significant down-modulation of apoptosis when either Ph+ cell line or primary CD34+ progenitor cells derived from patients with CML are treated with TKIs in the presence of a direct mesenchymal stroma cell interaction or exposition to SCM. Finally, I proved that JAK inhibitor Ruxolitinib, that inhibits STAT3 phosphorylation (a marker of JAK activity), synergizes with TKIs in the induction of apoptosis in CML primary cells. Indeed, compared with single agent treatment, exposure of CML cells to the combination of TKI and JAK inhibitor Ruxolitinib significantly decreased viability of CML cells and increased their apoptosis in vitro. Taken together, our data show that the rational drug combination of TKI and Ruxolitinib may enhance the eradication of primary human Ph+ cells homed in BM stroma niche.

CML: **Disease Overview**

Chronic myeloid leukemia (CML) is a myeloproliferative neoplasm with an incidence of one–two cases per 100,000 adults for year, and accounts for around 15% of newly diagnosed cases of leukemia in adults.[1]

Chronic myeloid leukemia (CML) is rare in children, representing 3% of pediatric and adolescent leukemia's.[2] In adults, CML represents about 15% of all cases of leukaemia[3] and is less common than acute myeloid leukaemia and myelodysplastic syndrome (AML/MDS) and chronic lymphocytic leukaemia (CLL). The median age of onset is 45 to 55 years. Half of CML patients are older than 60 years.

The CML is a lethal hematological malignancy resulting from the transformation of a primitive hematopoietic stem cell. These primitive hematopoietic stem cells are Philadelphia chromosome positive (Ph1) and express the oncogenic tyrosine kinase BCR-ABL[4]. The history of the hybrid BCR/ABL gene started in 1960, when an abnormal, shortened chromosome 22, termed the Philadelphia chromosome, was described in the leukemic cells of a patient affected by CML. Only 13 years later, the use of quinacrine fuorescence and Giemsa banding in chromosome studying, allowed clarifying that Ph1 chromosome was the result of a translocation of part of chromosome 22 to chromosome 9.[5] [6] Figure 1A.

This malignancy is almost unique among human neoplasms in that a specific genetic lesion, the t(9;22) chromosomal translocation, is invariably associated with the malignant phenotype.

Molecular structure of BCR/ABL genes

This chromosomal translocation results in the fusion between the 5' part of BCR (breakpoint cluster region) serine/threonine kinase gene, normally located on chromosome 22, and the 3' part of the ABL tyrosine kinase gene on chromosome 9 giving origin to a BCR/ABL fusion gene which is transcribed and then translated into a hybrid protein (Figure 1)[7]. This hybrid gene is present in almost all the CML cases with a classical clinical picture, which is now considered the hallmark.[8] The BCR-ABL oncoprotein, unlike the primarily nuclear c-ABL, is distributed throughout the cytoplasm and interacts with various proteins involved in signal transduction pathways leading to deregulated proliferation, differentiation, survival and DNA repair.[9] [10] Three main variants of the BCR/ABL gene have been described, that, depending on the length of the sequence of the BCR gene included, encode for the p190(BCR/ABL), P210(BCR/ABL), and P230(BCR/ABL) proteins. These three main variants are associated with distinct clinical types of human leukemias. [7] The ABL (Abelson leukemia virus) gene is a gene encoding a non receptor tyrosine kinase, which spans a 230 kb region at band q34 of chromosome 9 and consists of 11 exons, with two first alternative exons i.e. exons Ia and Ib. [11] In the vast majority of the Ph positive patients, breakpoints in the ABL gene appeared to be distributed over a rather large 300 kb fragment of chromosome 9 at band q34, which comprises the 5' end of this gene, and may occur either upstream of the alternative first exon (exon Ib), or downstream of the other first exon (Ia) or more frequently between these two (Figure 1B). [12] By the effect of the Ph chromosomal translocation, ABL sequences sited downstream (telomeric) of breakpoint move to the der(22) and are joined to the 5' part of the BCR gene.

The function of the normal BCR gene product is not clear. The protein has serine/threonine kinase activity and is a GTPase-activating protein for p21rac. Two transcript variants encoding different isoforms have been found for this gene.

The 23 exons of the BCR gene (Figure 1B top panel) are shown with respect to the translocation breakpoints that give rise to the P190, P210 and P230 Bcr/Abl proteins.
The BCR gene contains three hotspots for translocation breakpoints designated as major breakpoint cluster region (M-bcr), is a 5.8 kb chromosomal region spanning exons 12–16 (originally named b1 to b5) [13]; M-bcr breakpoints are detectable in more than 95% of cases. [14] However, breakpoints in this region can be detected in about one third of adult acute lymphoid leukemias (ALLs) with the t(9;22) translocation and in a small fraction of Ph positive ALL childhood cases. [15, 16] Depending on the position of breakpoint in this region, the 5' end of the BCR gene comprising either the exon 13 (formerly b2) or exon 14 (formerly b3) is joined to the 3' part of ABL gene, giving rise to a BCR/ABL hybrid gene encoding the chimeric 210 kDa protein (P210-BCR/ABL). The corresponding fusion mRNAs shows either the b2a2 or the b3a2 type of junctions.[17]
In 70–80% of Ph positive ALLs [15] [16], and in rare cases of [18], breakpoints of chromosome 22 span a 55 kb intronic sequence between the two alternative exons e2' and e2 ([19], called minor breakpoint cluster region (m-bcr). In these cases only the extreme 5' end of the BCR gene is joined to the 3' sequences of the ABL gene, and although the deriving BCR/ABL fusion gene contains both the e1' and the e2' BCR exons and may contain ABL alternative first exons, all these exonic sequences are removed by splicing and the hybrid transcript shows a junction between the BCR exon e1 and ABL exon a2. This type of ela2 transcript is smaller (7.4 kb) than that normally found in CML patients and encodes a 185 kDa chimeric protein (P190 BCR/ABL) (Clark et al., 1987; Hermans et al., 1987; Kurzrock et al., 1987).
A rare variant encoding a P230 is generated by an e19a2 fusion type junction encoding for the largest BCR/ABL chimeric protein of predicted 230 kDa. Interestingly, the leukemic phenotype in these patients was very close to that of the chronic neutrophilic leukemia (CNL), therefore, Pane et al. proposed the name of μBCR (Micro-BCR) for the breakpoints, located at the intron 19 of the BCR gene, which were associated to a distinct form of mild Ph positive myeloproliferative disease, the neutrophilic-chronic myeloid leukemia (CML-N).[20]

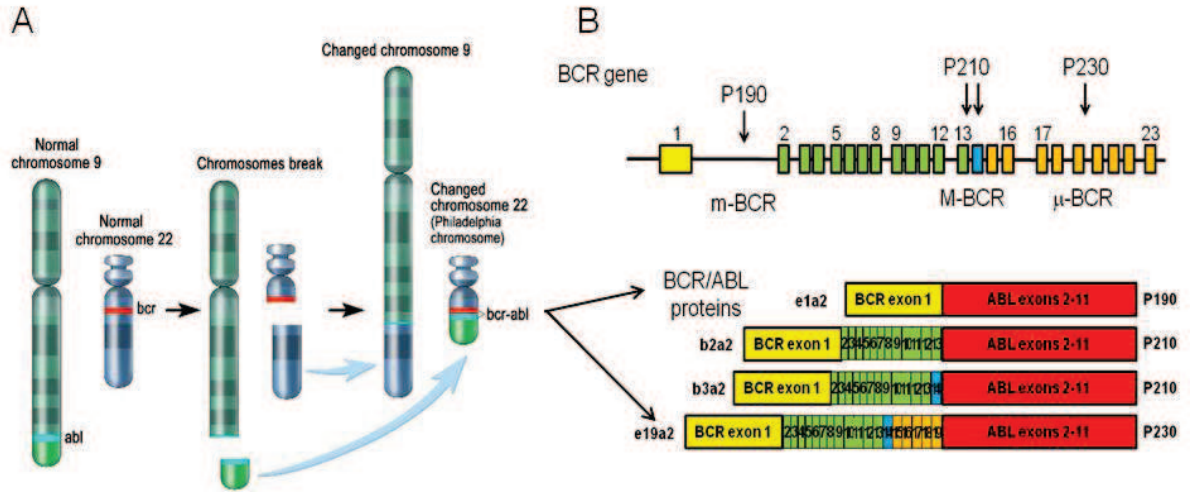

Figure1. **Schematic representation of formation of the Philadelphia Chromosome**. (**A**) Philadelphia chromosome is a translocation, in which parts of two chromosomes, 9 and 22, exchange places. The result is that a fusion gene is created by juxta-positioning the *Abl1* gene on chromosome 9 (region q34) to a part of the *BCR* ("breakpoint cluster region") gene on chromosome 22 (region q11). This is a reciprocal translocation, creating an elongated chromosome 9 (der9), and a truncated chromosome 22 (the Philadelphia chromosome*)*. (**B**) The 23 exons of the BCR gene (top panel) are shown with respect to the translocation breakpoints that give rise to the P190, P210 and P230 Bcr/Abl proteins (down panel). The BCR gene contains three hotspots for translocation breakpoints designated as minor BCR (m-BCR), Major BCR (M-BCR) and micro BCR (μ-BCR) underneath the gene.

Manifestations and Staging
CML can be classified into three disease phases: chronic phase (CP), accelerated phase (AP), and blast phase (BP).

Chronic phase
Approximately 85% of patients with CML are in the CP at the time of diagnosis. About 30 to 50% of patients with CML diagnosed in CP are asymptomatic. Common signs and symptoms of CML in CP, when present, result from anemia and splenomegaly (detected in 50 to 60% of cases). Hepatomegaly is less common (10 to 20%). Lymphadenopathy and infiltration of skin or other tissues are uncommon. The duration of chronic phase is variable and depends on how early the disease was diagnosed as well as the therapies used. In the absence of treatment, the disease progresses to an accelerated phase.

Accelerated phase
Criteria for diagnosing transition into the accelerated phase are somewhat variable; the most widely used criteria are those put forward by investigators at M.D. Anderson Cancer Center,[21] by Sokal et al., and the World Health Organization (WHO).[22] The WHO criteria are perhaps most widely used, and define the accelerated phase by any of the following:

- 10–19% myeloblasts in the peripheral blood or bone marrow
- >20% basophils in the blood or bone marrow
- Platelet count <100,000, unrelated to therapy
- Platelet count >1,000,000, unresponsive to therapy
- Cytogenetic evolution with new abnormalities in addition to the Philadelphia chromosome
- Increasing splenomegaly or white blood cell count, unresponsive to therapy

The patient is considered to be in the AP-LMC if any of the above is present. The accelerated phase is significant because it signals that the disease is progressing and transformation to blast crisis is imminent. Drug treatment often becomes less effective in the advanced stages.

Blast crisis
Blast crisis is the final phase in the evolution of CML, and behaves like an acute leukemia, with rapid progression and short survival. Blast crisis is diagnosed if any of the following are present in a patient with CML: [23]

- >20% myeloblasts or lymphoblasts in the blood or bone marrow
- Large clusters of blasts in the bone marrow on biopsy
- Development of a chloroma (solid focus of leukemia outside the bone marrow)

Progression to AP and BP is associated with occurrence of additional genetic defects that cooperate with BCR/ABL in leukemogenesis and lead to resistance against anti leukemic drugs. Most patients evolve into AP before BP, but 20% transit into BP without AP warning signals. AP might be insidious or present with worsening anemia, splenomegaly, and organ infiltration; BP presents as an acute leukemia with worsening constitutional symptoms, bleeding, fever, and infections.[3]

CML: Response Definition and Prevalent Methodologies

Hematological Response (**HR**) is a normalization of the blood counts, particularly white blood cell counts. This is the first noticeable indicator that treatment is beginning to work, though not necessarily in the bone marrow. The response can be **partial HR** (reduction in white cells, but not down to normal range) or **complete CHR** (white blood count at normal range or below to approximately 12,000 white cells/microliter) and non-palpable spleen.

Cytogenetic Response is a response to treatment of CML that occurs in the marrow, rather than just in the blood.

There are 3 levels of cytogenetic response:

1) Cytogenetic response (CR or CyR): A cytogenetic response means any Ph+ chromosome reading less than what you began with at diagnosis;
2) Partial cytogenetic response (PCyR); Partial mean 36-65% metafase positive for the Philadelphia chromosome;
3) Major cytogenetic response (MCR or MCyR); Major means 35% or less of the cells in your marrow test positive for the Philadelphia chromosome, but more than 0%;
4) Complete cytogenetic response (CCR or CCyR): Complete cytogenetic response means no Ph+ cells can be measured by either conventional or FISH cytogenetic testing (though the PCR test may still be positive).

Fluorescence in situ Hybridization (FISH)

FISH is a molecular cytogenetic technique that can detect chromosomal abnormalities that cannot be appreciated by standard chromosomal analysis (e.g. microdeletion syndromes) or when mitotic cells are not available for chromosomal analysis (e.g. X/Y FISH for cross-sex transplants). FISH uses fluorescent probes that bind to only those parts of the chromosome with which they show a high degree of sequence complementarity.

The polymerase chain reaction (**PCR**)

PCR is a biochemical technology in molecular biology to amplify a single or a few copies of a piece of DNA or c-DNA (complimentary DNA) across several orders of magnitude, generating thousands to millions of copies of a particular DNA sequence.

Reverse Transcription PCR (RT-PCR)

RT-PCR is a biochemical technology in molecular biology to amplify DNA from RNA. Reverse transcriptase reverse transcribes RNA into cDNA, which is then amplified by PCR. RT-PCR is widely used in expression profiling, to determine the expression of a gene or to identify the sequence of an RNA transcript, including transcription start and termination sites.

Real-time quantitative PCR (RQ-PCR)

RQ-PCR is a biochemical technology in molecular biology is allow to monitor the progress of the PCR as it occurs (i.e., in real time). Data is therefore collected throughout the PCR process, rather than at the end of the PCR. This completely revolutionizes the way one approaches PCR-based quantization of DNA and RNA. In real-time PCR, reactions are characterized by the point in time during cycling when amplification of a target is first detected rather than the amount of target accumulated

after a fixed number of cycles. The higher the starting copy number of the nucleic acid target, the sooner a significant increase in fluorescence is observed.
Since the advent of real-time PCR, several groups have published reports that describe the feasibility of monitoring CML patients with this technique. A total of 26 European university laboratories from 10 countries have collaborated to establish a standardized protocol for TaqMan-based real-time quantitative PCR (RQ-PCR) analysis of the main leukemia-associated FGs (fusion genes) within the Europe Against Cancer (EAC) program. The major aim was to establish a standardized protocol allowing comparison of minimal residual disease (MRD) data in order to assess the relative efficiency of each therapeutic strategy for leukemia bearing an appropriate molecular marker. [24]

Frontline Treatment Options
Tyrosine kinase inhibitors (TKIs) have transformed the natural history of CML by inducing cytogenetic and molecular responses in the majority of patients in chronic phase [25] resulting in transient deep responses in many cases of advanced disease. [26] Currently, there are three commercially available TKIs for the treatment of CML; these include Imatinib, Dasatinib, and Nilotinib.

Imatinib mesylate (Gleevec, Novartis Pharmaceutical Corporation, NJ, USA) was the first TKI to receive approval by the Food and Drug Administration (FDA) for the treatment of patients with CML-CP, and its introduction was associated with substantial improvements in response and survival compared with previous therapies. Imatinib mesylate,(IM) belongs to a class of compounds known as the 2-phenylaminopyrimidines. It acts via competitive inhibition at the ATP-binding site of the BCR-ABL protein, which results in the inhibition of phosphorylation of proteins involved in cell signal transduction. The drug is a potent inhibitor of three tyrosine kinases: Abelson (ABL), platelet derived growth-factor receptor (PDGFR) α and β, and C-KIT tyrosine Kinase.[27] The International Randomized Study of Interferon and STI571 (IRIS) study is considered a landmark clinical trial for TKIs and CML.[28] In this study, the investigators randomized 1106 patients to receive IM (553 patients, 50%) or interferon alfa plus low-dose cytarabine (553 patients, 50%). After a median follow-up of 18 months, the estimated rate of a MCyR was 87.1% in the IM group and 34.7% in the group given interferon alfa plus cytarabine (P<0.001). The rate of complete cytogenetic response CCyR was 76% in the IM group and 14.5% in the group given interferon alfa plus Cytarabine (P<0.001). The rate of freedom from progression to accelerated-phase or blast-crisis CML was 96.7% in the IM group and 91.5% in the combination-therapy group (P<0.001). In conclusion, in terms of hematologic and CyR, tolerability, and progression to accelerated-phase or blast-crisis CML, IM was superior to interferon alfa plus low-dose cytarabine as first-line therapy in newly diagnosed chronic-phase CML. The responses to IM were also durable, as shown in an 8-year follow up of the IRIS study.[29] Although the results using IM was quite impressive, only 55% of patients enrolled in the IRIS study remained on therapy at the 8-year follow up point.
Many patients responding to IM will also achieve a major molecular response (MMR), defined in the IRIS trial as a 3-log reduction in BCR-ABL transcript levels from a standardized baseline representing the median value of BCR-ABL/BCR present at diagnosis. [30] This 3-log reduction has subsequently been defined as a major molecular remission defined as a BCR-ABL transcript lower than 0.1 % expressed in International Scale, which was a way of the Scientific Community to agree on the

same results and to confer a prognostic significance universally shared ($BCR\text{-}ABL^{IS}$). [31] Only a minority of IM-treated patients achieve what has been termed complete MR (CMR), defined initially by the European LeukemiaNet as undetectable BCR-ABL mRNA transcripts by quantitative reverse transcriptase PCR (qRT-PCR) and/or nested PCR in two consecutive high-quality samples with a sensitivity $>10^4$. [32] Recent data, however, has highlighted the shortcomings of this definition. So, just as MMR corresponds to ≤ 0.1% $BCR\text{-}ABL^{IS}$, the terms CMR4, CMR4.5 and CMR5 have started to be used to indicate levels of disease that are ≤ 0.01% $BCR\text{-}ABL^{IS}$ (≥4-log reduction from IRIS baseline), ≤ 0.0032% $BCR\text{-}ABL^{IS}$ (4.5-log reduction from IRIS baseline) and ≤ 0.001% $BCR\text{-}ABL^{IS}$ (5-log reduction from IRIS baseline),respectively, as showed in Figure 2.

IM which binds to the ABL1 kinase domain and inhibits phosphorylation of substrates, has been used to treat CML, but it is not curative because, as reported by several authors, the leukemia stem cells that propagate the leukaemia are resistant to therapy and are not eradicated, because CML stem cells remain viable in a quiescent state. [33],[34] This led to the rational development of 2nd generation TKIs with hopes they would effectively treat patients unable to continue on imatinib therapy.

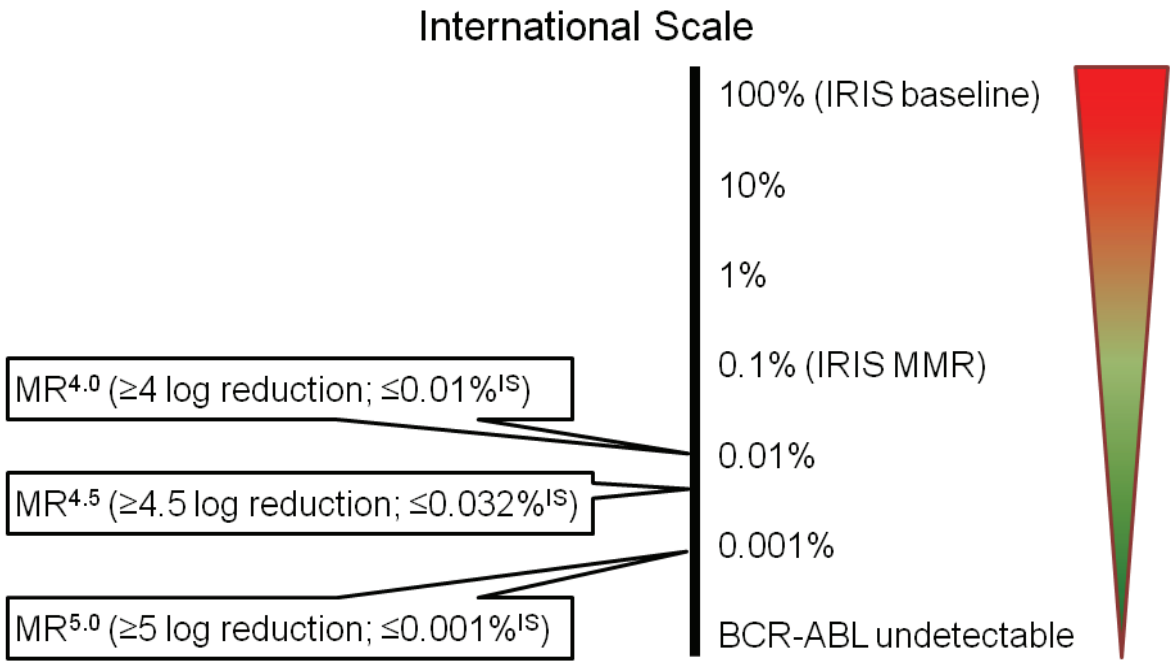

Figure 2. **Definitions of MR**. The international scale for BCR-ABL Q-RTPCR measurement is expressed as a percentage and is fixed to two key points: 100% corresponds to the IRIS standardized baseline and 0.1% corresponds to the upper limit of MMR. $MR^{4.0}$ corresponds to ≤0.01% $BCR\text{-}ABL^{IS}$, $MR^{4.5}$ corresponds to ≤0.0032% $BCR\text{-}ABL^{IS}$ and MR^{5} corresponds to ≤0.001% $BCR\text{-}ABL^{IS}$. Note that all log reductions are from the IRIS baseline and not from individual pretreatment levels.

Nilotinib

Nilotinib (Tasigna, Novartis Pharmaceutical Corporation, NJ, USA) is a structural analog of IM, though its affinity for the ATP binding site on BCR-ABL is up to 50 times more potent in vitro.[35] The drug is an Abl tyrosine kinase inhibitor (TKI) specifically developed to be more selective for Bcr-Abl and that also maintains activity against the most common mutations associated with clinical resistance to IM. Similar to IM, Nilotinib binds to the inactive conformation of Abl. In leukemia stem cells CD34+ the predominant effect of Nilotinib, like IM**,** is antiproliferative rather than proapoptotic.[36] ENEST trial was a randomized, phase III, international study comparing two doses of nilotinib to imatinib once daily.[37] In this phase 3, randomized, multicenter study, the investigators assigned 846 patients with chronic-phase Philadelphia chromosome-positive CML in a 1:1:1 ratio to receive Nilotinib (at a dose of either 300 mg or 400 mg twice daily) or IM (at a dose of 400 mg once daily). At 12 months, the rates of MMR for Nilotinib (44% for the 300-mg dose and 43% for the 400-mg dose) were nearly twice that for IM (22%) ($P<0.001$ for both comparisons). The rates of CCyR by 12 months were significantly higher for Nilotinib (80% for the 300-mg dose and 78% for the 400-mg dose) than for IM (65%) ($P<0.001$ for both comparisons). In conclusion Nilotinib at a dose of either 300 mg or 400 mg twice daily was superior to IM in patients with newly diagnosed chronic-phase Philadelphia chromosome-positive CML. There was also less progression to AP or BP noted in the groups randomized to Nilotinib. At 36 months of follow up, the benefits conferred by Nilotinib persisted. Nevertheless in leukemia stem cells CD34+ the predominant effect of Nilotinib, like IM**,** was antiproliferative rather than proapoptotic. [36].

Dasatinib (Sprycel, Bristol-Myers Squibb) is an oral, 2nd generation TKI that is 350 times more potent than IM in vitro. [38], [39, 40] This drug is a SRC/BCR-ABL kinase inhibitor that binds both active and inactive BCR-ABL conformations, and inhibits many of the kinase mutations that lead to IM resistance. This enhanced efficacy is likely mediated via BCR-ABL rather than SRC, which is not thought to contribute a major role to the pathogenesis of early chronic phase CML. However, the quiescent fraction of stem cells appears to be inherently resistant to IM, Nilotinib and Dasatinib.[41] The DASISION trial was a randomized, phase III, international study comparing IM 400 mg daily versus Dasatinib 100 mg daily in newly diagnosed patients with CML-CP.[42] In a multinational study, 519 patients with newly diagnosed chronic-phase CML were randomly assigned to receive Dasatinib at a dose of 100 mg once daily (259 patients) or IM at a dose of 400 mg once daily (260 patients). The primary endpoint of the study was confirmed CCyR at 12 months, and this was achieved in a higher percentage of patients randomized to dasatinib (77% vs. 66%, $P=0.007$). The rate of major molecular response was higher with Dasatinib than with IM (46% vs. 28%, $P<0.0001$), and responses were achieved in a shorter time with dasatinib ($P<0.0001$). Progression to the accelerated or blastic phase of CML occurred in 1.9% of patients who were receiving Dasatinib and in 3.5% of patients who were receiving IM. The safety profiles of the two treatments were similar. Importantly, with 18 months of follow-up, the benefits of Dasatinib persisted.[43] Taken together, these results demonstrate that the difference in the rates of response between second-generation TKIs and IM becomes more pronounced as the depth of MR increases.[44] Interestingly, although second-generation TKIs yield higher rates of CMR versus IM, there is no evidence to support

the eradication of CML stem cells. On the contrary, there are data suggesting an inability of TKIs to eliminate precursor CD34+ CML cells.[33] Currently, the only treatment modality available to CML patients that is considered potentially curative is allogeneic stem cell transplantation (ASCT), which may induce remission via elimination of CML stem cells through a graft vs leukemia effect.[45] Still, the morbidity and mortality rate following ASCT remains prohibitively high, precluding ASCT as a first-line or even second-line treatment option for most CML patients.
Therefore the kinase inhibitors, Imatinib, Nilotinib, Dasatinib although exhibiting potent antiproliferative effects, are only weak inducers of apoptosis in CML stem and progenitor cells. Thus, new treatment strategies are required.

Combination therapy strategy
Several trials are evaluating novel combinations of TKI therapy with agents that target CML stem cells to determine if it is possible to increase the percentage of patients who are able to achieve deep CMRs. Moreover the combination of Nilotinib with stem-cell active drugs, such as Janus kinase (JAK) inhibitors, MEK inhibitors and the hedgehog pathway inhibitors, may have a synergistic effect and could provide a rationale for future combination trials.[46], [47], [48]
These data suggest that CML stem cell survival may be also Bcr-Abl kinase independent and suggest curative approaches in CML must focus on kinase-independent mechanisms of resistance. Multiple reports have demonstrated that CML leukemia stem cells (LSCs) initiation and propagation occurs as a result of aberrant activation of pro-survival and self-renewal pathways regulated by stem-cell related signaling molecules including Sonic Hedgehog (Shh) and β-catenin. Enhanced survival in LSC protective microenvironments, such as the bone marrow niche, as well as acquired dormancy of cells in these niches, also contributes to LSC persistence. Key components of these cell-intrinsic and cell-extrinsic pathways provide novel potential targets for therapies aimed at eradicating this dynamic and therapeutically recalcitrant LSC population.[49] In leukemic disorders, LSC can hibernate in supportive hematopoietic microenvironments such as the bone marrow niche.

Bone Marrow Niche

Bone Marrow (BM) is a hematopoietic organ that resides within the protected confines of the bones and is the major location for the hematopoiesis. In adults, 4.6% of body weight is due to the BM that is distributed throughout the vertebrae, ribs, pelvis, skull and proximal ends of the long bones.[50] The structure of the BM consists of a rigid bone cortex enclosing a cavity containing the arterial vascular system, a complex sinusoidal system, hematopoietic cells and the stroma. The cellular component of the BM can be divided into hematopoietic cells and mesenchymal-derived cells.

The mesenchymal-derived cells, along with the macrophages and the extracellular matrix (ECM), form the BM stroma. The BM hematopoietic cells consist of hematopoietic stem cells (HSCs) hematopoietic progenitor cells (HPCs) and mature plasma cells. One of the best characterized stem cell is the hematopoietic stem cells (HSC). HSCs function to generate a lifelong supply of all blood cell types. HSCs have the ability to differentiate into all myeloid and lymphoid cell lineages and reproduce the entire hematopoietic and immune systems.

The ability to reconstitute all the blood-cell lineages in lethally irradiated mice is the most common assay to assess the stemness in HSCs [51] In the past few years, the microenvironment, which regulates HSCs, has been characterized. Within adult BM, self-renewal and differentiation are regulated by two major cellular components: osteoblasts and vascular endothelial cells.[52]

In the BM, quiescent or slow-cycling HSC have been identified close to the endosteal surface in the trabecular bone; constituting a reservoir of HSC that can be mobilized and restore the hematopoiesis in response of tissue injury.

The HSCs and HPCs are held within the BM stroma not only through the adhesive interactions between VCAM-1, expressed by stromal cells, and integrin $\alpha 4\beta 1$ (alpha 4 beta 1) expressed by the HSCs and HPCs, but also by the *chemotactic interaction* between the chemokine CXCL12 and its receptor CXCR4 expressed on the HSCs and HPCs. In steady-state conditions the majority of the HSCs reside in the BM with a few circulating in the peripheral blood. HSCs are localized in a non random manner at the bone–BM interface (osteoblastic niche) and around the blood vessels (vascular niche).[53]

The Osteoblastic Niche

The majority of HSCs in the endosteum are found to be in direct contact with the osteoblasts. The HSCs home in on the endosteum with the help of a chemotactic Ca2+ sensing receptor that senses the Ca2+ gradient within the BM. The gradient is created by the release of Ca2+ in the BM due to the constitutive osteoclasts and osteoblasts-mediated bone remodeling.[54] Once reaching the endosteum, the HSCs are held in the endosteum by the expression of:

- Adhesive molecules like osteopontin,
- N-cadherin,
- Transmembrane c-KIT ligand stem cell factor (SCF)
- The polysaccharide hyaluronic acid.

This interaction is strengthened by the cytokines and chemokines that are produced by the osteoblasts, like:

- Chemokine CXCL12, also known as SDF-1

- Angiopoietin-1 (Ang1),
- Jagged-1, a ligand for Notch1 receptor also expressed by HSCs.

Osteopontin, a matrix glycoprotein expressed by the osteoblasts supports the adhesion of HSC to the osteoblastic niche and negatively regulates HSC proliferation, contributing to the maintenance of a quiescent state.[55]
N-cadherin, is expressed in HSCs or HPCs and they plays a critical role in the regulation of HSCs/HPCs engraftment.
Osteoblasts in the bone marrow produce a significant amount of membrane-bound stem cell factor (SCF), which has the capacity to enhance the adhesion of HSCs to stromal cells. [56] SCF binds and activate c-KIT (a receptor tyrosine kinase), which is highly expressed by HSCs.
Hyaluronan is synthesized by primitive HSCs, participates in their lodgment at the endosteum.

Secreted Factors
The bone-forming osteoblasts are crucial players for the homeostasis of the hematopoietic tissue with its high turn-over. Indeed, osteoblasts express several cell-signaling molecules such as BMP4, Jagged-1, and angiopoietin-1 (Ang1), both are important for HSCs self-renewal, survival, and maintenance.[57]
CXCL12 a member of the CXC subfamily of cytokines, also known as Stromal derived factor-1 (SDF-1) is produced by stromal cells and, acting through the G protein–coupled CXCR4, the sole receptor for SDF-1 [58]
SDF-1 functions as both a chemo-attractant and a modulator of cellular growth/ survival.
Ang1 in osteoblasts interacts with the tyrosine kinase receptor Tie-2, a type of receptor tyrosine kinase that is expressed in HSCs, and the Tie-2/Ang1 interaction activates β1-integrin and N-cadherin. This enhanced adhesion contributes to the maintenance of the stem cell quiescence.
Osteoblasts expressing the Notch ligand: Jagged1. Jagged1-mediated Notch1 signaling is dispensable for HSCs self-renewal and differentiation.

The Vascular Niche
The vascular niche promotes proliferation, differentiation of actively cycling, and short-term HSCs.[59] The most purified HSCs, fractioned as CD150+ CD48− CD41− Lin−cells, were found in majority to be associated with the sinusoidal endothelium lining blood vessels, suggesting that endothelial cells create a cellular niche for HSCs.[60]

Secreted Factors
The vascular niche has been shown to produce factors important for mobilization, homing, and engraftment of HSCs, such as CXCL12 (SDF-1, stromal cell derived factor-1) important for mobilization, homing, and engraftment for HSCs.
SDF-1 and FGF-4 (fibroblast growth factor-4) induce upregulation of adhesion molecules, including VLA4/VCAM1, facilitating localization to the vascular niche.[61]
CXCL12/CXCR4 signaling plays important roles in HSCs trafficking and HSCs mobilization. HSCs were specifically located adjacent to cells expressing a high level of CXCL12, which surrounded the sinusoidal endothelial cells. They named these cells CXCL12-abundant reticular cells (CAR). HSCs have been shown to be associated with CAR cells in the sinusoidal region and are located between CAR and

osteoblastic cells in the endosteal region, suggesting that those cells might be an important component of both the osteoblastic and the vascular niches in adult BM.

Membrane-Bound Factors

During the bone marrow transplantation, the ability of HSCs to “home” and engraft in the recipient’s bone marrow requires a cascade of events which includes specific molecular recognition. Adhesion molecules on the HSCs involved in the process of rolling are VLA4 (CD49d), LFA-1 (CD11a), and hyaluronan binding cellular adhesion molecule (HCAM/CD44) whereas the complementary binding partners on the BM endothelial cells are VCAM-1, ICAM-1 (CD54), and E- and P-selectin (CD62E and CD62P).[62]

Difference between vascular and osteoblastic niches.

The major difference between both microenvironments is the oxygen level. Higher in the vascular niche than in the osteoblastic niche under hypoxia, HSCs would move to the vascular niche and resume then cell cycle in order to restore hematopoiesis.[63] The osteoblastic niche localized at the inner surface of the bone cavity and with abundant osteoblasts, might serve as a reservoir for long-term HSC storage in a quiescent state.

Whereas the vascular niche, which consists of sinusoidal endothelial cell lining blood vessel, provides an environment for short-term HSC proliferation and differentiation. Both niches act together to maintain hematopoietic homeostasis or restore it after damage. Figure 3.

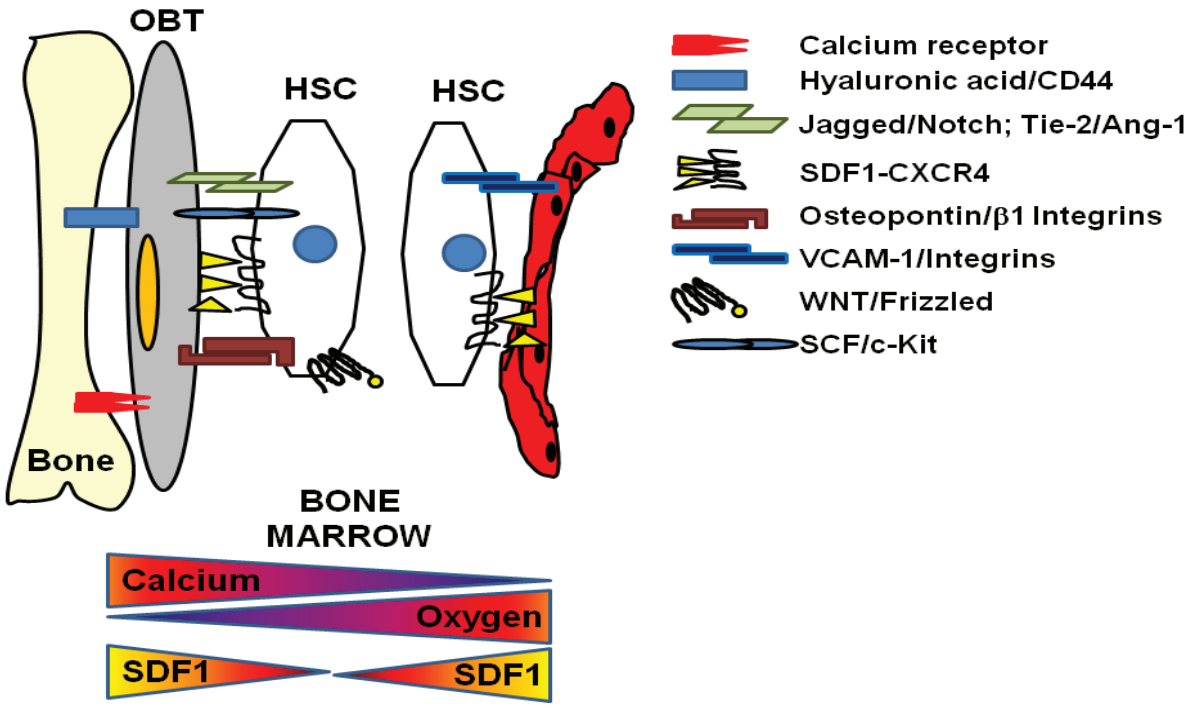

Figure 3. **Schematic representation of the molecular interactions between hematopoietic stem cells and their niches in the bone marrow**. In normal physiological conditions, the hematopoietic stem cells (HSCs) reside either at the endosteum, lodged with the osteoblasts (OBT) (osteoblastic niche) or at the sinusoidal vessels (SV) (vascular niche). The osteoblastic niche provides the microenvironment for HSC maintenance and quiescence and the vascular niche provides the microenvironment for HSC proliferation and differentiation. The oxygen and the calcium gradient might play a crucial role in maintenance of the different niches within the bone marrow.

Role of the Niches in the Leukemia Development and Treatment Resistance
Cancer stem cells have been described in a number of cancers including acute myeloid leukemia (AML), breast cancer, brain cancer, colon cancer, pancreatic cancer and CML.[64],[65],[66],[67],[68],[69]
CML, is a stem cell derived hematopoietic cancer that can be effectively treated with the use of bcr-abl kinase inhibitors. However, failure to eliminate minimal residual disease (MRD) found in the BM compartment due to the existence of the CML stem cells (that closely resemble normal HSCs), leads to the relapse of the disease.[70]
In vitro, it was demonstrated that osteoblasts or osteoblast-like cells seeded on the bio-derived bone scaffold could maintain stem/progenitor cells from CML bone marrow primary cells in a long term culture.[71]
In vivo, the CML stem cells utilize CD44 to home into and subsequently engraft in to the BM HSCs niche.[72] Once within the BM, the CML stem cells utilize the survival pathways that are active in normal HSCs. Also, CML cells when adhered to fibronectin, a component of the BM microenvironment, demonstrated significant resistance to BCR-ABL inhibitors via the phenomenon referred to as cell adhesion mediated drug resistance (CAM-DR).[73]
Microenvironment-mediated chemoresistance, including through CXCR4/SDF-1 axis in different hematologic malignancies, including multiple myeloma, acute myelogenous leukemia, acute lymphoblastic leukemia, and chronic lymphocytic leukemia. In CML it has been shown that p210 BCR-ABL can down regulate the CXCR4 expression with an abnormal release of immature myeloid cells (LSC) from the BM into the circulation. However IM or Nilotinib treatment, via inhibition of BCR-ABL will restore CXCR4/SDF-1a interactions and subsequently cause CML cells to migrate and attach to supportive milieu of bone marrow microenvironment. This is associated with inhibition of proliferation of CML cells concomitant with enhanced survival. In addition to the physical components, the BM microenvironment contains a milieu of cytokines and growth factors that contribute to drug resistance in CML.[74],[75],[76] The selective CXCR4 antagonist Plerixafor (previously AMD3100) sensitizes CML cells to the tyrosine kinase inhibitors IM and Nilotinib and was so able to overcome the protective effects of the BM stromal environment.[77]
In this study, we show that conditioned media (CM) generated from bone marrow (BM)-derived mesenchymal stromal cells or HS-5 cells lead to BCR-ABL independent STAT3 activation. Activation of STAT3 is important not only for survival of CML cells but also for its protection against TKI, within the BM microenvironment. The co-treatment of TKI and JAK2 inhibitors are able to significantly reduce cell viability and induce apoptosis in Ph+ cells or CD34+CML cells treated in the presence of stroma conditioned media (HS-5/CM) (separated by 0.4-μm thick micropore membranes; that interrupted cell-to-cell contact but allowed them to be bathed by the same culture medium). This experiment proves a strong synergistic effect of TKI and JAK2 inhibitors to overcome stroma derived TKI resistance. Finally, we demonstrate that in patient-derived primitive leukemic cells, co-cultured with BM stromal cells, inhibition of BCR-ABL and JAK activity was a successful strategy to potentiate their elimination.

Materials and Methods

Cell lines and tumor cells

K562 cell line

K-562 (obtained from the American Type Culture Collection) is an erythroleukemia cell line derived from the pleural effusion of a 53-year-old female with chronic myelogenous leukemia in terminal blast crisis. The cell population has been characterized as highly undifferentiated and of the granulocytic series. The morphology is round large, single cells in suspension. Cells carry the BCR-ABL1 e14-a2 (b3-a2) fusion gene. Human CML K562 cells were cultured in RPMI supplemented with 10% fetal bovine serum (FBS), 1% L-glutamine (L-Glu), and 1% penicillin/streptomycin (P/S), defined as regular media (RM), at 37°C in 5% CO_2 in a humidified incubator. K562 cells were kept at 0.5 x 10^6 cells/ml.

KT1 cell line

KT1 (CML) kindly provided by Dr Fujita (First Department of Internal Medicine, School of Medicine, Ehime University, Japan) is a leukemia cell line established from a patient in the blast crisis phase of CML. KT-1 has undifferentiated morphology that exhibited a high nuclear/cytoplasm ratio without cytoplasmic granules. Positive reactions for intracellular myeloperoxidase (MPO) and the myeloid marker CD33 indicated that KT-1 cells possessed the features of myeloid-lineage cells. KT-1 cells showed two Ph1 chromosomes and an absence of normal copies of chromosomes 9 and 22. The KT-1 cells are IFN-alpha or IFN-gamma sensitive.[78]
Human CML KT1 cells were cultured in RPMI supplemented with 10% fetal bovine serum (FBS), 1% L-glutamine (L-Glu), and 1% penicillin/streptomycin (P/S), defined as regular media (RM), at 37°C in 5% CO_2 in a humidified incubator. K562 cells were kept at 0.5 x 10^6 cells/ml.

BV173 cell line

BV173 (obtained from Leibniz Institute DSMZ-German Collection of Microorganisms and Cell Cultures) is a B cell precursor leukemia cell line established from the peripheral blood of a 45-year-old man with chronic myeloid leukemia (CML) in blast crisis in 1980. The morphology of cell is round to elongate. Cells grow in suspension. Cells carry the t(9;22) leading to BCR-ABL1 e13-a2 (b2-a2) fusion gene. Human BV173 cells were cultured in RPMI supplemented with 20% FBS, 1% L-Glu and 1% P/S, defined as regular media (RM), at 37°C in 5% CO_2 in a humidified incubator. BV173 were maintained at 0.5 x 10^6 cells/ml.

HS-5 cell line

The human bone marrow stromal cell line HS-5 (obtained from the American Type Culture Collection) is a fibroblastoid cell line immortalized by transduction with the human papilloma virus E6/E7 genes. Cells grow in adherent manner. it secretes detectable amounts of granulocyte colony-stimulating factor (G-CSF), granulocyte-macrophage colony-stimulating factor (GM-CSF), macrophage colony-stimulating factor (M-CSF), macrophage inhibitory protein 1-α, stem cell factor (SCF), leukemia-inhibitor factor, IL-11, IL-8, IL-6, and IL-1; and it is capable of sustaining proliferation of normal hematopoietic progenitors cells in serum-free media without additional growth factors.[79] Human HS-5 cell were seeded 1,5 × 10^6 cells in α-MEM

supplemented with 20% FBS, 1% L-Glu, and 1% P/S at 37°C in 5% CO2 in a humidified incubator. To achieve complete confluence and the formation of a stable feeder monolayer, $1x10^5$ HS-5 cells were plated in 24 well plates at least 48–72 hours to achieve 75% to 80% confluence, before the addition of primary leukemic cells. To evaluate the soluble factors produced by HS-5, the conditioned media (HS-5/SCM) was collected after 48-72 hours of culture and filtred with 0.22 μm filter, aliquoted and stored at -80°C.

Samples from CML Patients and Healthy Donors

Bone marrow samples and peripheral blood were collected from 20 newly diagnosed patients with CML-CP patients enrolled in our Institution and two healthy donors (HD), after signed informed consent was obtained in accordance with the Declaration of Helsinki and after approval by the Institutional Review Board (IRB) of University of Naples Federico II.

Isolation of CML Progenitor Cells

Mononuclear cells, from peripheral blood (PB) or bone marrow (BM) samples of patients with CML-CP at the untreated stage were isolated by centrifugation on a Ficoll-Hypaque gradient. CD34+ cells were sorted with Miltenyi Biotec CD34 MicroBead Kit human. Briefly, the CD34+ cells are magnetically labeled with CD34 MicroBeads. Then, the cell suspension is loaded onto a MACS® Column which is placed in the magnetic field of a MACS Separator. The magnetically labeled CD34+ cells are retained within the column. The unlabeled cells run through; this cell fraction is thus depleted of CD34+ cells. After removing the column from the magnetic field, the magnetically retained CD34+ cells can be eluted as the positively selected cell fraction. The CD34+ cells were cultured in AIM-V serum-free media (Invitrogen) supplemented with 2nM L-glutamine (GIBCO-BRL Invitrogen), 1% penicillin/streptomycin (Gibco-Invitrogen) at a starting density of $1x10^5$ cells/ml at 37°C, 5% CO_2, in a humidified incubator for 4 days. When specified, the following cytokines were included [high grow factor (GF) cocktail]:100 ng/ml SCF, 100 ng/ml FLT3 ligand, 20 ng/ml G-CSF, 20 ng/ml IL-3, and 20 ng/ml IL-6 (all from R&D Systems). Depending on the individual experiment, TKI were added at approximely a clinical relevant concentration (1μM Imatinib, 400nM Nilotinib and 2.5nM Dasatinib).[32]

Generation of Mesenchymal Stroma Cell (MSC) and Mesenchymal Stroma Conditioned Media (SCM)

Mononuclear cells were isolated from BM aspirates by centrifugation on a Ficoll-Hypaque gradient. MSC cells were sorted with Miltenyi Biotec Anti MSCA-1 MicroBead kit human. Briefly, the MSC+cells are magnetically labeled with MSC MicroBeads. Then, the cell suspension is loaded onto a MACS® Column which is placed in the magnetic field of a MACS Separator. The magnetically labeled MSC cells are retained within the column. The unlabeled cells run through; this cell fraction is thus depleted of MSC cells. After removing the column from the magnetic field, the magnetically retained MSC cells can be eluted as the positively selected cell fraction. Human MSCA-1+ cells were cultured in Mesenchymal Stem Cell Basal Medium (MSCBM) with Mesenchymal Cell Growth Supplement (MCGS), 2% (L-Glu), 1% Penicillin/Streptomycin and cultured at 37°C in 5% CO_2 in a humidified incubator. Conditioned Media (CM) was collected after at least two cell passages of two mesenchymaò stroma cell lines obtained from Healthy Donor (HD), named HD/SCM

and eight stroma cell lines obtained each from a BM sample of a patient with CML, named CML/SCM, and stored at -80°C. After SCM collection, mesenchymal stroma cell lines have been immunophenotypically analyzed for the positive expression of CD73, CD90, and CD105 and negative for CD45, CD34, CD14 or CD11b, CD79α or CD19, and HLA-DR surface antigens (human MSC Phenotyping Kit, Miltenyi).

Drugs and Reagents

Imatinib mesylate and Nilotinib (AMN107), both kindly supplied by Novartis Pharma, were dissolved in Dimethyl sulfoxide (DMSO) as a 10 mmol/L stock solution and stored in aliquots at −20°C. Dasatinib, kindly supplied by Bristol-Myers Squibb, was treated similarly. Ruxolitinib both also supplied by Novartis Pharma, were dissolved in DMSO as a 10 mmol/L stock solution and stored in aliquots at −20°C.

The Trypan Blue Method: Assessment of Percentage of Viable and Non Viable Cells

Cells were stained with trypan blue (Sigma, St Louis, MO). The reactivity of trypan blue is based on the fact that the chromopore is negatively charged and does not interact with the cell unless the membrane is damaged. Therefore, all the cells which exclude the dye are viable. The numbers of non-viable cells were determined by counting the cells that showed trypan blue uptake using the Burker's chamber, and reported as percentage of untreated control cells.

Apoptosis Assay

Apoptosis was measured using FITC Annexin V Apoptosis Detection Kit II BD Pharmingen. Briefly, we wash cells twice with cold PBS and then resuspend them in 1X Binding Buffer at a concentration of 1 x 10^6 cells/ml. We transfer 100 µl of the solution (1 x 10^5 cells) to a 5 ml culture tube and add 5 µl of FITC Annexin V and 5 µl propidium iodide (PI). We gently vortex the cells and incubate for 15 min at RT (25°C) in the dark. After incubation we add 400 µl of 1X Binding Buffer to each tube. Analyze by flow cytometry within 1 h.

In apoptotic cells, the membrane phospholipid phosphatidylserine (PS) is translocated from the inner to the outer leaflet of the plasma membrane, thereby exposing PS to the external cellular environment. FITC Annexin V is a 35-36 kDa Ca2+ dependent phospholipid-binding protein that has a high affinity for PS, and binds to cells with exposed PS. Since externalization of PS occurs in the earlier stages of apoptosis, FITC Annexin V staining can identify apoptosis at an earlier stage than assays based on nuclear changes such as DNA fragmentation. FITC Annexin V staining precedes the loss of membrane integrity which accompanies the latest stages of cell death resulting from either apoptotic or necrotic processes.

Therefore, staining with FITC Annexin V is typically used in conjunction with a vital dye such as propidium iodide (PI) or 7-Amino-Actinomycin (7-AAD) to allow the investigator to identify early apoptotic cells (PI negative, FITC Annexin V positive).

PI is an intercalating agent and a fluorescent molecule with a molecular mass of 668.4 Dalton that can be used to stain cells. Propidium iodide is used as a DNA stain for both flow cytometry to evaluate cell viability or DNA content in cell cycle analysis and microscopy to visualize the nucleus and other DNA containing organelles. It can be used to differentiate necrotic, apoptotic and normal cells.

Viable cells with intact membranes exclude PI, whereas the membranes of dead and damaged cells are permeable to PI. Cells that are considered viable are FITC Annexin V and PI negative; cells that are in early apoptosis are FITC Annexin V

positive and PI negative and cells that are in late apoptosis or already dead are both FITC Annexin V and PI positive.

Flow-Cytometric Assays
Apoptosis was measured using FITC Annexin V Apoptosis Detection Kit II (BD Pharmingen). The percentage of apoptotic cells was determined by flow cytometry. Cell cycle analysis was detrmined by BRdU Flow Kits (BD Pharmigen), as specified by the manufactory.

Evaluation of BCR-ABL Activity in K562 Cell Line
K562 cell have been treated with TKIs at the indicated concentration for 30' (minute), than cells were transferred in ice and washed with cold PBS. To simultaneously asses the phosphorylation status of BCR-ABL target, we carried out intracytoplasmatic immunostaining with antibody against p-CrkL (Tyr207), p-STAT5 (Tyr694), p-ERK1/2 (Thr202/Tyr204) and p-STAT3 (Tyr705) (Cell Signaling Technology), following the manufacturer's instructions. For each sample, a minimum of 100,000 cells were analyzed using a FACSCalibur (Becton Dickinson, San Diego, CA).

Cell Cycle Analysis
The immunofluorescent staining of incorporated bromodeoxyuridine (BrdU) and flow cytometric analysis provide to determine the frequency and nature of individual cells that have synthesized DNA. In this method, BrdU (an analog of the DNA precursor thymidine) is incorporated into newly synthesized DNA by cells entering and progressing through the S (DNA synthesis) phase of the cell cycle. The incorporated BrdU is stained with specific anti-BrdU fluorescent antibodies. The levels of cell-associated BrdU are then measured by flow-cytometry. Often, staining with a dye that binds to total DNA such as 7-aminoactinomycin D (7-AAD) is coupled with immunofluorescent BrdU staining. With this combination, two-color flow cytometric analysis permits the enumeration and characterization of cells that are actively synthesizing DNA (BrdU incorporation) in terms of their cell cycle position (ie, G0/1, S, or G2/M phase defined by 7-AAD staining intensities). The kit used is BRdU Flow Kits of Bd Pharmigen.

Colony-Forming Unit (CFU) Inhibition Assay of Leukemic and Normal Hematopoietic Progenitors
CD34+ cells were isolated from BM or PB of CML/Healthy Donors. CD34+ cells were cultured for 72 hours with the three BCR-ABL kinase inhibitors plus or minus the JAK Inhibitor Ruxolitinib in the presence of stroma cell line HS5 (HS5/SCM) or high grow factor cocktail. After co-incubation assay, cells were plated in triplicate in methylcellulose medium supplemented with recombinant cytokines (MethoCult; StemCell Technologies), and incubated at 37°C. Granulocyte-macrophage colony-forming units and erythrocyte colony-forming units (CFU) were scored using a high-quality inverted microscope after 2 weeks of culture. In selected experiments, colonies were collected to assess ABL and p210 expression by Q-RT-PCR. Total RNA was also isolated from single hematopoietic colonies as described previously.[80]

High Grow Factor Cocktail
We used the same high grow factor cocktail reported by Susan M. Graham et al; Briefly, CD34+ cells were grown in Iscoves modified Dulbecco medium (Sigma) supplemented with a serum substitute (BIT; StemCell), supplemented or not with 100ng/mL recombinant human Flt3-ligand (Immunex Corporation, Seattle,WA) and Steel factor (Terry Fox Laboratory, Vancouver, BC, Canada), and with 20 ng/mL recombinant human interleukin-3 (IL-3) (Novartis, Basel,Switzerland), IL-6 (Cangene, Mississauga, ON, Canada), and granulocyte–colony-stimulating factor (G-CSF) (Chugai Pharma, United Kingdom; abbreviated as 5 growth factors [GFs], like reported by Susan M. Graham et al.)[33]

Q-RT-PCR
Single cell clones have been evaluated for the expression of P210 mRNA by quantitative real-time PCR (Q-RT-PCR) as previously described. Briefly, all amplification reaction was carried out in triplicate and the mean Ct value was used to interpolate standard curves and calculate the transcript copy number.

Bioplex ELISA Assay
The Bio-Plex multiplex system enables the detection and quantification of multiple analytes in a single sample volume. Utilizing xMAP technology licensed from Luminex, the Bio-Plex Multiplex system can multiplex up to 500 different assays simultaneously. We evaluated the secretory profiles between the HS5/SCM and CML/SCM from 8 mesenchymal stromal cell lines obtained from CML patient, in particular we tested them for 20 different analytes, reported to be involved in leukemia signaling pathways: IL-1a, IL-3, M-CSF, SCF, SDF1-a, TRAIL, HGF, PDGF-bb, IL1b, IL-6, IL-7, IL-8, IL-10, IL-12, IL-15, G-CSF, GM-CSF, MIP-1a, TNF-a, and VEGF; using the Bio-PLEX-200 System.

Statistical Analysis
All in vitro experiments were summarized as mean plus or minus one standard Deviation (SD). Student *t* test was used to determine the statistical significant differences by non parametric Mann-Whitney test, between values obtained in a population of leukemic cells treated with different experimental conditions, with *P* value less than .05 indicating a significant difference. The half maximal inhibitory concentration (IC50) was calculated based on the level of viable cells (Annexin-$V^{neg.ve}/PI^{neg.ve}$) residual after treatment with increasing doses of TKI ranging from 0 to 100μM in the presence or absence of HS-5/SCM. Data were analyzed by a specific software (MasterPlexReaderFit), applying 4 Parameter Logistic (4-PL) and 5 Parameter Logistic (5-PL) model equations to calculate the IC50 for dose response curves. Combination index (CI), defined as quantitative measure of the degree of drug interaction in terms of synergism and antagonism for a given endpoint of the effect measurement [Z=(1-T/V), calculated from drug-treated samples with a measured response T (as a percentage of residual viable cells; Annexin-$V^{neg.ve}/PI^{neg.ve}$) relative to V, (a median level of viable cells of 10 vehicle-treated samples),[81] was calculated by CompuSyn software based on Chou's median-effect equation and its extension, combination index (CI) equation.[82],[83]
In particular, based on the CI value, we defined, as previously reported, a very strong synergism (CI<1), strong synergism (0.1-0.3), synergism (0.3-0.7), moderate synergism (0.7-0.85), slight synergism (0.85-0.9), nearly additive (0.90-1.10), slight

antagonism (1.10-1.20), moderate antagonism (1.20-1.45), antagonism (1.45-3.3), strong antagonism (3.3-10) and very strong antagonism (>10).

Results

Stroma Conditioned Media Derived from Healthy Donors or Patients with CML Protect Ph+ Cells from TKI-Related Apoptosis

To evaluate whether BM microenvironment significantly affects first and second generation TKI activity on Ph+ cells, we treated K562, BV173 and KT1 cell lines with Imatinib, Nilotinib or Dasatinib at clinical relevant concentrations,[84],[85] in the presence of a monolayer of BM stroma cell line HS-5. As shown in Figure 4 and 5, all the analyzed Ph+ cell lines are significantly protected from TKI-related cell apoptosis (Fig.4A-C) and mortality (Fig.5A-C) when incubated in direct contact of HS-5 stroma cell line. Indeed, when K562 cell line (Figure 4A) are treated with Imatinib, Nilotinib or Dasatinib in the presence of a HS-5 monolayer, apoptosis is significantly reduced (18%±13%, 50%±6%, or 10%±10%, respectively), respect to Ph+ cell line treated in RM (46%±12%, 84%±15%, or 53%±20%, respectively. $p<0.05$ in all the conditions. (Figure 4A). Similar results have been achieved in the context of BV173 and KT1 cell lines (Figure 5A and 5B). Moreover, we demonstrated that TKI-resistant is also related to soluble factors produced by HS-5 in the conditioned media (HS-5/SCM). Indeed, a significant level of protection is also achievable by treating Ph+ cells with TKIs in the presence of HS-5/SCM soluble factors (Figure 4A-C dark-gray barrel).

The apoptosis is also greatly reduced when K562 cell line is treated with Imatinib, Nilotinib or Dasatinib in the presence of HS-5/SCM (20%±9%, 29%±18%, or 17%±6%, respectively), respect to Ph+ cell line treated in RM.

To evaluate if the observed stroma-related TKI resistance is merely associated to HS-5 intrinsic characteristics, we generated stroma cell lines directly from two healthy BM donor identified as healthy donor/stroma cells (HD/SC) and 8 patients at diagnosis affected by CML identified as CML/ stroma cells (CML/SC). We tested the effects of the derived conditioned media obtained from these stroma cell lines (HD/SCM and CML/SCM, respectively) on the regulation of TKI activities on Ph+ cell lines. As shown in Figure 4A-C, HD/SCM (white barrel) and CML/SCM (gray barrel) are equally able to significantly reduce TKI-related apoptosis in K562 (Figure 4A), KT1 (Figure 4B) or BV173 cell lines (Figure 4C). Indeed TKI-induced apoptosis is significantly inhibited in K562 cell line by CML/SCM exposition (22%±12%, 40%±16%, or 31%±16%, respectively) respect to control cell line treated in RM (46%±12%, 84%±15%, or 53%±20%, respectively. (Figure 4A). $p<0.05$ in all the conditions. Similarly, apoptosis was greatly reduced when KT1 and BV173 cell lines were treated with TKIs in the presence of HD/SCM or CML/SCM (Fig. 4B and 4C, respectively).

Thus, we demonstrated that BM mesenchymal stroma microenvironment, either represented by the selected clone HS-5 or by mesenchymal stroma cell lines derived from HD and patients with CML, provides survival factor able to protect Ph+ cells from TKI-related apoptosis or cell death.

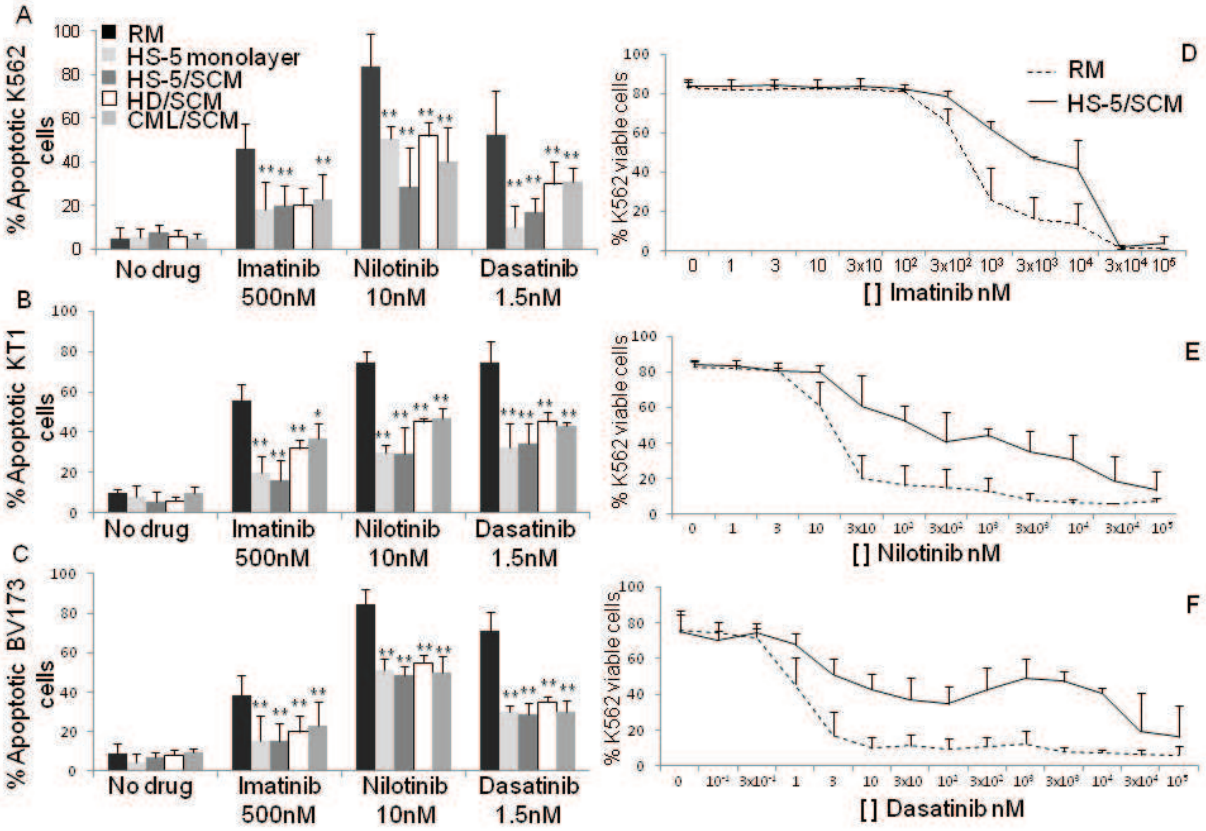

Figure 4. **Analysis of Imatinib, Nilotinib and Dasatinib activity modulation by Mesenchymal Stroma cells exposition.**
Ph+CML cell lines, K562, BV173 and KT1 were treated with the indicated concentrations of Imatinib, Nilotinib or Dasatinib in different culture conditions: in regular media (RM) (black barrel), in the presence of a HS-5 monolayer (light-gray barrel), in media supplemented with 50% of HS-5/SCM (dark-gray barrel), in media supplemented with 50% of HD/SCM (white barrel), or in media supplemented with 50% of patients derived CML/SCM (gray barrel). Apoptosis were monitored by Annexin V/PI staining after 24 hrs in K562 cell line (**A**), KT1 cell line (**B**) and BV173 cell line (**C**). Results represent the mean ± SD from 3 independent experiments. $p<0.01$ for all the condition. IC50 was calculated based on the level of viable cells (Annexin-$V^{neg.ve}$/$PI^{neg.ve}$) residual after treatment with increasing doses of Imatinib (**D**), Nilotinib (**E**) or Dasatinib (**F**) ranging from 0 to 100.000nM in the presence (continuous line) or absence (dot line) of HS-5/SCM.

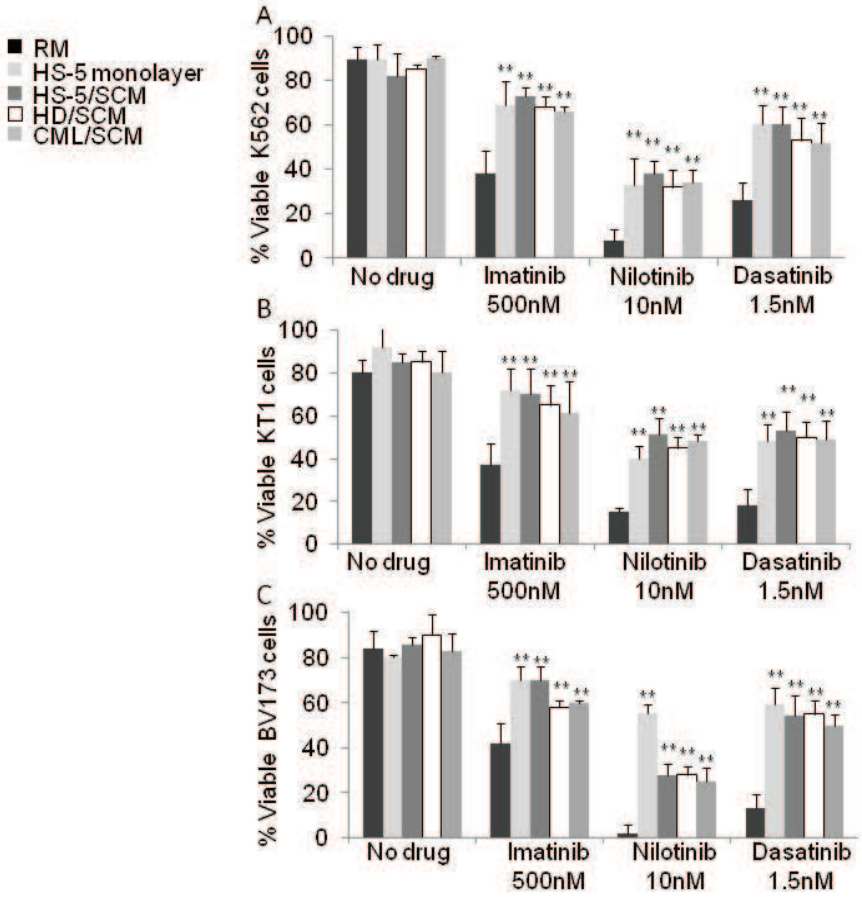

Figure 5. Cell viability in Ph+ cell lines treated with TKI upon Mesenchymal Stroma cells exposition.

Ph+CML cell lines, K562, BV173 and KT1 were treated with the indicated concentrations of Imatinib, Nilotinib or Dasatinib in different culture conditions: in regular media (RM) (black barrel), in the presence of a HS-5 monolayer (light-gray barrel), in media supplemented with 50% of HS-5/SCM (dark-gray barrel), in media supplemented with 50% of HD/SCM (white barrel), or in media supplemented with 50% of patients derived CML/SCM (gray barrel). Cell viability were monitored by Annexin V/PI staining after 72hrs, in K562 cell line (**A**), KT1 cell line (**B**) and BV173 cell line (**C**). Results represent the mean ± SD from 3 independent experiments. Significance values: * $p<0.05$; ** $p<0.01$.

CML/SCM increase the IC50 of Imatinib, Nilotinib and Dasatinib in Ph+ cell lines
To quantify the effect of HS-5/SCM exposition on TKI activity, K562 cell line has been treated with an escalation dose of Imatinib, Nilotinib or Dasatinib (range 0.1-100,000 nM) in the presence or in the absence of HS-5/SCM and cellular viability has been monitored after 72hrs. As shown in table1, we demonstrated that the IC50 of Imatinib, Nilotinib or Dasatinib is significantly increased when the Ph+ cell line K562 is cultured in the presence of HS-5/SCM (5309.29nM, 381.14nM, 2.31nM, respectively) vs the IC50 calculated on K562 viable cells residual after TKI treatment in RM (564.97nM, 14.26nM and 1.13nM, respectively). In particular the IC50 of K562 cell line, based on cell viability at 72hrs after Imatinib treatment, increases about ten times from 564.97 nM in RM to 5309.29 nM in cell treated in presence of HS-5/SCM (Fig.4C), the IC50 increases about thirty times from 14.26 nM in RM to 381.14 nM in HS-5/SCM after Nilotinib treatment and the IC50 increases about two times from 1.13 nM in RM to 2.31 nM in HS-5/SCM, after Dasatinib treatment. Moreover, in average 47%, 40% and 51% of K562 cells exposed to HS-5/SCM were still viable after treatment with 3000nM Imatinib, 300nM Nilotinib or 3nM Dasatinib, respectively (11%, 15% and 17% of K562 cells treated with the same concentration of TKIs in the absence of HS-5/SCM (Fig.5A); $p<0.001$ in all the conditions). Similarly, we observed the same results when KT1 and BV173 cell lines were exposed to HS-5/SCM. (Fig.5B and 5C, respectively).
Finally, to evaluate whether the viable Ph+ cells residual after TKI treatments in the presence of HS-5/SCM are able to further expand or, instead, apoptosis is just delayed by the presence of soluble factors produced by stroma cell line, we cultured K562 cell line with TKIs at the calculated IC50 (Table 1) for 72 hrs in the presence of HS-5/SCM. Cells were then collected, washed and re-plated in complete media for a total of 14 days without addition of TKIs. As shown in Fig 6A, residual K562 cells after TKIs treatment upon stroma exposition were able to significantly expand after drug withdrawal, respect to K562 cells exposed to a single dose of TKIs in the absence of HS-5/SCM. However, HS-5/SCM withdrawal before TKI treatment is able to completely overcome the stroma-mediated TKI protection (Fig 6B). Moreover, serial dilutions of HS-5/SCM, ranging from 50% to 0.05%, show that soluble factors are associated to stroma-related TKI resistance in a dose dependent manner (Fig.6C).

	RM IC50 (nM)	HS5-SCM IC50 (nM)
Imatinib	564.97	5309.29
Nilotinib	14.26	381.14
Dasatinib	1.13	2.31

Table1. IC50 modulation in K562 cell line by stroma conditioned media.
Data were analyzed by specific software (MasterPlex ReaderFit), applying 4 Parameter Logistic (4-PL) and 5 Parameter Logistic (5-PL) model equations to calculate IC50 for each dose response curve.

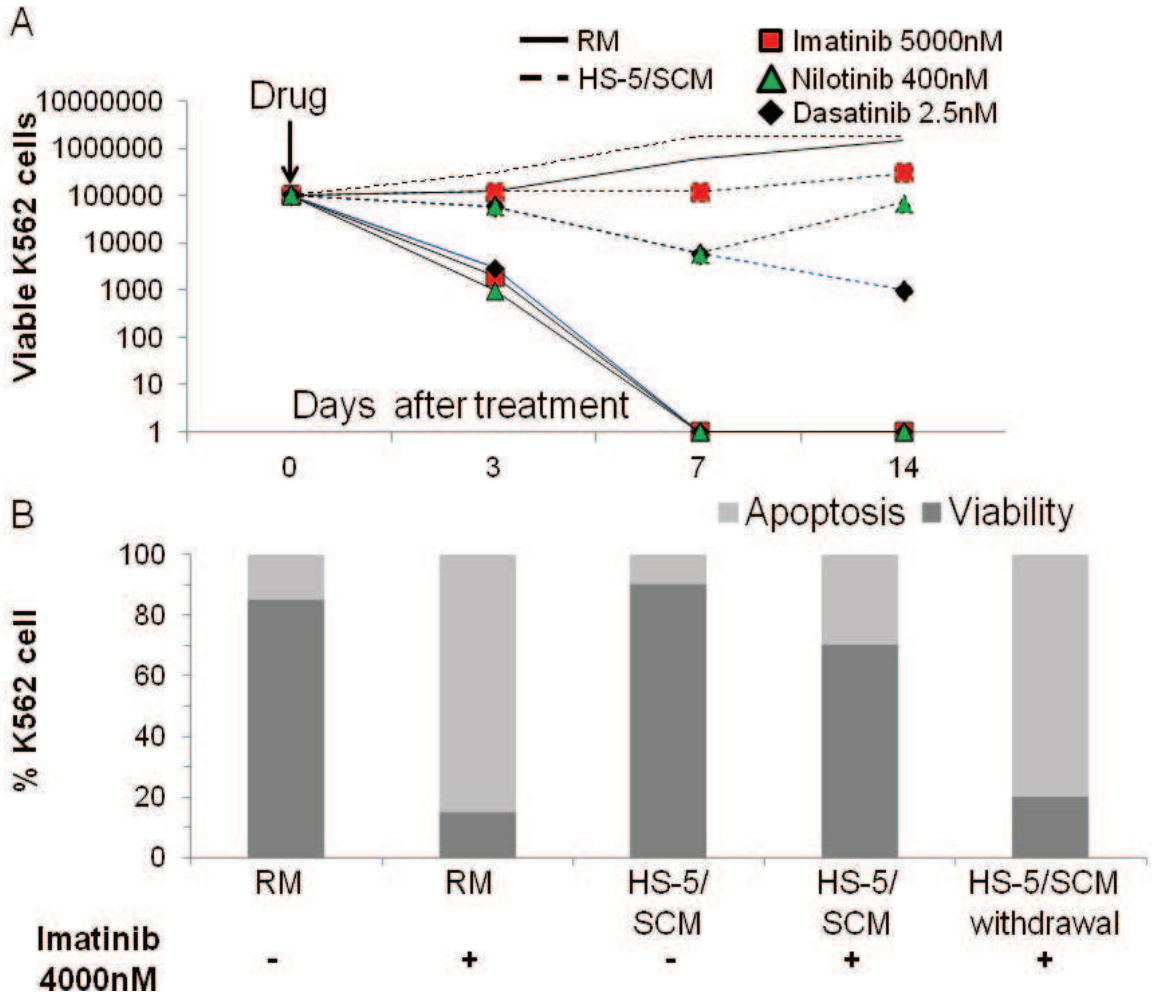

Figure 6A. Residual number of K562 cells after TKIs treatment upon stroma exposition were able to significantly expand after drug withdrawal. Cell proliferation has been monitored by trypan blu exclusion methode at the indicated time point. Long viability experiment: K562 cell line was treated with 5µM Imatinib (red square), 400nM Nilotinib (green triangle) and 2.5nM Dasatinib (black rhombus) at time 0 and day 3, day 7 and day 14 in RM (continuous lines) or HS-5/SCM (dotted lines).

Figure 6B. HS-5 media withdrawal before TKI treatment doesn't not protect from TKI induced apoptosis. K562 cell line was treated with 4000nM Imatinib at time 0 in RM or presence of HS-5/SCM. Cell viability (dark gray barrel) and apoptosis (light gray barrel) were monitored by Annexin-V/PI staining after 72hrs of treatment.

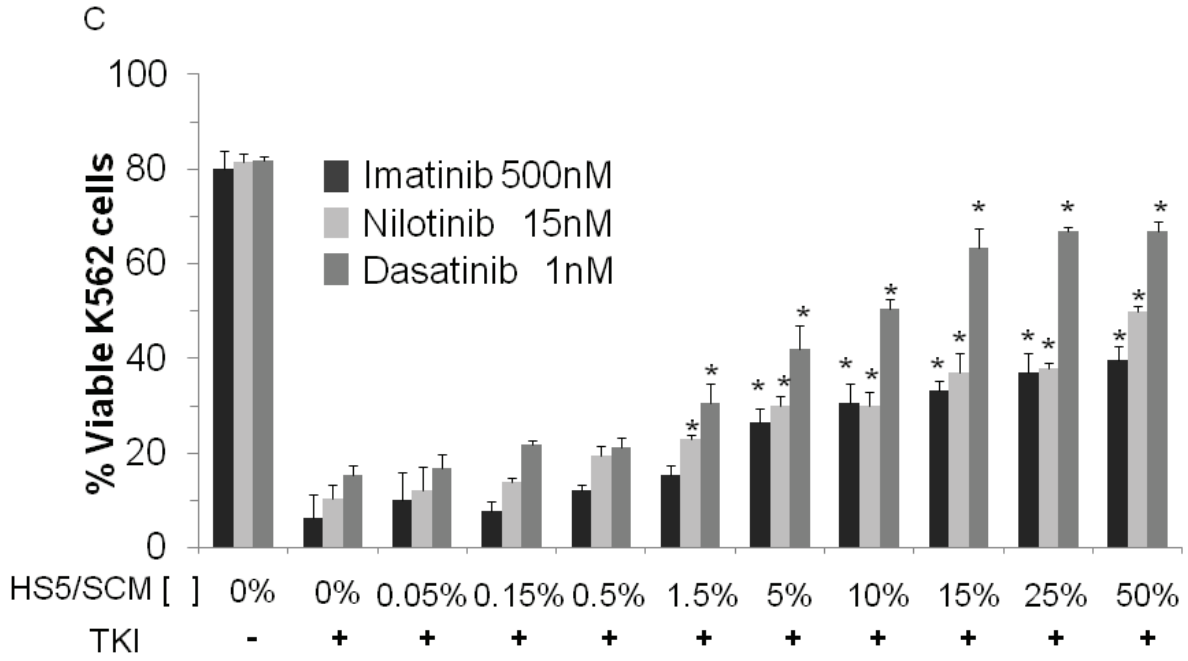

Figure 6C. **SCM protects K562 cell line from apoptosis in a dose dependent manner**. K562 cell line was evaluated for cell viability, by Annexin-V/PI staining after 72hrs of TKI treatment, in cell culture conditions where media was supplemented with increasing percentage of HS5/SCM. (N=3. * indicates p<0.005).

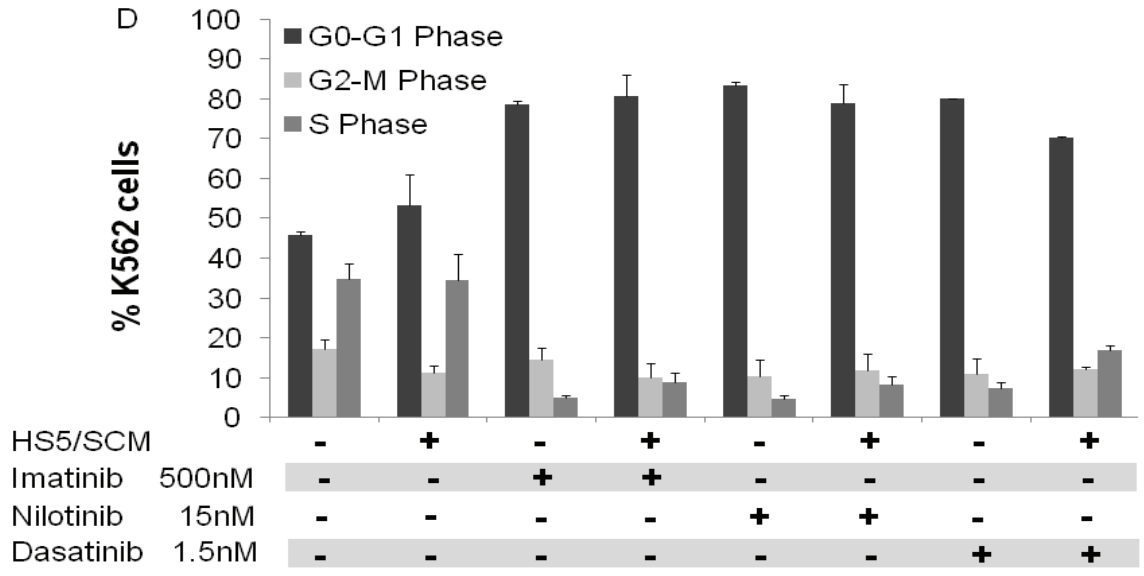

Figure 6D: TKI treatment significantly induce G0-G1 cell cycle arrest in Ph+ cell line independently by HS5/SCM. The K562 cell cycle state was evaluated after 24hrs of TKI treatment by BrdU assay. The graphic show the percentage of K562 cell line in the G_0-G_1 phase (black barrel); the percentage of K562 cell line in the G_2-M (gray-white barrel) and the percentage of K562 cell line in the S-phase (gray-iron barrel).

Stroma Conditioned Media Phosphorylates STAT3 without Cell Cycle Modification in K562 Cell Line

It was already reported that TKIs fail to eliminate primitive quiescent leukemia stem cells (LSC) in patients with CML, despite effective inhibition of BCR-ABL kinase activity.[86],[87] Thus, to assess the effects of BM stroma microenvironment on the cell cycle regulation of Ph+ cells during TKI exposition, we carried out cell cycle analysis on K562 cell line treated with TKIs at the IC50 concentration (RM) for 24hrs. As shown in Fig.6D on a set of four independent experiments, either G0-G1 or S phase of cell cycle in K562 cell line was not significantly modified by HS-5/SCM exposition. Moreover, TKI treatment significantly induce G0-G1 cell cycle arrest in Ph+ cell line and decrease the fraction of cells in S phase, as previously reported.[88] Because most available chemotherapeutic agents show some degree of S-phase specificity, cells that are not actively dividing may prove resistant to such drugs. The quiescent leukemic cells are likely to survive to standard chemotherapy regimens, and it may explain the clinical observation that, unlike CML cannot be eradicated by TKI chemotherapy alone. TKI treatment effect was not modified in the K562 cell line by the presence of HS-5/SCM, despite the effective inhibition of BCR-ABL kinase activity. Indeed, Imatinib (500nM), Nilotinib (15nM) or Dasatinib (1.5nM) treatment was able to reduce the phosphorylation level of the considered BCR/ABL targets as CkrL, STAT5 and ERK in Ph+ cells when cultured in either RM or in the presence of HS-5/SCM (Fig.7A-C respectively). In contrast, STAT3-Y705 was detected at the activated level in K562 cell line only when the cell line was exposed to HS-5/SCM, independently of TKI treatments (Fig. 7D), as previously reported.[47, 76] Constitutively active STAT3 induces the expression of anti-apoptotic genes including Bcl-2, Bcl-xl, Mcl-1, and also up-regulates the expression of inhibitors of apoptotic machinery like survivin and c-IAP2.[89], [90], [91]

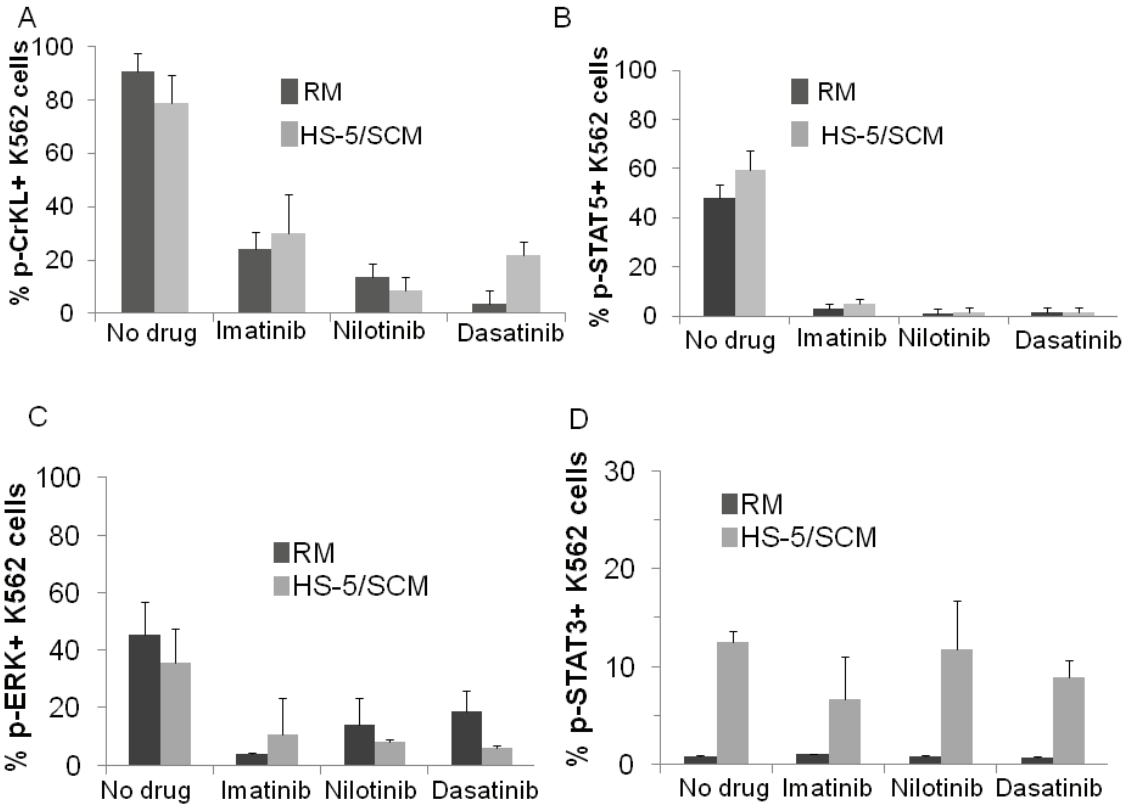

Figure 7. **HS-5/CM phosphorylates STAT3 and confers BCR/ABL indipendent resistance against TKI treatment**. K562 cells were treated with Imatinib (500nM), Nilotinib (15nM) or Dasatinib (1.2 nM) for 2.5 hours, and the extracts from these cells were subjected to immunoblot analysis for phosphorylated (p) or total forms of proteins (not showed) associated with the BCR/ABL signaling pathway. The immunoblot analyses were showed for p-CrKL (**A**), pSTAT5 (Tyr694) (**B**), p-ERK (**C**) and pSTAT3 (Tyr705) (**D**).

Since, STAT3 has been demonstrated to be activated by a variety of cytokine receptors including G-CSF and members of the IL-3/IL-5/GM-CSF family,[92] we also quantified by Bioplex ELISA assay the amount of several cytokines known to be related to survival signaling, in HS-5/SCM and CML/SCM derived from 8 BM mesenchymal stromal cell lines generated from BM samples of 8 patients affected by CP-CML. As shown in Figure 8, the majority of the cytokines are present at a significant higher level in HS-5/SCM than in CML/SCM (IL-1a, M-CSF, SCF, PDGF-bb, IL-1b, IL-6, IL-7, IL-8, IL-10, IL-12, IL-15, G-CSF, GM.CSF, MIP-1a, TNF-a and VEGF), whereas SDF-1a, TRAIL and HGF cytokines are present in HS-5/SCM and CML/SCM supernatants at similar levels. As already observed IL-3 was not found in any supernatant but not in one single tested CML/SCM at the concentration of 9pg/ml. Interesting we observed that both cell lines HS-5/SCM and CML/SCM produce high level of cytokine IL-6 which serves as a positive feedback loop to sustain CML development and acts at the level of leukemic MPPs (CML multipotent progenitors cells) to promote myeloid development at the expense of lymphoid differentiation. IL-6 is a major player in CML pathogenesis. Indeed BCR/ABL regulates IL-6 mRNA levels through a complex and indirect mechanism involving, at least, BCL6 and the LIN28/28b-Let-7 pathway, which are two known transcriptional regulators of the IL-6 gene.[93] This paracrine mechanism appears exacerbated in CML myeloid blast crisis, most likely due to increased IL-6 production by blast cells. Pharmacological inhibition of BCR/ABL activity with TKIs in K562 cell line or in CML cells downregulate STAT5 activation and both LIN28 and LIN28b expression, that increase BCL-6 expression, a direct transcriptional repressor of the *IL-6* gene (Yu et al., 2005).[94] Then exogenous IL-6 may activates the JAK-STAT pathway in CML CD34+ cells treated with TKIs. In our experiment we show that stroma cell lines producing high level of IL-6 may protect leukemic cell fate by TKI effect.

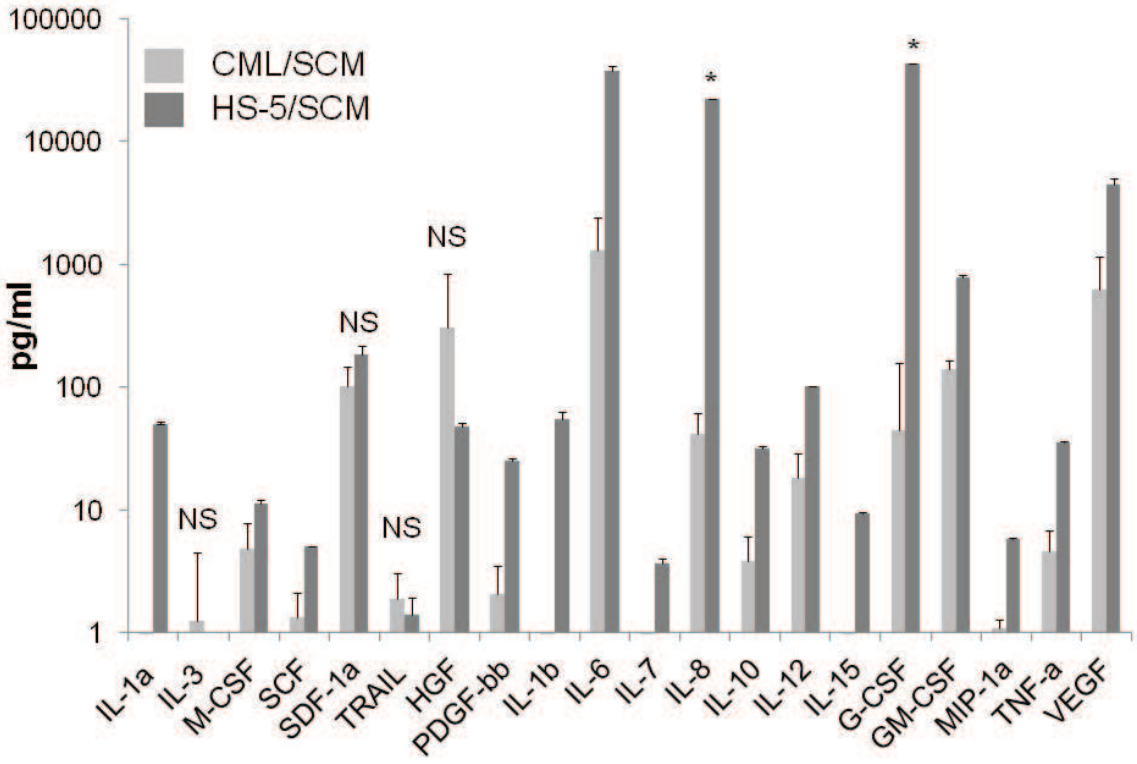

Figure 8. Bioplex ELISA assay. Comparation of secretory profiles between the HS5/SCM and CML/SCM. The human bone marrow stromal cell line HS-5 or the mesenchymal stromal cell derived from 8 BM CML patients were seeded in 75-cm^2 flasks and grown to 70%–80% confluency. Thereafter, culture media were exchanged for in α-MEM supplemented with 20% FBS, 1% L-Glutamine, and 1% penicillin/streptomycin. After 24 hours, the conditioned medium was carefully harvested, centrifuged for 10 minutes at 5,000*g to remove debris, 0.22 µm filtered and stored at* -80°C before the Bioplex ELISA analysis.

CD34+ CML Progenitor Cells are Protected from TKI Toxicity by Stroma Conditioned Media and Cytokines

To determine whether CML CD34+ cells would be susceptible to bone marrow stroma protection from TKI induced apoptosis, we treated CD34+ cells derived from 10 untreated patients affected by chronic phase of CML with clinical relevant concentration of TKIs, and drug-related cell death and apoptosis have been monitored after 72 and 24hrs, respectively. As shown in Fig. 9A-B, and as already demonstrated by several other independent groups, immature CML CD34+ cells, grown in the absence of grow factors, are inherently resistant to TKI treatment since 20±11%, 19±11% and 19±9% of CD34+ cells are still viable after treatment with Imatinib, Nilotinib or Dasatinib, respectively. Moreover, drug-related cell death and apoptosis are significantly reduced when CML CD34+ cells are treated with Imatinib, Nilotinib or Dasatinib in the presence of either high growth factor cocktail or HS5/SCM (Figure 10A-B). To confirm that the viable residual cells were not irreversible un-functional after TKI treatment, primary progenitor CML CD34+ cells residual after TKI treatment in the presence or absence of stroma derived grow factors, were washed and plated in a CFC assays (Figure 9C). Imatinib, Nilotinib and Dasatinib treatments significantly reduce CFU growth of progenitor CD34+ from CML patients. Nevertheless, a significant increase in CFU grow was observed when progenitor CD34+ from CML patients were treated with TKIs in the presence of high growth factor cocktail or HS5/SCM. These data indicate that not only stroma SCM protects from apoptosis or cell death but also results in a higher percentage of cells capable of dividing and repopulating. Moreover, after 14 days of colony grow, hematopoietic colonies were single plucked from methylcellulose and analyzed by Q-RTPCR for the presence of BCR-ABL mRNA, revealing that a large proportion of CD34+ cells remain BCR-ABL positive, after TKI treatment, independently from the in vitro applied culture conditions (Figure 9D).

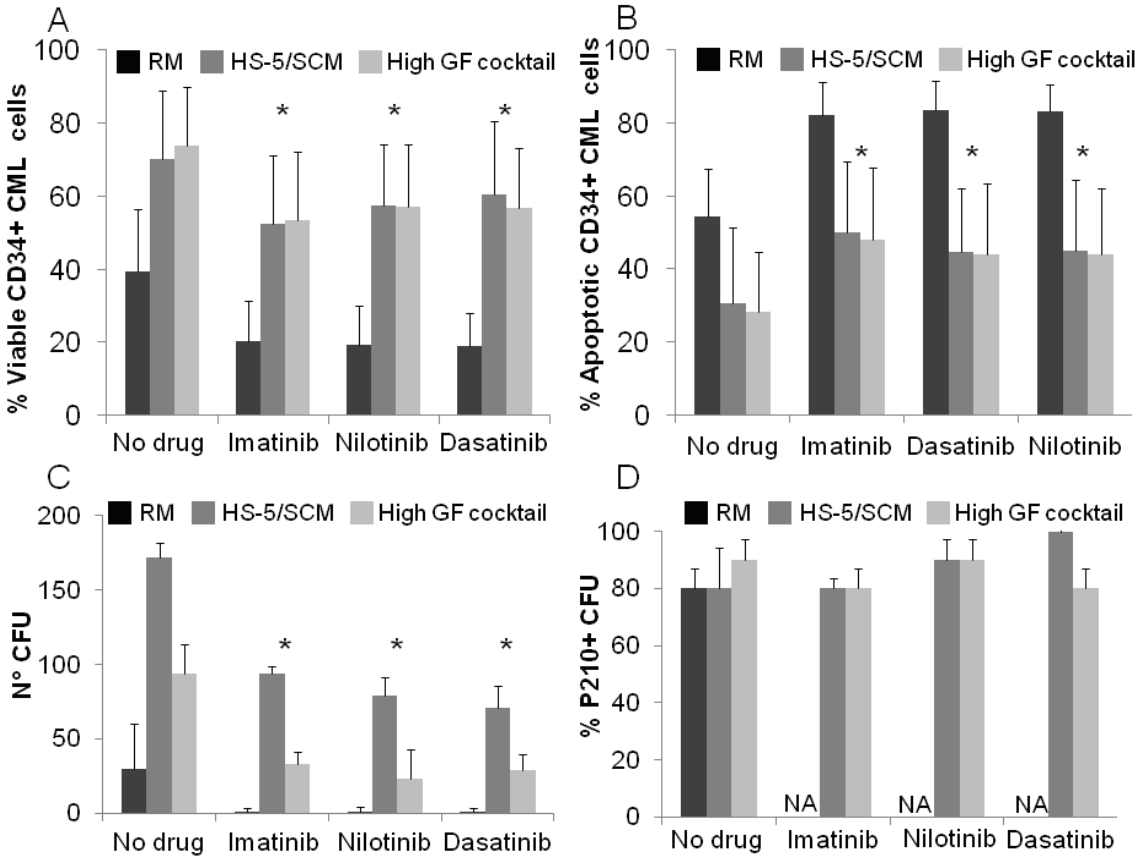

Figure 9. CD34+ CML progenitor cells are protected from TKI toxicity by stroma conditioned media. CD34+ CML progenitor cells (**A**) cells were treated respectively in regular media (RM) (black barrel), or with 50% HS-5/SCM (gray-iron barrel), or high grow factor (GF) cocktail (gray-white barrel) with clinical relevant concentrations of Imatinib (500nM), Nilotinib (15nM) or Dasatinib (1.2 nM) for 72 hours. The Figure 9A show that the residual percentage of viable cells after TKI treatment, assessed by flow cytometry, was significantly higher in CD34+ cell treated in presence of HS5/SCM or high GF cocktail. (**B**) The induction of overall apoptosis (early + late) was significantly reduced in presence of HS5/SCM or high GF cocktail. The Figure **C** show that granulocyte-macrophage colony-forming units and erythrocyte colony-forming units (CFU) originate from CD34+CML progenitor cells was significantly reduced but persistent, after TKI exposition in HS-5/SCM or high GF cocktail. The Figure **D** show that a percentage of CFU BCR-ABL positive, after TKI treatment, is independently from the in vitro applied culture conditions. Results are expressed as mean ± SD from 10 independent experiments. The symbol [*] is for p value ≤0.05.

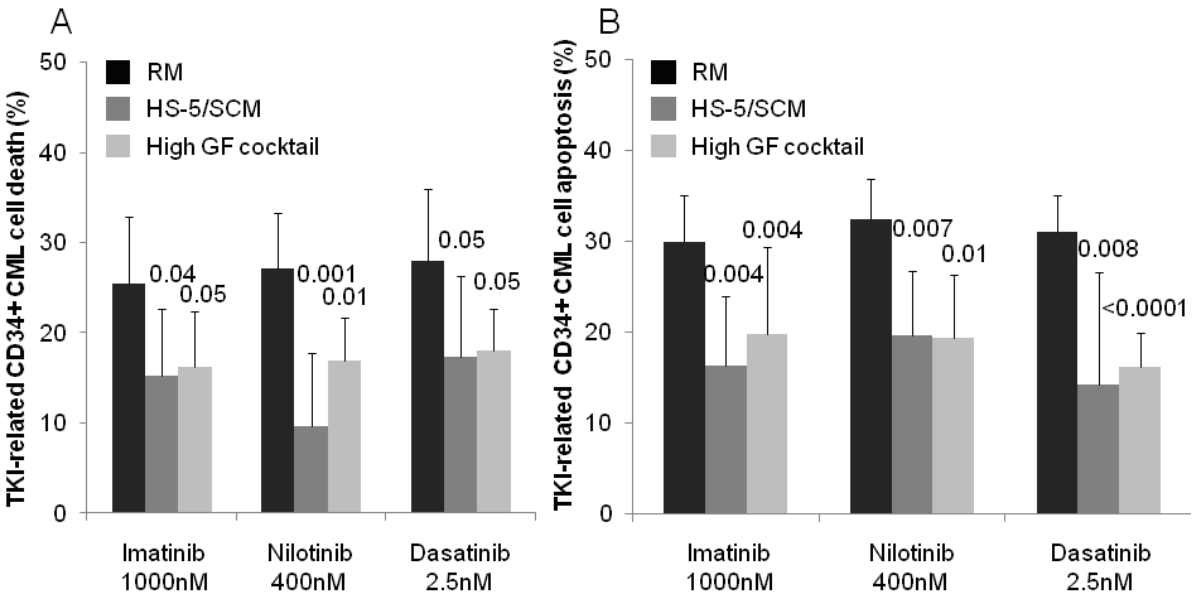

Fig10: SCM or stroma derived cytokines protects CML CD34+ from TKI-specific cell death and apoptosis.

TKI-specific cell death (**A**) and apoptosis (**B**) were calculated by subtracting the percentage of Annexin-V+/PI+ CML CD34+ cells from un-treated samples to the percentage of Annexin-V+/PI+ CML CD34+ cells relative to the specified samples treated with TKIs in the presence of RM (black barrel), in media supplemented with 50% of HS-5/SCM (dark gray barrel) or in media supplemented with high grow factor (GF) cocktail (light-gray barrel).

Synergistic Effect of JAK2 Inhibitors and TKI to overcome Stroma Related Drug Resistance

It has been recently proved by a carefully conducted study that BM stroma conditioned media activates Jak2-Tyk2-Stat3 pathway in CML cells and that knocking down JAK signaling by the JAK inhibitor Ruxolitinib (INCB018424), CML cells are sensitized to a subsequent Nilotinib treatment.[47] We next sought to determine a potential synergistic effect between TKIs and JAK inhibitor Ruxolitinib, by applying a dose matrix cell-based assay. In particular, drugs were serially diluted and all possible pairs of diluted drug combinations were tested on three independent experiments. In particular, K562 cell line was exposed to increasing dose of Imatinib or Nilotinib in combination with Ruxolitinib. Cell survival was assessed by AnnexinV/PI staining at 72 hours after treatment. Treatment with Ruxolitinib alone was not effective on K562 cells, demonstrating a modest effect on overall viability relative to untreated controls (Fig. 11 and Fig. 12). However, the combination of Imatinib or Nilotinib and Ruxolitinib demonstrated greater toxicity in K562 cells than treatment with either TKI alone or Ruxolitinib alone. Next, we tested the effects of drug synergy in the presence of HS-5/SCM, with similar results. In particular, combination indices (CIs) to determine synergy for the drug combinations (ie, CI<1) were calculated according to Chou-Talalay method, which indicated that the combinations were synergistic either in the absence or in the presence of HS-5/SCM (Fig. 11 and Fig. 12).

Nevertheless, a very strong synergism has been achieved in K562 cell line treated with Nilotinib in combination with Ruxolitinib in the presence of HS-5/SCM. Moreover, we looked after to evaluate the relevance of these findings, also in the modulation of the survival of progenitor CD34+ cells from patients with CML. Thus, we co-treated BM CD34+ cells with TKIs and Ruxolitinib for 72hrs in the presence or absence of stroma conditioned media (HS5/SCM). As shown in Fig. 13A, Ruxolitinib significantly synergize with either Imatinib or Nilotinib to reduce cell viability in CD34+ cells derived from CML patients, treated in the presence of either HS-5/SCM or high growth factor cocktail. In particular, although Ruxolitinib exert a significant cellular effect as single agent in CD34+ cells from both CML patients (Figure 13A), or healthy donors treated in the presence of stroma conditioned media or high growth factor cocktail (Figure 13C), the observed increase in cell death is significantly lower than the one observed by applying the proposed drug combination. Moreover, the synergistic effect of TKI and Ruxolitinib on the modulation of cell viability seems to be selective for CD34+ cells derived from patients with CML, since we observed a modest cell death when we treated CD34+ cells from healthy donors (CD34+HD cells), irrespective of the concomitant TKI treatment (Figure 13C). Indeed, Imatinib, Nilotinib and Ruxolitinib each demonstrated a moderate ability to impair the formation of CML colonies (CFU) in the presence of HS5/SCM (83%, 50% and 61% colonies, respectively, relative to untreated controls). However, Imatinib or Nilotinib in combination with Ruxolitinib demonstrated a substantial improvement over either Imatinib alone ($p<0.0001$) or Nilotinib alone ($p<0.0001$), significantly reducing the formation of CML colonies to 6% and 2%, respectively, relative to untreated controls (Figure 13B). Importantly, Imatinib, Nilotinib, and Ruxolitinib, alone or in combination did not significantly impair formation of normal erythroid and myeloid colonies (Figure 13D).

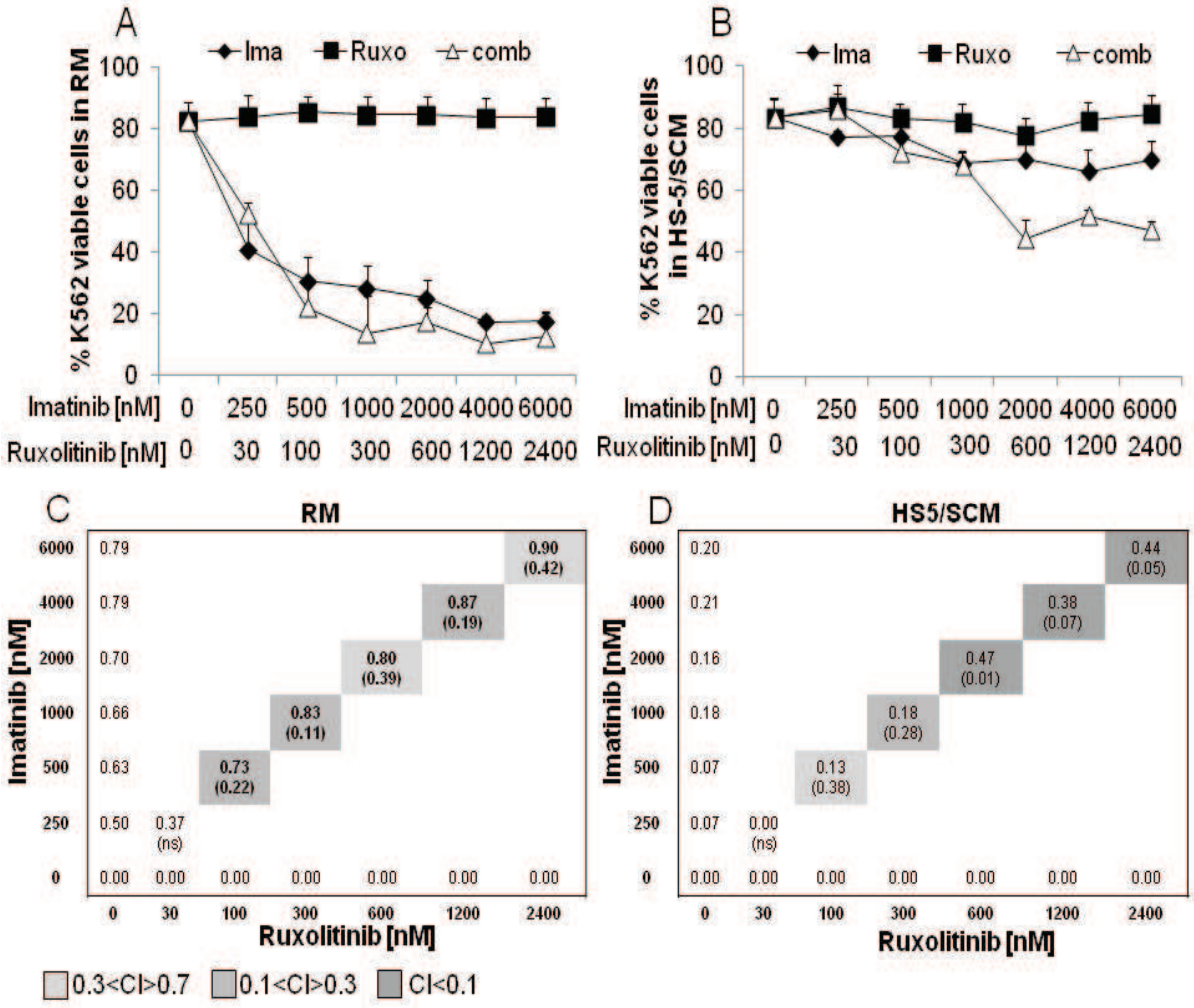

Figure 11: Very strong synergism of Imatinib and JAK2 inhibitor Ruxolitinib on overcoming stroma derived TKI resistance. K562 cell line was exposed to increasing dose of Imatinib (Ima) in combination with increasing doses of Ruxolitinib (Ruxo). Cell viability was assessed by AnnexinV/PI staining at 72 hours after treatment in RM (**A**) or in media supplemented with 50% of HS-5/SCM (**B**). Dose matrix summarizes the cell based cytotoxic effect (Z) relative to the drug combination (comb) of Imatinib and Ruxolitinib in K562 cells treated in RM (**C**) or in media supplemented with 50% of HS-5/SCM (**D**). Cell based cytotoxic effect (Z) for each combination dose is reported into the tables C and D; and CI value for each combination dose are reported in parenthesis. In particular, based on the CI value, we defined, as previously reported, a very strong synergism (dark gray), strong synergism (gray), synergism (light gray), from moderate synergism to no synergism (white).

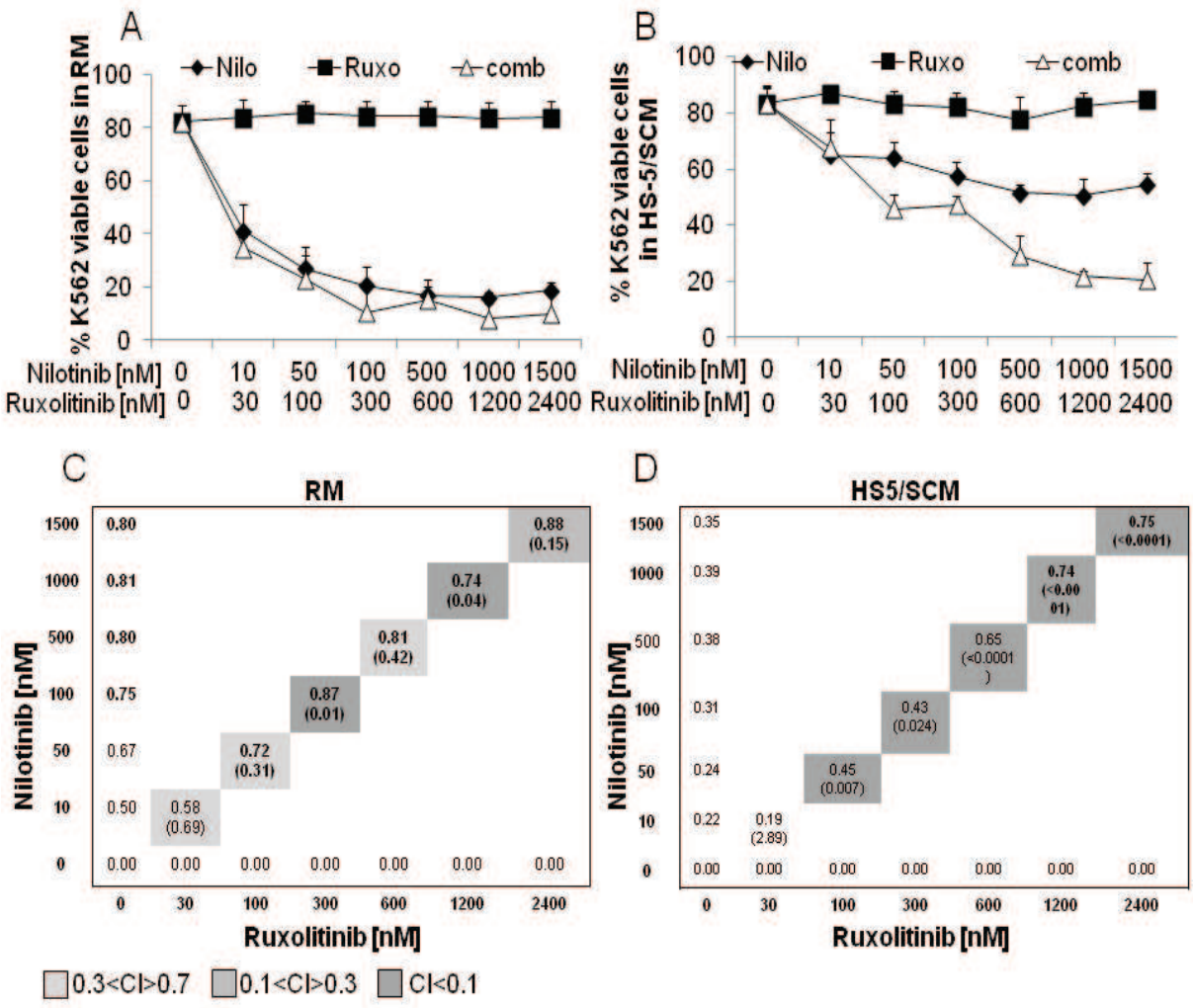

Figure 12: Very strong synergism of Nilotinib and JAK2 inhibitor Ruxolitinib on overcoming stroma derived TKI resistance. K562 cell line was exposed to increasing dose of Nilotinib (Nilo) in combination (comb) with increasing doses of Ruxolitinib (Ruxo). Cell viability was assessed by AnnexinV/PI staining at 72 hours after treatment in RM (**A**) or in media supplemented with 50% of HS-5/SCM (**B**). Dose matrix summarizes the cell based cytotoxic effect (Z) relative to the drug combination of Nilotinib and Ruxolitinib in K562 cells treated in RM (**C**) or in media supplemented with 50% of HS-5/SCM (**D**). Cell based cytotoxic effect (Z) for each combination dose is reported into the tables. CI value for each combination dose are reported in parenthesis. In particular, based on the CI value, we defined, as previously reported, a very strong synergism (dark gray), strong synergism (gray), synergism (light gray), from moderate synergism to no synergism (white).

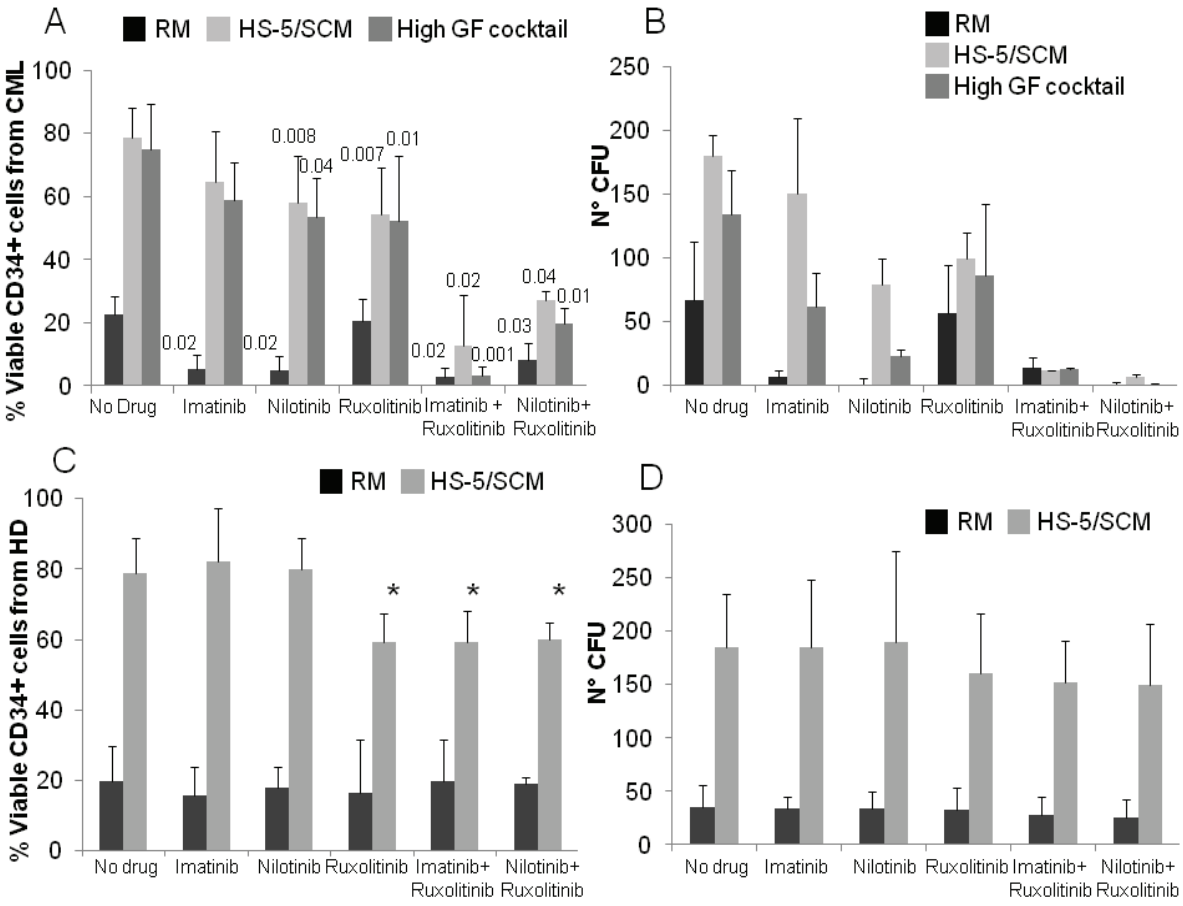

Figure13. Ruxolitinib synergize with TKI in the elimination of CFU from patients with CML.

CD34+cells derived from either BM of five patients with CML-CP or PB of two immobilized HDs, were treated respectively in regular media (RM) (black barrel), or with 50% HS-5/SCM (gray-white barrel), or high grow factor (GF) cocktail (gray-iron barrel) with clinical relevant concentrations of Imatinib (500nM), Nilotinib (15nM), Ruxolitinib (300nM) or drug combination for 72 hours. The Figure **A** show that the residual percentage of viable CD34+ CML progenitor cells after TKI treatment or/and Ruxolitinib, assessed by flow cytometry, was higher in CD34+ CML progenitor cell treated in presence of HS5/SCM or high GF cocktail than RM, but significantly lower in cells treated with the drug combination (TKI+ JAK2 inhibitor). Interesting the CFU originate from CD34+CML progenitor cells (**B**) were significantly reduced, but still persistents, after Nilotinib or Ruxolitinib exposition in HS-5/SCM or high GF cocktail. (**B**) Data from a clonogenic assay clearly evidenced a significant down-regulation of CFU grow when CD34+ CML progenitor cells were treated with the drug combination (TKI+JAK2 inhibitor).

The Figure **C** show that the residual percentage of viable CD34+HD cells exposed to HS-5/SCM and treated with Ruxolitinib or drug combination was slightly but significantly reduced. (The symbol [*] is for p value ≤0.05). (**D**) Data from a clonogenic assay clearly evidenced that CFU originate from CD34+HD cells still grow when treated with clinical concentrations of TKI or/and Ruxolitinib in RM and in HS5/SCM.

Discussion

Philadelphia positive (Ph+) chronic myeloid leukemia (CML) is a chronic disease with a tendency of progression into an accelerated and a blastic phase. When the disease becomes advanced, it is almost incurable.[95] Over the past decade, tyrosine kinase inhibitors (TKIs) have become the standard treatment for CML. First of all the 2-phenylaminopyrimidine Imatinib has transformed CML in a life-threatening disease into a chronic condition. Newly diagnosed patients with chronic phase CML have an almost 90% chance of being alive at 60 months after diagnosis.[25] In addition the 8-year update of the IRIS trial confirmed the long-term efficacy and safety of Imatinib, with an overall survival (OS) of 85%;[29] and with second generation TKIs, Dasatinib and Nilotinib, almost 50% of the Imatinib-resistant patients gained a remission with an OS over 90% at 2 years.[95] However, most patients continue to test positive by RT-PCR, and disease recurrence upon discontinuation of drug is the rule even in the minority of patients that become PCR undetectable.[30], [96], [97] This indicates that CML stem cells survive in the presence of TKIs and suggests lifelong continuation of therapy, at considerable expense and sometimes despite significant side effects. Elucidating the mechanism by which persistent CML stem cells escape the effects of TKIs will be crucial for directing strategies to eradicate residual leukemia. The central question is what role has the BM microenvironment in the persistence of CML stem cells survival in patients treated with TKIs; and whether disease persistence is BCR-ABL dependent, like many cases of resistance, or BCR-ABL independent.

In this thesis, I evaluate the effect on clinical IC50 of three TKI alone or in combination with JAK inhibitor Ruxolitinib on leukemia cell line Ph+ and in CD34+CML stem cells in RM or in HS-5/SCM, to establish the role of the BM microenvironment in the persistence of CD34+ leukemia progenitor cells.

I found that the resistance of CD34+CML stem cells to BCR-ABL tyrosin kinase inhibitors may be related to soluble factors produced by mesenchymal stroma cells derived from patients at diagnosis of CML-CP. Indeed, I proved that stroma-derived microenvironment drug protection is achievable not only by leukemia cell exposition to a direct stroma cell contact during TKI treatment, but also by setting up cell culture condition implying soluble factors produced by either HS-5 immortalized cell line or CML patient-derived BM stroma cells. Thus, co-culturing Ph+ cell lines with the CML/SCM, CML cells survive to the action of drugs by observing a significant increase of viability and reduction of apoptosis, compared to controls, despite the quiescent state that has been observed when Ph+ cells are treated with TKI either in the presence or absence of SCM. Indeed, I demonstrated that the higher cell viability, noticed in K562 cells treated with TKI in the presence of stroma conditioned media respect to control cell culture condition (RM), is not related to cytokine cell cycle regulation but to a significant reduction in apoptosis induction. In fact, BrdU analysis show a relevant accumulation in G0-G1 cell cycle phase of K562 cells treated with TKI either in the presence or absence of SCM, with no significant differences between the two culture conditions. To understand whether TKI treatment is able to completely eliminate leukemic cells, I conducted a long-term experiment, in which K562 cell viability and proliferation were monitored overtime for 14 consecutive days after TKI treatment in presence or absence of conditioned media derived from the stroma cell line HS-5. I observed that K562 cells treated with TKI in the absence of HS-5/CM cease to proliferate and are not more able to encounter cell divisions. In contrast, if K562 cells are treated with TKI in the presence of HS-5/CM, after a steady-state of three days from the TKI culture addition, cells start to proliferate at the same level of the untreated cells. This evidence, strongly suggests that TKIs are not

able to completely eradicate leukemic cells when stroma derived factors are present in the microenvironment. The study may have a interesting clinical relevance, since I also demonstrated in vitro that IC50s of the three studied TKI (Imatinib, Nilotinib and Dasatinib) are strongly modulated by HS-5/CM. Indeed, I show that I can reduce the Ph+ cell viability below the 50% only implying high TKI concentration that are not reasonable achieved in vivo in patients. These evidences also confirm what it is coming out from several clinical trials applying TKI: target molecular therapy, including Imatinib, induces remission in patients with CML but does not eliminate leukemia stem cells, which remain a potential source of relapse.
Thus, I investigated the activity of JAK inhibitor Ruxolitinib, to be synergic with TKI in the elimination of CML stem cells. The inhibitor Ruxolitinib is a potent and selective JAK1- and JAK2-inhibitor (IC50 of 3.3±1.2 and 2.8±1.2 nmol/L, respectively, in "naked" kinase assays in cell-free in vitro systems). It demonstrates modest selectivity against Tyk2 (IC50 of 19±3.2 nmol/L) and 130-fold less selectivity against JAK3 (IC50 of 428±243 nmol/L).[98] Treatment with Ruxolitinib is associated with a dramatic decrease in circulating levels of proinflammatory cytokines, IL-6, and tumor necrosis factor (TNF)-α, which have been implicated in the pathogenesis of MPNs.[99] I showed that co-treatment with a combination of the JAK inhibitor Ruxolitinib and the TKI Imatinib/Nilotinib synergistically induced apoptosis of different cultured leukemia cell lines and human CML cells. The combination is also more active than either drug alone against all leukemia cell lines and human CML cells.
In particular, in K562 cell line, Imatinib (500nM), Nilotinib (15nM) or Dasatinib (1.2 nM) treatment was able to reduce the phosphorylation level of the considered BCR/ABL targets as CkrL, ERK and STAT5 in Ph+ cells when cultured in either RM or in the presence of HS-5/SCM. In contrast, STAT3-Y705 was detected at the activated level in K562 cell line only when the cell line was exposed to HS-5/SCM, independently of TKI treatments. Moreover, this STAT3 activity was sustained by HS-5/SCM even in the presence of TKIs, confirming the hypothesis that disease persistence in the context of the BM microenvironment is BCR/ABL independent.
I observed that immature CML CD34+ cells, grown in the absence of grow factors, are inherently resistant to TKI. Moreover, drug-related cell death and apoptosis are significantly reduced when CML CD34+ cells are treated with Imatinib, Nilotinib or Dasatinib in the presence of either high growth factor cocktail or HS5/SCM.
Finally, I attempted to evaluate if the synergic combination of TKI and JAK2 inhibitors is able to significantly reduce leukemia clonogenic activity in an in vitro assay. Thus, I selected CD34+ progenitor cells from BM samples of patients with CML. After 72hrs of treatment with TKI and JAK2 inhibitors, residual cells were plated in methylcellulose media supplemented with cytokine allowing grow of CFU-E, BFU-E, CFU-G, CFU-M, CFU-GM and CFU-GEMM. CFUs were encountered after 14 days and I observed that Imatinib or Nilotinib treatment are able to significantly reduce colony grow only in the absence of conditioned media from HS-5 or stroma derive cytokines with anti-apoptotic and pro-proliferating activity. Moreover, the co-treatment of Ph+ CD34+ cells with Imatinib/Nilotinib and Ruxolitinib strongly decrease CFU counting in a stroma-independent manner. This data strongly suggest that stroma related drug resistance has a relevant role in the regulation of TKI responsiveness in patient with CML and that the drug concentration needed to eliminate in vitro Ph+ cells in the presence of stroma microenvironment is not achievable in vivo clinical trial. Thus, I propose a novel drug combination able to be effective in the leukemia eradication: the combined down regulation of the BCR/ABL oncogene plus the down-regulation of the signalling induced by soluble factors present in the stroma BM

microenvironment through JAK/STAT pathway may be likely relevant in vivo for the treatment of patients and the reduction of relapses.
Furthermore, combination strategies targeting LSC may have the potential to dramatically improve response for patients that are resistant to current therapies.

References

1. Jemal, A., et al., *Cancer statistics, 2010.* CA Cancer J Clin. **60**(5): p. 277-300.
2. Bansal D, *Imatinib has adverse effect on growth in children with chronic myeloid leukemia.* Pediatr Blood Cancer, 2012. **59**(3): p. 481–484.
3. Jabbour, E., *Chronic myeloid leukemia: 2012 Update on diagnosis, monitoring, and management.* American Journal of Hematology, 2012. **87**(11): p. 1037-1045.
4. Sawyers, C.L., *Chronic myeloid leukemia.* New England Journal of Medicine, 1999. **340**(17): p. 1330-1340.
5. Heisterkamp, N., et al., *Structural organization of the bcr gene and its role in the Ph' translocation.* Nature, 1985. **315**(6022): p. 758-61.
6. JD, R., *A new consistent chromosomal abnormality in chronic myelogenous leukaemia identified by quinacrine fluorescence and Giemsa staining.* Nature, 1973. **243**(5405): p. 290-293.
7. Pane, F., et al., *BCR/ABL genes and leukemic phenotype: from molecular mechanisms to clinical correlations.* Oncogene, 2002. **21**(56): p. 8652-67.
8. Bennett, J.M., et al., *The chronic myeloid leukaemias: guidelines for distinguishing chronic granulocytic, atypical chronic myeloid, and chronic myelomonocytic leukaemia. Proposals by the French-American-British Cooperative Leukaemia Group.* Br J Haematol, 1994. **87**(4): p. 746-54.
9. Sattler, M. and J.D. Griffin, *Molecular mechanisms of transformation by the BCR-ABL oncogene.* Semin Hematol, 2003. **40**(2 Suppl 2): p. 4-10.
10. Penserga, E.T. and T. Skorski, *Fusion tyrosine kinases: a result and cause of genomic instability.* Oncogene, 2007. **26**(1): p. 11-20.
11. Kurzrock, R., J.U. Gutterman, and M. Talpaz, *The molecular genetics of Philadelphia chromosome-positive leukemias.* N Engl J Med, 1988. **319**(15): p. 990-8.
12. Melo, J.V., et al., *The ABL-BCR fusion gene is expressed in chronic myeloid leukemia.* Blood, 1993. **81**(1): p. 158-65.
13. Stam, K., et al., *Evidence of a new chimeric bcr/c-abl mRNA in patients with chronic myelocytic leukemia and the Philadelphia chromosome.* N Engl J Med, 1985. **313**(23): p. 1429-33.
14. Faderl, S., et al., *The biology of chronic myeloid leukemia.* N Engl J Med, 1999. **341**(3): p. 164-72.
15. Arico, M., et al., *Outcome of treatment in children with Philadelphia chromosome-positive acute lymphoblastic leukemia.* N Engl J Med, 2000. **342**(14): p. 998-1006.
16. Gleissner, B., et al., *Leading prognostic relevance of the BCR-ABL translocation in adult acute B-lineage lymphoblastic leukemia: a prospective study of the German Multicenter Trial Group and confirmed polymerase chain reaction analysis.* Blood, 2002. **99**(5): p. 1536-43.
17. Kawasaki, E.S., et al., *Diagnosis of chronic myeloid and acute lymphocytic leukemias by detection of leukemia-specific mRNA sequences amplified in vitro.* Proc Natl Acad Sci U S A, 1988. **85**(15): p. 5698-702.
18. Melo, J.V., et al., *P190BCR-ABL chronic myeloid leukaemia: the missing link with chronic myelomonocytic leukaemia?* Leukemia, 1994. **8**(1): p. 208-11.

19. Chissoe, S.L., et al., *Sequence and analysis of the human ABL gene, the BCR gene, and regions involved in the Philadelphia chromosomal translocation.* Genomics, 1995. **27**(1): p. 67-82.
20. Pane, F., et al., *Neutrophilic-chronic myeloid leukemia: a distinct disease with a specific molecular marker (BCR/ABL with C3/A2 junction).* Blood, 1996. **88**(7): p. 2410-4.
21. Kantarjian, H.M., et al., *Characteristics of accelerated disease in chronic myelogenous leukemia.* Cancer, 1988. **61**(7): p. 1441-6.
22. Vardiman, J.W., N.L. Harris, and R.D. Brunning, *The World Health Organization (WHO) classification of the myeloid neoplasms.* Blood, 2002. **100**(7): p. 2292-302.
23. Karbasian Esfahani, M., et al., *Blastic phase of chronic myelogenous leukemia.* Curr Treat Options Oncol, 2006. **7**(3): p. 189-99.
24. Gabert, J., et al., *Standardization and quality control studies of 'real-time' quantitative reverse transcriptase polymerase chain reaction of fusion gene transcripts for residual disease detection in leukemia - a Europe Against Cancer program.* Leukemia, 2003. **17**(12): p. 2318-57.
25. Druker, B.J., et al., *Five-year follow-up of patients receiving imatinib for chronic myeloid leukemia.* N Engl J Med, 2006. **355**(23): p. 2408-17.
26. Druker, B.J., et al., *Activity of a specific inhibitor of the BCR-ABL tyrosine kinase in the blast crisis of chronic myeloid leukemia and acute lymphoblastic leukemia with the Philadelphia chromosome.* N Engl J Med, 2001. **344**(14): p. 1038-42.
27. Druker, B.J. and N.B. Lydon, *Lessons learned from the development of an abl tyrosine kinase inhibitor for chronic myelogenous leukemia.* J Clin Invest, 2000. **105**(1): p. 3-7.
28. O'Brien, S.G., et al., *Imatinib compared with interferon and low-dose cytarabine for newly diagnosed chronic-phase chronic myeloid leukemia.* N Engl J Med, 2003. **348**(11): p. 994-1004.
29. **Deininger, M.**, ***International Randomized Study of Interferon Vs STI571 (IRIS) 8-Year Follow up: Sustained Survival and Low Risk for Progression or Events in Patients with Newly Diagnosed Chronic Myeloid Leukemia in Chronic Phase (CML-CP) Treated with Imatinib.*** Blood (ASH Annual **M**eeting Abstracts) 2009. **114**.
30. Hughes, T.P., et al., *Frequency of major molecular responses to imatinib or interferon alfa plus cytarabine in newly diagnosed chronic myeloid leukemia.* N Engl J Med, 2003. **349**(15): p. 1423-32.
31. Hughes, T., et al., *Monitoring CML patients responding to treatment with tyrosine kinase inhibitors: review and recommendations for harmonizing current methodology for detecting BCR-ABL transcripts and kinase domain mutations and for expressing results.* Blood, 2006. **108**(1): p. 28-37.
32. Baccarani, M., et al., *Chronic myeloid leukemia: an update of concepts and management recommendations of European LeukemiaNet.* J Clin Oncol, 2009. **27**(35): p. 6041-51.
33. Graham, S.M., et al., *Primitive, quiescent, Philadelphia-positive stem cells from patients with chronic myeloid leukemia are insensitive to STI571 in vitro.* Blood, 2002. **99**(1): p. 319-25.
34. Hu, Y., et al., *Targeting multiple kinase pathways in leukemic progenitors and stem cells is essential for improved treatment of Ph+ leukemia in mice.* Proc Natl Acad Sci U S A, 2006. **103**(45): p. 16870-5.

35. Weisberg, E., et al., *Characterization of AMN107, a selective inhibitor of native and mutant Bcr-Abl.* Cancer Cell, 2005. **7**(2): p. 129-41.
36. Jorgensen, H.G., et al., *Nilotinib exerts equipotent antiproliferative effects to imatinib and does not induce apoptosis in CD34+ CML cells.* Blood, 2007. **109**(9): p. 4016-9.
37. Saglio, G., et al., *Nilotinib versus imatinib for newly diagnosed chronic myeloid leukemia.* N Engl J Med. **362**(24): p. 2251-9.
38. Lombardo, L.J., et al., *Discovery of N-(2-chloro-6-methyl- phenyl)-2-(6-(4-(2-hydroxyethyl)- piperazin-1-yl)-2-methylpyrimidin-4- ylamino)thiazole-5-carboxamide (BMS-354825), a dual Src/Abl kinase inhibitor with potent antitumor activity in preclinical assays.* J Med Chem, 2004. **47**(27): p. 6658-61.
39. O'Hare, T., et al., *In vitro activity of Bcr-Abl inhibitors AMN107 and BMS-354825 against clinically relevant imatinib-resistant Abl kinase domain mutants.* Cancer Res, 2005. **65**(11): p. 4500-5.
40. Tokarski, J.S., et al., *The structure of Dasatinib (BMS-354825) bound to activated ABL kinase domain elucidates its inhibitory activity against imatinib-resistant ABL mutants.* Cancer Res, 2006. **66**(11): p. 5790-7.
41. Copland, M., et al., *Dasatinib (BMS-354825) targets an earlier progenitor population than imatinib in primary CML but does not eliminate the quiescent fraction.* Blood, 2006. **107**(11): p. 4532-9.
42. Kantarjian, H., et al., *Dasatinib versus imatinib in newly diagnosed chronic-phase chronic myeloid leukemia.* N Engl J Med. **362**(24): p. 2260-70.
43. **Shah, N.**, *Dasatinib Versus Imatinib In Patients with Newly Diagnosed Chronic Myeloid Leukemia In Chronic Phase (CML-CP) In the DASISION Trial: 18-Month Follow-up.* Blood (ASH A**nn**ual Meeti**n**g Abstracts), 2010. **116**(206).
44. Kantarjian, H.M., et al., *Second-generation tyrosine kinase inhibitors: the future of frontline CML therapy.* Clin Cancer Res. **17**(7): p. 1674-83.
45. Kolb, H.J., et al., *Graft-versus-leukemia effect of donor lymphocyte transfusions in marrow grafted patients.* Blood, 1995. **86**(5): p. 2041-50.
46. Zhang, B., *Inhibition of chronic myeloid leukemia stem cells by the combination of the hedgehog pathway inhibitor LDE225 with nilotinib. .* Blood (ASH Annual Meeting Abstracts), 2010. **116**(227).
47. Nair, R.R., et al., *Potentiation of Nilotinib-mediated cell death in the context of the bone marrow microenvironment requires a promiscuous JAK inhibitor in CML.* Leuk Res. **36**(6): p. 756-63.
48. Packer, L.M., et al., *Nilotinib and MEK inhibitors induce synthetic lethality through paradoxical activation of RAF in drug-resistant chronic myeloid leukemia.* Cancer Cell. **20**(6): p. 715-27.
49. Crews, L.A. and C.H. Jamieson, *Selective elimination of leukemia stem cells: Hitting a moving target.* Cancer Lett.
50. Lord, B.I., N.G. Testa, and J.H. Hendry, *The relative spatial distributions of CFUs and CFUc in the normal mouse femur.* Blood, 1975. **46**(1): p. 65-72.
51. Purton, L.E. and D.T. Scadden, *Limiting factors in murine hematopoietic stem cell assays.* Cell Stem Cell, 2007. **1**(3): p. 263-70.
52. Perry, J.M. and L. Li, *Disrupting the stem cell niche: good seeds in bad soil.* Cell, 2007. **129**(6): p. 1045-7.
53. Nair, R.R., J. Tolentino, and L.A. Hazlehurst, *The bone marrow microenvironment as a sanctuary for minimal residual disease in CML.* Biochem Pharmacol. **80**(5): p. 602-12.

54. Adams, G.B., et al., *Stem cell engraftment at the endosteal niche is specified by the calcium-sensing receptor.* Nature, 2006. **439**(7076): p. 599-603.
55. Nilsson, S.K., et al., *Osteopontin, a key component of the hematopoietic stem cell niche and regulator of primitive hematopoietic progenitor cells.* Blood, 2005. **106**(4): p. 1232-9.
56. Kinashi, T. and T.A. Springer, *Adhesion molecules in hematopoietic cells.* Blood Cells, 1994. **20**(1): p. 25-44.
57. Arai, F., et al., *Tie2/angiopoietin-1 signaling regulates hematopoietic stem cell quiescence in the bone marrow niche.* Cell, 2004. **118**(2): p. 149-61.
58. Lataillade, J.J., et al., *Stromal cell-derived factor 1 regulates primitive hematopoiesis by suppressing apoptosis and by promoting G(0)/G(1) transition in CD34(+) cells: evidence for an autocrine/paracrine mechanism.* Blood, 2002. **99**(4): p. 1117-29.
59. Kopp, H.G., et al., *The bone marrow vascular niche: home of HSC differentiation and mobilization.* Physiology (Bethesda), 2005. **20**: p. 349-56.
60. Kiel, M.J., et al., *SLAM family receptors distinguish hematopoietic stem and progenitor cells and reveal endothelial niches for stem cells.* Cell, 2005. **121**(7): p. 1109-21.
61. Avecilla, S.T., et al., *Chemokine-mediated interaction of hematopoietic progenitors with the bone marrow vascular niche is required for thrombopoiesis.* Nat Med, 2004. **10**(1): p. 64-71.
62. Mazo, I.B., et al., *Hematopoietic progenitor cell rolling in bone marrow microvessels: parallel contributions by endothelial selectins and vascular cell adhesion molecule 1.* J Exp Med, 1998. **188**(3): p. 465-74.
63. Parmar, K., et al., *Distribution of hematopoietic stem cells in the bone marrow according to regional hypoxia.* Proc Natl Acad Sci U S A, 2007. **104**(13): p. 5431-6.
64. Bonnet, D. and J.E. Dick, *Human acute myeloid leukemia is organized as a hierarchy that originates from a primitive hematopoietic cell.* Nat Med, 1997. **3**(7): p. 730-7.
65. Al-Hajj, M., et al., *Prospective identification of tumorigenic breast cancer cells.* Proc Natl Acad Sci U S A, 2003. **100**(7): p. 3983-8.
66. Singh, S.K., et al., *Identification of human brain tumour initiating cells.* Nature, 2004. **432**(7015): p. 396-401.
67. Dalerba, P., et al., *Phenotypic characterization of human colorectal cancer stem cells.* Proc Natl Acad Sci U S A, 2007. **104**(24): p. 10158-63.
68. Li, C., et al., *Identification of pancreatic cancer stem cells.* Cancer Res, 2007. **67**(3): p. 1030-7.
69. Wang, J.C., et al., *High level engraftment of NOD/SCID mice by primitive normal and leukemic hematopoietic cells from patients with chronic myeloid leukemia in chronic phase.* Blood, 1998. **91**(7): p. 2406-14.
70. Eaves, C., et al., *The biology of normal and neoplastic stem cells in CML.* Leuk Lymphoma, 1993. **11 Suppl 1**: p. 245-53.
71. Hou, L., et al., *Long-term culture of leukemic bone marrow primary cells in biomimetic osteoblast niche.* Int J Hematol, 2009. **90**(3): p. 281-91.
72. Krause, D.S., et al., *Requirement for CD44 in homing and engraftment of BCR-ABL-expressing leukemic stem cells.* Nat Med, 2006. **12**(10): p. 1175-80.
73. Damiano, J.S., L.A. Hazlehurst, and W.S. Dalton, *Cell adhesion-mediated drug resistance (CAM-DR) protects the K562 chronic myelogenous leukemia*

cell line from apoptosis induced by BCR/ABL inhibition, cytotoxic drugs, and gamma-irradiation. Leukemia, 2001. **15**(8): p. 1232-9.
74. Jin, L., et al., *CXCR4 up-regulation by imatinib induces chronic myelogenous leukemia (CML) cell migration to bone marrow stroma and promotes survival of quiescent CML cells.* Mol Cancer Ther, 2008. **7**(1): p. 48-58.
75. Hiwase, D.K., et al., *Blocking cytokine signaling along with intense Bcr-Abl kinase inhibition induces apoptosis in primary CML progenitors.* Leukemia. **24**(4): p. 771-8.
76. Bewry, N.N., et al., *Stat3 contributes to resistance toward BCR-ABL inhibitors in a bone marrow microenvironment model of drug resistance.* Mol Cancer Ther, 2008. **7**(10): p. 3169-75.
77. Dillmann, F., et al., *Plerixafor inhibits chemotaxis toward SDF-1 and CXCR4-mediated stroma contact in a dose-dependent manner resulting in increased susceptibility of BCR-ABL+ cell to Imatinib and Nilotinib.* Leuk Lymphoma, 2009. **50**(10): p. 1676-86.
78. Yanagisawa, K., et al., *Suppression of cell proliferation and the expression of a bcr-abl fusion gene and apoptotic cell death in a new human chronic myelogenous leukemia cell line, KT-1, by interferon-alpha.* Blood, 1998. **91**(2): p. 641-8.
79. Roecklein, B.A. and B. Torok-Storb, *Functionally distinct human marrow stromal cell lines immortalized by transduction with the human papilloma virus E6/E7 genes.* Blood, 1995. **85**(4): p. 997-1005.
80. Savoldo, B., et al., *Reverse transcription polymerase chain reaction is a reliable assay for detecting leukemic colonies generated by chronic myelogenous leukemia cells.* Leukemia, 1998. **12**(3): p. 434-40.
81. Lehar, J., et al., *Synergistic drug combinations tend to improve therapeutically relevant selectivity.* Nat Biotechnol, 2009. **27**(7): p. 659-66.
82. Chou, T.C. and P. Talalay, *Quantitative analysis of dose-effect relationships: the combined effects of multiple drugs or enzyme inhibitors.* Adv Enzyme Regul, 1984. **22**: p. 27-55.
83. Chou, T.C., *Drug combination studies and their synergy quantification using the Chou-Talalay method.* Cancer Res. **70**(2): p. 440-6.
84. Soverini, S., et al., *Choosing the best second-line tyrosine kinase inhibitor in imatinib-resistant chronic myeloid leukemia patients harboring Bcr-Abl kinase domain mutations: how reliable is the IC(5)(0)?* Oncologist. **16**(6): p. 868-76.
85. Deguchi, Y., et al., *Comparison of imatinib, dasatinib, nilotinib and INNO-406 in imatinib-resistant cell lines.* Leuk Res, 2008. **32**(6): p. 980-3.
86. Holtz, M.S., S.J. Forman, and R. Bhatia, *Nonproliferating CML CD34+ progenitors are resistant to apoptosis induced by a wide range of proapoptotic stimuli.* Leukemia, 2005. **19**(6): p. 1034-41.
87. **Corbin, A.**, *Human chronic myeloid leukemia stem cells are insensitive to imatinib despite inhibition of BCR-ABL activity* J Clin Invest. , 2011. **121**(1): p. 396-409.
88. Gomez-Casares, M.T., et al., *MYC antagonizes the differentiation induced by imatinib in chronic myeloid leukemia cells through downregulation of p27(KIP1).* Oncogene.
89. Epling-Burnette, P.K., et al., *Inhibition of STAT3 signaling leads to apoptosis of leukemic large granular lymphocytes and decreased Mcl-1 expression.* J Clin Invest, 2001. **107**(3): p. 351-62.

90. Bhattacharya, S., R.M. Ray, and L.R. Johnson, *STAT3-mediated transcription of Bcl-2, Mcl-1 and c-IAP2 prevents apoptosis in polyamine-depleted cells.* Biochem J, 2005. **392**(Pt 2): p. 335-44.
91. Gritsko, T., et al., *Persistent activation of stat3 signaling induces survivin gene expression and confers resistance to apoptosis in human breast cancer cells.* Clin Cancer Res, 2006. **12**(1): p. 11-9.
92. Chakraborty, A. and D.J. Tweardy, *Granulocyte colony-stimulating factor activates a 72-kDa isoform of STAT3 in human neutrophils.* J Leukoc Biol, 1998. **64**(5): p. 675-80.
93. Iliopoulos, D., H.A. Hirsch, and K. Struhl, *An epigenetic switch involving NF-kappaB, Lin28, Let-7 MicroRNA, and IL6 links inflammation to cell transformation.* Cell, 2009. **139**(4): p. 693-706.
94. Reynaud, D., et al., *IL-6 controls leukemic multipotent progenitor cell fate and contributes to chronic myelogenous leukemia development.* Cancer Cell. **20**(5): p. 661-73.
95. Fava, C., G. Rege-Cambrin, and G. Saglio, *Chronic myeloid leukemia: state of the art in 2012.* Curr Oncol Rep. **14**(5): p. 379-86.
96. Merante, S., et al., *Outcome of four patients with chronic myeloid leukemia after imatinib mesylate discontinuation.* Haematologica, 2005. **90**(7): p. 979-81.
97. Rousselot, P., et al., *Imatinib mesylate discontinuation in patients with chronic myelogenous leukemia in complete molecular remission for more than 2 years.* Blood, 2007. **109**(1): p. 58-60.
98. Quintas-Cardama, A., et al., *Preclinical characterization of the selective JAK1/2 inhibitor INCB018424: therapeutic implications for the treatment of myeloproliferative neoplasms.* Blood. **115**(15): p. 3109-17.
99. Verstovsek, S., *Therapeutic potential of JAK2 inhibitors.* Hematology Am Soc Hematol Educ Program, 2009: p. 636-42.

Addendum I

Oral and Poster Presentations At The National And International Meeting
CO: Oral Comunication; **P**: Poster

Anno 2010, I Anno

1. **CO-24**, "XI National Meeting of the Italian Society of Hematology Experimental SIES", October 6-8 2010, Torino, Italy. "Induction of Preferentially Expressed Antigen of Melanoma (PRAME)-Specific Immunity by PRAME-Overlapping Pentadecapeptides In Patients with Hematologic Malignancies, including Chronic Myelogenenous Leukemia." Quintarelli C., **De Angelis B**, Errichiello S,Accetta R,Musella F,Savoldo B,Dotti G, Luciano L, Heslop H, Rooney C, Brenner M,Camera A, Pane.

2. **P-147**, "XI National Meeting of the Italian Society of Hematology Experimental SIES", October 6-8 2010, Torino, Italy. "High JAK-1 mRNA Levels May Be Prognostic of Poor Response To Interferon-Alfa Treatment In Patient With Essential Trombocythemia." Pugliese N, Quintarelli C, Gravetti A, **De Angelis B**,Pane F,Martinelli V.

3. **P-179**, "XI National Meeting of the Italian Society of Hematology Experimental SIES", October 6-8 2010, Torino, Italy. "The Incidence and Clinical Value of Quantitative Monitoring of Preferentially expressed Antigen of Melanoma (PRAME) as a Marker of Disease Activity In Acute Myeloid Leukemia (AML)." **De Angelis B**, Quintarelli C, Errichiello S, Accetta R, Camera A, Pane F.

4. **CO-334,** XV Giornate Scientifiche Polo Delle Scienze E Delle Tecnologie Per La Vita 24-26 novembre 2010 Tensostruttura Facolta' Medicina E Chirurgia Facolta' Scienze Biotecnologiche, Napoli, Italy. "Attivazione Di Un'immunità Specifica Per PRAME Mediante L'utilizzo Di Una Libreria Peptidica In Pazienti Affetti Da Patologie Ematologiche." **De Angelis B.**, Quintarelli C., Errichiello S., Accetta R., Musella F., Izzo B., Muccioli Casadei G., Peluso A.L., Esposito N., Farina V., Rinaldi P., Pugliese N., Cosenza M., Pisano I., Savoldo B., Dotti G., Luciano L., Heslop H., Rooney C., Brenner M., Camera A., Pane F.

Anno 2011, II Anno

1. **C0-18**, 43° Congresso Nazionale SIE 16-17-18-19 ottobre 2011. Napoli, Italy. "Frequenza Delle Mutazioni Ckit In Pazienti Affetti Da Leucemia Mieloide Acuta (Lam) Caratterizzati Da Alterazioni Del Gene Del Core Binding Factor (CBF)." Peluso A.L., Izzo B., Musella F., Rinaldi P., Esposito N., **De Angelis B.**, Errichiello S., Muccioli Casadei G., Quintarelli C., Pane F. (Napoli)

2. **C0-80**,43° Congresso Nazionale SIE 16-17-18-19 ottobre 2011. Napoli, Italy. "Una Bassa Espressione Della Fosfatasi SHP-1 Correla Con La Resistenza Al Trattamento Con Inibitori Delle Tirosin Kinasi In Pazienti Affetti Da Leucemia Mieloide Cronica." Esposito N., Quintarelli C., Colavita I., Sica A.R., Peluso A.L., Errichiello S., **De Angelis B.**, Musella F., Izzo B., Muccioli Casadei G.,

Rinaldi P., Cosenza M., Pisano I., Cacciapuoti V., Luciano L., Picardi M., Del Vecchio L., Buonomo T., Hughes T.P., Radich J.P., Russo D., Branford S., Saglio G., Melo J.V., Martinelli R., Ruoppolo M., Kalebic T., Martinelli G., Pane F.(Napoli, Adelaide - AUS, Seattle - USA, Brescia, Orbassano, New Jersey - USA, Bologna, Roma)

3. **C0-81**,43° Congresso Nazionale SIE 16-17-18-19 ottobre 2011. Napoli, Italy. "L'attività Degli Inibitori Di Tirosina Kinasi (TKI) Sulla Proliferazione E L'attivazione Delle Cellule T." Quintarelli C., **De Angelis B.**, Errichiello S., Accetta R., Palma M.D., Esposito N., Peluso A.L., Izzo B., Muccioli Casadei G., Musella F., Rinaldi P., Cosenza M., Pisano I., Cacciapuoti V.,Luciano L., Pane F. (Napoli)

4. **P-088**, 43° Congresso Nazionale SIE 16-17-18-19 ottobre 2011. Napoli, Italy. "Generazione Di Linfociti T Citotossici Specifici Per Un Nuovo Peptide Derivante Dalla Proteina Preferenzialmente Espressa In Melanoma (PRAME) Capaci Di Riconoscere Ed Eliminare Progenitori Cellulari Ematopoietici Derivanti Da Pazienti Leucemici." Quintarelli C., **De Angelis B.**, Errichiello S., Accetta R., Palma M.D., Esposito N., Peluso A.L.,Izzo B., Muccioli Casadei G., Musella F., Rinaldi P., Cosenza M., Pisano I., Cacciapuoti V.,Luciano L., Brenner M.K., Dotti G., Savoldo B., Pane F. (Napoli, Houston - USA)

5. **P-196**,43° Congresso Nazionale SIE 16-17-18-19 ottobre 2011. Napoli, Italy. "L'attivazione Costitutiva Della Tirosina Chinasi Janus Kinase 2 (JAK2) Mediata Dalla Mutazione V617F Induce Alterazioni Del Centrosoma." **De Angelis B.**, Cosenza M.R., Errichiello S., Pisano I., Accetta R., Palma M.D., Esposito N.,Peluso A.L., Pugliese N., Rinaldi P., Izzo B., Muccioli-Casadei G., Musella F., Pisano I.,Cacciapuoti V., Martinelli V., Quintarelli C., Pane F. (Napoli)

6. **P-275**, 43° Congresso Nazionale SIE 16-17-18-19 ottobre 2011. Napoli, Italy. "La Proteina Da Shock Termico Hsp90 Regola L'espressione Della Proteina Preferenzialmente Espressa In Melanoma (PRAME) In Linee Cellulari Derivanti Da Pazienti Affetti Da Leucemia Mieloide Cronica." **De Angelis B.**, Quintarelli C., Accetta R., Palma M.D., Errichiello S., Pugliese N., Esposito N., Peluso A.L., Izzo B., Muccioli Casadei G., Musella F., Rinaldi P., Cosenza M., Pisano I.,Cacciapuoti V., Luciano L., Pane F. (Napoli)

7. **P-276**, 43° Congresso Nazionale SIE 16-17-18-19 ottobre 2011. Napoli, Italy. "Le Cellule Staminali Mesenchimali (MSC) Ottenute Da Pazienti Affetti Da Leucemia Mieloide Cronica (CML) Proteggono Le Cellule Leucemiche Ph+ Dai Processi Apoptotici Indotti Da Inibitori Delle Tyrosina Kinasi (TKI)." Quintarelli C., **De Angelis B.**, Errichiello S., Esposito N., Peluso A.L., Accetta R., Palma

M.D., Izzo B., Muccioli-Casadei G., Musella F., Rinaldi P., Cosenza M., Pisano I., Cacciapuoti V., Luciano L., Pane F. (Napoli).

8. **P-278**, 43° Congresso Nazionale SIE 16-17-18-19 ottobre 2011. Napoli, Italy. "Delezioni Ed Inserzioni Nucleotidiche Nel Dominio Chinasico Di Bcrabl Sono Comuni Nella Leucemia Mieloide Cronica." Peluso A.L., Cosenza M.R., Seneca E., Quintarelli C., Musella F., Esposito N., **De Angelis B**.,Izzo B., Muccioli-Casadei G., Rinaldi P., Cosenza M., Pisano I., Cacciapuoti V., Errichiello S.,Villa M.R., Pezzullo L., Palmieri F., Annunziata M., D'Anise P., Vallone R., Esposito M.R.,Luciano L., Pane F. (Napoli, Roma, Avellino, Benevento).

Anno 2012, III Anno

1. **P-0381,** 17TH Congress of The European Hematology Association Amsterdam, The Netherlands June 14 - 17, 2012. "Effectiveness of Interferon Alpha Therapy In Essential Thrombocythemia." N Pugliese, L Marano, C Quintarelli, M Gherghi, G Ciancia, **B De Angelis**, S Errichiello, B Izzo, A Peluso, V Martinelli, F Pane University of Naples Federico II, Napoli, Italy. Haematologica | 2012; 97(s1) |155.

2. **P-0904**, 17TH Congress Of The European Hematology Association Amsterdam, The Netherlands June 14 - 17, 2012. "In Vitro And In Vivo Data Confirmed Jak1 Gene Expression As Predictor Marker Of Response To IFN In Essential Thrombocythemia (ET)." N Pugliese, C Quintarelli, **B De Angelis**, S Errichiello, L Marano, N Esposito, MRaia, L Del Vecchio, V Martinelli, F Pane University of Naples Federico II, Napoli, Italy Haematologica | 2012; 97(s1) |373.

3. **C0-54,** XII Congresso Nazionale Sies 2012. "Analisi Funzionale Della Nicchia Midollare Per La Regolazione Dell'attività Degli Inibitori Delle Tirosina Kinasi In Linee Cellulari Philadelphia Positive E Progenitori Cellulari CD34+ Derivanti Da Pazienti Affetti Da Leucemia Mieloide Cronica." Quintarelli C., **De Angelis B.**, Errichiello S., Caruso S., Esposito N., Raia M., Pagliuca S.,Picardi M., Luciano L., Pane F. *(Napoli).* Haematologica | 2012.

4. **C091**, XII Congresso Nazionale SIES 2012. "La Proteina JAK2 E La Sua Controparte Mutata JAK2V617F si Localizzano Differenzialmente A Livello Centrosomico." **De Angelis B.**, Quintarelli C., Errichiello S., Sarnataro D., Palma M.D., Pugliese N., Caruso S., Accetta R., Cosenza M.R., Martinelli V. *(Napoli).* Haematologica | 2012.

5. **C096**, XII Congresso Nazionale Sies 2012. "JAK1 E SOCS3 Rappresentano Dei Predittori Molecolari Di Risposta All'ifn Nella Trombocitemia Essenziale."

Pugliese N., Quintarelli C., **De Angelis B.**, Santa E., Marano L., Esposito N., Raia N.,Del Vecchio L., Martinelli V., Pane F. *(Napoli).* Haematologica | 2012.

6. **P-019**, XII Congresso Nazionale SIES 2012. “La Proteina Indotta Da Shock Termico Hsp90 Regola L’espressione Della Proteina Preferenzialmente Espressa In Melanoma (PRAME) In Linee Cellulari Derivanti Da Pazienti Affetti Da Leucemia Mieloide Cronica. **De Angelis B.**, Quintarelli C., Accetta R., Palma M.D., Errichiello S., Pugliese N., Pane F. *(Napoli).* Haematologica | 2012.

7. **P-028**, XII Congresso Nazionale SIES 2012. “In Vitro Ed In Vivo Analisi Della Proliferazione e Dell’attivazione Linfocitaria Dopo Trattamento Con Inibitori Delle Tirosino Chinasi (TKI).” Quintarelli C., **De Angelis B.**, Errichiello S., Caruso S., Raia M., Annunziata M., Seneca E., Luciano L., Pane F. (Napoli). Haematologica | 2012.

8. **P106**, XII Congresso Nazionale SIES 2012. Mutazioni Del Gene cKIT In Pazienti Affetti Da Leucemia Mieloide Acuta (LAM) Caratterizzati Da Alterazioni Del Gene Del Core Binding Factor (CBF).” Peluso A.L., Izzo B., Musella F., Muccioli-Casadei G., Rinaldi P., Esposito N., **De Angelis B.**, Quintarelli C., Pane F. *(Napoli, Roma).* Haematologica | 2012.

9. **P-173,** XII Congresso Nazionale SIES 2012. “ATRA Sinergizza Con Interferone Alfa Nell’inibizione In Vitro Di Cellule Derivanti Da Pazienti Affetti Da Neoplasia Mieloproliferativa Cronica.” Pugliese N., Quintarelli C., **De Angelis B.**, Santa E., Marano L., Raia N., Del Vecchio L., Martinelli V., Pane F. *(Napoli).* Haematologica | 2012.

10. **P-174,** XII Congresso Nazionale SIES 2012. “Efficacia Della Terapia Con Interferone Alfa Nella Trombocitemia Essenziale.” Pugliese N., Marano L., Quintarelli C,. Beneduce G., Gherghi M., Ciancia G., **De Angelis B.**, Errichiello S., Izzo B., Muccioli Casadei G., Martinelli V., Pane F. *(Napoli).* Haematologica | 2012.

11. **P-2795,** 54th ASH Annual Meeting and Exposition. Atlanta, GA. December 8-11, 2012. “Analysis of Bone Marrow Microenviroment Factors As Early Markers of Response in Patients with Newly Diagnosed BCR-ABL Positive CML in Chronic Phase Treated with Nilotinib. Concetta Quintarelli, **Biagio De Angelis**, Santa Errichiello, Simona Caruso, Nicola Esposito, Luigia Luciano, Simona Paratore, Claudia Galimberti, Simona Soverini, Carolina Terragna, Daniela Cilloni, Giuseppe Saglio, Giovanni Martinelli, Frank Giles, Andreas Hochhaus, and Fabrizio Pane. Blood.

Addendum II
Academic Articles: 2008-2009 (pre-fellow Doc)

1. Giuliana Alimena, Massimo Breccia, Luigia Luciano, Fabrizio Quarantelli, Daniela Diverio, Barbara Izzo, **Biagio De Angelis**, et al.*"Imatinib mesylate therapy in chronic myeloid leukemia patients in stable complete cytogenic response after interferon-alpha results in a very high complete molecular response rate."* Leuk Res. 2008 Feb; 32(2):255-61. IF 2.39

2. Quintarelli C, Dotti G, **De Angelis B**, et al."Cytotoxic T lymphocytes directed to the Preferentially Expressed Antigen of Melanoma (PRAME) target chronic myeloid leukemia" Blood. 2008 Sep 1;112(5):1876-85. IF 10.432

3. **Biagio De Angelis**, Gianpietro Dotti, Concetta Quintarelli, et al. **"**Generation of Epstein-Barr-Virus-specific Cytotoxic T lymphocytes Resistant to the Immunosuppressive Drug Tacrolimus (FK506)". Blood 2009 Nov 26; 114(23): 4784-4791. IF 10.555

4. Di Stasi A, **De Angelis B**, et al. "T lymphocytes coexpressing CCR4 and a chimeric antigen receptor targeting CD30 have improved homing and antitumor activity in a Hodgkin tumor model. Blood. 2009 Jun 18; 113(25):6392-402. IF 10.555

Academic Articles: 2010-2013 (PhD period)

5. Di Stasi A, **De Angelis B**, Savoldo B. "Gene therapy to improve migration of T cells to the tumor site. Methods in Molecular Biology, Chapter 7, **2010**. **Methods Mol Biol. 2010**; 651:103-18.

6. Concetta Quintarelli, Gianpietro Dotti, Tooba Hasan, **Biagio De Angelis**, Valentina Hoyos, Santa Errichiello, Martha P Mims, Luigia Luciano, Jessica Shafer, Ann M Leen, Helen E Heslop, Cliona M Rooney, Fabrizio Pane, Malcolm K Brenner, and Barbara Savoldo. High-avidity cytotoxic-T-lymphocytes specific for a new preferentially expressed antigen of melanoma (PRAME)-derived peptide can target leukemic- and leukemic-precursor cells**. Blood. 2011** Mar 24;117(12):3353-62. Impact Factor : **10.555**

7. Giampaolo Merlini, Fabrizio Pane con la collaborazione di **Biagio De Angelis**, Francesca Lavatelli, Anna Lucia Peluso, Concetta Quintarelli. "Biochimica del plasma e sistema ematopoietico." Capitolo 1, 2013. **Casa Editrice Idelson Gnocchi.** Italian book forthcoming. 2013

8. Perna SK, **De Angelis B**, Pagliara D, Hasan ST, Zhang L, Mahendravada A, Heslop HE, Brenner MK, Rooney CM, Dotti G, Savoldo B. "Interleukin 15 provides relief to cytotoxic T lymphocytes from regulatory T cell-mediated

inhibition: implications for adoptive T-cell based therapies of lymphoma." **Clin Cancer Res**. 2013 Jan 1;19(1):106-17. IF **7.742**

Available online at www.sciencedirect.com
ScienceDirect
Leukemia Research 32 (2008) 255–261
Leukemia Research
www.elsevier.com/locate/leukres

Imatinib mesylate therapy in chronic myeloid leukemia patients in stable complete cytogenic response after interferon-alpha results in a very high complete molecular response rate

Giuliana Alimena [a,*], Massimo Breccia [a], Luigia Luciano [b], Fabrizio Quarantelli [b], Daniela Diverio [a], Barbara Izzo [b], Biagio De Angelis [b], Marco Mancini [a], Roberto Latagliata [a], Ida Carmosino [a], Mauro Nanni [a], Marco Picardi [b], Bruno Rotoli [b], Franco Mandelli [a], Fabrizio Pane [b]

[a] *Department of Cellular Biotechnologies and Hematology, University "La Sapienza", Rome, Italy*
[b] *CEINGE Biotecnologie Avanzate and Department of Biochemistry and Medical Biotechnology, University of Naples Federico II, Italy*

Received 8 April 2007; received in revised form 4 June 2007; accepted 6 June 2007
Available online 10 August 2007

Abstract

To determine the impact on minimal residual disease by switching to imatinib chronic phase chronic myeloid leukaemia (CP-CML) patients responsive to interferon-alpha (IFNα), in stable complete cytogenetic response (CCR) but with persistent PCR positivity.

Twenty-six Philadelphia positive (Ph+) CML patients in stable CCR after IFNα but persistently positive at PCR analysis during this treatment, were given imatinib mesylate at standard dose.

At enrolment into the study, median IFN treatment and CCR duration were 88 months (range 15–202) and 73 months (range 10–148), respectively. Imatinib treatment resulted in a progressive and consistent decline of the residual disease as measured by quantitative PCR (RQ-PCR) in all but one of the 26 patients; at the end of follow-up, after a median of 32 months (range 21–49) of treatment, a major molecular response (BCR/ABL levels <0.1) was reached in 20 patients (77%), and BCR/ABL transcripts were undetectable in 13 (50%). The achievement of molecular response was significantly correlated with post-IFN baseline transcript level (mean 1.194 for patients achieving complete molecular response versus 18.97 for those who did not; $p < 0.001$), but not with other clinical/biological disease characteristics.

These results indicate that patients induced into CCR by IFN treatment represent a subset with very favourable prognosis, which can significantly improve molecular response with imatinib and further support investigative treatment schedules combining these two drugs.

Keywords: Chronic myeloid leukemia; Interferon alpha; Imatinib; Minimal residual disease

1. Introduction

Chronic myeloid leukemia (CML) is a malignant hematopoietic disease whose molecular hallmark is the BCR/ABL gene rearrangement originating from a t(9;22) translocation. The BCR/ABL fusion product encodes for a deregulated tyrosine kinase (TK), which has a central role in the pathogenesis of the disease [1]. Until recently, interferon-α (IFN) was considered the gold standard for drug therapy of CML, as it yielded complete cytogenetic response (CCR) in 10–25% of patients with significant survival prolongation, particularly in low risk patients usually obtaining a higher response rate [2,3]. However, even in best responding patients, the disease still remained detectable at a molecular level, and the majority of patients eventually relapsed [4–7]. Only consistently negative RT-PCR patients

* Corresponding author at: Department of Cellular Biotechnologies and Hematology, Via Benevento 6, 00161 Rome, Italy.
E-mail address: alimena@bce.uniroma1.it (G. Alimena).

0145-2126/$ – see front matter © 2007 Elsevier Ltd. All rights reserved.
doi:10.1016/j.leukres.2007.06.008

appeared to remain 100% in CCR at 10 years follow-up [7].

The introduction of imatinib mesylate (STI571, Gleevec), a selective inhibitor of the BCR/ABL TK, has revolutionized the disease management, as it induces CCR in 50–90% of chronic phase (CP) CML patients, including those resistant or refractory to IFNα [8,9]. Furthermore, molecular monitoring using quantitative PCR (RQ-PCR) has shown a consistent reduction of the transcript level in a high proportion of responder patients, and the degree of the molecular response strongly correlates with the probability of progression-free survival. A reduction of the BCR/ABL transcript level ≥3 log at 12 or 18 months predicts almost 100% long-term remission [8–12]. However, residual disease still remains detectable using PCR standard procedures in the majority of patients, and development of imatinib resistance is the main cause of therapy failure [11–17].

In this study, we administered standard dose imatinib to 26 CML patients in late CP, who were in stable CCR induced by IFN, but had persistent residual disease by molecular analysis. We monitored the level of BCR/ABL fusion transcript by RQ-PCR to assess the impact on residual disease of crossover from IFN to imatinib in this subset of IFN-responding patients and the possible correlations between response to imatinib and clinical-biological characteristics of patients at diagnosis and during follow-up.

2. Materials and methods

2.1. Patients and study design

Twenty-six Ph+ CP-CML patients who had been diagnosed in our institutions between December 1985 and March 2000 entered this study. Inclusion criteria were: (a) having received an IFNα based treatment, (b) being in stable CCR defined as the absence of Ph+ mitoses in at least two consecutive analyses (6 months apart), and (c) being persistently positive at qualitative PCR analysis for the BCR/ABL transcript.

At presentation all patients were previously untreated and in first CP according to the standard criteria [18]. All patients had been receiving IFN from diagnosis at the maximum tolerated dose (up to 5 MU/m^2/day); following CCR, the initial IFN scheduled dosage was adjusted to maintain WBC count between 1.5 and 4×10^9 L^{-1}. From the time of imatinib treatment, quantitative PCR analysis of residual disease was regularly assessed. A reduction in the dose of imatinib because of non-hematologic or hematologic toxicities was allowed according to common toxicity criteria [18]. Complete blood counts and serum chemistry evaluations were performed before starting imatinib, weekly during the first 6 weeks, every 2 weeks for the next 6 weeks, and every 6 months thereafter.

2.2. Cytogenetics

Cytogenetic analyses were performed on bone marrow (BM) aspirates at diagnosis, every 6 months during IFN treatment, before starting imatinib (baseline), and after 3, 6, and 12 months of therapy and thereafter every 6 months, according to standard methods. Only results obtained from at least 20 metaphases were considered as evaluable. Cytogenetic response was categorized according to standard criteria [2]: CCR was defined as the presence of 100% Ph- metaphases.

2.3. FISH analysis

FISH analysis was performed on unseparated nucleated cells using differently labeled BCR and ABL probes (LSI BCR/ABL ES Dual Color Translocation Probe, Abbott Molecular Diagnostics) with a minimum of 150 cells in interphase being scored for each sample. Normal cells display two red signals (ABL gene) and two green signals (BCR gene), while the FISH pattern of Ph positive cells consists of one red, one green and two yellow signals. The cut-off limit for BCR/ABL positive analysis was set at 0.2%, i.e. the mean + 2 S.D. of positive FISH pattern detected by scoring 1000 nuclei of bone marrow cells from patients affected by other hemopoietic diseases.

2.4. Quantitative evaluation of minimal residual disease

2.4.1. Organization, sampling schedule and storage of samples

Quantitative assays of minimal residual disease (MRD) were centrally performed in Naples at the CEINGE-Biotecnologie Avanzate [19]. BM samples for MRD analysis were collected from all patients enrolled into the study prior to imatinib treatment (baseline), after 3, 6, 12 and 18 months; a further assay of MRD was also carried out at the latest follow-up.

2.4.2. Cell separation and RNA extraction

Leukocyte pellets were isolated from BM aspirates by lysis of red blood cells, and re-suspended in aliquots of 5×10^6 in 600 μL of 4 M guanidium isothiocyanate solution (GITC). Total RNA was extracted using ion exchange chromatography on minicolumn (GeneElute, Total RNA Purification kit, Sigma, St. Louis, MO, USA), according to the manufacturer directions.

2.4.3. Real time quantitative RT-PCR assay of minimal residual disease

MRD was detected during follow-up by a recently standardized RQ-PCR method [20]. The method independently measures in each sample by real time PCR, the copy number of both mRNA encoding for the P210 BCR/ABL protein and for Abelson (ABL); the latter was used as a control gene to verify sample-to-sample RNA quality variations. In this study, for each amplification run, both a BCR/ABL and ABL

standard curve were independently generated by assaying, in parallel with the samples, 1:10 serial dilutions (from 10^6 to 10^2 copies, each in triplicate) of plasmid DNA calibrators containing the target sequences diluted in a solution of *E. coli* RNA (20 ng/μL). The copy number (CN) of BCR/ABL and ABL transcript are derived by the interpolation of the cycle threshold (C_t—the number of PCR cycles necessary to detect a signal above the threshold) values to the appropriate standard curve; the result for each sample was expressed as ratio of BCR/ABL mRNA copies to ABL mRNA × 100 (normalized copy number—NCN).

2.4.4. Real Time quantitative PCR reaction conditions

The reaction conditions were the same for both BCR/ABL and ABL mRNA RQ-PCR. Briefly, 1 μg of total RNA extracted from the patient samples was pre-warmed for 10 min at 70 °C and incubated for 10 min at 25 °C; the RNA solution was then incubated for 42 min at 45 °C in a 20 μL reaction mixture containing 10 mM Tris–HCl (pH 8.3), 50 mM KCl, 5.5 mM $MgCl_2$, 1 mM of each deoxyribonucleotide, 20 U of RNAsin (Pharmacia, Upsala, Sweeden), 25 mM random examers (Pharmacia), 10 mM of DTT (Pharmacia), and 100 U of MoMLV reverse transcriptase (BRL, Bethesda, MD). PCR amplification of p210- and ABL-encoding cDNAs were separately carried out in a reaction mixture consisting of 1 × Master Mix (Applied BioSystem, Foster City, CA USA), 300 nM of the appropriate primer pair and 200 nM of the appropriate probe in a final volume of 25 μL using the following time/temperature profile: 95 °C, 15 s, and 60 °C, 1 min, for 50 cycles. All amplification reactions were carried out in triplicate. Primers and probe sequences for RQ-PCR of BCR/ABL and ABL were designed, tested and standardized within the EU concerted action (Table 1). Plasmid dilution used to generate the standard curves of the assays, were purchased by IPSOGEN Inc. (Marseille, France).

Sample results and all analytical series underwent to a rigorous check, as follow: (i) RNA samples that repeatedly gave ABL Ct values higher than 28.7 were operationally considered degraded and eliminated from further evaluation to ensure a sensitivity of at least 4 logs in all samples assayed; (ii) in the case of BCR/ABL C_t value higher than the intercept value of the relative standard curve of the run (C_t value corresponding to one copy), the samples were considered negative (MRD below the detection limit of the technique); (iii) in the case that the slope of a standard curve was not comprised within the mean ±2 standard deviations, all the samples of the analytical series were re-assayed.

Table 2
Patient features

Number of patients	26
Age	
Mean (years)	40
Range	21–64
Sokal Risk	
Low	18
Intermediate	8
High	–
Follow-up (months)	
Median	122
Range	49–236
IFN-α treatment	
Duration (months)	
Median	88
Range	15–202
Weekly dose (MU)	
Median	26
Imatinib treatment	
Duration (months)	
Median	32
Range	21–49
Daily dose (mg)	
Median	400

2.5. Statistics

Statistical analysis was performed using SPSS version 6.0 software; Wilcoxon–Mann–Whitney test was performed for comparison of non-parametric series and Fisher's exact test was used to compare categories. Values of $p < 0.05$ were considered of statistical significance.

3. Results

3.1. Pre-Imatinib features of patients

Clinical features of the 26 patients enrolled into the study are summarized in Table 2.

At diagnosis median age was 40 years (range 21–64), and baseline Sokal risk score was low in 18 patients and intermediate in the remaining 8, whereas no patient was in high risk

Table 1
Sequences of primers and probes used for the assay of BCR/ABL and ABL mRNA levels

#	Sequence (5′ → 3′)	Description
ENF501	TCCGCTGACCATCAACAAGGA	Sense—BCR exon 13
ENP541	Fam-CCCTTCAGCGGCCAGTAGCATCTGA-Tamra	Probe—ABL exon 2
ENR561	CACTCAGACCCTGAGGCTCAA	Antisense—uABL exon 2
ENF1302	GAGTATGCCTGCCGTGTG	Sense—ABL exon 2
ENPr1342	Fam-CCTCCATGATGCTGCTTACATGTCTC-Tamra	Probe—ABL exon 3
ENR1362	AATCCAAATGCGGCATCT	Antisense—ABL exon 4

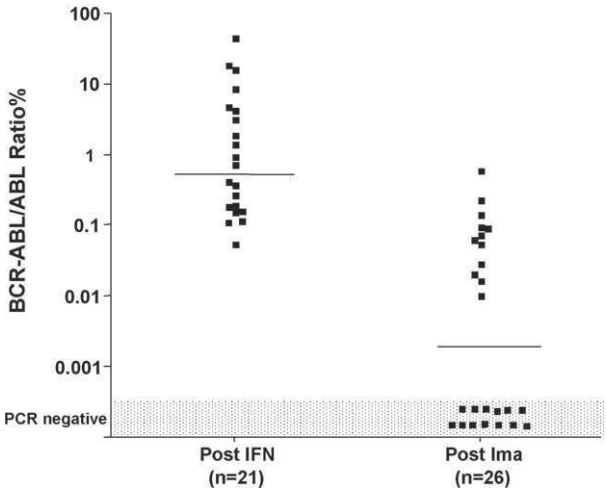

Fig. 1. MRD levels at baseline and at end of follow-up. MRD levels assessed by RQ-PCR in patients at IFN treatment discontinuation before imatinib therapy and at the end of the follow-up. Dotted lines indicate median values of the two groups of MRD values.

category. Overall, median weekly dose of IFN received from the patients was 26 MU, the median duration of IFN treatment being 88 months (range 15–202). All the 26 patients had sustained CCR from a median of 73 months (range 10–148) at the start of imatinib. Total follow-up from diagnosis of the patients was 122 months (range 49–236). During the course of IFN treatment, qualitative RT-PCR analysis tested always positive for all the patients. At the end of IFN treatment, median BCR/ABL transcripts level in BM samples of patients, assayed by RQ-PCR analysis, was 0.89 (range 0.06–100.04), and was considered as study baseline level of MRD (see Fig. 1). In three patients, RQ-PCR showed a level of MRD higher than 10, despite the confirmed status of CCR. Therefore, FISH analysis was performed on interphase marrow cells of patients given the possible presence, in the marrow of the three patients, of Ph positive cells still inhibited by IFN in their capability to proliferate in vitro. Consistently with the RQ-PCR data, all these patients had up to 8% of analyzed nuclei positive for the BCR/ABL translocation, thus suggesting the possibility of an impending disease relapse (Table 3). None of the other patients had BCR/ABL positive cells detectable by interphase FISH.

Table 3
FISH analysis of the three patients with high MRD level at the treatment switch to Imatinib

Patient	IFN treatment duration (months)	MRD level	Interphase FISH	
			Analyzed nuclei	BCR/ABL+ve (%)
#1	202	52.84	291	8
#2	66	100.04	190	7
#3	96	20.77	290	2

3.2. Imatinib treatment

Imatinib treatment was well tolerated by all 26 patients; no patient needed dose reduction or drug discontinuation for hematological or extra hematological side effects. At the present time, after a median of 37 months (range 26–54) of clinical observation, all patients are still on imatinib treatment at the full 400 mg/die dose. No patient showed loss of either hematological or cytogenetic complete response. Overall, total follow-up from diagnosis of the 26 patients is 122 months (range 49–236).

Imatinib treatment induced in all but one patient a significant decrease of MRD level: median BCR/ABL ratio reached <0.01, a level more than two-log lower with respect to the baseline post-IFN value (Fig. 1). Noteworthy, 20 patients (77%) had PCR results below 0.1%, with 13 of them (50%) being in complete response (BCR/ABL transcript not detectable by PCR) (Table 4). The levels of MRD at the end of follow-up did not correlate with overall disease length, IFN treatment duration and the Sokal risk at presentation (data not shown). Conversely, the levels of MRD reached after IFN (baseline level in this study) of the 13 patients who obtained complete molecular response under imatinib were significantly lower than those of the remaining patients (1.194 versus 18.97, $p < 0.001$). Sensitivity of PCR analysis was assessed as previously published in single patient samples [19] to avoid any influence on results by sample degradation. Mean ABL copy number of the analyzed samples was 8500 (range 1300–48,000) with a calculated sensitivity of the assays never lower than 10^{-4}, and in the case of samples who gave negative PCR results the mean ABL copy number was 7200 (range 1300–21,100). Overall, MRD monitoring (Fig. 2) showed a progressive decline of median values over the various time points, thus indicating a continuous reduction of the leukemic burden. Remarkably, the response to imatinib treatment was very rapid in a significant proportion of patients; MRD level was evaluable in 18 samples after the first 3 months of imatinib treatment, and in seven of these BCR/ABL transcripts were no longer detectable (PCR negative), while in other two the level was below 0.1 (major molecular response) (Fig. 2). In a single patient, MRD level showed almost one log increase at the last follow-up. This patient had, at presentation, an intermediate Sokal risk of progression, and, at start of imatinib treatment, more than 15

Table 4
Minimal residual level by RQ-PCR of BCR/ABL in the 26 patients

	Baseline	Last follow-up
Mean[a]	10.51	0.09
Median[a]	0.89	0.01
Range[a]	0.06–100.04	0–1.02
MRD <0.1 (no.)	1	20[b]
PCR negative (no.)	–	13[c]

[a] Value expressed as BCR/ABL-ABL ratio%.
[b] Including the 13 PCR negative patients.
[c] Baseline MRD level of these patients was 1.194 vs. 18.97 ($p < 0.001$) of the remaining patients.

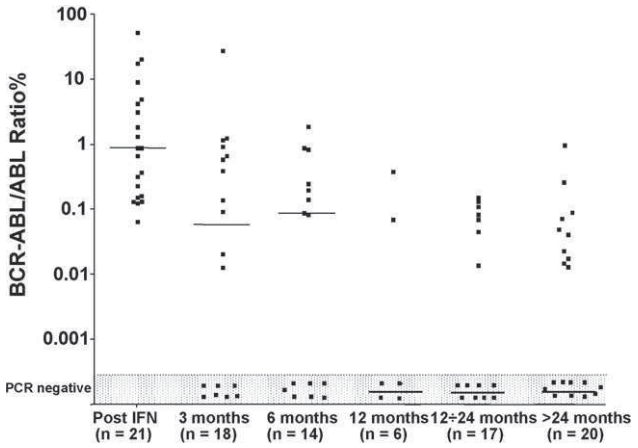

Fig. 2. Progressive effect of imatinib on MRD level. Representation of the progressive decline of MRD levels observed in CML patients under imatinib treatment. Dotted lines indicate median values of MRD at single time points.

years of IFN therapy with an overall follow-up duration of 220 months.

4. Discussion

In the present study, we analysed the effect of switching to imatinib 26 CML patients with long term cytogenetic but not molecular response to IFN. The main reason for this therapeutical decision was to evaluate whether a stable cytogenetic response to IFN could be improved at the molecular level through the possible complementary actions of the two drugs.

We found that 77% of our patients treated with a standard dose of imatinib reached BCR/ABL levels <0.01 over a median follow-up period of 32 months. These data were obtained from an unusual subset of selected patients; therefore, they cannot be extrapolated to the general CML patient population. However, some considerations may be done. Using IFN, 10–25% of CP-CML patients obtain CCR, but only a minority of them achieve and maintain very low levels of residual disease and do not experience disease relapse or progression [4–7,21,22]. When imatinib is given at 400–800 mg/day, CCR is obtained in 50 to >90% of patients with new diagnosis or late CP-CML, including those pre-treated with IFN [9,23,24]. Furthermore, molecular monitoring by quantitative RQ-PCR, has shown consistent reduction of the transcript level in a high proportion of responder patients, and the degree of the molecular response strongly correlates with the probability of long-term progression-free survival [12,17,24]. However, transcript undetectability only reached a limited number of patients. The dynamics of the molecular response has been analysed in large series of patients in CCR after imatinib, the percentage of cases with undetectable transcripts ranging from 4 to 8% to near 40% of the cases, depending on disease status (late or early CP), prior IFN treatment or not, imatinib dosage (400 or 800 mg/day) [9,23]. Therefore, the heterogeneity of previously investigated cases precludes direct comparison with the data obtained from the present study.

In our series of selected patients in minimal disease status, the molecular response was very rapid and residual disease undetectability was achieved in a high proportion of patients. Furthermore, transcript reduction in almost all our patients appeared to be sustained, and progressively increasing over time, thus indicating ongoing disease depletion, as previously observed [9,12,13]. Also the three patients who had a high MRD level following IFN treatment showed a rapid decline of the BCR/ABL transcript levels as assessed by RQ-PCR. This subset of patients with a high level of BCR/ABL transcript was already indicated in the IFN era as candidate for an imminent relapse [4]; noteworthy, these three subjects showed a small percentage (2–8%) of BCR/ABL positive nuclei at FISH analysis and they were likely going into relapse.

Despite being in late disease, our patients obtained improved molecular response on imatinib. This apparently contrasts with the observations that better results are usually reached in earlier disease due to the enhanced probability of developing imatinib-resistant mutations over time [9,16,25]. We could thus infer that the significant reduction of the BCR/ABL positive cells induced by IFN made the development of resistance less likely to occur in our patients. Alternatively, some biological factors may exist in this subset of patients with particularly good prognosis, capable of preventing clonal evolution. We only observed a rough correlation between the baseline (post-IFN) level of BCR/ABL transcripts and the degree of molecular response under imatinib, while we did not find, in our series of patients, a correlation between molecular response to imatinib and disease duration, length and weekly dose of IFN, and Sokal score. It should be underlined that no high Sokal risk patient was included in our study group, may be as a consequence of the unsatisfactory response to IFN usually seen in this subset of CML patients. The prognostic impact of high Sokal risk was also confirmed in imatinib era by large cooperative clinical trials: the CCR rate in this subgroup of patients never exceeds 70% even under high dose imatinib treatment [17,23]. Finally, the mechanisms by which imatinib improved molecular status in our IFN-responsive patients remain to be elucidated. It is well known that these two drugs act through different molecular mechanisms, and it is thus expected that their effects may be mutually potentiated [26]. The complex action of IFN, which includes direct antineoplastic effect and immunomodulatory activity, is not fully understood [26]. However, it has been suggested that it induces control, rather than eradication, of the disease [27]. In contrast, imatinib and the new generation TK inhibitors act directly on the oncogenic protein of the leukemic clone; however even imatinib may fail to completely eliminate primitive quiescent Ph+ progenitor cells [27]. Thus, it is possible that IFN and imatinib exerted a complementary effect in our patients, while showing no cross drug resistance.

Much has been discussed about curtailing treatment in patients with persistent CCR after IFN, given that very low number of Ph+ cells does not necessarily imply relapse, and that patients with molecularly negative disease do not seem to experience relapse [5,6,7]. This issue applies now also to patients in CCR after imatinib, especially to those achieving persistently undetectable levels of residual disease, in whom divergent outcome have been observed after imatinib discontinuation [28]. Furthermore, as a high number of patients in CCR on imatinib still remain molecularly positive and at potential risk of relapse, strategies aiming at increasing PCR negativity need to be explored, which include combining or adding synergistic drugs to imatinib [29].

The concurrent use of imatinib and IFN has been recently studied in multicenter trials but results have demonstrated additive cytotoxic effects, limiting the possibility to apply this approach in the clinical practice [26]. Though the use of imatinib is at present the first choice for CML therapy, the complementary actions of the two drugs could be investigated in sequential or low-dose combination, also in patients reaching stable CCR on imatinib but still having detectable molecular disease.

Longer follow-up and strict monitoring of these patients, with improving technologies over time is required to determine to what extent they will become molecularly negative and whether patients with undetectable transcripts are indeed cured of their disease.

Acknowledgements

Supported by a grant from ROMAIL, Regione Campania, PRIN e FIRB (MIUR, Rome), Ministero della Salute (Rome).

References

[1] Daley GQ, Van Etten RA, Baltimore D. Induction of chronic myelogenous leukemia in mice by the P210bcr/abl gene of the Philadelphia chromosome. Science 1990;247:824–30.
[2] The Italian Cooperative Study Group on Chronic Myeloid Leukemia. Interferon alfa-2a compared with conventional chemotherapy for the treatment of chronic myeloid leukemia. N Engl J Med 1994;330:820–5.
[3] Hehlmann R, Berger U, Pfirrmann M, et al. Randomized comparison of interferon alpha and hydroxyurea with hydroxyurea monotherapy in chronic myeloid leukemia (CML-study II): prolongation of survival by the combination of interferon alpha and hydroxyurea. Leukemia 2003;17:1529–37.
[4] Hochhaus A, Reiter A, Saussele S, et al. Molecular heterogeneity in complete cytogenetic responders after interferon-alpha therapy for chronic myelogenous leukemia: low levels of minimal residual disease are associated with continuing remission. Blood 2000;95:62–6.
[5] Bonifazi F, de Vivo A, Rosti G, et al. Chronic myeloid leukemia and interferon-alpha: a study of complete cytogenetic responders. Blood 2001;98:3074–81.
[6] Mahon FX, Delbrel X, Cony-Makhoul P, et al. Follow-up of complete cytogenetic remission in patients with chronic myeloid leukemia after cessation of interferon alfa. J Clin Oncol 2002;20:214–20.
[7] Kantarjian HM, O'Brien S, Cortes J, et al. Complete cytogenetic and molecular responses to IFN-alpha based therapy for chronic myeloid leukemia are associated with excellent long-term prognosis. Cancer 2003;97:1033–41.
[8] Druker BJ, Talpaz M, Resta DJ, et al. Efficacy and safety of a specific inhibitor of the BCR-ABL tyrosine kinase in chronic myeloid leukemia. N Engl J Med 2001;344:1031–7.
[9] Kantarjian HM, Cortes JE, O'Brien S, et al. Long-term survival benefit and improved complete cytogenetic and molecular response rates with imatinib mesylate in Philadelphia chromosome-positive, chronic-phase chronic myeloid leukemia after failure of interferon-{alpha}. Blood 2004;104:1979–88.
[10] O'Brien SG, Guilhot F, Larson RA, et al. IRIS Investigators. Imatinib compared with interferon and low-dose cytarabine for newly diagnosed chronic-phase chronic myeloid leukemia. N Engl J Med 2003;348:994–1004.
[11] Branford S, Rudzki Z, Harper A, et al. Imatinib produces significantly superior molecular responses compared to interferon alfa plus cytarabine in patients with newly diagnosed chronic myeloid leukemia in chronic phase. Leukemia 2003;17:2401–9.
[12] Druker BJ, Guilhot FG, O'Brien SG, et al. Five-year follow-up of patients receiving imatinib for chronic myeloid leukemia. N Engl J Med 2006;355:2408–17.
[13] Hughes TP, Kaeda J, Branford S, et al. Frequency of major molecular responses to imatinib or interferon alfa plus cytarabine in newly diagnosed chronic myeloid leukemia. N Engl J Med 2003;349:1423–32.
[14] Muller MC, Gattermann N, Lahaye T, et al. Dynamics of BCR-ABL mRNA expression in first-line therapy of chronic myelogenous leukemia patients with imatinib or interferon alpha/ara-C. Leukemia 2003;17:2392–400.
[15] Paschka P, Muller MC, Merx K, et al. Molecular monitoring of response to imatinib (Glivec) in CML patients pre-treated with interferon alpha, low levels of residual disease are associated with continuous remission. Leukemia 2003;17:1687–94.
[16] Hochhaus A, La Rosee P. Imatinib therapy in chronic myelogenous leukaemia: strategies to avoid and overcome resistance. Leukemia 2004;18:1321–31.
[17] Baccarani M, Saglio G, Goldman J, et al. Evolving concepts in the management of chronic myeloid leucemia:recommendations from an export panel on behalf of the European LeukemiaNet. Blood 2006;108:1809–20.
[18] Kantarjian H, Sawyers C, Hochhaus A, et al. Hematologic and cytogenetic responses to imatinib mesylate in chronic myelogenous leukemia. N Engl J Med 2002;346:645–52.
[19] van Dongen JJ, Macintyre EA, Gabert JA, et al. Standardized RT-PCR analysis of fusion gene transcripts from chromosome aberrations in acute leukemia for detection of minimal residual disease. Report of the BIOMED-1 Concerted Action: investigation of minimal residual disease in acute leukemia. Leukemia 1999;13:1901–28.
[20] Gabert J, Beillard E, van der Velden VH, et al. Standardization and quality control studies of 'real-time' quantitative reverse transcriptase polymerase chain reaction of fusion gene transcripts for residual disease detection in leukaemia—a Europe Against Cancer program. Leukemia 2003;17:2318–57.
[21] Chronic myeloid leukaemia Trialists' Collaborative Group. Interferon alpha versus chemotherapy for chronic myeloid leukaemia: a meta-analysis of seven randomized trials. J Natl Cancer Inst 1997;89:1616–20.
[22] Guilhot F, Chastang C, Michallet M, et al. Interferon alfa-2b combined with cytarabine versus interferon alone in chronic myelogenous leukemia. French Chronic Myeloid Leukemia Study Group. N Engl J Med 1997;337:223–9.
[23] Kantarjian H, Talpaz M, O'Brien S, et al. High-dose imatinib mesylate therapy in newly diagnosed Philadelphia chromosome-positive chronic phase chronic myeloid leukemia. Blood 2004;103:2873–8.

[24] Mauro MJ, Deininger MW. Chronic myeloid leukemia in 2006: a perspective. Haematologica 2006;91:152.
[25] Branford S, Rudzki Z, Parkinson I, et al. Real-time quantitative PCR analysis can be used as a primary screen to identify patients with CML treated with imatinib who have BCR-ABL kinase domain mutations. Blood 2004;104:2926–32.
[26] Baccarani M, Martinelli G, Rosti G, et al. GIMEMA Working Party on Chronic Myeloid Leukemia. Imatinib and pegylated human recombinant interferon-alpha2b in early chronic-phase chronic myeloid leukemia. Blood 2004;104:4245–51.
[27] Bhatia R, Holtz M, Niu N, et al. Persistence of malignant hematopoietic progenitors in chronic myelogenous leukemia patients in complete cytogenetic remission following imatinib mesylate treatment. Blood 2003;101:4701–7.
[28] Rousselot P, Huguet F, Rea D, et al. Imatinib mesylate discontinuation in patients with chronic myelogenous leukemia in complete molecular remission for more than 2 years. Blood 2007;109:58–60.
[29] Hehlmann R, Berger U, Hochhaus A. Chronic myeloid leukemia: a model for oncology. Ann Hematol 2005;84:487–97.

Cytotoxic T lymphocytes directed to the preferentially expressed antigen of melanoma (PRAME) target chronic myeloid leukemia

Concetta Quintarelli,[1-3] Gianpietro Dotti,[1,4,5] Biagio De Angelis,[1,3,6] Valentina Hoyos,[1] Martha Mims,[1,4] Luigia Luciano,[7] Helen E. Heslop,[1,4,8] Cliona M. Rooney,[1,5,8,9] Fabrizio Pane,[3,6,7] and Barbara Savoldo[1,8]

[1]Center for Cell and Gene Therapy, Baylor College of Medicine, The Methodist Hospital and Texas Children's Hospital, Houston; [2]School of Biotechnological Sciences, University of Naples Federico II, Naples, Italy; [3]CEINGE-Biotecnologie Avanzate SCARL, Naples, Italy; Departments of [4]Medicine and [5]Immunology, Baylor College of Medicine, The Methodist Hospital and Texas Children's Hospital, Houston; [6]Dipartimento di Biochimica e Biotecnologie Mediche, University of Naples Federico II, Naples, Italy; [7]Hematology Unit, CEINGE-Biotecnologie Avanzate, Naples, Italy; and Departments of [8]Pediatrics and [9]Molecular Virology and Microbiology, Baylor College of Medicine, The Methodist Hospital and Texas Children's Hospital, Houston

The cancer testis antigen (CTA) preferentially expressed antigen of melanoma (PRAME) is overexpressed in many hematologic malignancies, including chronic myeloid leukemia (CML). The sensitivity of CML to donor lymphocyte infusion after allogeneic stem cell transplantation suggests this tumor can be highly susceptible to cellular immunotherapy targeted to tumor associated antigens. We therefore tested whether functional PRAME-specific cytotoxic T lymphocytes (PRAME CTLs) could be generated and expanded from healthy donors and CML patients, or whether the limited immunogenicity of this CTA coupled with tumor-associated anergy would preclude this approach. Using optimized culture conditions and HLA-A*02–restricted PRAME-peptides, we have consistently generated PRAME CTLs from 8/9 healthy donors and 5/6 CML patients. These CTLs released IFNγ in response to PRAME peptides (between 113 ± 8 and 795 ± 23 spot forming cells/10^5 T cells) and lysed PRAME peptide–loaded cells (45 ± 19% at an effector:target [E:T] ratio of 20:1) in a MHC-restricted fashion. Importantly, these CTLs recognized and had cytotoxic activity against HLA-A*02$^+$/PRAME$^+$ tumor cell lines, and could recognize and respond to primary CML cells. PRAME CTLs were generated almost exclusively from the naive T-cell compartment, and clonal analysis showed these cells could have high αβTCR-peptide avidity. PRAME CTLs or vaccines may thus be of value for patients with CML. (Blood. 2008;112: 1876-1885)

Introduction

Achievement of complete cytogenetic remission in chronic myeloid leukemia (CML) has dramatically improved with the introduction of imatinib.[1,2] Nonetheless, allogeneic hematopoietic stem cell transplantation (HSCT) remains a valid option for patients losing or not achieving cytogenetic response with imatinib.[3-6] This benefit is mediated largely by T lymphocytes in the donor graft, and donor lymphocyte infusion can rescue 80% of CML patients who develop cytogenetic relapse after allogeneic HSCT.[6-8] Unfortunately, the advantages of this graft-versus-leukemia (GVL) effect are frequently offset by the occurrence of severe graft-versus-host disease (GVHD).[9] Considerable efforts have therefore been directed toward separating GVL from GVHD by identifying tumor-associated antigens (TAAs), such as proteinase-3 (PR3)[10-12] or p210 bcr/abl proteins,[13,14] and generating T lymphocytes that specifically recognize these antigens. Encouragingly, recent studies using whole-cell vaccines or peptides have successfully generated tumor-specific cytotoxic T lymphocytes (CTLs) in vivo and showed evidence for disease control.[12,14]

Cancer testis antigens (CTAs) represent a class of potential target antigens expressed on leukemic cells.[15] One such antigen is preferentially expressed antigen of melanoma (PRAME),[16] which is overexpressed in many acute and chronic leukemias.[17] In malignant melanoma cells, PRAME overexpression makes a significant contribution to oncogenesis by inhibiting retinoic acid receptor signaling, which is crucial for development and cell differentiation.[18] Although PRAME's contribution to leukemogenesis is not yet clear, its broad expression in CML cells and their known sensitivity to appropriately targeted effector T cells encouraged us to explore the generation of PRAME-specific cytotoxic T lymphocytes (PRAME CTLs) in healthy donors and in patients with CML.

Several obstacles must be addressed in effort to prepare TAA-specific CTLs for adoptive immunotherapy in cancer patients. First, with the exception of viral-associated antigens, such as Epstein-Barr virus (EBV)–derived antigens,[19] most TAAs are only weakly stimulatory to the immune system. Second, many TAAs, including CTAs such as PRAME, are self-antigens, and responding T cells may be anergized or clonally deleted, leaving only small numbers of low-affinity or unresponsive circulating T cells available for expansion.[20] Third, many patients with advanced hematologic malignancy have been treated extensively and may have few or abnormal professional antigen-presenting cells (APCs) capable of recruiting an immune response against such weakly stimulatory antigens. Finally, aberrant antigen processing mechanisms in tumor cells may preclude presentation even of highly expressed TAAs in a way that can be recognized by major histocompatibility class (MHC) I– and II–restricted CTLs.

Submitted April 6, 2008; accepted June 16, 2008. Prepublished online as *Blood* First Edition paper, June 30, 2008; DOI 10.1182/blood-2008-04-150045.

The online version of this article contains a data supplement.

The publication costs of this article were defrayed in part by page charge payment. Therefore, and solely to indicate this fact, this article is hereby marked "advertisement" in accordance with 18 USC section 1734.

Table 1. PRAME mRNA expression in CML samples from patients at different stage of disease

Pt	Disease stage	Treatment	Copy number of PRAME, average ± SD (range)	Level of PRAME mRNA expression			
				N < 0.1	0.1 < N < 1	1 < N < 10	N > 10
20	Dx	None	3.46 ± 4.34 (0-18.3)	1 (5%)	4 (20%)	14 (70%)	1 (5%)
14	CP	< 60 mo IFN-α	11.17 ± 22.79 (0-83.12)	1 (7%)	4 (29%)	6 (43%)	3 (21%)
6	CP	> 60 mo IFN-α	24.31 ± 46.60 (0.4-118.8)	0	1 (16%)	3 (50%)	2 (34%)
8	CP	< 60 mo IM	17.85 ± 25.80 (0-65.83)	1 (12%)	3 (38%)	1 (12%)	3 (38%)
10	BC	IFN-α/IM	95.97 ± 163.49 (1.19-515.98)	0	0	3 (30%)	7 (70%)

Pt indicates patient number; N, normalized mRNA copy number (mRNA copy PRAME/Gusb*10^4); Dx, CML at diagnosis; CP, CML in chronic phase; BC, CML in blastic phase; IFN-α, interferon-α; and IM, imatinib (STI-571).

In this paper we describe the use of an artificial APC line to overcome the need for large numbers of professional APCs to generate tumor-specific T cells, and the development of culture conditions that expand PRAME CTLs. We found that PRAME CTLs generated from normal donors and from patients with CML are specific for HLA-A*02–restricted PRAME peptides, and respond in a MHC-restricted manner to HLA-A*02$^+$ /PRAME$^+$ tumor cell lines and autologous CML blasts. These data suggest that PRAME is a suitable target for CML immunotherapy.

Methods

Cell lines and tumor cells

The following tumor cell lines were used: KT1 (CML) kindly provided by Dr Fujita (First Department of Internal Medicine, School of Medicine, Ehime University, Japan); BV173 (CML), L428 and HDLM-2 (Hodgkin lymphoma) and ME1 (acute myelogenous leukemia) from German Collection of Cell Cultures (DSMZ, Braunschweig, Germany); and U266B1 and ARH77 (multiple myeloma), K562 (erythroleukemia), and MRC-5 (normal human fetal lung fibroblasts) from ATCC (Rockville, MD). Cells were maintained in culture with RPMI 1640 medium (Hyclone, Logan, UT) containing 10% fetal bovine serum (FBS; Hyclone), 2 mM L-glutamine (GIBCO-BRL Invitrogen, Gaithersburg, MD), 25 IU/mL penicillin, and 25 mg/mL streptomycin (Lonza Walkersville, Walkersville, MD) in a humidified atmosphere containing 5% CO_2 at 37°C.

Samples from CML patients and healthy donors

Bone marrow samples were collected from 50 CML patients after signed informed consent was obtained in accordance with the Declaration of Helsinki and after approval by the Institutional Review Board (IRB) of University of Naples Federico II (Table 1). For 8 CML patients (7 HLA-A*02$^+$ and 1 HLA-A*02$^-$) and 9 HLA-A*02$^+$ healthy donors, peripheral blood was collected according to the local IRB-approved protocol (Baylor College of Medicine, Houston, TX). This protocol was approved for collecting anonymized CML samples (stripped of identifiers), as the major goal of this study was to evaluate the feasibility of generating PRAME CTLs.

Professional and artificial APCs

Professional APCs: dendritic cells. To generate dendritic cells (DCs), peripheral blood mononuclear cells (PBMCs) were selected for the CD14$^+$ population using anti-CD14 beads (Miltenyi Biotech, Auburn, CA) and cultured in media (CellGenix, Antioch, IL) with IL-4 (1000 U/mL) and GM-CSF (800 U/mL; R&D Systems, Minneapolis, MN). On day 5, cells were matured with IL-6 (1 μg/mL), TNF-α (1 μg/mL), IL-1β (1 μg/mL), and PGE (1 μg/mL; all from R&D Systems) for 48 hours and then used to prime T cells after loading them with specific peptides.

Professional APCs: CD40-activated B cells. To generate CD40-activated B lymphocytes, PBMCs were cocultured with MRC-5 cell line engineered to stably express human CD40L (> 90% positive) in AIM-V media (Invitrogen, Carlsbad, CA) supplemented with 5% human AB serum (Valley Biomedical, Winchester, VA) in the presence of IL-4 (500 U/mL) and Cyclosporine-A (1 mg/mL; Sandoz Pharmaceutical, Washington, DC).[21] After 7 days of culture, the cells were plated under the same conditions. On day 14 of culture, more than 90% of the cells were CD19$^+$ based on phenotypic analysis, and after loading them with specific peptides they were used to prime T cells.

Artificial APCs. To generate artificial APCs (aAPCs), the K562 cell line was modified to express human HLA-A*02, CD80, CD40L, and OX40L[22] molecules using sequential transduction with retroviral vectors. After transduction, K562 cells were selected by drug resistance (puromycin and neomycin), and single-cell fluorescence-activated cell–sorted (CD40L and OX40L) to obtain a K562/HLA-A*02$^+$/CD80$^+$/CD40L$^+$/OX40L$^+$ clone (K562/aAPCs). This clone was then expanded, and the expression of the transgenic molecules was monitored by fluorescence-activated cell sorting (FACS) analysis over time.

Generation and expansion of specific CTLs

CTL lines were generated from PBMCs obtained from 9 HLA-A*02$^+$ healthy donors and 6 HLA-A*02$^+$ CML patients.

Generation of virus-specific CTLs. PBMCs were stimulated with K562/aAPCs (PBMCs:K562/aAPCs ratio 20:1) loaded either with NLVPMVATV (pp65-cytomegalovirus (CMV) or CLGGLLTMV (LMP-2 EBV) HLA-A*02–restricted peptides at 5 μM for 2 hours, then washed twice in complete media [RPMI 1640 45%, Click medium (Irvine Scientific, Santa Ana, CA) 45%, supplemented with 5% human AB serum (hABS) and 2 mmoL L-glutamine]. T cells were collected and stimulated weekly with K562/aAPCs loaded with the same peptides. After second round of stimulation, cells were expanded using IL-2 (50 U/mL; Proleukin, Chiron, Emeryville, CA) and hABS in the complete media was replaced with FBS.

Generation of PRAME peptide–specific CTLs. The previously identified HLA-A*02–restricted PRAME peptides used in this study included ALYVDSLFFL, VLDGLDVLL, SLYSFPEA and SLLQHILGL.[16] CD8$^+$ cells were selected using magnetic antibodies (Miltenyi). These cells were primed with professional APCs (pAPCs; T cells:APCs ratio 20:1) loaded with tumor-associated HLA-A*02–restricted peptides, in complete media and in the presence of IL-7 (10 ng/mL), IL-12 (1 ng/mL), and IL-15 (2 ng/mL; all from R&D Systems). For peptide loading, pAPCs and aAPCs were incubated with a pool of the 4 HLA-A*02–restricted PRAME-peptides, each at 5 μM. This optimal peptide concentration was determined in preliminary titration experiments (Figure S1, available on the *Blood* website; see the Supplemental Materials link at the top of the online article). After 2 hours incubation at 37°C in 5% CO_2, cells were washed twice in PBS-1× to remove unbound peptides, resuspended in the appropriate media, and then used as stimulator cells for T lymphocyte activation. In a second set of experiments we used PBMCs from healthy donors and generated CTL lines using pAPCs and aAPCs loaded with the HLA-A*02–restricted ALY-peptide, which consistently recruits specific T cells from healthy donors.

After the first stimulation, T cells were collected and stimulated weekly with K562/aAPCs loaded with the same peptides. IL-7, IL-12, and IL-15 cytokines were added for the second stimulation. Subsequently, cells were expanded using IL-2 (50 U/mL) and complete media with FBS.

The same culture conditions were also used for additional HLA-A*02–restricted TAA, including ELAGIGILTV (from MART-1),[23] RMFPNAPYL (from Wilms tumor-1, WT-1),[12] VLQELNVTV (PR1 peptide from PR3

protein),[11] KVAELVHFL (from MAGE-A3),[24] ILAKFLMWL and RLVDDFLLV (from human telomerase, hTERT)[25,26] and YMDGTMSQV (from tyrosinase, TYR).[27] All peptides were obtained from Genemed Synthesis (San Antonio, TX).

In selected experiments, PRAME ALY-specific CTLs were generated using $CD8^+CD45RO^+$or $CD8^+CD45RA^+$ T cells obtained by negative immunomagnetic sorting (Miltenyi Biotech).[28]

Isolation and expansion of PRAME peptide–specific T-cell clones

Polyclonal T-cell lines obtained after 3 stimulations with K562/aAPCs loaded with ALY peptide were cloned by limiting dilution assay in 96-well plates in the presence of IL-2 (100 U/mL), CD3 antibody (50 ng/mL OKT3; Ortho Biotech, Bridgewater, NJ), and irradiated (4000 rad) allogeneic PBMCs as feeder cells, as previously described.[19] The specificity of the T-cell clones was evaluated by measuring the IFNγ release in response to the specific PRAME peptide (ELIspot assay), and their cytotoxic activity was determined with a standard ^{51}Cr-release assay against autologous phytohaemagglutinin (PHA)–activated blasts loaded with the specific PRAME peptide.

Immunophenotyping

Phycoerythrin (PE)–conjugated, fluorescein isothiocyanate (FITC)–conjugated and periodin chlorophyll protein (PerCP)–conjugated CD3, CD4, CD8, and CD56 monoclonal antibodies were used to stain T lymphocytes. Control samples labeled with an appropriate isotype-matched antibody were included in each experiment. Cells were analyzed by a FACScan (BD Biosciences, San Jose, CA) equipped with the filter set for 4 fluorescence signals. CTL lines were also analyzed for binding with specific tetramers, as previously described.[29] Tetramers were prepared by Baylor College of Medicine core facility. For each sample, a minimum of 100 000 cells were analyzed using a FACSCalibur with the CellQuest software (BD Biosciences). To determine whether samples from normal donors and CML patients were HLA-$A*02^+$, we used a specific FITC-labeled antibody. To evaluate the percentage of circulating malignant cells in CML samples, we used CD33 and CD34 monoclonal antibodies. All antibodies were from BD Biosciences.

ELIspot assay

The IFNγ ELIspot assay was performed as previously described.[30] T cells were plated in triplicate and serially diluted from 10^5 to 10^4 cells/well, and then each PRAME peptide (5 μM) was added. In all experiments, T cells were also incubated with an irrelevant peptide to show the specificity of IFNγ release. As positive control, T cells were stimulated with 25 ng/mL phorbol myristate acetate (PMA) and 1 μg/mL ionomycin (Iono; Sigma-Aldrich, St Louis, MO). To measure the αβTCR avidity, CTL lines and clones were stimulated with specific peptides from 200 to 0.02 nM and $IFN\gamma^+$ SFC enumerated (Zellnet Consulting, Fort Lee, NJ).

Chromium release assay

The cytotoxic specificity of T cells was evaluated using a standard 4-hour ^{51}Cr release assay, as previously described.[29] Target cells incubated in media alone or in 1% Triton X-100 (Sigma-Aldrich) were used to determine spontaneous and maximum ^{51}Cr release, respectively. The mean percentage of specific lysis of triplicate wells was calculated as follows: [(test counts − spontaneous counts)/(maximum counts − spontaneous counts)] × 100.

Western blot analysis

Tumor cell line lysates, obtained from 5×10^6 cells, were resolved on a 7.5% SDS-PAGE. PRAME protein was detected by immunoblot using a rabbit polyclonal antibody (Ab32185; AbCAM, Cambridge, MA). Immunoblots were developed using enhanced chemoluminescence detection reagents (GE Healthcare, Little Chalfont, United Kingdom). Membranes were reprobed using the monoclonal anti-GAPDH Ab (Sigma-Aldrich).

Real-time qRT-PCR and fluorescence in situ hybridization analysis

PRAME mRNA was measured by real-time quantitative reverse transcription–polymerase chain reaction (qRT-PCR) analysis. Total RNA was isolated using the RNeasy Mini kit (Qiagen, Valencia, CA) following the manufacturer's instructions. One microgram total RNA was reverse transcribed using SuperScript First-strand Synthesis System (Invitrogen) following the manufacturer's instructions. cDNAs from PRAME and beta-glucuronidase (GUSb, as housekeeping control) were separately amplified using primer and probe sequences that were designed, tested, and standardized by Applied Biosystems (Foster City, CA; HS00196132_m1 and Hs99999908_m1, respectively). All reactions were amplified in triplicate on an ABI Prism 7700 Sequence Detector (Perkin-Elmer, Foster City, CA) and the mean Ct values were used to calculate the transcript copy number by the formula: mRNA copy number = power (10,(Ct − 39.7)/ − 3.47), where 39.7 and 3.47 are the intercept and the slope, respectively, of the appropriate plasmid standard curve. The normalized copy number for PRAME was determined as follows: (mRNA Copy number PRAME/mRNA copy number GUSb)*10^4. The threshold was systematically set at 0.1 to avoid problems of baseline creeping. The sensibility of PRAME detection by the described method is 10^{-1} normalized copies.

Fluorescence in situ hybridization (FISH) analysis was performed as previously reported[31,32] on unseparated nucleated cells using differently labeled BCR and ABL probes (LSI BCR/ABL ES Dual Color Translocation Probe, Abbott Molecular Diagnostics, Abbott Park, IL).

Statistical analysis

All in vitro data are presented as means plus or minus SD. Student *t* test was used to determine the statistical significant differences between samples, and *P* at less than .05 was accepted as indicating a significant difference.

Results

Functional validation of K562/HLA-A*02/CD80/CD40L/OX40L aAPC line (K562/aAPCs)

Many efforts to generate TAA-specific CTLs are limited by their requirement for large numbers of autologous professional APCs for repeated target cell stimulations. To overcome this problem, we prepared aAPCs derived from the K562 cell line that does not express MHC molecules. We engineered this line to express the HLA-A*02 molecule, and improved its costimulatory properties by coexpressing CD80, CD40L and OX40L molecules as described in "Methods." This aAPC line stably expressed transgenic HLA-A*02, CD80, CD40L, and OX40L for more than 6 months (Figure 1A). In addition, expression was stable after several freeze-thaw cycles (data not shown).

To measure the function of these aAPCs, we first used 2 virus-derived antigens, pp65 (from CMV) and LMP-2 (from EBV). K562/aAPCs were loaded either with HLA-A*02–restricted NLV (CMV) or CLG (EBV) peptides and used to stimulate unfractionated PBMCs or $CD8^+$ T cells obtained from CMV- or EBV-seropositive HLA-$A*02^+$ healthy donors. As shown in Figure 1B, after 3 weeks of culture, a significant percentage of T cells was specific for either NLV or CLG peptides, as assessed by tetramer staining. These T-cell lines were also functional since they produced IFNγ on exposure to either NLV or CLG peptides (Figure 1C), and were cytotoxic to autologous PHA blasts loaded with NLV or CLG peptides and to autologous EBV-lymphoblastoid cell lines (EBV-LCL) transduced with an adenoviral vector to express pp65[33] or LMP-2 proteins[34] (Figure 1D). These data confirmed that K562/aAPCs can be used to generate and expand functional CTLs

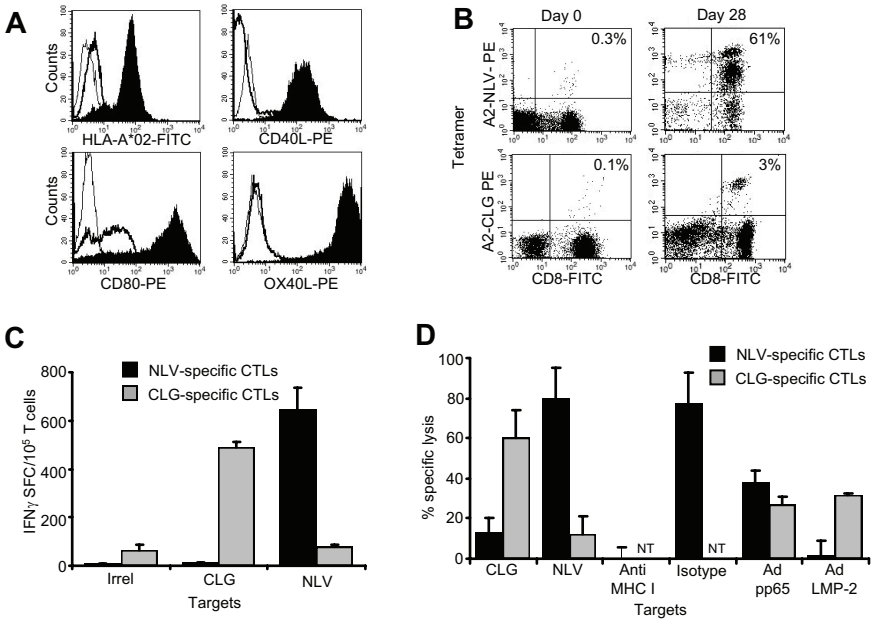

Figure 1. Generation and validation of artificial antigen-presenting cells. The K562 cell line was modified using retroviral vectors to stably express transgenic HLA-A*02, CD80, CD40L, and OX40L. (A) The expression of the transgenic molecules in modified (K562/aAPC; filled profiles) and nontransduced cells (bold lines). Isotype controls are illustrated as thin lines. To assess functionality, K562/aAPCs loaded with either NLV or CLG peptides were used to reactivate NLV- or CLG-specific CTLs, respectively, from PBMC of CMV- or EBV-seropositive HLA-A*02 healthy donors. (B) Tetramer staining illustrates the enrichment of expanded CTLs in NLV and CLG T-cell precursors (right panels) after 28 days of culture, compared with PBMCs before ex vivo culture (left panels). (C) Frequency of CTLs responding to NLV (■) or CLG peptides (□) as assessed by IFNγ ELIspot assay in a representative donor after 3 stimulations with aAPCs loaded with the specific peptides. IFNγ production in response to an irrelevant peptide (ELA peptide) was negligible. (D) Cytotoxic activity of these CTLs using a standard ^{51}Cr release assay at an effector:target ratio of 20:1. Target cells were autologous PHA blasts loaded either with NLV or CLG-peptides, and autologous EBV lymphoblastoid cell lines (LCL) transduced with an adenoviral vector encoding the full protein of either pp65[33] or LMP-2.[34] Specific killing was MHC-restricted because it was inhibited by preincubation of PHA blasts with class I MHC blocking antibodies, but not with isotype. Shown is 1 representative experiment of 5 donors. NT indicates not tested.

derived from effector-memory T cells and directed to immunogenic viral antigens.

Characterization of PRAME CTLs generated from HLA-A*02$^+$ healthy donors

Having generated an unlimited source of biologically active aAPCs, we determined whether these cells were sufficiently potent to generate PRAME CTLs from the PBMCs of healthy individuals.

Initial priming with pAPCs and IL-15 is required to generate PRAME CTLs. We stimulated CD8$^+$ cells from healthy HLA-A*02$^+$ donors with aAPCs loaded with PRAME peptides, using the same methodology validated for the generation of viral specific CTLs. In contrast to viral-specific CTL generation, however, K562/aAPCs loaded with PRAME peptides (ALY, VLD, SLY, and SLL) were insufficient to generate PRAME CTLs from PBMC (data not shown). We therefore substituted pAPCs (DCs or CD40-activated B cells) loaded with PRAME-peptides, and we also added a combination of cytokines that included IL-7, IL-12, and IL-15. As shown in Figure 2A, priming with pAPCs in combination with IL-7 and IL-12 cytokines induced the generation of PRAME CTLs. The addition of IL-15 to the cytokine cocktail, but not IL-15 alone, significantly improved the generation of these CTLs. We also found that both DCs and CD40L-activated B cells were equally efficient in generating PRAME CTLs (data not shown). Once generated, PRAME CTL lines could then be significantly expanded to numbers potentially useful for clinical application by substituting PRAME-peptides loaded K562/aAPCs and IL-2 in subsequent cultures to produce a median 102-fold expansion after 3 rounds of K562/aAPCs exposure (range, 13- to 218-fold; Figure 2B).

As a control, we also generated T-cell lines from HLA-A*02$^+$ donors using K562/aAPCs without PRAME peptide loading. None of these T-cell lines had measurable specific response to PRAME peptides or PRAME-positive target cells (data not shown). To further validate the culture protocol optimized for the generation and expansion of PRAME CTLs, we used the same in vitro condition to generate CTLs specific for other TAAs such as WT1, MART-1, PR3, MAGE-A3, hTERT, and Tyr. These results are summarized in Figure S2, and they confirm that this approach was applicable to a variety of TAAs.

PRAME CTLs originate from a different T-cell subset to viral-specific CTLs. We next investigated the mechanism responsible for the observed difference in APC requirements between CTLs specific for viral antigens versus the cancer testis antigen PRAME. Effector T cells specific for CMV/EBV derived viral antigens are primarily generated from memory T-cell subsets.[35] We assessed whether CTLs specific for the self-antigen PRAME had the same origin. We prepared ALY-peptide specific CTLs from 3 healthy donors using sorted CD45RO$^+$ and CD45RA$^+$ T-cell fractions and the same culture conditions and cytokines described above. As shown in Figure 2C, ALY-peptide–responsive T cells were detected only in CTL lines originating from the naive (CD45RA$^+$) T-cell subsets. In contrast, CTLs specific for the CMV-derived NLV peptide generated using the same culture conditions, were preferentially expanded from the memory (CD45RO$^+$) T-cell population (Figure 2D). Hence antigen-dependent expansion of the (naive) PRAME-specific T-cell population has more rigorous requirements for costimulation during initial antigen presentation than (memory) viral-specific T cells.

Specificity and functionality of PRAME CTLs

We used multiple approaches to ensure that the PRAME CTLs expanded from the naive subset of T cells were specific and active against antigen-expressing targets.

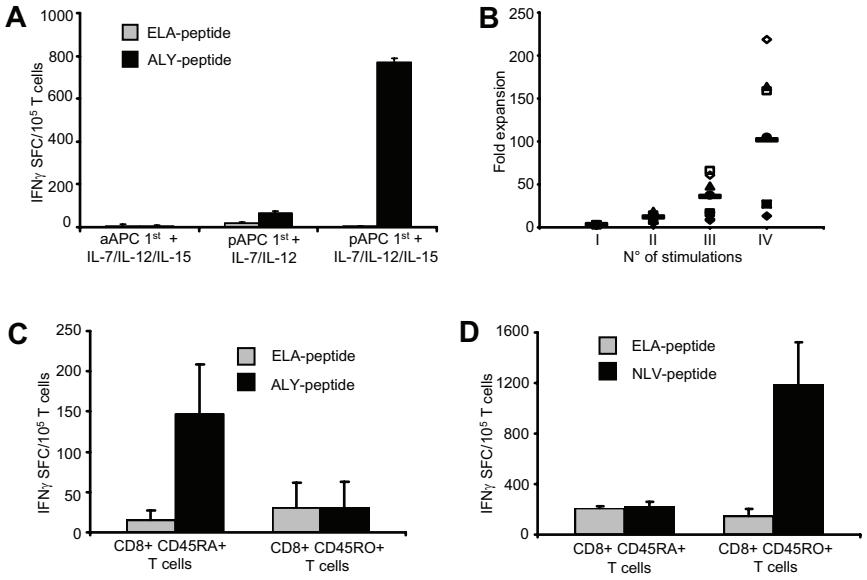

Figure 2. PRAME CTLs derive from the naive T-cell subset. To generate PRAME CTLs from healthy donors, $CD8^+$ T cells were stimulated weekly with peptide-loaded K562/aAPCs in the presence of IL-7, IL-12, and IL-15, or primed with peptide-loaded autologous pAPCs in the presence of IL-7 and IL-12 with or without IL-15, then expanded with peptide-loaded K562/aAPCs. (A) Frequency of T cells responding (in an IFNγ ELIspot assay) to PRAME peptides; shown is ALY as representative peptide, ■) or an irrelevant peptide (ELA, □). The number of $IFN\gamma^+$ SFC was negligible when T cells were stimulated weekly only with peptide loaded K562/aAPCs. Although $IFN\gamma^+$ SFC were detectable when T cells were primed with peptide-loaded pAPCs, only the addition of IL-15 to the cytokine cocktail significantly increased the generation of ALY-specific CTLs. Shown is 1 representative of 4 donors. (B) Fold expansion of PRAME CTLs primed with autologous pAPCs and stimulated with aAPCs for 3 weeks. Each symbol represents one of the 8 individual PRAME CTL lines and the horizontal lines represent the mean group value. (C) $IFN\gamma^+$ SFC in response to ALY-peptide (■) or ELA-irrelevant peptide (□) of ALY-specific CTLs expanded from 3 donors from sorted naive ($CD45RA^+$) and memory ($CD45RO^+$) T-cell subsets. T cells producing IFNγ in response to the ALY peptide were significantly higher in CTL lines that originated from the naive ($CD45RA^+$) T-cell subset. In contrast, CTLs generated against the viral peptide NVL (from the pp65 protein of CMV), were originated predominantly from the memory ($CD45RO^+$) T-cell subset (D).

Cytokine release

CTL lines generated using the peptide pool were tested for IFNγ release in response to each peptide individually, using a specific ELIspot assay. As shown in Figure 3A, we found that the majority of the expanded PRAME CTLs released IFNγ in response to at least 2 PRAME peptides (ALY and VLD in 8/9 and 5/7 donors, respectively). In addition, 2 CTL lines released IFNγ in response to SLY- or SLL-PRAME peptides. CTL line #2 recognized ALY, VLD, and SLY peptides and CTL line #1 responded to ALY, VLD, and SLL peptides. This observation suggests that ALY and VLD peptides are more dominant.[16] IFNγ production was specific, as fewer than 25 IFNγ SFC/10^5 cells were produced when PRAME CTLs were incubated with media alone or with an irrelevant peptide (Figure 3A). Although $IFN\gamma^+$ T cells were detectable in 8 of 9 ALY-specific CTL lines, we could clearly identify ALY-$tetramer^+$ cells in only 2 CTL lines (Figure 3B). To evaluate whether this discrepancy between IFNγ release and tetramer staining was due to variable affinity/avidity of the αβTCRs, we compared the numbers of $IFN\gamma^+$ SFCs produced in response to decreasing concentrations of ALY-peptide (ranging from 200 to

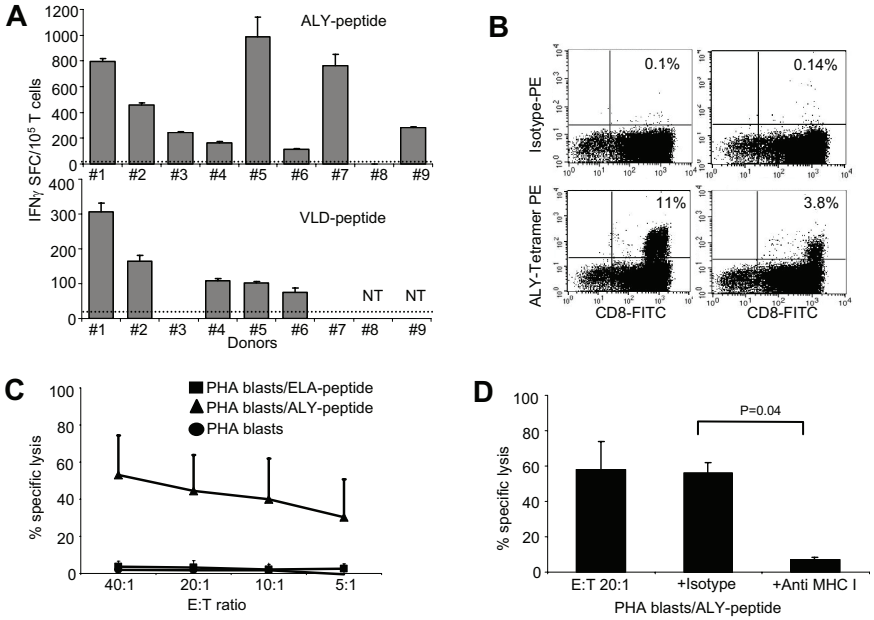

Figure 3. PRAME CTLs can be reproducibly generated from HLA-A*02$^+$ healthy donors. (A) illustrates the frequency of IFNγ + T cells responding to 2 PRAME peptides (ALY and VLD peptides) for PRAME CTL lines generated from 9 HLA-A*02^+ healthy donors after 3 stimulations, as assessed by ELIspot assay. PRAME CTLs from donors 1 and 2 also targeted SLL and SLY peptides, respectively (see "Cytokine release"). Fewer than 25 $IFN\gamma^+$ SFC were counted when CTL lines were pulsed with the ELA-irrelevant peptide (indicated by ----). (B) Staining with the ALY-specific tetramer of 2 PRAME CTL lines generated from healthy donors. (C) PRAME CTLs expanded from healthy donors were evaluated for their cytotoxic activity, using a standard 4-hour ^{51}Cr release assay, against autologous PHA blasts loaded with ALY peptide (▲), ELA-irrelevant peptide (■), or no peptide (●). Data represent the means plus or minus SD of PRAME CTLs from 5 healthy donors. (D) Killing (20:1 E:T ratio) of ALY-loaded autologous PHA blasts by CTLs was significantly inhibited by preincubation of the targets with MHC class I antibody, but not by an isotype control, indicating MHC restricted killing. NT indicates not tested.

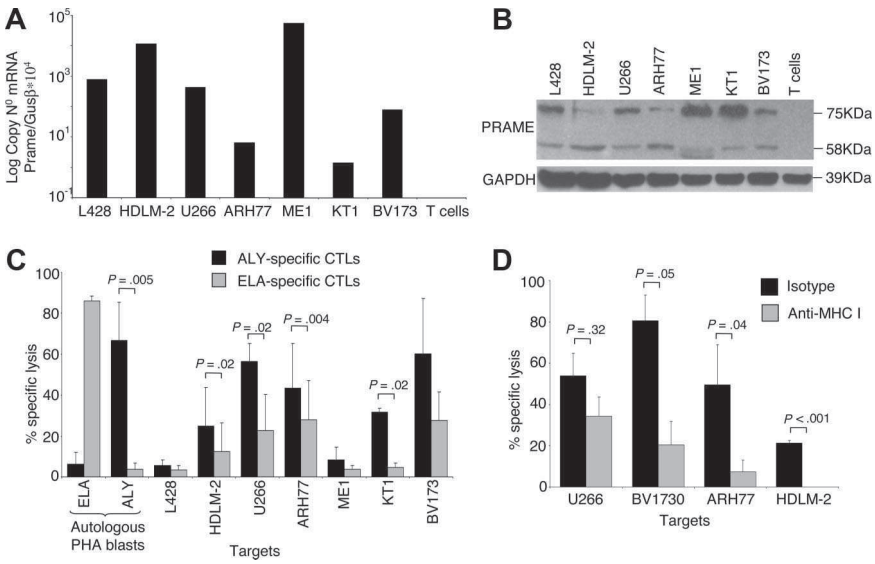

Figure 4. ALY-specific CTLs are cytotoxic to PRAME$^+$ tumor cell lines. (A) Expression of PRAME in several tumor cell lines as assessed by qPCR. (B) Expression of PRAME in the same cell lines by Western blot analysis. In addition to the predicted band (58 kDa), another band of approximately 75kDa was observed, likely originated from posttranscriptional modifications. (C) Cytotoxic activity of ALY-specific CTLs (■) toward tumor cell lines, evaluated using a standard ^{51}Cr release assay. As negative controls, we used (i) CTLs specific for another HLA-A2*02 tumor-restricted epitope (ELA from MART-1 protein; ▩); (ii) autologous PHA blasts loaded with ELA-irrelevant peptide; (iii) the L428 tumor cell line (PRAME$^+$ but HLA-A*02$^-$). As positive control we used autologous PHA blasts loaded with the ALY peptide. Data at a CTLs:tumor cells ratio of 40:1 are shown. Overall, killing of PRAME$^+$/HLA-A*02$^+$ was significantly higher than control cell killing. (D) Killing of PRAME$^+$/HLA-A*02$^+$ cell lines was inhibited by preincubation with MHC class I antibody but not with isotype control, confirming MHC class I restriction.

0.02 nM) between ALY-tetramer$^+$ and ALY-tetramer$^-$ CTLs. We found that ALY-tetramer$^+$ CTLs produced more than 600 IFNγ^+ SFC/10^5 cells when pulsed with 0.2 nM of peptide, whereas only 35 ($\pm$ 8) IFNγ^+ SFC/10^5 were produced by ALY-tetramer$^-$ CTLs (Figure S3A), suggesting that only CTLs with high avidity for ALY peptide were detected by staining with the specific tetramer.

Cytotoxic activity

We evaluated the cytotoxic activity of PRAME CTLs using standard 4-hour ^{51}Cr release assays with autologous PHA blasts loaded with ALY peptide (as the response to this peptide was the most consistently detectable) or irrelevant peptide as target cells. As shown in Figure 3C, PRAME CTLs lysed PHA-blasts loaded with the ALY peptide (average 45% $\pm$ 19%; effector:target [E:T] ratio, 20:1; $P < .001$), but not PHA blasts loaded with an irrelevant peptide (< 10%). The killing mediated by PRAME CTLs was MHC class I–restricted since it was significantly inhibited by preincubation of target cells with anti-HLA class I antibody (7% $\pm$ 1.5%; E:T ratio 20:1), but not by preincubation with the appropriate isotype control antibody (56% $\pm$ 6%; E:T ratio 20:1; $P = .04$; Figure 3D). Notably, not only CTL lines with high avidity but also CTL lines with low avidity for PRAME peptides were cytotoxic to peptide-loaded PHA blasts (data not shown).

PRAME CTLs recognize naturally processed PRAME peptides

The capacity of PRAME CTLs to lyse target cells pulsed with peptides may not predict their recognition and lysis of tumor cells that are naturally expressing and processing PRAME antigens. Therefore, we measured the cytotoxic activity of PRAME CTLs against PRAME-expressing tumor cell lines. As shown in Figure 4A,B, screening of multiple HLA-A*02$^+$ tumor cell lines using both qPCR and Western blot analysis demonstrated that HDLM-2, U266-B1, ARH77, ME1, KT1, and BV173 tumor cell lines expressed PRAME. We then used these tumor cell lines as targets to determine the cytotoxic activity of PRAME CTLs in a standard 4-hour ^{51}Cr release assay. Because CTLs recognizing ALY peptide were consistently generated from healthy donors, we also generated CTLs in which pAPCs and aAPCs were loaded with ALY peptide exclusively. Cytotoxic activity against HLA-A*02$^+$/PRAME$^+$ tumor cell lines was evaluated in CTLs generated using pAPCs and aAPCs loaded either with the peptide pool (data not shown) or with the ALY peptide alone (ALY-specific CTL lines). CTL lines expanded using APCs loaded with the ALY peptide showed more consistent cytotoxic activity. As shown in Figure 4C, killing of HDLM-2, U266-B1, KT1, and BV173 tumor cells by ALY-specific CTL lines was higher than that mediated by CTLs reactivated against ELA peptide from MART-1 (lysis at 40:1 E:T ratio was 25% $\pm$ 19% vs 12% $\pm$ 14% for HDLM-2, $P = .02$; 57% $\pm$ 9% vs 23% $\pm$ 18% for U266-B1, $P = .02$; 49.4% $\pm$ 21.8% vs 27.9% $\pm$ 19% for ARH-77, $P = .004$; 8% $\pm$ 6% vs 4% $\pm$ 2% for ME-1, $P = .5$; 32% $\pm$ 2% vs 5% $\pm$ 2% for KT1, $P = .02$; 60% $\pm$ 27% vs 28% $\pm$ 14% for BV173, $P = .088$; Figure 4C). Killing of autologous PHA blasts loaded with an irrelevant peptide and killing of the PRAME$^+$ but HLA-A*02$^-$ L428 cell line were both less than 10%. Killing mediated by CTLs was MHC class I–restricted (Figure 4D), as it was inhibited by preincubation of target cells with an anti-HLA class I antibody (U266-B1: 34% $\pm$ 13%; BV173: 21% $\pm$ 16%; ARH77: 8% $\pm$ 8%; HDLM-2: 0% $\pm$ 5%), but not with the appropriate isotype control antibody (U266-B1: 54% $\pm$ 15%, $P = .32$; BV173: 80% $\pm$ 16%, $P = .05$; ARH77: 50% $\pm$ 26%, $P = .04$; HDLM-2: 22% $\pm$ 5%, $P = .001$).

PRAME CTLs target PRAME$^+$ CML tumor cells

Because PRAME has been reported previously to be overexpressed in CML tumor cells,[17] we have analyzed its expression in 58 samples obtained from CML patients in different stages of disease.

As shown in Table 1, PRAME mRNA was broadly detectable using qPCR assay in our group of patients, since 46% of them showed between 1/10^4 and 10/10^4 copies of PRAME/GUSb mRNA, and 27% more than 10/10^4 copies. For 7 HLA-A*02$^+$ CML patients (Figure 5A), sufficient PBMCs were available to perform culture experiments. To assess disease stage in these patients we evaluated the percentage of circulating CD33$^+$ and CD34$^+$ cells[36,37] and FISH analysis.[31,32] Samples from patients 1, 2, and 5 lacked circulating CD33$^+$ or CD34$^+$ cells, and cytogeneic analysis showed 100% of Philadelphia (Ph)–negative metaphases. In patient samples 3 and 6, circulating CD33$^+$ cells were 41% and 44%, respectively, whereas CD34$^+$ cells were 0% and 1.5%, respectively, suggesting that these patients were in chronic phase. For the sample obtained from patient 3, cytogenetic analysis showed 80% Ph$^+$ metaphases. In patient sample 4 the

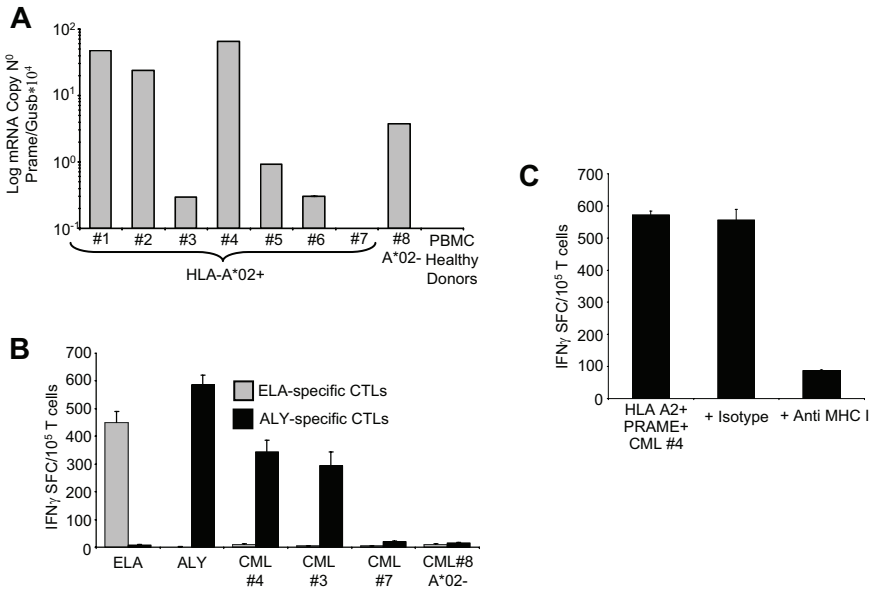

Figure 5. PRAME CTLs can target PRAME$^+$ CML tumor cells. (A) Expression of PRAME mRNA in PBMCs isolated from 8 patients with CML and from a pool of 4 representative healthy donors. In 1 of the HLA-A*02$^+$ CML patients, PRAME mRNA was undetectable ($< 10^{-1}$ normalized copies) as in healthy donors. (B) shows IFNγ production by PRAME CTLs (■) or by ELA-specific CTLs (▩) generated from healthy donors against blasts obtained from CML patients. Significant numbers of IFNγ + SFC were detected in response to PRAME$^+$/HLA-A*02$^+$ CML cells (patients 3 and 4) but not in response to HLA-A*02$^+$ CML cells with undetectable PRAME expression (patient 7) or PRAME$^+$/HLA-A*02$^-$ CML cells (patient 8). Negligible numbers of IFNγ$^+$SFC were released by ELA-specific CTLs. (C) IFNγ production by PRAME CTLs in response to PRAME$^+$/HLA-A*02$^+$ CML cells is reduced by MHC class I antibody.

percentages of circulating CD33$^+$ cells and CD34$^+$ cells were 86% and 50%, respectively, suggesting that this patient was in accelerated/blastic phase. Because CML samples 3 and 4 contained significant numbers of CD33$^+$ cells, we used these samples as a target for PRAME CTLs generated from HLA-A*02$^+$ healthy donors, measuring the CTLs response by IFNγ ELIspot assays. As controls, we used PRAME$^+$ CML blasts from an HLA-A*02$^-$ patient (no. 8) with circulating blasts (CD33$^+$:77% and CD34$^+$: 3%), or incubated MART-1-ELA-peptide specific CTLs with autologous CML blasts. As shown in Figure 5B, ALY-specific CTLs responded both to ALY peptide and to PRAME$^+$/HLA-A*02$^+$ CML blasts. In contrast, few IFNγ$^+$ SFC were detected in response to CML blasts which lacked significant PRAME expression or which were PRAME$^+$ but HLA-A*02$^-$ (Figure 5B). ELA-specific CTLs from the same donors also failed to respond to autologous CML cells (Figure 5B). Furthermore, blocking experiments using anti-HLA class I antibody showed that the production of IFNγ by ALY-specific CTLs in response to CML blasts was MHC restricted (Figure 5C).

PRAME CTL single-cell clones

Because PRAME CTLs generated from healthy donors could be matched with primary PRAME$^+$ cell lines or CML blasts only for HLA-A*02, to ensure that the reactivity we observed was genuinely PRAME-specific and not a manifestation of residual alloreactivity in the CTL lines, we cloned ALY-specific T lymphocytes from the bulk CTL cultures by limiting dilution. We were able to identify several clones (66/111 of the expanded clones) that produced IFNγ in response to the ALY peptide but not to an irrelevant peptide (Figure 6A). As shown in Figure 6B, we also confirmed that these clones were cytotoxic to HLA-A*02$^+$PRAME$^+$ cell lines (such as BV173 and U266-B1), but not to the HLA-A*02$^-$PRAME$^+$ cell line L428. In addition, we found that these clones could target primary CML blasts as assessed by IFNγ ELISpost assay. Figure 6C shows the response of 2 clones to CML blasts. Recognition was mediated through the conventional TCR as it was inhibited by preincubation with MHC class I antibodies.

Generation of PRAME CTLs from CML patients

We next obtained T cells from the peripheral blood of 6 HLA-A*02$^+$ CML patients, and primed them with autologous pAPCs loaded with the pool of PRAME-derived peptides (ALY, VLD, SLY, and SLL) in the presence of IL-7, IL-12, and IL-15. Subsequently we stimulated these cells with peptide loaded K562/aAPCs and IL-2. We were able to detect and expand PRAME CTLs from 5 of the 6 patients tested.

As shown in Figure 7A, in 3 patients we expanded T cells that produced significant amount of IFNγ in response to 2 different PRAME-peptides [ALY (205 ± 24 and 78 ± 11 IFNγ SFC/10^5 T cells) and VLD (20 ± 2 and 103 ± 14 IFNγ SFC/10^5 T cells), or SLY (175 ± 18 IFNγ SFC/10^5 T cells) and VLD (33 ± 6 IFNγ SFC/10^5 T cells)]. In 2 other patients, T cells generated responded to a single PRAME peptide, either ALY (45 ± 4 IFNγ SFC/10^5 T cells) or VLD (33 ± 2 IFNγ SFC/10^5 T cells), but not in response to an irrelevant peptide (all < 5 IFNγ SFC/10^5 T cells) as assessed by the specific ELIspot assay.

These PRAME CTLs obtained from CML patients also recognized autologous tumor cells. As shown in Figure 7B,C, we found that PRAME CTLs from the 2 donors tested produced IFNγ$^+$ SFC when incubated with autologous PRAME$^+$ CML blasts (56 ± 11 IFNγ$^+$ SFC/10^5 T cells for patient 3 and 33 ± 6 IFNγ$^+$ SFC/10^5 T cells for patient 6) but not with PRAME$^-$ CML blasts (Figure 7C). In contrast, CTLs generated from the same patient against the ELA peptide did not produce IFNγ when incubated with PRAME peptides (< 5 SFC/10^5 T cells) or with autologous CML blasts (3 ± 2 IFNγ$^+$ SFC/10^5 T cells; Figure 7B). Unlike those from healthy donors, PRAME CTLs expanded from leukemic patients had low avidity for PRAME-derived peptides, as CTLs did not recognize PRAME tetramers (data not shown) and produced low amounts of IFNγ$^+$ SFC when exposed to low concentrations (<2 nM) of specific peptides (Figure S3B).

Discussion

CML is highly susceptible to control by the immune system, and effector T cells recognizing TAAs overexpressed in tumor cells

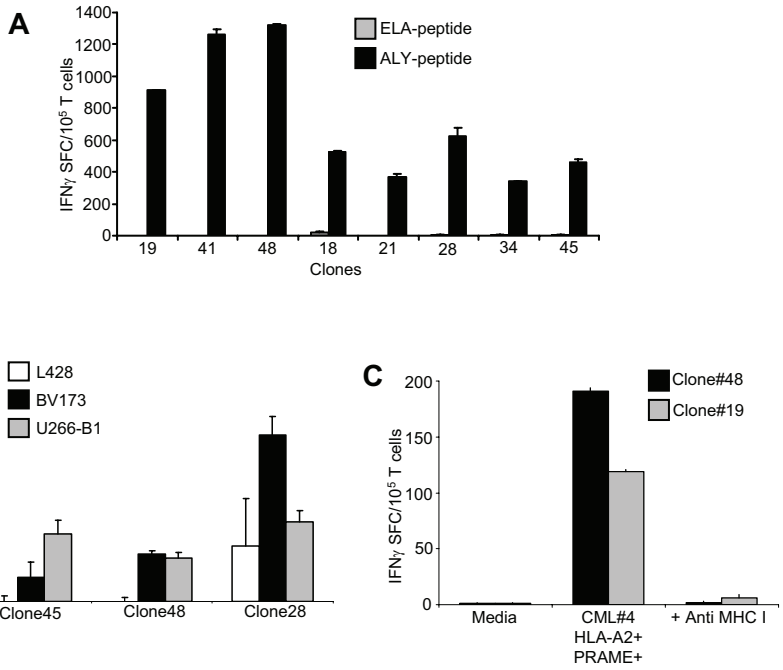

Figure 6. Analysis of clones derived from PRAME CTLs. (A) Specificity of representative single-cell clones targeting the ALY peptide, generated by limiting dilution assay. These representative CTL clones produced significant amounts of IFNγ in response to the ALY peptide but not to ELA-irrelevant peptide. (B) Functional specificity of 3 representative ALY-specific T-cell clones against PRAME$^+$ tumor cell lines. These clones lysed HLA-A*02$^+$/PRAME$^+$ cell lines (BV173, ■ and U266-B1, ▒) but not the HLA-A*02$^-$/PRAME$^+$ cell line (L428, □). (C) Two representative ALY-specific T-cell clones produce significant amounts of IFNγ in response to blasts isolated from a HLA-A*02$^+$/PRAME$^+$ CML patient (patient 4) in a MHC class I–restricted fashion.

may play an important role in this process.[6-8] The identification and validation of candidate antigens with clinical promise is crucial for developing immunotherapies for CML that can be translated to clinical trials. Here, we show that the cancer testis antigen PRAME is one such target. A combination of professional and artificial APCs and cytokines allows PRAME CTLs to be obtained from healthy donors and from CML patients with active disease. These PRAME CTLs recognize and kill tumor cell lines expressing PRAME and also specifically recognize blasts from CML patients expressing endogenous PRAME.

Our results suggest that PRAME may be a suitable target antigen for immunotherapy aimed at control of CML. The 2 most widely considered means of obtaining such an immune response are the use of peptide vaccination to recruit CTLs in vivo ("active" immunity), and the preparation of CTLs ex vivo for adoptive transfer ("passive" immunity). Both strategies are currently being evaluated in patients with hematologic malignancies and solid tumors using other putative target antigens.[12,14,38,39]

Although both active and passive approaches can induce objective clinical responses, adoptive transfer of tumor-specific CTLs, may be better suited than vaccination for the control of advanced disease, at least in patients with melanoma[40] and EBV-associated malignancies.[19,41-43] But although tumor-specific CTLs targeting viral antigens, such as those derived from EBV, are consistently expanded ex vivo from a pool of memory T cells,[44] it has proved harder to consistently prepare CTLs specific for nonviral TAAs such as PRAME. The frequency of CTL precursors specific for TAA/CTA-derived peptides is usually very low, and these cells are rarely detectable in the peripheral blood of healthy individuals.[12] Although it has been reported that PRAME CTL precursors can be detected in PBMCs freshly isolated from healthy donors,[45] we found the frequency to be too low to be quantitated by

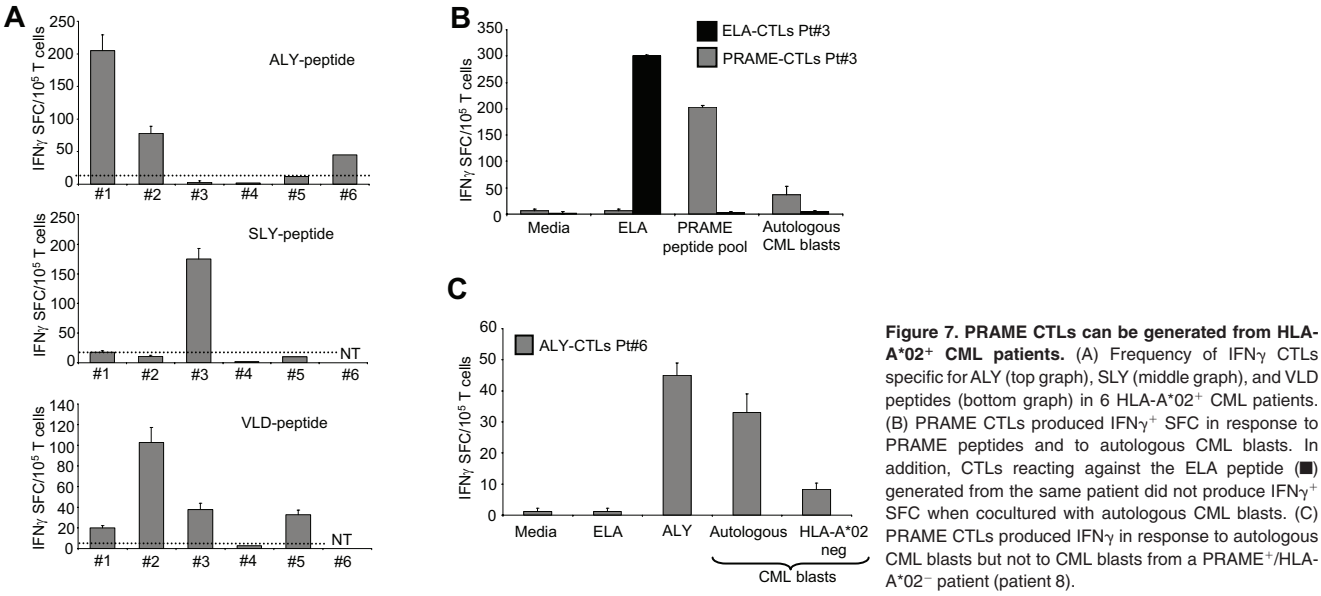

Figure 7. PRAME CTLs can be generated from HLA-A*02$^+$ CML patients. (A) Frequency of IFNγ CTLs specific for ALY (top graph), SLY (middle graph), and VLD peptides (bottom graph) in 6 HLA-A*02$^+$ CML patients. (B) PRAME CTLs produced IFNγ$^+$ SFC in response to PRAME peptides and to autologous CML blasts. In addition, CTLs reacting against the ELA peptide (■) generated from the same patient did not produce IFNγ$^+$ SFC when cocultured with autologous CML blasts. (C) PRAME CTLs produced IFNγ in response to autologous CML blasts but not to CML blasts from a PRAME$^+$/HLA-A*02$^-$ patient (patient 8).

IFNγ ELIspot assay in our cohort of healthy donors. Moreover, these low frequency cells may reside in the naive T-cell subpopulation, or be anergized, so that their recruitment and expansion require the use of potent APCs in combination with several cytokines. Our results show that PRAME CTLs were derived from naive $CD45RA^+/CD8^+$ T cells and that the requirement for pAPCs could not be overcome even by substituting an aAPC with a broad array of costimulatory components (CD80, CD40L, and OX40L), so that pAPCs provide more effective priming for naive T cells. We used B cells exposed to CD40L[21] as our pAPCs because these cells could be reproducibly generated in sufficient numbers from the limited amount of blood available for the study. Although we did not perform a formal comparison between the effectiveness of CD40-activated B cells and DCs, in 1 case in which DCs and CD40-activated B cells were both available, we found no apparent difference. IL-15, a cytokine that plays an important role in breaking immunotolerance and in restoring the function of T cells that have been anergized or tolerized,[46] was also essential for optimal expansion of PRAME CTLs from both healthy donors and CML patients. Fortunately, however, once this initial priming step is overcome, our results show that subsequent expansion steps have less stringent requirements and can be accomplished with an artificial APC and IL-2, simplifying implementation in clinical practice where autologous pAPCs may be limited in number.

The antitumor effect of adoptive T-cell therapies is likely to be enhanced when the infused T cells recognize more than one epitope of viral and/or tumor-associated antigens,[19] because the risk of tumor escape is reduced.[47] Therefore, we determined whether our PRAME responses were directed to more than one of the previously identified HLA-A*02–restricted PRAME epitopes.[16] We found that CTL lines from both healthy donors and CML patients were directed against at least 2 PRAME-derived peptides, ALY and VDL. These CTL lines and clones were functional and could target not only peptide-loaded cells, but also tumor cell lines expressing PRAME and $PRAME^+$ primary CML tumor cells. Hence, the PRAME peptides targeted by these CTL lines are naturally processed and presented in the context of MHC class I even by tumor cells.

In patients with leukemia, CTLs with the highest avidity for tumor-associated antigens such as PR1 may be deleted.[20] Therefore, we examined whether CTL lines generated from healthy donors and CML patients had a different range of avidities for PRAME-derived peptides. We found that PRAME CTLs generated from CML patients with active disease were characterized by a lower avidity for PRAME-derived peptides than CTLs from normal donors. Thus, selective depletion of high-avidity CTLs in patients with leukemia may occur not only for PR1-specific CTLs,[20] but also for PRAME CTLs, and may be a general immune evasion strategy. Our study was not designed to correlate PRAME expression specifically with disease stage, cytogenetic response, or treatment, so we cannot correlate these parameters with the generation of PRAME CTLs from CML patients. Of note, PRAME expression by CML cells may be regulated by epigenetic mechanisms,[48] so that treatment with IFN and/or imatinib may alter PRAME expression and further modify the ability to expand PRAME CTLs from patients in any given stage of disease.

Given our results showing the antileukemic effects of PRAME CTLs, the administration of PRAME peptides to generate T cells in vivo represents a simple, and hence appealing, alternative to the preparation of PRAME CTLs for adoptive transfer ex vivo. Vaccine trials using peptides derived from other leukemia-associated antigens including p210 bcr/abl, PR1, and WT1 have shown promise, although their overall potency may be lower than that of adoptively transferred CTLs.[12,14,20] However, the predominance of low-avidity CTLs in patients with active disease suggests that achievement of minimal residual disease with more conventional therapies before peptide vaccination may be required to allow the generation of T cells with higher avidity for the antigen.[20]

In conclusion, we have confirmed that PRAME is expressed by a significant proportion of CML samples[17] and represents a potential target antigen both for adoptive T-cell therapy and for vaccination of CML patients. Because the highest-avidity CTLs are obtained from healthy donors, this antigen may be of particular value for generating a selective GvL effect after allogeneic stem cell transplantation. Ultimately, CTL administration may be used in sequence with peptide vaccines to maintain long-term immune surveillance.

Acknowledgments

We would like to thank Linda Chapman Golden Funds for the support and Dr Malcolm Brenner for critical revision of the manuscript.

This work was supported in part by the Leukemia & Lymphoma Society Specialized Center of Research (SCOR; grant no. 7018) and Leukemia & Lymphoma Society Translational Research grants (G.D. and B.S.), and by PRIN, MIUR-Rome PS35-126/IND Grants (Rome, Italy), Progetto Integrato Oncologia, Ministero Salute (Rome, Italy), Regione Campania.

Authorship

Contribution: C.Q., B.S., B.D.A., V.H., and G.D. designed and performed experiments; C.Q., G.D., F.P., and B.S. designed the research and analyzed the data; L.L., F.P., and M.M. provided CML samples; H.E.H. and C.M.R. provided expertise in T-cell generation and analyzed the data; C.Q., G.D., F.P., and B.S. wrote the manuscript; and all authors reviewed the manuscript.

Conflict-of-interest disclosure: The authors declare no competing financial interests.

Correspondence: Barbara Savoldo, MD, Center for Cell and Gene Therapy, Baylor College of Medicine, 6621 Fannin Street, MC 3-3320, Houston, TX 77030; e-mail: bsavoldo@bcm.tmc.edu.

References

1. Hehlmann R, Berger U, Pfirrmann M, et al. Drug treatment is superior to allografting as first-line therapy in chronic myeloid leukemia. Blood. 2007;109:4686-4692.
2. Deininger M, Buchdunger E, Druker BJ. The development of imatinib as a therapeutic agent for chronic myeloid leukemia. Blood. 2005;105:2640-2653.
3. Druker BJ, Guilhot F, O'Brien SG, et al. Five-year follow-up of patients receiving imatinib for chronic myeloid leukemia. N Engl J Med. 2006;355:2408-2417.
4. Baccarani M, Saglio G, Goldman J, et al. Evolving concepts in the management of chronic myeloid leukemia: recommendations from an expert panel on behalf of the European LeukemiaNet. Blood. 2006;108:1809-1820.
5. Goldman JM, Melo JV. Chronic myeloid leukemia–advances in biology and new approaches to treatment. N Engl J Med. 2003;349:1451-1464.
6. Dazzi F, Szydlo RM, Goldman JM. Donor lymphocyte infusions for relapse of chronic myeloid leukemia after allogeneic stem cell transplant: where we now stand. Exp Hematol. 1999;27:1477-1486.
7. Luznik L, Fuchs EJ. Donor lymphocyte infusions to treat hematologic malignancies in relapse after allogeneic blood or marrow transplantation. Cancer Control. 2002;9:123-137.
8. Giralt S, Hester J, Huh Y, et al. CD8-depleted donor lymphocyte infusion as treatment for relapsed

chronic myelogenous leukemia after allogeneic bone marrow transplantation. Blood. 1995;86: 4337-4343.

9. Kolb HJ, Schmid C, Barrett AJ, Schendel DJ. Graft-versus-leukemia reactions in allogeneic chimeras. Blood. 2004;103:767-776.
10. Molldrem JJ, Clave E, Jiang YZ, et al. Cytotoxic T lymphocytes specific for a nonpolymorphic proteinase 3 peptide preferentially inhibit chronic myeloid leukemia colony-forming units. Blood. 1997; 90:2529-2534.
11. Molldrem JJ, Lee PP, Wang C, Champlin RE, Davis MM. A PR1-human leukocyte antigen-A2 tetramer can be used to isolate low-frequency cytotoxic T lymphocytes from healthy donors that selectively lyse chronic myelogenous leukemia. Cancer Res. 1999;59:2675-2681.
12. Rezvani K, Yong AS, Mielke S, et al. Leukemia-associated antigen-specific T-cell responses following combined PR1 and WT1 peptide vaccination in patients with myeloid malignancies. Blood. 2008;111:236-242.
13. Yotnda P, Firat H, Garcia-Pons F, et al. Cytotoxic T cell response against the chimeric p210 BCR-ABL protein in patients with chronic myelogenous leukemia. J Clin Invest. 1998;101:2290-2296.
14. Bocchia M, Gentili S, Abruzzese E, et al. Effect of a p210 multipeptide vaccine associated with imatinib or interferon in patients with chronic myeloid leukaemia and persistent residual disease: a multicentre observational trial. Lancet. 2005;365:657-662.
15. Scanlan MJ, Gure AO, Jungbluth AA, Old LJ, Chen YT. Cancer/testis antigens: an expanding family of targets for cancer immunotherapy. Immunol Rev. 2002;188:22-32.
16. Kessler JH, Beekman NJ, Bres-Vloemans SA, et al. Efficient identification of novel HLA-A(*)0201-presented cytotoxic T lymphocyte epitopes in the widely expressed tumor antigen PRAME by proteasome-mediated digestion analysis. J Exp Med. 2001;193:73-88.
17. Paydas S, Tanriverdi K, Yavuz S, Seydaoglu G. PRAME mRNA levels in cases with chronic leukemia: clinical importance and review of the literature. Leuk Res. 2007;31:365-369.
18. Epping MT, Wang L, Edel MJ, et al. The human tumor antigen PRAME is a dominant repressor of retinoic acid receptor signaling. Cell. 2005;122: 835-847.
19. Rooney CM, Smith CA, Ng CY, et al. Infusion of cytotoxic T cells for the prevention and treatment of Epstein-Barr virus-induced lymphoma in allogeneic transplant recipients. Blood. 1998;92: 1549-1555.
20. Molldrem JJ, Lee PP, Kant S, et al. Chronic myelogenous leukemia shapes host immunity by selective deletion of high-avidity leukemia-specific T cells. J Clin Invest. 2003;111:639-647.
21. Coughlin CM, Vance BA, Grupp SA, Vonderheide RH. RNA-transfected CD40-activated B cells induce functional T-cell responses against viral and tumor antigen targets: implications for pediatric immunotherapy. Blood. 2004;103:2046-2054.
22. Biagi E, Dotti G, Yvon E, et al. Molecular transfer of CD40 and OX40 ligands to leukemic human B cells induces expansion of autologous tumor-reactive cytotoxic T lymphocytes. Blood. 2005;105: 2436-2442.
23. Dudley ME, Wunderlich JR, Yang JC, et al. Adoptive cell transfer therapy following nonmyeloablative but lymphodepleting chemotherapy for the treatment of patients with refractory metastatic melanoma. J Clin Oncol. 2005;23:2346-2357.
24. Kawashima I, Hudson SJ, Tsai V, et al. The multi-epitope approach for immunotherapy for cancer: identification of several CTL epitopes from various tumor-associated antigens expressed on solid epithelial tumors. Hum Immunol. 1998;59:1-14.
25. Vonderheide RH, Hahn WC, Schultze JL, Nadler LM. The telomerase catalytic subunit is a widely expressed tumor-associated antigen recognized by cytotoxic T lymphocytes. Immunity. 1999;10: 673-679.
26. Minev B, Hipp J, Firat H, et al. Cytotoxic T cell immunity against telomerase reverse transcriptase in humans. Proc Natl Acad Sci U S A. 2000; 97:4796-4801.
27. Wolfel T, Van Pel A, Brichard V, et al. Two tyrosinase nonapeptides recognized on HLA-A2 melanomas by autologous cytolytic T lymphocytes. Eur J Immunol. 1994;24:759-764.
28. Anichini A, Molla A, Mortarini R, et al. An expanded peripheral T cell population to a cytotoxic T lymphocyte (CTL)-defined, melanocyte-specific antigen in metastatic melanoma patients impacts on generation of peptide-specific CTLs but does not overcome tumor escape from immune surveillance in metastatic lesions. J Exp Med. 1999;190: 651-667.
29. Savoldo B, Huls MH, Liu Z, et al. Autologous Epstein-Barr virus (EBV)-specific cytotoxic T cells for the treatment of persistent active EBV infection. Blood. 2002;100:4059-4066.
30. Savoldo B, Rooney CM, Quiros-Tejeira RE, et al. Cellular immunity to Epstein-Barr virus in liver transplant recipients treated with rituximab for post-transplant lymphoproliferative disease. Am J Transplant. 2005;5:566-572.
31. Alimena G, Breccia M, Luciano L, et al. Imatinib mesylate therapy in chronic myeloid leukemia patients in stable complete cytogenic response after interferon-alpha results in a very high complete molecular response rate. Leuk Res. 2008; 32:255-261.
32. Palandri F, Iacobucci I, Martinelli G, et al. Long-term outcome of complete cytogenetic responders after imatinib 400 mg in late chronic phase, Philadelphia-positive chronic myeloid leukemia: the GIMEMA Working Party on CML. J Clin Oncol. 2008;26:106-111.
33. Sili U, Huls MH, Davis AR, et al. Large-scale expansion of dendritic cell-primed polyclonal human cytotoxic T-lymphocyte lines using lymphoblastoid cell lines for adoptive immunotherapy. J Immunother. 2003;26:241-256.
34. Gahn B, Siller-Lopez F, Pirooz AD, et al. Adenoviral gene transfer into dendritic cells efficiently amplifies the immune response to LMP2A antigen: a potential treatment strategy for Epstein-Barr virus–positive Hodgkin's lymphoma. Int J Cancer. 2001;93:706-713.
35. Quintarelli C, Vera JF, Savoldo B, et al. Co-expression of cytokine and suicide genes to enhance the activity and safety of tumor-specific cytotoxic T lymphocytes. Blood. 2007;110:2793-2802.
36. Banavali S, Silvestri F, Hulette B, et al. Expression of hematopoietic progenitor cell associated antigen CD34 in chronic myeloid leukemia. Leuk Res. 1991;15:603-608.
37. Lanza F, Moretti S, Castagnari B, et al. CD34+ leukemic cells assessed by different CD34 monoclonal antibodies. Leuk Lymphoma. 1995;18 Suppl 1:25-30.
38. Biagi E, Rousseau R, Yvon E, et al. Responses to human CD40 ligand/human interleukin-2 autologous cell vaccine in patients with B-cell chronic lymphocytic leukemia. Clin Cancer Res. 2005;11: 6916-6923.
39. Heslop HE, Stevenson FK, Molldrem JJ. Immunotherapy of hematologic malignancy. Hematology (Am Soc Hematol Educ Program). 2003;331-349.
40. Dudley ME, Wunderlich J, Nishimura MI, et al. Adoptive transfer of cloned melanoma-reactive T lymphocytes for the treatment of patients with metastatic melanoma. J Immunother. 2001;24: 363-373.
41. Savoldo B, Goss JA, Hammer MM, et al. Treatment of solid organ transplant recipients with autologous Epstein Barr virus-specific cytotoxic T lymphocytes (CTLs). Blood. 2006;108:2942-2949.
42. Bollard CM, Aguilar L, Straathof KC, et al. Cytotoxic T lymphocyte therapy for Epstein-Barr virus+ Hodgkin's disease. J Exp Med. 2004;200: 1623-1633.
43. Straathof KC, Bollard CM, Popat U, et al. Treatment of nasopharyngeal carcinoma with Epstein-Barr virus–specific T lymphocytes. Blood. 2005; 105:1898-1904.
44. Savoldo B, Cubbage ML, Durett AG, et al. Generation of EBV-specific CD4+ cytotoxic T cells from virus naive individuals. J Immunol. 2002; 168:909-918.
45. Griffioen M, Kessler JH, Borghi M, et al. Detection and functional analysis of CD8+ T cells specific for PRAME: a target for T-cell therapy. Clin Cancer Res. 2006;12:3130-3136.
46. Teague RM, Sather BD, Sacks JA, et al. Interleukin-15 rescues tolerant CD8+ T cells for use in adoptive immunotherapy of established tumors. Nat Med. 2006;12:335-341.
47. Gottschalk S, Ng CY, Perez M, et al. An Epstein-Barr virus deletion mutant associated with fatal lymphoproliferative disease unresponsive to therapy with virus-specific CTLs. Blood. 2001;97: 835-843.
48. Roman-Gomez J, Jimenez-Velasco A, Agirre X, et al. Epigenetic regulation of PRAME gene in chronic myeloid leukemia. Leuk Res. 2007;31: 1521-1528.

T lymphocytes coexpressing CCR4 and a chimeric antigen receptor targeting CD30 have improved homing and antitumor activity in a Hodgkin tumor model

Antonio Di Stasi,[1] Biagio De Angelis,[1] Cliona M. Rooney,[1-4] Lan Zhang,[1] Aruna Mahendravada,[1] Aaron E. Foster,[1] Helen E. Heslop,[1,2,5] Malcolm K. Brenner,[1,2,5] Gianpietro Dotti,[1,4,5] and Barbara Savoldo[1,2]

[1]Center for Cell and Gene Therapy and Departments of [2]Pediatrics, [3]Molecular Virology and Microbiology, [4]Immunology, and [5]Medicine, Baylor College of Medicine, Methodist Hospital and Texas Children's Hospital, Houston

For the adoptive transfer of tumor-directed T lymphocytes to prove effective, there will probably need to be a match between the chemokines the tumor produces and the chemokine receptors the effector T cells express. The Reed-Stemberg cells of Hodgkin lymphoma (HL) predominantly produce thymus- and activation-regulated chemokine/CC chemokine ligand 17 (TARC/CCL17) and macrophage-derived chemokine (MDC/CCL22), which preferentially attract type 2 T helper (Th2) cells and regulatory T cells (Tregs) that express the TARC/MDC-specific chemokine receptor CCR4, thus generating an immunosuppressed tumor environment. By contrast, effector CD8$^+$ T cells lack CCR4, are nonresponsive to these chemokines and are rarely detected at the tumor site. We now show that forced expression of CCR4 by effector T cells enhances their migration to HL cells. Furthermore, T lymphocytes expressing both CCR4 and a chimeric antigen receptor directed to the HL associated antigen CD30 sustain their cytotoxic function and cytokine secretion in vitro, and produce enhanced tumor control when infused intravenously in mice engrafted with human HL. This approach may be of value in patients affected by HL. (Blood. 2009;113:6392-6402)

Introduction

Adoptive transfer of Epstein-Barr virus (EBV)–specific cytotoxic T lymphocytes (CTLs) can induce prolonged disease stabilization and complete remissions in patients with EBV-associated Hodgkin lymphoma (HL).[1,2] The great majority of HL, however, lack EBV antigens and so cannot benefit from this promising approach.[3] CD30 is an alternative target antigen because it is expressed by virtually all Reed-Stemberg cells.[4] Adoptive transfer of T lymphocytes that are genetically modified to express a CD30-specific chimeric antigen receptor (CAR-CD30), which combines the antigen-binding domain of a monoclonal CD30 antibody (scFv) with the ζ chain of the CD3/T-cell receptor complex, may therefore be of value in HL that lacks EBV antigens.[5]

Previous studies have shown that retargeting effector T cells to tumor antigens by the expression of CAR molecules is necessary but not sufficient for clinical responses.[6] One additional requirement is that modified T cells should effectively traffic to the tumor sites.[7] This aspect may be particularly problematic for HL as the tumor generates a chemokine milieu that significantly influences which T-cell subtypes traffic to and accumulate in the tumor.[8,9] For instance, Reed-Stemberg cells produce the chemokines thymus- and activation-regulated chemokine/CC chemokine ligand 17 (TARC/CCL17) and macrophage-derived chemokine (MDC)/CCL22 that attract T helper (Th2) cells and regulatory T cells (Tregs),[9,10] which express CCR4, the receptor for these chemokines.[9-14] In contrast, CD8$^+$ effector T cells, which lack CCR4 expression, are rarely detected within HL tumors, a result probably attributable to an incompatible match between the chemokines secreted by the tumor cells and the chemokine receptors expressed by the effector T cells.

The abundance of Tregs (and Th2 cells) in tumors including HL can create a hostile immune microenvironment by impairing the antitumor activity of the few cytotoxic-effector T lymphocytes able to reach the tumor site.[11] Thus, increasing the number of cytototxic T cells that efficiently reach the tumor site should enhance antitumor responses.

We now show that migration of CAR-CD30-redirected, effector T lymphocytes toward an HL-generated TARC gradient is improved by forced expression of CCR4. Transgenic expression of CCR4 does not impede the functionality of these cells; consequently, their overall antilymphoma activity is enhanced in vivo.

Methods

Tumor cell lines

The HL-derived cell lines HDLM-2, L-428, L-1236, L-540, KM-H2, and the anaplastic large cell lymphoma-derived cell line Karpas-299 were obtained from the German Collection of Cell Cultures (DMSZ, Braunschweig, Germany). These cell lines are CD30$^+$ but lack expression of EBV-associated antigens. All cells were maintained in culture with RPMI 1640 medium (HyClone Laboratories, Logan, UT) containing 10% fetal bovine serum (HyClone Laboratories) and 2 mM L-glutamine (Invitrogen, Carlsbad, CA). Cells were maintained in a humidified atmosphere containing 5% CO_2 at 37°C.

Retroviral constructs

Full-length human CCR4 was cloned by reverse-transcribed polymerase chain reaction from OKT3-(Ortho Biotech Products, Bridgewater, NJ) activated CD4$^+$ cells cultured for 5 days with IL-4 (1000 U/mL; R&D

Submitted March 8, 2009; accepted April 6, 2009. Prepublished online as *Blood* First Edition paper, April 17, 2009; DOI 10.1182/blood-2009-03-209650.

The publication costs of this article were defrayed in part by page charge payment. Therefore, and solely to indicate this fact, this article is hereby marked "advertisement" in accordance with 18 USC section 1734.

Table 1. Tumor cell lines

	TARC, pg/mL	MDC, pg/mL
HL		
HDLM-2	> 2000	> 4000
L428	> 2000	< 62.5
L540	691 ± 116	285 ± 94
KH-M2	918 ± 183	< 62.5
L1236	> 2000	657 ± 60
ALCL		
Karpas-299	93 ± 33	< 62.5
Karpas-299/TARC	> 2000	Not done

ALCL indicates anaplastic large-cell lymphoma; TARC, thymus- and activation-regulated chemokine; and MDC, macrophage-derived chemokine.

Systems, Minneapolis, MN). CCR4 was cloned into the SFG retroviral vector.[15] The retroviral vector encoding the CAR-CD30 was kindly provided by Drs H. Abken and A. Hombach and previously described.[5,16] For this study, we constructed a second-generation CAR-CD30 in which we included the CD28 endodomain to augment costimulation of the modified T cells after antigen engagement of their chimeric receptor.[17,18] We also generated a bicistronic retroviral construct encoding both CCR4 and CAR-CD30 in which CAR-CD30 is driven by an internal ribosome entry site [CCR4(I)CAR-CD30]. The chemokine TARC was cloned by reverse-transcribed polymerase chain reaction from the HDLM-2 cell line and subcloned into a retroviral vector (PL-x-SP) containing the puromycin resistance gene as a selectable marker (PL-TARC-SP). Two additional retroviral vectors encoding eGFP-Firefly-Luciferase (eGFP-FFLuc) and Firefly-Luciferase gene (FFLuc) were used to label T lymphocytes and tumor cells, respectively, for in vivo study as previously described.[16,18] Transient retroviral supernatant was produced using 293T cells, as previously described.[16,18] Karpas-299 cell line (Karpas/wt) that does not produce the chemokine TARC was genetically modified with PL-TARC-SP and selected using puromycin (Sigma-Aldrich, St Louis, MO) to generate Karpas/TARC cells that produce significant amounts of TARC that could be detected in the supernatant by specific enzyme-linked immunosorbent assay (ELISA).

Generation and transduction of effector cells

Peripheral blood mononuclear cells (PBMCs) were activated in 24-well plates coated with OKT3 and CD28 antibodies (BD Biosciences PharMingen, San Diego, CA) in the presence of recombinant human interleukin-2 (IL-2, 100 U/mL; Proleukin, Chiron, Emeryville, CA). Activated T cells were transduced on day 3 in 24-well plates precoated with recombinant fibronectin fragment (FN CH-296; Retronectin; Takara, Kyoto, Japan) using specific retroviral supernatant and IL-2, as previously described.[18,19] T cells were then collected and expanded in T-cell media (50% RPMI, 50% Click [Irvine Scientific, Santa Ana, CA], 10% fetal bovine serum, and 2 mM L-glutamine) using IL-2 (50-100 U/mL) to obtain sufficient number of cells to perform the experiments in vitro and in vivo.

Transwell migration assay

Migration was assessed using 5-μm pore 24-transwell plates (Corning Life Sciences, Acton, MA). The lower chamber was loaded with culture supernatant containing the chemokine of interest. To obtain supernatant, cell lines (HDLM-2, L428, Karpas/wt, and Karpas/TARC) were cultured for 16 hours in serum-free medium (AIM-V, Invitrogen) at a concentration of 10^6 cells/mL. Supernatant was then collected and centrifuged before being loaded in the lower chamber. Effector cells (10^5) labeled with ^{51}Cr (100 μCi) were added to the upper chamber. As a positive control, effector cells were placed directly into the lower chamber. As a negative control, medium without chemokine was placed into the lower chamber. Plates were incubated for 4 to 5 hours at 37°C, 5% CO_2. At the end of the incubation period, the transwell inserts were removed and the content of the lower compartment carefully recovered. Cells were lysed with Triton-X (Sigma-Aldrich) and chromium release measured using a gamma counter (PerkinElmer Life and Analytical Sciences, Waltham, MA). The percentage of migrating cells was calculated as follows: 100× [cpm from experimental supernatant (cells migrated in the lower chamber) − cpm in the presence of media only (random migration)]/[cpm of positive control − cpm random migration]. To evaluate specific migration, neutralizing antibodies for the chemokine TARC (R&D Systems) or appropriate isotype controls (R&D Systems) were added to lower chamber before the chemotactic assay.

Enzyme-linked immunosorbent assay and cytometric bead array

The production of the chemokines TARC and MDC were quantified by specific ELISA using commercially available kits (R&D Systems, Pepro-Tech, Rocky Hill, NJ). Supernatants tested with ELISA were collected from the cultures used for the chemotactic assay. Supernatants collected 24 hours after activation with OKT3 (100 ng/mL) of transduced or control T cells was tested using the Th1/Th2 CBA assay (BD Biosciences PharMingen).

Phenotypic analysis

Expression of cell surface molecules was determined by flow cytometry using standard methodology. The following monoclonal antibodies conjugated with phycoerythrin, fluorescein isothiocyanate, and/or peridinin chlorophyll protein were used: CD3, CD4, CD8, CD30, CCR4, CD45RA, CD45RO, CCR7, CD62L, CD56, αβT-cell receptor (BD Biosciences PharMingen). Expression of CAR by T cells was detected using Cy-5–conjugated goat anti–human IgG (H+L) antibodies (Jackson ImmunoResearch Laboratories, West Grove, PA), which recognizes the human IgG1-CH2-CH3 component incorporated as a spacer region within the CAR. Samples were analyzed using a FACSCalibur (BD Biosciences PharMingen), and data were analyzed by CellQuest Pro software (BD Biosciences, San Jose, CA). At least 10 000 positive events were measured for each sample.

Cytotoxicity assay

The cytotoxic activity of transduced effector cells was evaluated using a 4-hour ^{51}Cr release assay as previously described.[16] Target cells were: Daudi cell line ($CD30^+ < 0.1\%$), HDLM-2 ($CD30^+ = 100\%$), and Karpas-299 ($CD30^+ = 100\%$). ^{51}Cr labeled target cells incubated in complete medium or 1% Triton X-100 were used to determine spontaneous and maximal ^{51}Cr release, respectively. After 4 hours, supernatants were collected and radioactivity was measured on a gamma counter. The mean percentage of specific lysis of triplicate wells was calculated as 100 × (experimental release − spontaneous release)/(maximal release − spontaneous release).

Inhibition assay

PBMCs were labeled with carboxyfluorescein succinimidyl ester (CFSE, Invitrogen) following the manufacturer's instructions. PBMCs were then stimulated with irradiated (40 Gy) allogeneic PBMCs (at a 4:1 effector/target ratio) and OKT3 0.5 μg/mL. Control or transduced T cells were added to the culture (at a 1:1 ratio) to evaluate inhibition of proliferation. As positive control, naturally occurring Treg cells ($CD4^+CD25^{bright}$), were isolated from PBMCs using immunomagnetic selection with CD25 magnetic beads (2 μL/10^7 cells), followed by selection of $CD4^+$, according to Godfrey et al.[20] On day 6, cells were labeled with CD4 peridinin chlorophyll protein and CD8 phycoerythrin and CFSE dilution analyzed using a FACSCalibur to assess cell division.

In vivo experiments

All mouse experiments were performed in accordance with Baylor College of Medicine Animal Husbandry and Institutional Animal Care and Use

Table 2. Expression of CCR4 on T cells

Cell type	$CD3^+$	$CD4^+$	$CD8^+$
Circulating T cells	5.6% ± 3.2%	5.0% ± 3.4%	0.7% ± 0.8%
OKT3/CD28-activated T cells	19.1% ± 8.8%	13.5% ± 3.8%	3.0% ± 3.8%

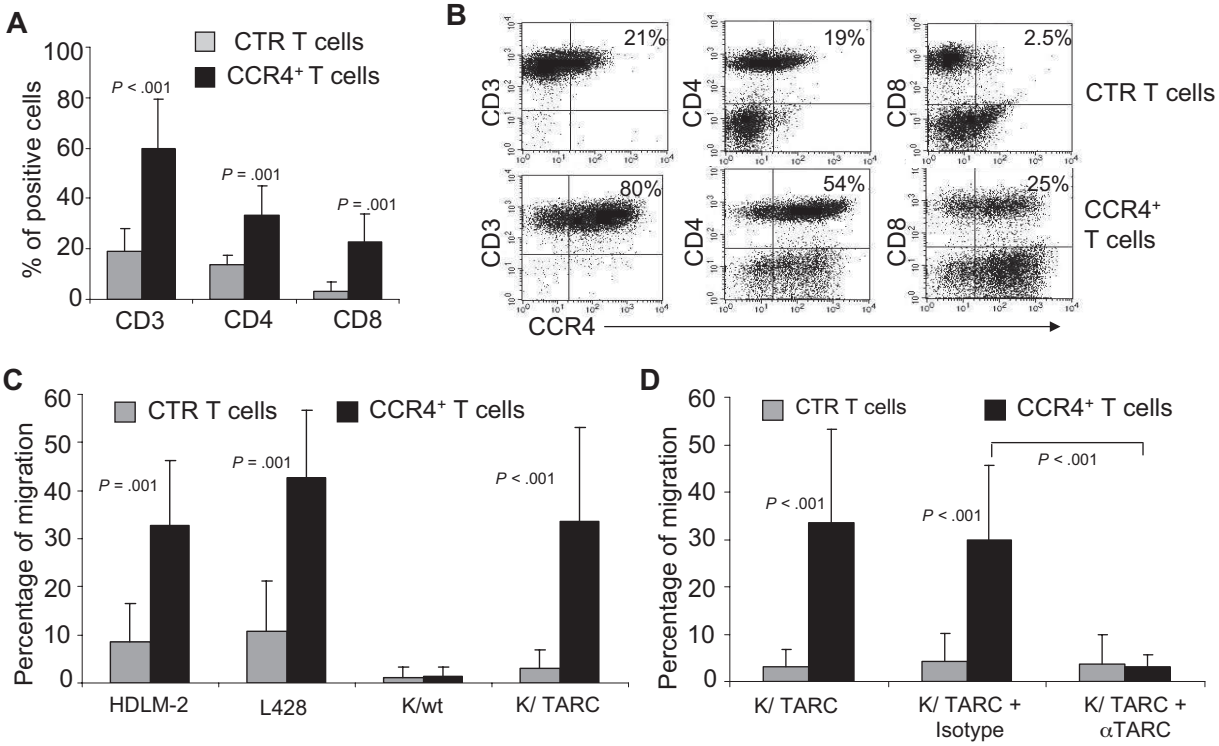

Figure 1. Improved migration of activated T lymphocytes genetically modified to overexpress CCR4. (A) The expression of CCR4 in control (CTR) T cells and in T lymphocytes transduced with a retroviral vector encoding CCR4. Surface expression of CCR4 was evaluated by FACS analysis of $CD3^+$, $CD4^+$, and $CD8^+$ T lymphocytes. represent the mean ± SD of control T cells; ■, mean ± SD of $CCR4^+$ T cells. The data summarize the results of T-cell lines generated from 7 healthy donors. (B) A representative phenotypic analysis. (C) The migration of CTR ( ) and $CCR4^+$ (■) T cells toward TARC gradients, using a transwell migration assay. T-cell migration was evaluated using culture supernatants collected from 2 HL-derived cell lines (HDLM-2 and L428) that physiologically produce high amounts of TARC, and against the Karpas-299 cell line genetically modified to produce TARC (K/TARC). K/wt was used as a control. The panel indicates that migration toward TARC is significantly improved if T cells are genetically modified to overexpress CCR4. The data are the mean ± SD for T-cell lines generated from 7 healthy donors. (D) The improved migration of $CCR4^+$ T cells (■) is TARC mediated as it is inhibited by addition of anti-TARC antibodies but not by the addition of an isotype control.

Committee guidelines and were approved by the Baylor College of Medicine's Institutional Review Board.

Homing

To assess homing and localization of control and genetically modified T cells in vivo, we used a severe combined immunodeficiency (SCID) mouse model and the In Vivo Imaging System (IVIS) imaging system (Xenogen, Caliper Life Sciences, Hopkinton, MA). Six- to 8-week-old CB17/SCID mice (Harlan, Indianapolis, IN) were sublethally irradiated (230 cGy) and engrafted subcutaneously with 5×10^6 $CD30^+$ tumor cells (Karpas/wt) on the left side and with the same tumor cells engineered to secret TARC (Karpas/TARC) on the contralateral side. Five to 7 days later, the mice received intravenous injection of 10×10^6 control or genetically modified T cells and IL-2 (Teceleukin, Fisher Bioservices, Rockville, MD) intraperitoneally (500 U/mouse) 3 times a week. To track the cells in vivo, both control and genetically modified cells were transduced with the eGFP-FFLuc vector. T-cell migration was evaluated using the IVIS imaging system. Briefly, a constant region of interest was drawn over the tumor regions and the intensity of the signal measured as total photon/sec/cm^2/sr (p/s/cm^2/sr) as previously described.[16,18,21]

Antitumor activity

Because there are few reproducible systemic models of HL, we assessed the antitumor activity of T cells transduced with the bicistronic vector CCR4(I)CAR-CD30 using NOG/SCID/γc^{null} mice that reproducibly allow subcutaneous engraftment of $CD30^+TARC^+$ HL cell lines, including HDLM-2.[22] To measure the in vivo growth of these cells, HDLM-2 were transduced with the FFLuc vector and selected in puromicin. $FFLuc^+$ HDLM-2 cells (3×10^6 cells/mice) were resuspended in Matrigel (BD Biosciences, San Jose, CA) and injected subcutaneously. Three to 5 days later, when the light emission of the tumor was consistently measurable, mice received intravenous control or genetically modified T cells (10×10^6 cells/mouse) and IL-2 intraperitoneally (500 U/mice) twice a week. To monitor tumor growth, the IVIS imaging system (Xenogen) was used as described in "Homing."

Statistical analysis

All in vitro data are presented as average plus or minus SD. Student *t* test was used to determine the statistical significance of differences between samples, and *P* values less than .05 were accepted as indicating a significant difference. For the bioluminescence experiments, the homing of T cells to the tumor site was expressed as fold expansion of the light intensity and compared between light intensity at Karpas/wt and Karpas/TARC tumor sites. Changes in intensity of signal from baseline at each time point were calculated and compared using paired *t* tests or Wilcoxon signed-ranks test.

Results

HL cell lines secrete TARC and MDC chemokines but activated T lymphocytes lack CCR4 expression

Identification of cell lines producing TARC and MDC chemokines. We first evaluated the production of TARC and MDC by HL-derived cell lines (HDLM-2, L428, L540, KH-M2, and L1236) and confirmed that all lines released significant amounts of TARC (ranging from 700 pg/mL/10^6 cells to > 2000 pg/mL/10^6 cells) and 3 lines (HDLM-2, L540, and L1236) also released MDC (ranging from 200 pg/mL/10^6 cells to 700 pg/mL/10^6 cells; Table 1). We

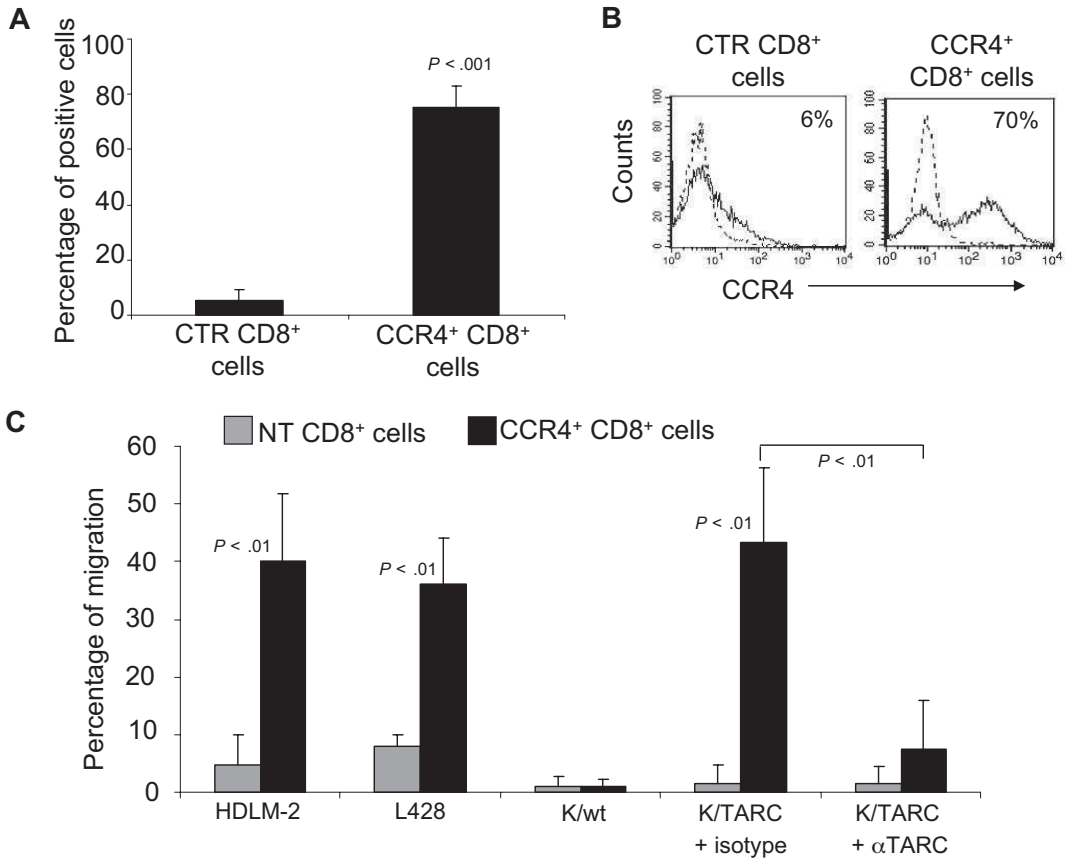

Figure 2. Improved migration of CD8$^+$ T lymphocytes genetically modified to overexpress CCR4. (A) The expression of CCR4 by CTR and transduced CD8$^+$ T cells, using FACS analysis. The data summarize the results of T-cell lines generated from 4 healthy persons. (B) A representative phenotypic analysis. Dotted lines indicate isotype control. (C) The migration of CTR (▒) and CCR4$^+$ (■) CD8$^+$ T cells toward TARC gradients, using a transwell migration assay. The panel indicates that migration toward TARC is significantly increased when CD8$^+$ T cells overexpress CCR4. The data are the mean ± SD for CD8$^+$ T-cell lines generated from 4 healthy donors.

selected 2 cell lines, HDLM-2, producing both chemokines, and L428, producing only TARC, in which to evaluate the effects of TARC/MDC and CCR4 interaction. In addition, we used Karpas-299, an anaplastic large cell lymphoma cell line that expresses the target antigen CD30 but does not secrete TARC or MDC, as a negative control (Table 1).

Expression of CCR4. We next determined the expression of CCR4 by freshly isolated and recently activated T cells. Only a small fraction of freshly isolated CD3$^+$ cells expressed CCR4 (5.6% ± 3.2%). Cells expressing CCR4 were mainly CD4$^+$ (5.0% ± 3.4%), and expression was almost undetectable in CD8$^+$ cells (0.7% ± 0.8%; Table 2). Five days after activation with OKT3 and CD28 antibodies, T lymphocytes showed a modest increase of CCR4 expression on CD4$^+$ cells (13.5% ± 3.8%), but CD8$^+$ cells continued to have low or undetectable levels of the chemokine receptor (3.0% ± 3.8%; Table 2).

Hence, TARC production is a consistent biologic property of HL cells, and the lack of CCR4 expression by activated CD8$^+$ T lymphocytes may impede their migration to sites of disease.

Functional expression of CCR4 can be obtained in activated T lymphocytes using gene transfer. PBMCs isolated from 7 healthy donors were activated and then transduced with a retroviral vector encoding CCR4. After transduction, CCR4 expression increased from 19% plus or minus 9% to 60% plus or minus 19% ($P < .001$; Figure 1A,B), as assessed by FACS analysis. In the transgenic population, CCR4 was expressed by both CD4$^+$ (33% ± 12%) and CD8$^+$ T lymphocytes (23% ± 12%). Receptor expression was stable over 4 weeks of culture (data not shown). To discover whether transgenic CCR4 was functional, we compared the migration of control and CCR4-transduced (CCR4$^+$) T lymphocytes toward TARC gradients using a transwell migration assay. As shown in Figure 1C, CCR4$^+$ T lymphocytes had significantly improved migration toward culture supernatant collected from HL cell lines that naturally secrete TARC (percentage migration, 32% ± 13% and 43% ± 14% toward HDLM-2 and L-428 supernatants, respectively) compared with control T cells (percentage migration, 8% ± 6% and 11% ± 10% toward HDLM-2 and L-428 supernatants, respectively; both $P = .001$). To further confirm that the migration was exclusively mediated by TARC/CCR4 interaction, we compared the migration activity of control and CCR4$^+$ T cells toward the supernatants collected from the wild-type Karpas tumor cell line (Karpas/wt, TARC negative) and its counterpart that had been genetically modified to produce TARC (Karpas/TARC; TARC > 2000 pg/mL/10^6 cells in the supernatant, as assessed by ELISA; Table 1). Both control and CCR4$^+$ T cells had negligible migration toward Karpas/wt supernatant (percentage migration, 1.2% ± 2.2% and 1.3% ± 2%, respectively; Figure 1C). In contrast, we observed significant migration of CCR4$^+$ T cells (percentage migration, 34% ± 20%), but not of control T cells (percentage migration, 4% ± 4%; $P < .001$), toward Karpas/TARC supernatant (Figure 1C). Importantly, migration of CCR4$^+$ T cells was inhibited by the addition of a TARC-blocking antibody (percentage migration, 3% ± 3%) but not by an isotype control (percentage migration, 30% ± 16%; $P < .001$; Figure 1D).

Because control T cells showed some migration when incubated with supernatant collected from HL cell lines, which is

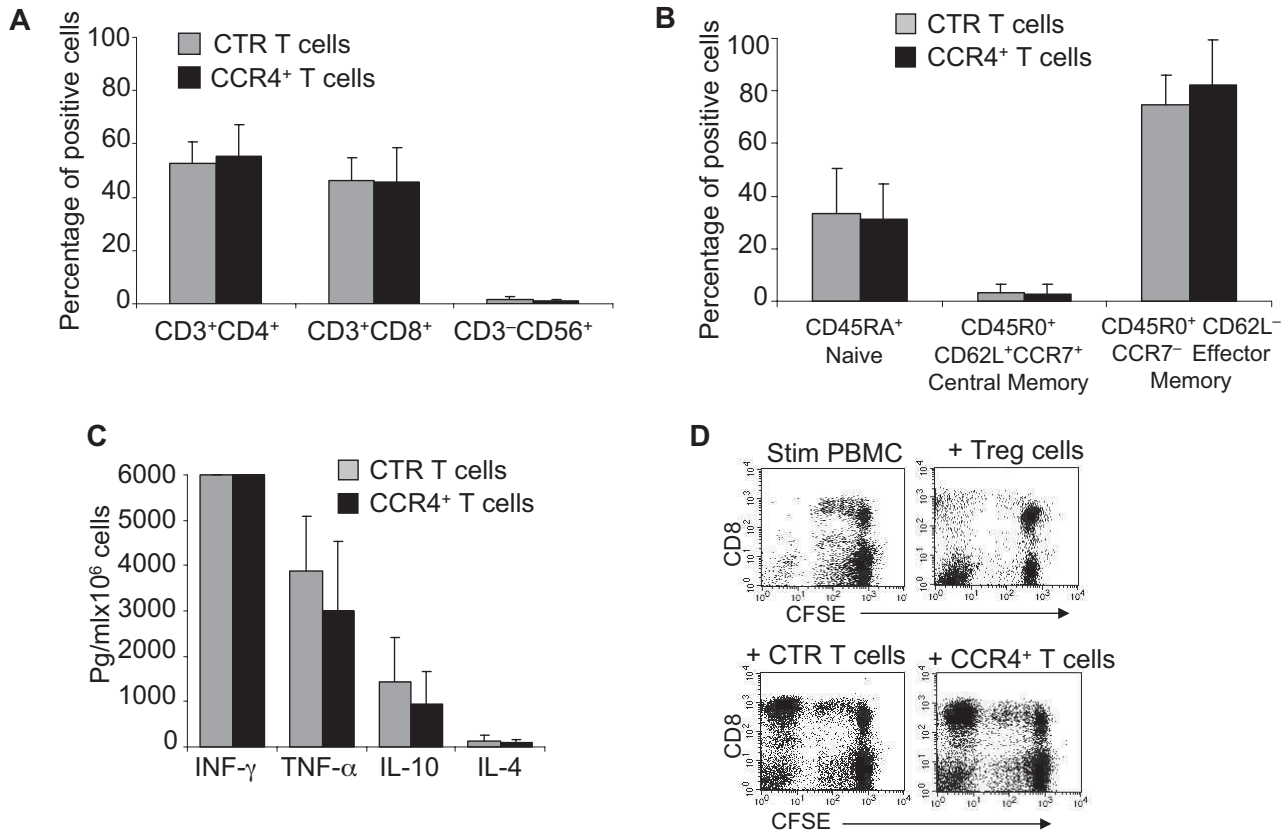

Figure 3. Immunophenotype and function of T cells overexpressiong CCR4 are retained. (A) The phenotypic composition of NT (▒) and CCR4$^+$ (■) T cells. The data are mean ± SD of 5 healthy donors. T-cell markers are shown on the x-axis. No significant differences were observed if cells overexpressed CCR4. (B) Expression of naive, central memory, and effector memory surface markers on CTR (▒) and CCR4$^+$ (■) T cells is not significantly different. The data are mean ± SD of 4 donors. (C) The production of Th1 (IFN-γ and TNF-α) and Th2 (IL-10 and IL-4) cytokines by CTR (▒) and CCR4$^+$ (■) T cells 24 hours after stimulation with OKT3. No significant differences in cytokine production were detected, suggesting that the transgenic expression of CCR4 does not induce the acquisition of a Th2 profile. (D) CCR4$^+$ T cells do not acquire inhibitory function. The inhibitory activity of T cells was evaluated using a CFSE-based suppression assay in which PBMCs labeled with CFSE are stimulated with irradiated allogeneic PBMCs and OKT3 in the absence (top left graph) or in the presence of freshly isolated CD4$^+$CD25^{bright} cells (top right graph), CTR (bottom left graph), or CCR4$^+$ T cells (bottom right graph). The panel indicates a significant number of divisions (CFSE partitioning) of T cells in the absence or presence of CTR or CCR4$^+$ T cells (evident in the left quadrants). In contrast, the divisions are significantly reduced in the presence of Treg cells. Shown is one of 3 donors studied, illustrative of results from all.

probably mediated by the fraction of CD4$^+$ T cells that physiologically express CCR4, we repeated the migration assays using only CD8$^+$ T lymphocytes, which lack CCR4 (5% ± 4% by FACS analysis; Figure 2A,B), and compared them with the migration of CD8$^+$ cells genetically modified to express CCR4 (75% ± 7% by FACS analysis; Figure 2A,B). We found that TARC-mediated migration of CD8$^+$CCR4$^+$ cells toward supernatant collected from HDLM-2 and L428 cells was significantly increased (40% ± 12% and 36% ± 15%, respectively) compared with control CD8$^+$ T cells (4.7% ± 5% and 8% ± 2%; $P < .01$; Figure 2C). Similarly, migration of CD8$^+$ CCR4$^+$ T cells toward Karpas/TARC (43% ± 13%) was improved compared with Karpas/wt (1% ± 1%; $P < .001$). In addition, this migration was specifically inhibited by a TARC-blocking antibody (7% ± 8%) but not by an isotype control (43% ± 13%; $P = .001$). As expected, no significant migration was observed for control CD8$^+$ T cells toward Karpas/wt (1% ± 2%) or Karpas/TARC (3% ± 4%; Figure 2C).

T lymphocytes expressing transgenic CCR4 do not acquire inhibitory properties. As TARC/CCR4 interaction seems to play an important role in attracting Th2 and Tregs,[10,13] we next determined whether forced expression of CCR4 conferred inhibitory properties to the modified cells. We first compared the expression of T-cell markers (CD3, CD4, CD8, CD56, CD45RA, CD45RO, CD62L, and CCR7) by control and CCR4$^+$-activated T cells and found that CCR4$^+$ cells were comparable phenotypically to control T cells (Figure 3A), including the components of naive and effector-memory cells described previously[23] (Figure 3B). We then examined the cytokines released by these cells after activation with OKT3 monoclonal antibody. As shown in Figure 3C, CCR4$^+$ T cells continued to secrete interferon-γ (IFN-γ, > 6000 pg/mL per 10^6 cells) and tumor necrosis factor-α (TNF-α, 2900 ± 1550 pg/mL per 10^6 cells) similar to control T cells (> 6000 pg/mL per 10^6 cells and 3890 ± 1200 pg/mL per 10^6 cells, respectively). Moreover, production of the cytokines IL-4 and IL-10, which are associated with Th2 or Treg cells, was not significantly increased in CCR4$^+$ cells (101 ± 76 pg/mL per 10^6 cells and 960 ± 688 pg/mL per 10^6, respectively) compared with control T cells (130 ± 109 pg/mL per 10^6 cells and 1450 ± 955 pg/mL per 10^6, respectively). To discover whether CCR4$^+$ T cells acquired suppressive function, PBMCs were labeled with CFSE and then stimulated with irradiated allogeneic antigen-presenting cells (APCs) and OKT3, with or without the addition of control or CCR4$^+$ T cells. As shown in Figure 3D, the proliferation of CD8$^+$ T cells was unaffected by either control or CCR4$^+$ T cells, suggesting that CCR4$^+$ cells do not acquire inhibitory properties. In contrast, the proliferation of CD8$^+$ T cells was significantly inhibited when CD4$^+$CD25^{bright} Tregs were added to the culture.

Forced expression of CCR4 can be obtained in T lymphocytes isolated from HL patients. To ensure this approach was feasible in patients affected by HL, we evaluated whether CCR4 could be

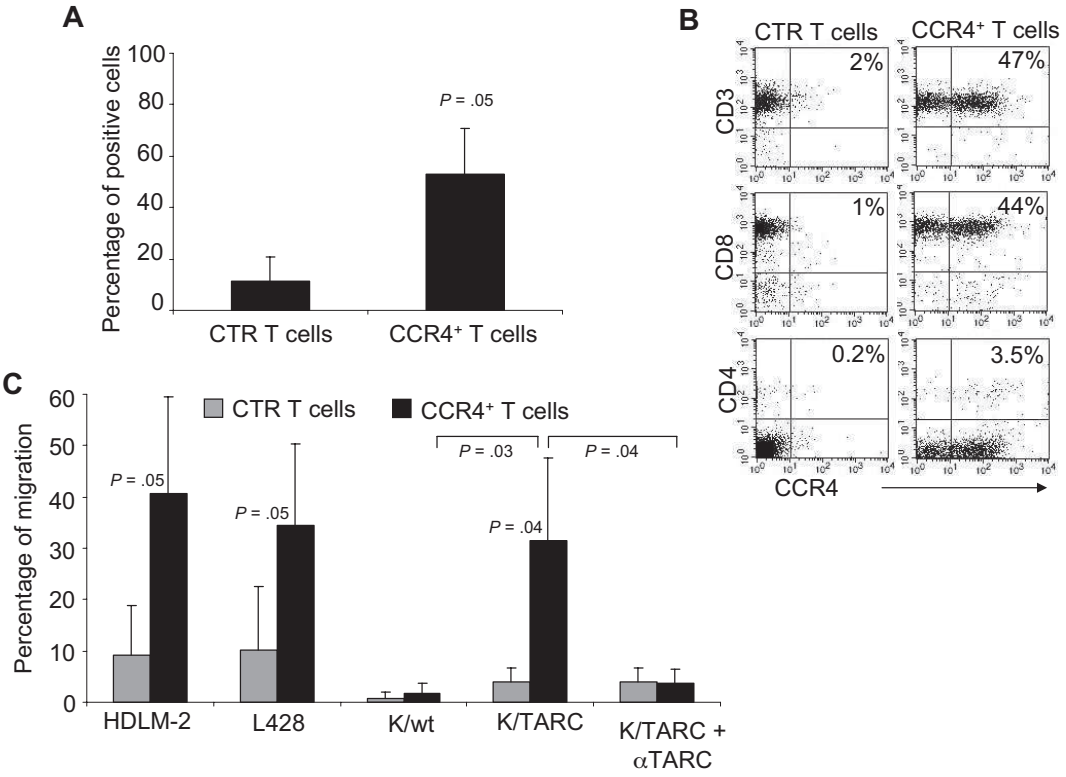

Figure 4. Expression and improved migration of CCR4$^+$ T cells established from persons affected by HL. (A) The expression of CCR4 by CTR (▒) and transduced (■) T cells established from 4 persons with HL. The data are mean ± SD. (B) A representative phenotypic analysis. (C) The migration of CTR (▒) and CCR4$^+$ (■) T cells toward TARC gradients, using a transwell migration assay. T-cell migration was evaluated using culture supernatants collected from HDLM-2 and L428, which physiologically produce high amounts of TARC, and against Karpas genetically modified to produce TARC (K/TARC). K/wt represents migration toward Karpas wild-type, which produces a negligible amount of TARC, as a negative control. Migration is significantly increased for CCR4$^+$ T cells compared with CTR T cells. In addition, the figure shows that the improved migration of CCR4$^+$ T cells (■) is TARC mediated as it is inhibited by addition of anti-TARC antibodies but not by addition of an isotype control.

expressed in primary T cells from the peripheral blood of HL patients with active disease. After transduction, CCR4 was expressed by 53% plus or minus 18% of T cells, whereas only 11% plus or minus 9% of control T cells expressed this chemokine receptor (Figure 4A). Similar to observations made with T cells from healthy donors, expression of CCR4 could be detected on both CD4$^+$ and CD8$^+$ T cells after transduction (Figure 4B). CCR4 was also functional in these patient-derived T lymphocytes. As shown in Figure 4C, migration in TARC gradients toward HDLM-2 and L428 was significantly improved for CCR4$^+$ T cells (41% ± 18% and 34% ± 16%) compared with control T cells (9% ± 19% for HDLM-2 and 10% ± 12% for L428; $P = .05$). In addition, improved migration was observed toward Karpas/TARC (32% ± 16%) compared with Karpas/wt (2% ± 2%; $P = .03$), whereas no migration was observed for control T cells to Karpas/wt (1% ± 1%) or Karpas/TARC (4% ± 2%). As anticipated, migration was TARC specific as it was significantly inhibited in the presence of TARC-blocking antibodies but not by an isotype control (percentage migration, 4% ± 3% vs 32% ± 16%; $P = .04$).

T lymphocytes expressing transgenic CCR4 have improved migration toward TARC-secreting tumors in vivo. We next determined whether forced expression of CCR4 by activated T cells produced improved migration in vivo. Sublethally irradiated SCID mice were engrafted subcutaneously with 5×10^6 Karpas/wt on the left flank and 5×10^6 Karpas/TARC on the right flank to evaluate TARC-mediated T-cell migration within the same animal. Thus, each mouse acted as a "self-control" for unmodified and CCR4$^+$ T cells. We ensured that the 2 cell lines Karpas/wt and Karpas/TARC had comparable in vivo growth (data not shown) and that TARC could be detected in the plasma of mice engrafted with tumor cells (696 ± 141 pg/mL when the engrafted tumor was 1 cm^3). After tumor engraftment, mice were infused intravenously with either 10×10^6 control or CCR4$^+$ T lymphocytes. To monitor the migration over time of infused T cells using the IVIS Xenogen imager, control and CCR4$^+$ T cells were further modified to express eGFP-FFLuc as previously described (Figure 5A).[16,18,21] As shown in Figure 5B and C, we observed that CCR4$^+$ T cells preferentially accumulated at tumors producing TARC by days 9 to 12 (Karpas/TARC = $4.4 \times 10^5 \pm 2.7 \times 10^5$ p/sec/cm^2/sr vs Karpas/wt = $5 \times 10^4 \pm 2.1 \times 10^4$ p/sec/cm^2/sr; $P = .04$). In contrast, the signals detected at the tumor sites for control T cells were low and showed no significant differences between Karpas/TARC ($2.7 \times 10^4 \pm 5.6 \times 10^3$ p/sec/cm^2/ser) or Karpas/wt ($2.6 \times 10^4 \pm 1 \times 10^4$ p/sec/cm^2/sr; $P = .8$). Figure 5D shows that the increase of the bioluminescence signal corresponded to an increase in T cells localized at the TARC-secreting tumor site.

Functional coexpression of CCR4 and CAR-CD30 in T lymphocytes can be achieved using a bicistronic vector. After establishing that the forced expression of CCR4 by activated T cells enhances their migration toward TARC-secreting tumors without altering their Th1/T effector profile, we determined whether the enhanced migration of these cells to HL tumors could be coupled with antilymphoma specificity by providing them with a CAR targeting the CD30 molecule (CAR-CD30).[5,16]

Transduction efficiency. Activated T cells established from 10 healthy donors were transduced with a CCR4(I)CAR-CD30 bicistronic vector. As a control, we used the same T cells transduced

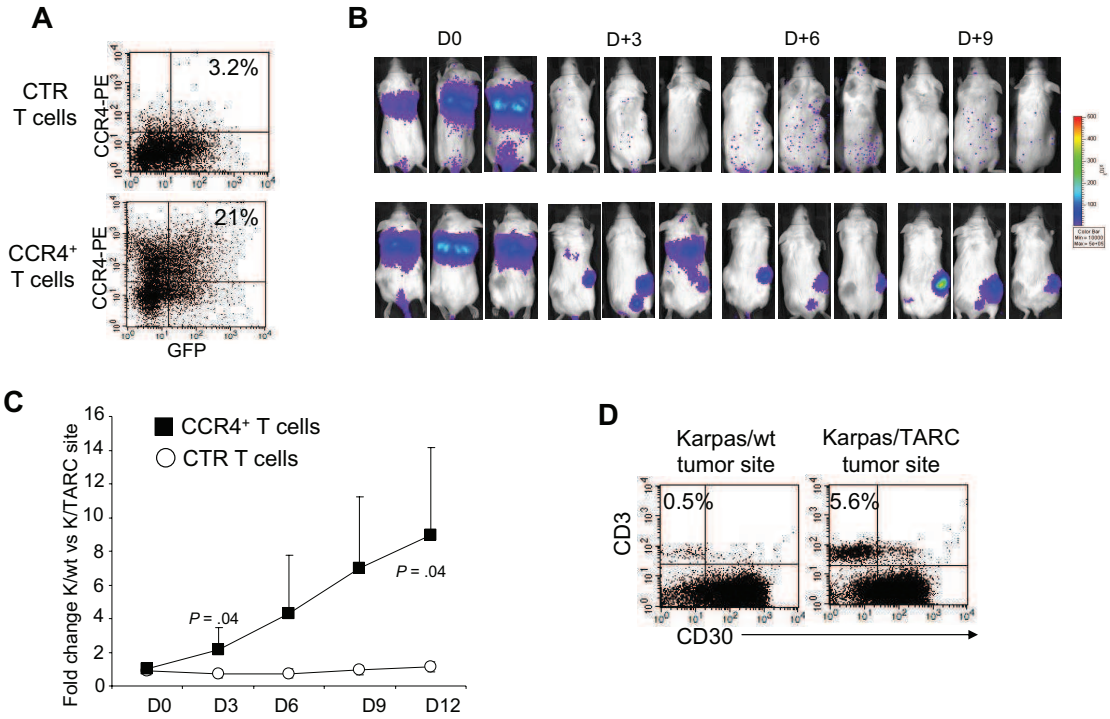

Figure 5. Improved in vivo migration of CCR4$^+$ T cells. CTR and CCR4$^+$ T cells were transduced to express eGFP-FFLuc to monitor their migration in vivo in SCID mice, using the IVIS imager system. (A) The expression of eGFP-FFLuc on CTR (top plot) and CCR4$^+$ (bottom plot) T cells evaluated by GFP. (B) The bioluminescence signal from CTR and CCR4$^+$ T cells in 3 representative SCID mice/group engrafted with TARC$^-$ tumor (K/wt) on the left side and the TARC$^+$ tumor (K/TARC) on the right side. Whereas no significant expansion of the bioluminescent signal was observed to either site of tumor in mice receiving CTR T cells (top picture in each pair), an increase in bioluminescence was observed in mice receiving CCR4$^+$ T cells (bottom picture in each pair) only at the site of the tumor producing TARC. (C) The fold change of bioluminescence signal between K/wt and K/TARC sites for CTR (○) and CCR4$^+$ (■) T cells. Data are mean ± SD of 6 mice. (D) The immunophenotype of K/wt (left plot) and K/TARC (right plot) tumors isolated from one representative mouse that received CCR4$^+$ T cells, killed on day 9. After removal, the tumors were homogenized and cells stained to distinguish T cells (using an antihuman CD3 antibody) from Karpas tumor cells (using an antihuman CD30 antibody). As shown in the panel, the proportion of cells detectable at the site of tumor-secreting TARC (5.6%) was more than 10-fold higher compared with K/wt (0.5%). This correlated with the increase in bioluminescence signal at the site of K/TARC tumor (2.1×10^6 p/sec/cm^2/sr) compared with the site of K/wt tumor (1.4×10^5 p/sec/cm^2/sr).

with a CAR-CD30 monocistronic vector. As shown in Figure 6A, T cells transduced with either the CAR-CD30 or CCR4(I)CAR-CD30 vector expressed significant levels of CAR-CD30, although the expression of this molecule was higher in cells transduced with the vector encoding CAR-CD30 alone (79% ± 8% vs 50% ± 6%; $P < .001$). In contrast, only T cells transduced with CCR4(I)CAR-CD30 expressed significant levels of CCR4, and the expression of this molecule remained low in cells transduced with CAR-CD30 alone (52% ± 14% vs 11% ± 8%; $P < .001$).

Migration. We then tested whether CCR4 expression obtained using the bicistronic vector improved migration in vitro, using the transwell migration assay. The migration of CCR4$^+$CAR-CD30$^+$ T cells toward HDLM-2 and L-428 supernatants was significantly increased (percentage migration, 17% ± 6% and 19% ± 9%, respectively) compared with T cells transduced with the monocistronic vector encoding CAR-CD30 (percentage migration, 4% ± 6% and 5% ± 4%, respectively; $P < .001$; Figure 6B). In addition, migration toward Karpas/TARC supernatant was significantly improved (percentage migration, 13% ± 5%) compared with migration toward Karpas/wt supernatant (percentage migration, 0.4% ± 1%; $P < .001$; Figure 6B). In contrast, migration of T cells transduced with CAR-CD30 alone was minimal toward both Karpas/wt and Karpas/TARC supernatants (percentage migration, 0.6% ± 1% and 0.9% ± 1%, respectively; Figure 6B).

Effector function. We next tested whether the expression of CAR-CD30 from the bicistronic vector made T lymphocytes cytotoxic to CD30$^+$ tumor cells. T cells transduced with the bicistronic vector CCR4(I)CAR-CD30 retained their killing of CD30$^+$ tumor cells (39% ± 15% for HDLM-2 and 33% ± 16% for Karpas-299 at 20:1 effector/target ratio) at levels comparable with that of T cells transduced with the monocistronic vector CAR-CD30 (47% ± 11% and 36% ± 8%, respectively; Figure 6C). Killing of CD30$^-$ targets was always less than 10% for both CCR4$^+$CAR-CD30$^+$ and CAR-CD30$^+$ T lymphocytes. As expected, no cytotoxicity against CD30$^+$ targets was produced by control T cells (1.4% ± 0.5% for HDLM-2 and 2.7% ± 1% for Karpas-299, respectively), and no significant killing of CD30$^-$ targets was produced by control T cells (data not shown).

Because CAR-CD30 also contains the costimulatory endodomain CD28, we measured the IL-2 released by CAR-CD30$^+$ cells after exposure to CD30$^+$ targets. IL-2 was detected in supernatants collected from T cells transduced with either CAR-CD30 or CCR4(I)CAR-CD30 (5427 ± 427 pg/mL per 10^6 cells and 5238 ± 873 pg/mL per 10^6 cells, respectively), confirming that the CD28 pathway is not impaired by the coexpression of CCR4. As expected, T lymphocytes transduced with a CAR targeting CD30 but lacking the coexpression of CD28 endodomain did not produce significant amounts of IL-2 in response to CD30$^+$ tumor cells (Figure 6D).

Forced expression of CCR4 in CAR-CD30$^+$ T cells improves migration and antitumor activity in vivo

Improved in vivo migration. To evaluate the in vivo migration of T cells, SCID mice (8 mice/group) were engrafted subcutaneously with Karpas/wt and Karpas/TARC cells (5×10^6 cells/mice) on the

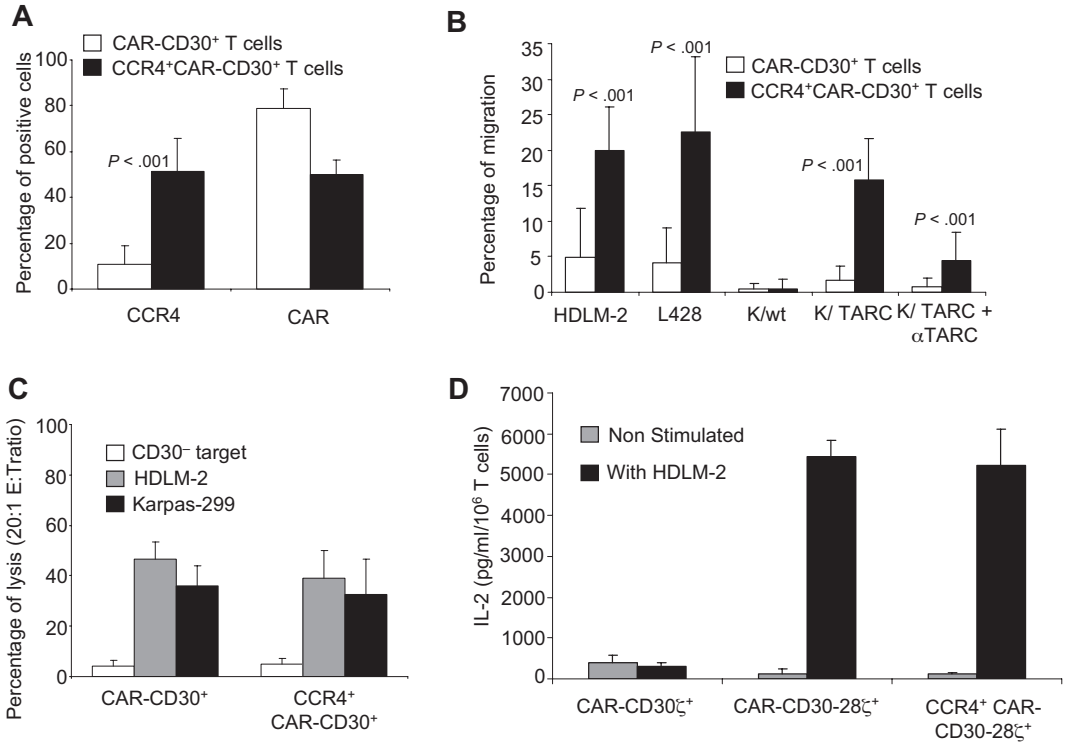

Figure 6. Improved migration of activated T lymphocytes genetically modified to overexpress CCR4 and a CAR targeting the CD30 antigen expressed by HL. A bicistronic vector encoding CCR4 and CAR-CD30 was constructed and used to transduce T cells from 8 healthy donors. (A) The expression of CCR4 and CAR-CD30 by T cells transduced with a retroviral vector encoding CAR-CD30 (□) or with a bicistronic retroviral vector encoding CCR4 and CAR-CD30 (■). Surface expression of the CCR4 and CAR was evaluated by FACS analysis. (B) The migration of CAR-CD30$^+$ (□) and CCR4$^+$CAR-CD30$^+$ (■) T cells toward TARC gradients, using a transwell migration assay. T-cell migration was evaluated using culture supernatants collected from HDLM-2 and L428, which physiologically produce high amounts of TARC, and against Karpas genetically modified to produce TARC (K/TARC). Karpas wild type (K/wt) was used as a control. The panel indicates that migration toward TARC is significantly improved for T cells genetically modified to overexpress CCR4 using the bicistronic vector CCR4(I)CAR-CD30. This improved migration was TARC mediated as it was inhibited by addition of anti-TARC antibodies but not by addition of an isotype control. (C) Killing of CD30$^+$ (HDLM-2, ▒; Karpas, ■) and CD30$^-$ (□) tumor cells by CAR-CD30$^+$ and CCR4$^+$CD30-CAR$^+$ T cells. (D) The measurement of IL-2 cytokine released in the supernatant of T cells cocultured with or without HDLM-2 and assessed using a specific ELISA assay. T cells were transduced with either CAR-CD30 or CCR4(I)CAR-CD30, where CAR molecules also incorporate the CD28 endodomain. As a control, T cells were also transduced with the same CAR targeting CD30 but lacking the CD28 endodomain (CD30CARζ). As anticipated, we observed enhanced production of IL-2 by T cells transduced with the CAR containing the CD28 endodomain (CAR-CD30), regardless of coexpression of CCR4, but not by T cells transduced with CD30CARζ lacking CD28. The figure indicates that T cells transduced with CCR4(I)CAR-CD30 vector produce IL-2 in amounts comparable with that of T cells transduced with the vector encoding CAR-CD30 alone, confirming that the CD28 pathway is not impaired by the coexpression of CCR4. Data are mean ± SD of 10 donors.

left and right flank, respectively. Seven days later, mice were infused intravenously either with CAR-CD30$^+$ or CCR4$^+$CAR-CD30$^+$ T cells (10×10^6 cells per mouse) expressing eGFP-FFLuc (Figure 7A). When mice were injected with CCR4$^+$CAR-CD30$^+$ cells, the bioluminescence signal, and thus T-cell migration, was greater at the site of the Karpas/TARC cells ($3.2 \times 10^5 \pm 1.9 \times 10^5$ p/sec/cm^2/sr) by days 6 to 9, compared with the Karpas/wt cell site ($5.5 \times 10^4 \pm 3.2 \times 10^4$ p/sec/cm^2/sr; $P = .01$; Figure 7B,C). In contrast, no significant signal accumulation was detected at the Karpas/wt site or Karpas/TARC site when mice were infused with T cells expressing only CAR-CD30 (Karpas/TARC cells = $3.7 \times 10^4 \pm 1.8 \times 10^4$ p/sec/cm^2/sr vs Karpas/wt cells = $4.4 \times 10^4 \pm 2.8 \times 10^4$ p/sec/cm^2/sr; $P = .2$).

Improved antitumor activity. We used NOG/SCID/γc^{null} mice that allow significant and consistent engraftment of the HL-derived cell line HDLM-2[22] to examine the antitumor activity of CCR4$^+$CAR-CD30$^+$ cells. These NOG/SCID/γc^{null} mice were engrafted subcutaneously with HDLM-2 tumor cells expressing FFLuc (3×10^6 cells/mouse) and 3 to 5 days later, the mice (7/group) were infused intravenously with either CCR4$^+$ or CAR-CD30$^+$ or CCR4$^+$CAR-CD30$^+$ T cells (10×10^6 cells per mouse). Tumor growth was monitored longitudinally using bioluminescence detected by the IVIS imager. As shown in Figure 7D and E, by day 25, bioluminescence signals from the tumor cells were progressively increasing in mice that received either CCR4$^+$ or CAR-CD30$^+$ T lymphocytes (tumor signals increased from $0.7 \times 10^6 \pm 0.8 \times 10^6$ p/sec/cm^2/sr to $92 \times 10^6 \pm 55 \times 10^6$ p/sec/cm^2/sr and from $0.9 \times 10^6 \pm 0.7 \times 10^6$ p/sec/cm^2/sr to $52 \times 10^6 \pm 37 \times 10^6$ p/sec/cm^2/sr, respectively). In contrast, tumor bioluminescence only slowly increased in mice treated with CCR4$^+$CAR-CD30$^+$ T lymphocytes (from $0.8 \times 10^6 \pm 0.7 \times 10^6$ p/sec/cm^2/sr to $2 \times 10^6 \pm 3 \times 10^6$ p/sec/cm^2/sr); and indeed, by day 30 after T-cell infusion, tumor regression was documented in 4 of 7 mice (57%).

Discussion

Coupling the effector function of tumor-specific T cells with enhanced migration toward a specific tumor chemokine gradient has the potential to improve the clinical benefits of adoptive T-cell therapy in cancer patients. Using CD30$^+$ HL that expresses the chemokine TARC as our model, we demonstrated that T lymphocytes engineered to coexpress the chemokine receptor, CCR4, and the effector molecule, CAR-CD30, have enhanced migration to the tumor when infused intravenously in a mouse model of HL and

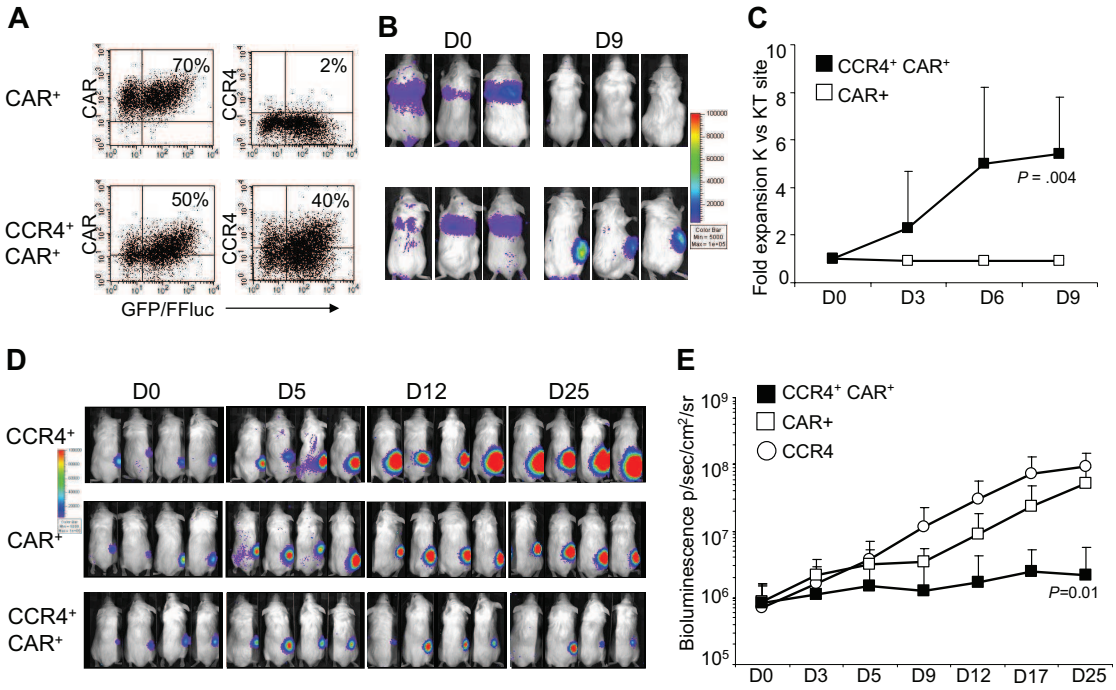

Figure 7. Improved in vivo migration and antitumor activity of T cells transduced with a bicistronic vector encoding both CCR4 and CAR-CD30. For in vivo experiments, T cells transduced with CAR-CD30 or the bicistronic vector encoding CCR4 and CAR-CD30 were further transduced to express eGFP-FFLuc to monitor their migration in vivo in SCID mice using the IVIS system. (A) The expression of eGFP-FFLuc on CAR-CD30$^+$ and CCR4$^+$CAR-CD30$^+$ cells in one representative donor. (B) The bioluminescence signal from T cells in 3 representative SCID mice engrafted with TARC$^-$ tumor (Karpas/wt) on the left side and the TARC$^+$ tumor (Karpas/TACR) on the right side. Whereas no significant expansion of the bioluminescent signal was observed at either tumor site in mice receiving CAR-CD30$^+$ T cells (top panels), a significant increase of bioluminescence was observed in mice receiving CCR4$^+$CAR-CD30$^+$ T cells (bottom panels) at the site of tumor-producing TARC. (C) The fold change of bioluminescence signal between K/wt and K/TARC site for CAR-CD30$^+$ (□) and CCR4$^+$CAR-CD30$^+$ (■) T cells. Data are mean ± SD of 8 mice. Data confirm that CCR4 expressed by T cells using a bicistronic vector remain functional in vivo. To evaluate in vivo antitumor activity of T cells transduced with the bicistronic vector, the HL-derived cell line HDLM-2 was further transduced with FFLuc and inplanted subcutaneously into NOG-SCID mice (7 mice/group). Tumor growth was monitored by measuring bioluminescence signals with the IVIS system. Mice then received intravenous T cells transduced with retroviral vectors encoding either CCR4 or CAR-CD30, or the bicistronic vector CCR4(I)CAR-CD30. (D) The bioluminescence signal of tumor cells in 4 representative mice/group. In mice receiving CCR4$^+$ or CAR-CD30$^+$ T cells, the bioluminescence signal, and thus tumor, increased over time. In contrast, in mice that received CCR4$^+$CAR-CD30$^+$ T cells, the signal remained stable, indicating tumor control. (E) The data from all 7 mice/group.

provide greater antilymphoma activity than T lymphocytes expressing the same CAR-CD30 receptor but lacking CCR4 expression.

The generation of T lymphocytes with specificity for tumor-associated antigens is the basis of most adoptive T-cell therapies. Using this approach, clinical responses have been obtained in a high proportion of EBV-positive HL patients receiving EBV-specific CTLs enriched for T-cell precursors targeting LMP-1 and LMP-2, the predominant EBV antigens expressed by Reed-Stenberg cells in EBV-positive HL.[24] As CD30 is highly expressed by Reed-Stenberg cells,[4] the infusion of T lymphocytes engineered to target CD30 by the expression of CAR-CD30 may be similarly effective in patients with EBV-negative HL. As previously reported, CAR-CD30-modified T cells do indeed show consistent cytotoxic activity against a variety of CD30$^+$ tumor cells,[5] and these benefits are seen without functional effects on other T cells because CD30 is only expressed by a small fraction of activated T cells, which may be nonessential to an effective immune response.[16]

Although the effectiveness of CAR-CD30 or other chimeric receptors can be enhanced by incorporation of costimulatory endodomains into the CAR molecules themselves[17,18,25,26] or by expressing the receptors in antigen-specific CTLs,[15,16,27,28] the antitumor effects of CTLs are also dependent on their ability to home to the sites of malignancy. Although gene marking[2] and multimer staining studies[1,24] showed that EBV-specific CTLs can accumulate in EBV-positive HL, these tumors, unlike EBV-negative HL, consistently express (IFN-γ)–inducible protein 10 (also known as CXCL10),[8,9] the receptor for which (CXCR3) is expressed on EBV-specific CTLs.[23] By contrast, the trafficking of CAR-expressing T lymphocytes to EBV-negative HL will probably be suboptimal because there is a disparity between the chemokines (such as TARC) produced by the tumors and the chemokine receptors expressed by CD8$^+$ effector cells.

Trafficking of T cells to lymphoid organs and peripheral tissues is a multistage process,[29] but soluble and tissue-bonded chemokines interacting with chemokine receptors expressed by T lymphocytes certainly play a pivotal role in determining migration under physiologic conditions and during inflammation.[29] The production of chemokines by tumor cells can disrupt this process. Hence, the Reed-Stenberg cells of HL produce the chemokines TARC and MDC that selectively recruit CCR4-expressing cell subsets, including eosinophils, histiocytes, macrophages, plasma cells, and Th2 and Treg lymphocytes,[8,9] which are all readily detected at tumor sites.[8-10] By contrast, effector CD8$^+$ cells express the chemokine receptors CCR2, CCR5, CXCR1, and CXCR3, allowing them to respond to the chemokines, including CCL2, CCL3, CCL4, CCL5 (Rantes), CXL10, and CXCL8,[29] released during inflammation. These CD8$^+$ effectors may still be able to traffic even to EBV-negative HL because molecular and histologic analyses of HL tissues indicate that some produce the monokine induced by IFN-γ (Mig) (CXCL9) and the chemokine CCL5 whose cognate receptors CXCR3 and CCR5 are indeed present on CD8$^+$ cells. But although this will allow limited migration, Th2 and Treg cells are overwhelmingly present so that TARC and MDC are the more important

determinants of migration. Further evidence for this importance comes from the observation that elevated serum levels of TARC/CCL17 correlate with unfavorable prognosis in patients with HL, so that this pattern of infiltrate has clinical correlates.[30,31]

Our data demonstrate that forced expression of CCR4 in $CD8^+$ T lymphocytes provides them with the capacity to migrate toward TARC gradient, so that the functionality of this receptor is not restricted to the subset of T cells in which it is physiologically expressed. Conversely, expression of CCR4 in $CD8^+$ T cells raises the concern that this molecule may also produce unwanted or altered functions, such as acquisition of inhibitory activity, diminished cytotoxic activity, or shifts in the polarity of released cytokines. Our data show that CCR4 expression in $CD8^+$ T cells does not confer on them any discernible Th2 or Treg properties or otherwise modulate their function. Hence $CCR4^+CD8^+$ cells maintain their cytotoxic activity through CAR-CD30 against $CD30^+$ tumors, produce IFN-γ, TNF-α, and IL-2 rather than IL-4 or IL-10, and do not acquire inhibitory function.

TARC and MDC are released by other tissues in which accumulation of $CD8^+$ T lymphocytes may be toxic. For instance, CCR4-TARC/MDC interaction may also direct $CD4^+$ cells to the skin, especially during inflammation.[32,33] CD30 antigen, however, is not physiologically expressed in the skin, so that the CAR-$CD30^+$ T cells should not produce cytotoxic, direct "off-target" effects even if they are present. Indeed, improved migration to the skin of $CCR4^+$CAR-$CD30^+$ T cells could be advantageous in extending this T-cell therapeutic approach form HL to cutaneous large cell anaplastic lymphomas that are frequently $CD30^+$.[34]

In conclusion, coexpression of CCR4 by T lymphocytes can be used to improve the homing of CAR-CD30-modified T cells to $CD30^+$ HL and thereby promote improved antilymphoma effects. A similar approach can be implemented for other types of cancer,[7] provided that the targeted tumors produce specific chemokines for which T cells may not express the receptor, to maximize the antitumor activity of adoptively transferred antitumor T cells.

Acknowledgments

This work was supported in part by the Leukemia & Lymphoma Society Specialized Center of Research (grant no. 7018; H.E.H.) and Specialized Programs of Research Excellence in Lymphoma (H.E.H.). A.D.S. is supported by Fondazione Marco Semenza per la Ricerca sul Cancro (Milano, Italy) and by American Italian Cancer Foundation (New York, NY). G.D. is supported by the Doris Duke Charitable Foundation/Clinical Scientist development award and by a Leukemia & Lymphoma Society Translational Research grant. B.S. is supported by National Institutes of Health (grant R01CA131027) and the Leukemia & Lymphoma Society Translational Research.

Authorship

Contribution: A.D.S., G.D., and B.S. designed the research, analyzed the data, and wrote the manuscript; A.D.S performed the majority of the experiments; B.D.A. and B.S. performed some in vitro and in vivo experiments; G.D. has supervised the generation of the retroviral vectors; A.E.F. provided assistance with some in vitro experiments; L.Z. and A.M. provided technical assistance for the in vitro and in vivo experiments, respectively; and C.M.R., H.E.H., and M.K.B. provided assistance in the design of the research and critically reviewed the manuscript. All authors approved the final version of the manuscript.

Conflict-of-interest disclosure: The authors declare no competing financial interests.

Correspondence: Barbara Savoldo, Center for Cell and Gene Therapy, Baylor College of Medicine, 6621 Fannin St, MC 3-3320, Houston, TX 77030; e-mail: bsavoldo@bcm.tmc.edu.

References

1. Bollard CM, Aguilar L, Straathof KC, et al. Cytotoxic T lymphocyte therapy for Epstein-Barr virus+ Hodgkin's disease. J Exp Med. 2004;200:1623-1633.
2. Roskrow MA, Suzuki N, Gan Y, et al. Epstein-Barr virus (EBV)-specific cytotoxic T lymphocytes for the treatment of patients with EBV-positive relapsed Hodgkin's disease. Blood. 1998;91:2925-2934.
3. Wu TC, Mann RB, Charache P, et al. Detection of EBV gene expression in Reed-Sternberg cells of Hodgkin's disease. Int J Cancer. 1990;46:801-804.
4. Falini B, Pileri S, Pizzolo G, et al. CD30 (Ki-1) molecule: a new cytokine receptor of the tumor necrosis factor receptor superfamily as a tool for diagnosis and immunotherapy. Blood. 1995;85:1-14.
5. Hombach A, Heuser C, Sircar R, et al. An anti-CD30 chimeric receptor that mediates CD3-zeta-independent T-cell activation against Hodgkin's lymphoma cells in the presence of soluble CD30. Cancer Res. 1998;58:1116-1119.
6. Walker RE, Bechtel CM, Natarajan V, et al. Long-term in vivo survival of receptor-modified syngeneic T cells in patients with human immunodeficiency virus infection. Blood. 2000;96:467-474.
7. Kershaw MH, Wang G, Westwood JA, et al. Redirecting migration of T cells to chemokine secreted from tumors by genetic modification with CXCR2. Hum Gene Ther. 2002;13:1971-1980.
8. Maggio EM, van den Berg A, Visser L, et al. Common and differential chemokine expression patterns in rs cells of NLP, EBV positive and negative classical Hodgkin lymphomas. Int J Cancer. 2002;99:665-672.
9. van den Berg A, Visser L, Poppema S. High expression of the CC chemokine TARC in Reed-Sternberg cells: a possible explanation for the characteristic T-cell infiltrate in Hodgkin's lymphoma. Am J Pathol. 1999;154:1685-1691.
10. Ishida T, Ishii T, Inagaki A, et al. Specific recruitment of CC chemokine receptor 4-positive regulatory T cells in Hodgkin lymphoma fosters immune privilege. Cancer Res. 2006;66:5716-5722.
11. Curiel TJ, Coukos G, Zou L, et al. Specific recruitment of regulatory T cells in ovarian carcinoma fosters immune privilege and predicts reduced survival. Nat Med. 2004;10:942-949.
12. Iellem A, Mariani M, Lang R, et al. Unique chemotactic response profile and specific expression of chemokine receptors CCR4 and CCR8 by CD4(+)CD25(+) regulatory T cells. J Exp Med. 2001;194:847-853.
13. D'Ambrosio D, Iellem A, Bonecchi R, et al. Selective up-regulation of chemokine receptors CCR4 and CCR8 upon activation of polarized human type 2 Th cells. J Immunol. 1998;161:5111-5115.
14. Marshall NA, Christie LE, Munro LR, et al. Immunosuppressive regulatory T cells are abundant in the reactive lymphocytes of Hodgkin lymphoma. Blood. 2004;103:1755-1762.
15. Rossig C, Bollard CM, Nuchtern JG, Rooney CM, Brenner MK. Epstein-Barr virus-specific human T lymphocytes expressing antitumor chimeric T-cell receptors: potential for improved immunotherapy. Blood. 2002;99:2009-2016.
16. Savoldo B, Rooney CM, Di Stasi A, et al. Epstein Barr virus specific cytotoxic T lymphocytes expressing the anti-CD30zeta artificial chimeric T-cell receptor for immunotherapy of Hodgkin disease. Blood. 2007;110:2620-2630.
17. Pule MA, Straathof KC, Dotti G, et al. A chimeric T cell antigen receptor that augments cytokine release and supports clonal expansion of primary human T cells. Mol Ther. 2005;12:933-941.
18. Vera J, Savoldo B, Vigouroux S, et al. T-lymphocytes redirected against the kappa light chain of human immunoglobulin efficiently kill mature B-lymphocyte derived malignant cells. Blood. 2006;108:3890-3897.
19. Dotti G, Savoldo B, Pule M, et al. Human cytotoxic T lymphocytes with reduced sensitivity to Fas-induced apoptosis. Blood. 2005;105:4677-4684.
20. Godfrey WR, Ge YG, Spoden DJ, et al. In vitro-expanded human CD4(+)CD25(+) T-regulatory cells can markedly inhibit allogeneic dendritic cell-stimulated MLR cultures. Blood. 2004;104:453-461.
21. Quintarelli C, Vera JF, Savoldo B, et al. Co-expression of cytokine and suicide genes to enhance the activity and safety of tumor-specific cytotoxic T lymphocytes. Blood. 2007;110:2793-2802.

22. Dewan MZ, Watanabe M, Ahmed S, et al. Hodgkin's lymphoma cells are efficiently engrafted and tumor marker CD30 is expressed with constitutive nuclear factor-kappaB activity in unconditioned NOD/SCID/gammac(null) mice. Cancer Sci. 2005;96:466-473.

23. Pule MA, Savoldo B, Myers GD, et al. Virus-specific T cells engineered to coexpress tumor-specific receptors: persistence and antitumor activity in individuals with neuroblastoma. Nat Med. 2008;14:1264-1270.

24. Bollard CM, Gottschalk S, Leen AM, et al. Complete responses of relapsed lymphoma following genetic modification of tumor-antigen presenting cells and T-lymphocyte transfer. Blood. 2007;110:2838-2845.

25. Maher J, Brentjens RJ, Gunset G, Riviere I, Sadelain M. Human T-lymphocyte cytotoxicity and proliferation directed by a single chimeric TCRzeta /CD28 receptor. Nat Biotechnol. 2002;20:70-75.

26. Zhang H, Snyder KM, Suhoski MM, et al. 4-1BB is superior to CD28 costimulation for generating CD8+ cytotoxic lymphocytes for adoptive immunotherapy. J Immunol. 2007;179:4910-4918.

27. Landmeier S, Altvater B, Pscherer S, et al. Gene-engineered varicella-zoster virus reactive CD4+ cytotoxic T cells exert tumor-specific effector function. Cancer Res. 2007;67:8335-8343.

28. Cooper LJ, Al Kadhimi Z, Serrano LM, et al. Enhanced antilymphoma efficacy of CD19-redirected influenza MP1-specific CTLs by cotransfer of T cells modified to present influenza MP1. Blood. 2005;105:1622-1631.

29. Bromley SK, Mempel TR, Luster AD. Orchestrating the orchestrators: chemokines in control of T cell traffic. Nat Immunol. 2008;9:970-980.

30. Niens M, Visser L, Nolte IM, et al. Serum chemokine levels in Hodgkin lymphoma patients: highly increased levels of CCL17 and CCL22. Br J Haematol. 2008;140:527-536.

31. Weihrauch MR, Manzke O, Beyer M, et al. Elevated serum levels of CC thymus and activation-related chemokine (TARC) in primary Hodgkin's disease: potential for a prognostic factor. Cancer Res. 2005;65:5516-5519.

32. Reiss Y, Proudfoot AE, Power CA, Campbell JJ, Butcher EC. CC chemokine receptor (CCR)4 and the CCR10 ligand cutaneous T cell-attracting chemokine (CTACK) in lymphocyte trafficking to inflamed skin. J Exp Med. 2001;194:1541-1547.

33. Kunkel EJ, Butcher EC. Chemokines and the tissue-specific migration of lymphocytes. Immunity. 2002;16:1-4.

34. Yamaguchi T, Ohshima K, Karube K, et al. Expression of chemokines and chemokine receptors in cutaneous CD30+ lymphoproliferative disorders. Br J Dermatol. 2006;154:904-909.

Generation of Epstein-Barr virus–specific cytotoxic T lymphocytes resistant to the immunosuppressive drug tacrolimus (FK506)

Biagio De Angelis,[1-3] Gianpietro Dotti,[1,4,5] Concetta Quintarelli,[1-3] Leslie E. Huye,[1] Lan Zhang,[1] Ming Zhang,[1] Fabrizio Pane,[2,3] Helen E. Heslop,[1,4,5] Malcolm K. Brenner,[1,4,5] Cliona M. Rooney,[1,5-7] and Barbara Savoldo[1,6]

[1]Center for Cell and Gene Therapy, Baylor College of Medicine, The Methodist Hospital and Texas Children's Hospital, Houston; [2]CEINGE Biotecnologie Avanzate, Napoli, Italy; [3]Hematology, Department of Biochemistry and Medical Biotechnology, University Federico II, Naples, Italy; and Departments of [4]Medicine, [5]Immunology, [6]Pediatrics, and [7]Molecular Virology and Microbiology, Baylor College of Medicine, The Methodist Hospital and Texas Children's Hospital, Houston

Adoptive transfer of autologous Epstein-Barr virus–specific cytotoxic T lymphocytes (EBV-CTLs) to solid organ transplant (SOT) recipients has been shown safe and effective for the treatment of EBV-associated posttransplantation lymphoproliferative disorders (PTLDs). SOT recipients, however, require the continuous administration of immunosuppressive drugs to prevent graft rejection, and these agents may significantly limit the long-term persistence of transferred EBV-CTLs, precluding their use as prophylaxis. Tacrolimus (FK506) is one of the most widely used immunosuppressive agents in SOT recipients, and its immunosuppressive effects are largely dependent on its interaction with the 12-kDa FK506-binding protein (FKBP12). We have knocked down the expression of FKBP12 in EBV-CTLs using a specific small interfering RNA (siRNA) stably expressed from a retroviral vector and found that FKBP12-silenced EBV-CTLs are FK506 resistant. These cells continue to expand in the presence of the drug without measurable impairment of their antigen specificity or cytotoxic activity. We confirmed their FK506 resistance and anti-PTLD activity in vivo using a xenogenic mouse model, suggesting that the proposed strategy may be of value to enhance EBV-specific immune surveillance in patients at high risk of PTLD after transplantation. (Blood. 2009;114:4784-4791)

Introduction

Adoptive transfer of Epstein-Barr virus–specific cytotoxic T lymphocytes (EBV-CTLs) can induce the regression of EBV-associated posttransplantation lymphoproliferative diseases (EBV-PTLDs) in recipients of allogeneic hematopoietic stem cell (HSC) grafts.[1,2] Moreover, prophylactic administration of EBV-CTLs can efficiently prevent the occurrence of EBV-PTLDs in these patients due to the long-term in vivo persistence of these cells after adoptive transfer.[1,2]

Although EBV-CTLs can also be effective to treat PTLDs occurring after solid organ transplantation,[3-9] it has proven difficult to obtain reduction in morbidity in these patients using a prophylactic approach.[10] Indeed, in contrast to allogeneic HSC transplantation, solid organ transplant (SOT) recipients require continued administration of immunosuppressive drugs to avoid graft rejection,[11,12] and these agents may significantly impair the growth, expansion, and long-term persistence of adoptively transferred EBV-CTLs.[13]

Although this inhibition evidently does not preclude the short-term in vivo cytotoxic activity of adoptively transferred EBV-CTLs and hence benefit in the case of established disease,[3-9] it effectively precludes their cost-effective use as prophylactic treatment for patients at high risk for PTLD development after solid organ transplantation. To overcome this obstacle and improve CTL proliferation and persistence despite continued immunosuppression, we have made EBV-CTLs resistant to the effects of tacrolimus (FK506), a commonly used immunosuppressive drug.

FK506 is widely used as an immunosuppressive drug to prevent rejection of renal, liver, and heart-lung transplant grafts.[14-17] FK506 inhibits host immune responses by binding to immunophilin FK506-binding proteins (FKBPs).[18] Of the 10 known mammalian FKBPs, the 12-kDa FK506-binding protein (FKBP12) appears to play a key role in mediating FK506 immunosuppression,[19] forming a complex with the drug that inhibits the Ca^{2+}-activated serine/threonine phosphatase calcineurin, and thereby preventing cytoplasmic nuclear factor of activated T cell (NFATc) dephosphorylation, which is required for interleukin-2 (IL-2) production and T-cell activation.[20,21]

We hypothesized that EBV-CTLs in which we prevented binding of FK506 to FKBP12 would retain their ability to proliferate even in the presence of the drug. To achieve this effect we selectively down modulated FKBP12 in EBV-CTLs using a specific small interference RNA (siRNA) expressed by a retroviral vector. We show that stable knockdown of FKBP12 in EBV-CTLs allows them to expand in the presence of therapeutic doses of FK506 without affecting their ex vivo or in vivo antigen specificity and function.

Methods

Plasmid construction and retrovirus production

We obtained the full-length human FKBP12 cDNA, by reverse-transcription polymerase chain reaction from peripheral blood mononuclear cells (PBMCs) and cloned it into the expression plasmid p.eGFP-C1

Submitted July 1, 2009; accepted August 21, 2009. Prepublished online as *Blood* First Edition paper, September 16, 2009; DOI 10.1182/blood-2009-07-230482.

An Inside *Blood* analysis of this article appears at the front of this issue.

The online version of this article contains a data supplement.

The publication costs of this article were defrayed in part by page charge payment. Therefore, and solely to indicate this fact, this article is hereby marked "advertisement" in accordance with 18 USC section 1734.

(Clontech Laboratories Inc) to generate the p-eGFP-hFKBP12-C1 plasmid. In this plasmid, FKBP12 was cloned in frame to the COOH-terminus of enhanced green fluorescent protein (eGFP) to obtain a fusion protein. We designed siRNA sequences targeting the FKBP12 mRNA using software from Ambion (http://www.ambion.com) and cloned them into the pSUPER vector (OligoEngine), containing the puromycin resistance gene, or pSUPER.eGFP vector, containing GFP as a selectable marker, as previously described.[22] Control vectors encoding an irrelevant siRNA were also used.[22,23] The vector encoding firefly luciferase (FFLuc) was constructed and used as previously described.[24] We prepared the retroviral supernatant using 293T cells cotransfected with 3 plasmids (the retroviral construct, Peg-Pam-e encoding *gag-pol,* and RDF encoding the RD114 envelop[25]) using the Gene Juice transfection reagent (Novagen Brand). Supernatants were collected 48 and 72 hours later.

Screening of FKBP12-siRNAs

We cloned 17 different siRNAs that targeted FKBP12 mRNA into the pSUPER retroviral vector. To evaluate the silencing activity of these siRNAs, we cotransfected 293T cells with the reporter plasmid (p-eGFP-hFKBP12-C1) and pSUPER vectors encoding siRNAs (ratio of 1:2). Silencing mediated by the siRNAs was measured by quantifying the expression of GFP in 293T cells using a BD FACSCalibur Flow Cytometer (BD Biosciences) 48 hours after plasmid transfection.

Western blot analysis

Cell lysates were resolved on sodium dodecyl sulfate–polyacrylamide gel electrophoresis. FKBP12 was detected using a rabbit polyclonal antibody (AbCAM Inc). Immunoblots were developed using enhanced chemiluminescence detection reagents (Amersham Biosciences). To evaluate the equal loading of the proteins, membranes were reprobed with glyceraldehyde-3-phosphate dehydrogenase (GAPDH) monoclonal antibody (mAb; Santa Cruz Biotechnology). To measure the relative intensity of bands, after drawing appropriate regions of interest around the bands, we used the Kodak Molecular Imaging Software Version 4.0.

Generation and transduction of effector T cells

Human PBMCs were activated in 24-well plates coated with OKT3 (Ortho Biotech) and CD28 (Pharmingen) mAbs in the presence of recombinant human IL-2 (100 U/mL; Proleukin; Chiron). Activated T cells were transduced on day 3 in 24-well plates precoated with recombinant fibronectin fragment (FN CH-296; Retronectin; Takara Shuzo) using specific retroviral supernatant and IL-2, as previously described.[24,26] T cells were then collected and expanded in T-cell medium (50% RPMI, 50% Click media [Irvine Scientific], 10% fetal bovine serum, and 2 mM L-glutamine) using IL-2 (50-100 U/mL) to obtain sufficient cells for in vitro experiments.

Generation and retroviral transduction of EBV-CTLs

EBV-CTLs were prepared by stimulating PBMCs with γ-irradiated (40 Gy) autologous EBV-transformed lymphoblastoid cell lines (EBV-LCLs) as previously described.[2,7,13] Stimulations with autologous EBV-LCLs were repeated weekly and IL-2 (50 U/mL) was added twice a week from day 14 of culture.[7] After the third stimulation, EBV-CTLs were transduced in Retronectin-precoated 24-well plates with the retroviral supernatant.[27] Three days after transduction, EBV-CTLs were collected and then stimulated weekly with autologous EBV-LCLs in the presence of low doses of IL-2 (20 U/mL) with or without the addition of FK506 (5 or 10 ng/mL; LC Laboratories), or with or without the addition of temsirolimus (25 ng/mL; LC Laboratories).

Immunophenotyping

Phycoerythrin-, fluorescein isothiocyanate–, peridinin chlorophyll protein–, and allophycocyanin–conjugated CD3, CD4, CD8, CD56, CD19, and αβ T-cell receptor (TCR) mAbs (Becton Dickinson) were used to stain EBV-CTLs and T cells. Control samples labeled with an appropriate isotype-matched Ab were included in each experiment. We analyzed cells using a FACSCalibur with a filter set for 4 fluorescence signals and CellQuest software (BD Biosciences). For each sample, we analyzed a minimum of 10 000 events.

Multimers

The antigen specificity of EBV-CTLs was evaluated with EBV-specific multimers, as previously described.[7] We chose multimers based on available donor human leukocyte antigen (HLA) types, which recognized the following EBV peptides: *EBNA3B,* HLA-A11: IVTDFSVIK, and *EBNA3B,* HLA-A11: AVFDRKSDAK; *EBNA3A,* HLA-B8: QAKWRLQTL; *BZLF1,* HLA-B8: RAKFKQLL (listed in Khanna and Burrows[28]; Houssaint et al[29]). Multimers were prepared by Proimmune. Samples were costained with CD8-allophycocyanin and CD3–peridinin chlorophyll protein mAbs. Isotype controls were included. For each sample, a minimum of 100 000 cells were analyzed using a FACSCalibur with a filter set for 4 fluorescence signals and CellQuest software.

Phosphorylation of S6K1

After transduction, T cells were stimulated overnight with bound-OKT3 mAb (1 μg/mL) in the presence of increasing concentration of temsirolimus (from 1 to 25 ng/mL). Cells were then collected, washed, fixed, permeabilized with methanol, and then stained with phospho-S6 ribosomal protein (Ser235/236) rabbit mAb Alexa Fluor 647 conjugate (Cell Signaling Technology). Control samples labeled with an appropriate isotype-matched Ab were included. Cells were then analyzed using a FACSCalibur and CellQuest software. For each sample, we analyzed a minimum of 10 000 events.

Enzyme-linked immunospot assay

The interferon-γ (IFNγ) enzyme-linked immunospot (ELIspot) assay (Mabtech, Inc) was performed as previously described.[7] Briefly, EBV-CTLs were plated in triplicate at 10^5 in the presence of the appropriate peptides (5 μM). Negative controls included EBV-CTLs alone and EBV-CTLs plated with irrelevant peptides. As positive controls, EBV-CTLs were stimulated with autologous EBV-LCLs.

Chromium release assay

The cytotoxic activity of EBV-CTLs was evaluated in a standard 4-hour ^{51}Cr release assay, as previously described.[7] Target cells included autologous and HLA class I and II mismatched EBV-LCLs, and the K562 cell line (as a natural killer cell target). Target cells incubated in media alone or in 1% Triton X-100 (Sigma-Aldrich) were used to determine spontaneous and maximum ^{51}Cr release, respectively. The mean percentage specific lysis of triplicate wells was calculated as follows: 100 × (test counts − spontaneous counts)/(maximum counts − spontaneous counts).

Proliferation assay

EBV-CTLs were plated in triplicate at 10^5 cells/well with γ-irradiated (40 Gy) autologous EBV-LCLs at an effector-target ratio of 4:1 in the presence of IL-2 (20 U/mL), with or without increasing doses of FK506 (from 5 ng/mL to 100 ng/mL). Transduced T cells were stimulated with bound-OKT3 mAb (1 μg/mL) in the presence of increasing concentrations of temsirolimus (from 5 ng/mL to 25 ng/mL). After 72 hours, CTLs or T cells were pulsed with 1 μCi (0.037 MBq) methyl-3[H]thymidine (Amersham Pharmacia Biotech), cultured for an additional 16 hours, and then harvested onto filters and dried. Thymidine uptake was measured as counts per minute in a β-scintillation counter (liquid scintillation analyzer TRI-CARB 2910 TR; Perkin Elmer). The percentage suppression was calculated using the following formula: 100 × [1 − (experimental cpm − control cpm)/(without drug cpm − negative control cpm)], as previously reported.[13]

Transduction of tumor cells with the luciferase vector

EBV-LCLs were transduced with the FFLuc vector on a Retronectin-coated plate and then selected using puromycin (Sigma-Aldrich) as previously

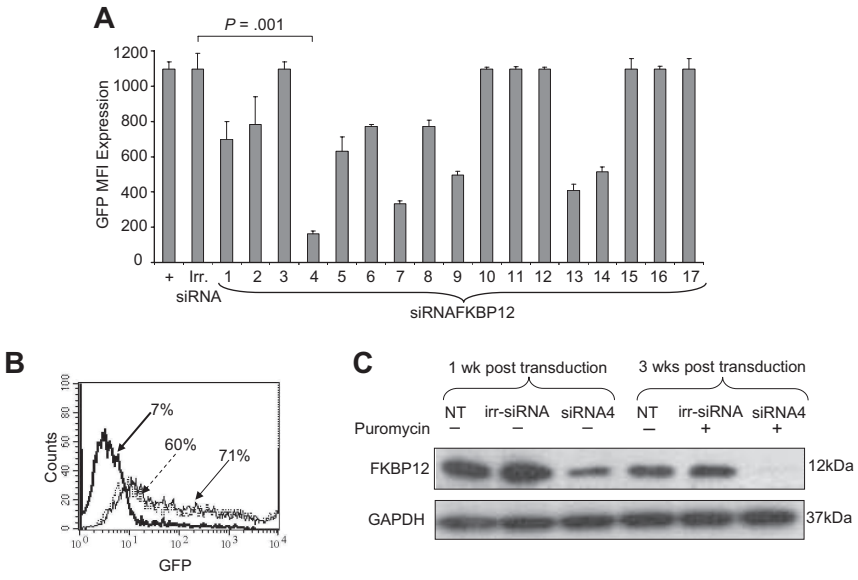

Figure 1. Identification of a siRNA vector that stably knocks down FKBP12. (A) GFP MFI of 293T cells transfected with eGFP-hFKBP12 (+) or cotransfected with eGFP-hFKBP12 and each of the 17 predicted siRNA sequences targeting the human FKBP12 mRNA or an irrelevant siRNA (irr-siRNA). siRNA4 resulted in > 85% reduction of the GFP MFI. (B) GFP was expressed by 60% of 293T cells transfected with the reporter plasmid eGFP-hFKBP12 alone, by 71% of 293T cells cotransfected with the irr-siRNA plasmid, and by 7% of 293T cells cotransfected with siRNA4 plasmid. (C) The expression of the FKBP12 in nontransduced (NT), irr-siRNA$^+$, and siRNA4$^+$ EBV-CTLs assessed by WB 1 week after transduction and after selection with puromycin for 3 weeks. FKBP12 expression is visibly reduced in siRNA4$^+$ EBV-CTLs after transduction. This effect is more evident after selection in the presence of puromycin. The bottom gel shows the membrane reprobed with anti-GAPDH antibody.

described.[30] To confirm transgene expression, 5×10^6 tumor cells were lysed and aliquots diluted in 100 μL of D-luciferin according to the manufacturer's instructions (Promega). Bioluminescence was measured using a luminometer (Monolight; BD Biosciences).

In vivo experiments

All mouse experiments were performed in accordance with Baylor College of Medicine Animal Husbandry and Institutional Animal Care and Use Committee guidelines and were approved by the Baylor College of Medicine's institutional review board.

Antitumor activity

To assess persistence and antitumor activity of control and genetically modified human EBV-CTLs in the presence of FK506 in vivo, we used a xenograft lymphoma severe combined immunodeficient (SCID) mouse model and the IVIS imaging system (Xenogen; Caliper Life Sciences) as previously described.[27,30] Six- to 8-week-old CB17/SCID mice (Harlan-Sprague) were sublethally irradiated (230 cGy) and engrafted intraperitoneally with 3×10^6 FFLuc$^+$ EBV-LCLs resuspended in Matrigel (BD Biosciences).[30] Three or 4 days after engraftment (when the light emission of the tumor was consistently measurable) and again 1 week later, mice received 10×10^6 autologous EBV-CTLs intraperitoneally. In addition, mice also received 3 times a week intraperitoneal injections of 1000 U/mouse IL-2 (Teceleukin; Fisher Bioservices) and 10 mg/kg body weight of FK506.[31] Control animals received only IL-2. Tumor growth was evaluated over time using the IVIS imaging system. Briefly, a constant region of interest was drawn over the tumor regions and the intensity of the signal measured as total photon/sec/cm^2/steradian (p/s/cm^2/sr) as previously described.[27,30]

Statistical analysis

All in vitro experiments were summarized as mean plus or minus SD. Student *t* test was used to determine the statistical significant differences between samples, with *P* value less than .05 indicating a significant difference. Survival was evaluated by Kaplan-Meier analysis (SPSS software) and the statistical significance of observed differences assessed by log-rank and Breslow testing.

Results

Selection of siRNAs targeting the human FKBP12 mRNA

To rapidly select functional siRNAs, the 17 predicted siRNA sequences targeting the human FKBP12 mRNA were cloned in the pSUPER vector.[22] FKBP12-siRNA-pSUPER or control siRNA-pSUPER (irr-siRNA) vectors were then cotransfected into 293T cells with the reporter plasmid eGFP-hFKBP12 (encoding the fusion protein eGFP-hFKBP12). GFP expression, measured by fluorescence-activated cell sorting (FACS) analysis 48 hours after transfection, was used as a surrogate marker of FKBP12 mRNA silencing by specific siRNAs. As shown in Figure 1A, the GFP mean fluorescence intensity (MFI) of eGFP-hFKBP12$^+$ 293T cells was 1067 (± 80) and remained stable in 293T cells cotransfected with the irr-siRNA (1097 ± 89). Variable decreases of the GFP MFI were observed in 293T cells after transfecting each FKBP12-siRNA-pSUPER vector. The siRNA designated siRNA4, which targets the GATGGAAAGAAATTTGATT mRNA sequence, significantly knocked down the GFP MFI to 163 (± 33), which is equivalent to a more than 85% reduction in the FKBP12 expression compared with irr-siRNA ($P = .001$; Figure 1A-B). The combination of siRNA4 with other siRNAs had no further effect on GFP expression or MFI (data not shown). Hence, siRNA4 was selected for all subsequent experiments.

siRNA4 significantly knocked down expression of endogenous FKBP12 in EBV-CTLs

We measured the effects of siRNA4 on the expression of endogenous FKBP12 in EBV-CTL lines generated from 6 EBV-seropositive donors. These CTLs were transduced after the third antigen stimulation either with the retroviral vector pSUPER encoding the siRNA4 or with the control irr-siRNA vector. After transduction, CTLs were maintained in culture and selected with puromycin (0.1-0.5 μg/mL). As shown in Figure 1C, FKBP12 expression, assessed by Western blot (WB) analysis, was reduced by 42% in EBV-CTLs transduced with siRNA4, but not in CTLs expressing the irr-siRNA. This effect was further increased when CTLs were selected in the presence of puromycin because we observed a 94% reduction of FKBP12 in siRNA4$^+$ EBV-CTLs (Figure 1C). FKBP12 knockdown was stable in EBV-CTLs maintained in culture for more than 2 months (data not shown).

Enrichment of FKBP12-silenced EBV-CTLs in the presence of FK506

We next measured the effects of reduced FKBP12 expression on the resistance of EBV-CTLs to FK506. We transduced EBV-CTLs

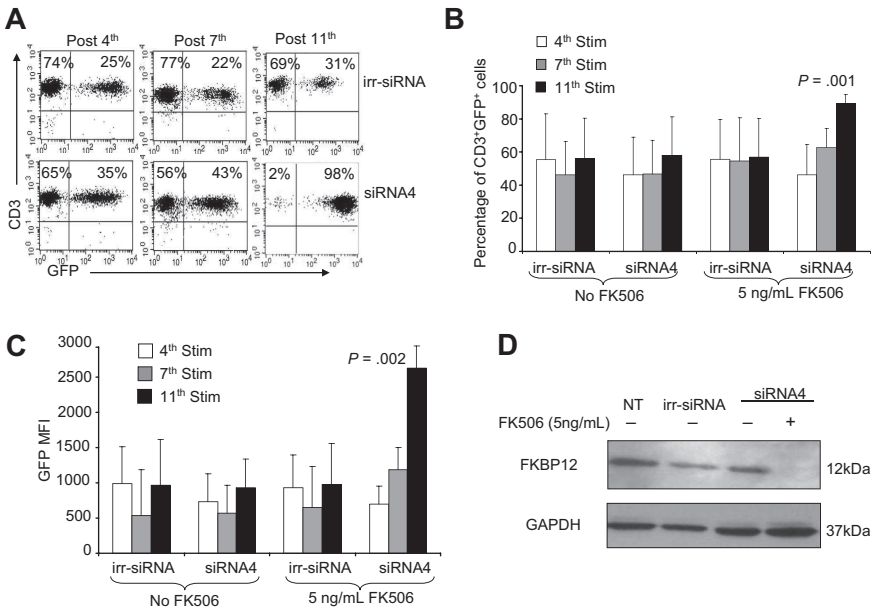

Figure 2. Selection of EBV-CTLs with a silenced FKBP12 occurs in the presence of FK506. EBV-CTLs were transduced with either the pSUPER.eGFP vector encoding the irrelevant siRNA (irr-siRNA) or pSUPER.eGFP encoding siRNA4. (A) GFP expression (as measure of transduction) of irr-siRNA$^+$ (top plots) and siRNA4$^+$ (bottom plots) EBV-CTLs stimulated with irradiated EBV-LCLs in the presence of IL-2 (20 U/mL) and FK506 (5 ng/mL) in a representative donor. The plots show a progressive increase of GFP$^+$ cells for siRNA4$^+$ CTLs, whereas the percentage of GFP$^+$ cells is stable for irr-siRNA$^+$ CTLs. (B) The data for the percentage of GFP$^+$ cells for 6 CTL lines. Bars represent mean ± SD. Shown is the percentage of GFP$^+$ cells after the 4th, 7th, and 11th stimulations, which significantly increased over time only for siRNA4$^+$ EBV-CTLs, whereas it remained stable for irr-siRNA$^+$ EBV-CTLs. (C) The MFI of GFP$^+$ cells significantly increased in siRNA4$^+$ EBV-CTLs compared with irr-siRNA$^+$ cells when cells were maintained in culture in the presence of FK506. Bars represent mean ± SD for 6 CTL lines. (D) The expression of FKBP12 in NT and irr-siRNA$^+$ EBV-CTLs and in siRNA4$^+$ EBV-CTLs after 5 weeks in culture in the absence or in the presence of FK506, as assessed by WB. FKBP12 is completely undetectable by WB in siRNA4$^+$ EBV-CTLs cultured in the presence of FK506.

with either pSUPER.eGFP encoding siRNA4 or pSUPER.eGFP encoding control siRNA and determined transduction efficiency by measuring GFP expression using FACS analysis. Transduction efficiency was 46% (± 22%) for siRNA4$^+$ CTLs and 56% (± 27%) for irr-siRNA$^+$ CTLs. After transduction, EBV-CTLs were maintained in culture by weekly stimulation with irradiated autologous EBV-LCLs and suboptimal doses of IL-2 (20 U/mL added twice a week) because ex vivo cultured EBV-CTLs become highly dependent on IL-2 for their proliferation and no expansion is observed in the absence of exogenous cytokines (data not shown and Quintarelli et al[32]), with or without the addition of FK506 (5 ng/mL added twice a week) starting 1 week after transduction (fourth stimulation). We determined whether CTL lines were selected/enriched over time in FK506-resistant cells by monitoring changes in the percentage of GFP$^+$ cells. As shown in Figure 2A and B, the percentage of GFP$^+$ CTLs significantly increased over the following 7 weeks of culture for siRNA4$^+$ EBV-CTLs cultured in the presence of FK506 (from 46% ± 22% at the fourth stimulation to 89% ± 5% at the 11th stimulation; $P = .001$). In contrast, the percentage of GFP$^+$ CTLs remained stable for irr-siRNA$^+$ EBV-CTLs cultured in the presence of FK506 (from 56% ± 27% at the 4th stimulation to 57% ± 23% at the 11th stimulation; P = not significant). In parallel with the increasing percentages of GFP$^+$ cells, the GFP MFI significantly increased in siRNA4$^+$ EBV-CTLs (from 692 ± 263 to 2625 ± 318; $P = .002$) when these cells were maintained in culture in the presence of FK506 (Figure 2C). These data show a selective enrichment of FKBP12-silenced EBV-CTLs, which suggests they had indeed become FK506 resistant. As expected, the percentage of GFP$^+$ cells did not increase when siRNA4$^+$ EBV-CTLs were cultured without FK506, confirming the lack of any intrinsic selective growth advantage for CTLs in which FKB12 was down-regulated (Figure 2B-C). The selection of siRNA4$^+$ EBV-CTLs was also maintained when a higher dose of FK506 (10 ng/mL) was added to the culture (supplemental Figure 1, available on the *Blood* website; see the Supplemental Materials link at the top of the online article).

Finally, we confirmed that the positive selection of siRNA4$^+$ EBV-CTLs in the presence of FK506 corresponded to an enrichment of EBV-CTLs with a significant down-regulation of FKBP12. As shown in Figure 2D, FKBP12 was detectable by WB in nontransduced (NT) EBV-CTLs and in those transduced with irr-siRNA cultured without FK506. In contrast, FKBP12 was completely undetectable in EBV-CTLs transduced with siRNA4 and maintained in culture for 5 weeks with antigen stimulation and in the presence of FK506 (Figure 2D). We have further supported the significance of this finding by exploring the NFAT pathway, which was partially preserved only in T cells expressing siRNA4 when stimulated in the presence of FK506 (supplemental Figure 1D).

siRNA4$^+$ EBV-CTLs retain antigen-specific expansion in the presence of FK506

To discover whether enrichment of CTLs with knocked-down FKBP12 observed in the previous experiments was determined by a preserved proliferation of siRNA4$^+$ EBV-CTLs in the presence of FK506, we measured EBV-CTL proliferation and numeric increase after antigen stimulation by a thymidine uptake assay and counting viable cells using trypan blue exclusion, respectively. Figure 3A shows the thymidine uptake of EBV-CTLs expressing either irr-siRNA or siRNA4 and cultured in the presence of increasing concentration of FK506. We observed that concentrations of FK506 as low as 5 ng/mL significantly reduced the proliferative capacity of NT and irr-siRNA$^+$ EBV-CTLs. In contrast, siRNA4$^+$ CTLs retained most of their proliferative capacity when FK506 was added, irrespective of the dose. Figure 3B shows data for 6 EBV-CTL lines cultured in the presence of 5 ng/mL FK506. Proliferation of both control NT and irr-siRNA$^+$ EBV-CTLs ($3.2 \times 10^4 \pm 0.7 \times 10^4$ cpm and $3.6 \times 10^4 \pm 1.4 \times 10^4$ cpm, respectively) was significantly reduced in the presence of 5 ng/mL FK506 ($0.9 \times 10^4 \pm 0.5 \times 10^4$ cpm and $1.5 \times 10^4 \pm 0.9 \times 10^4$ cpm, respectively; $P = .003$), which translates to 70% (± 14%) inhibition for NT EBV-CTLs and 60% (± 20%) inhibition for irr-siRNA$^+$ EBV-CTLs. By contrast, proliferation of siRNA4$^+$ EBV-CTLs in the presence of FK506 was substantially preserved. Thymidine incorporation in presence of FK506 was 3.3×10^4 ($\pm 1.3 \times 10^4$) cpm, which was only slightly reduced from that of siRNA4$^+$ EBV-CTLs cultured in the absence of FK506 ($4.4 \times 10^4 \pm 1.5 \times 10^4$ cpm; $P = .06$). Indeed, the percentage of inhibition of siRNA4$^+$ EBV-CTLs was 29% (± 7%) in

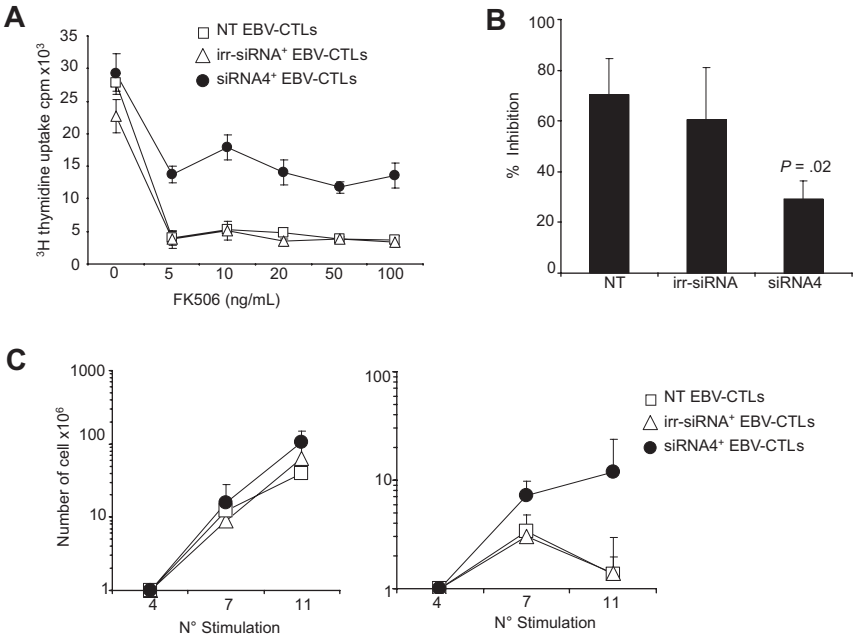

Figure 3. siRNA4$^+$ EBV-CTLs retain proliferative activity in the presence of FK506. (A) The thymidine uptake of NT, irr-siRNA$^+$, and siRNA4$^+$ EBV-CTLs after stimulation with autologous EBV-LCLs in the presence of increasing concentration of FK506. In the presence of FK506, proliferation of both NT and irr-siRNA$^+$ EBV-CTLs is significantly reduced compared with siRNA4$^+$ EBV-CTLs. (B) The percentage inhibition for NT, irr-siRNA$^+$, and siRNA4$^+$ EBV-CTLs grown in the presence of FK506. Bars represent mean ± SD of 4 CTL lines. (C) The expansion in cell numbers of NT, irr-siRNA$^+$, and siRNA4$^+$ EBV-CTLs stimulated weekly with EBV-LCLs and IL-2 (20 U/mL) with or without the addition of FK506 (5 ng/mL). T-cell numbers increased for all CTLs in the absence of FK506, but in the presence of FK506 increased only for siRNA4$^+$ CTLs. Shown are median ± SEM for 6 CTL lines.

the presence of FK506 (Figure 3B). This maintenance of thymidine uptake was significantly greater than that observed in NT or irr-siRNA$^+$ EBV-CTLs cultured in the presence of FK506 ($P < .01$).

When control EBV-CTLs and siRNA4$^+$ EBV-CTLs were maintained in culture for more than 7 weeks using weekly stimulation with EBV-LCLs, suboptimal doses of IL-2 (20 U/mL twice a week), with or without the addition of FK506 (5 ng/mL twice a week), only EBV-CTLs expressing siRNA4 numerically expanded in the presence of FK506 (median fold increase, 24; range, 3-70; Figure 3C). By contrast, the expansion of NT and irr-siRNA$^+$ EBV-CTLs was almost completely inhibited in the presence of FK506 (median fold expansion, 1; range 0-2; Figure 3C). Similar results were obtained when a dose of 10 ng/mL FK506 was added to the culture (supplemental Figure 2).

Silencing of FKBP12 does not affect EBV-CTL functionality

We evaluated the immunophenotype, cytotoxic activity, and EBV-antigen specificity of FKBP12-silenced EBV-CTLs using FACS analysis, ^{51}Cr release assay, and multimers and IFNγ ELIspot assay, respectively. As shown in Figure 4A, NT and irr-siRNA$^+$ EBV-CTLs were predominantly CD3$^+$CD8$^+$ T lymphocytes (88% ± 8% and 87% ± 6%, respectively). The majority of CTLs expressed the αβTCR (90% ± 1% and 88% ± 11%), with less than 2% of natural killer cells (CD3$^-$CD56$^+$). Selective expansion of siRNA4$^+$ EBV-CTLs in the presence of FK506 did not alter their phenotype (CD3$^+$CD8$^+$ = 83% ± 12%; αβTCR$^+$ = 82% ± 14%; and CD3$^-$CD56$^+$ = 0.3% ± 0.2%; Figure 4A). We evaluated the cytotoxic activity of EBV-CTLs using a standard 4-hour ^{51}Cr

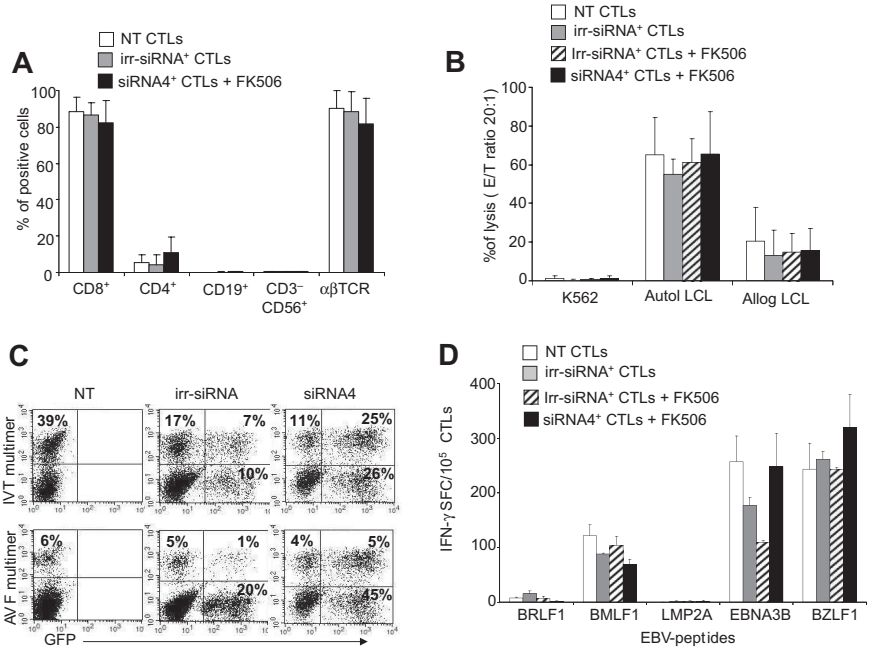

Figure 4. siRNA4$^+$ EBV-CTLs retain their immunophenotype, cytotoxic activity, and EBV-antigen specificity. (A) The immunophenotype of NT and irr-siRNA$^+$ EBV-CTLs and of siRNA4$^+$ EBV-CTLs cultured in the presence of FK506. Means ± SD are shown for the 6 CTL lines. No significant phenotypic differences were observed for siRNA4$^+$ CTLs expanded in the presence of FK506. (B) The results of a standard ^{51}Cr release assay of NT and irr-siRNA$^+$ EBV-CTLs and of irr-siRNA$^+$ and siRNA4$^+$ EBV-CTLs cultured in the presence of FK506. Targets were K562, autologous LCLs, and allogeneic LCLs. Shown is the CTL/tumor cell ratio of 20:1. Bars represent the mean ± SD of the EBV-CTLs generated from 6 donors. No significant differences in cytotoxic activity were observed for siRNA4$^+$ CTLs versus NT or irr-siRNA$^+$ CTLs. (C) The frequencies of multimers recognizing latent EBV-associated antigens (EBNA3B-AVF and EBNA3B-IVT) in NT (left plots) and irr-siRNA$^+$ (middle plots) EBV-CTLs and in siRNA4$^+$ (right plots) EBV-CTLs cultured in the presence of FK506 for 3 weeks in 1 representative donor. (D) The frequency of CTLs responding to the indicated EBV-specific peptides assessed by IFNγ ELIspot assay in another representative donor.

Table 1. Analysis of EBV specificity within the healthy donor CTL lines

Peptide	Lytic	EBNA1	EBNA3	Irrelevant
Donor 1				
NT CTLs	243 ± 47	1202 ± 154	257 ± 47	0 ± 0
irr-siRNA$^+$ CTLs	242 ± 4	ND	109 ± 4	1 ± 1.7
siRNA4$^+$ CTLs + FK506	319 ± 61	1050 ± 77	248 ± 61	1.7 ± 2.1
Donor 2				
NT CTLs	12 ± 1.5	ND	143 ± 23	0 ± 0
irr-siRNA$^+$ CTLs	14 ± 3.1	ND	224 ± 16	0.3 ± 0.6
siRNA4$^+$ CTLs + FK506	5 ± 1.2	ND	230 ± 16	0.7 ± 0.6
Donor 3				
NT CTLs	111 ± 10	ND	0 ± 0	1.3 ± 1.5
irr-siRNA$^+$ CTLs	41 ± 10	ND	0 ± 0	0.7 ± 0.6
siRNA4$^+$ CTLs + FK506	64 ± 15	ND	0 ± 0	2 ± 1
Donor 4				
NT CTLs	ND	ND	701.3 ± 89.5	0 ± 0
irr-siRNA$^+$ CTLs	ND	ND	356 ± 48.1	0 ± 0
siRNA4$^+$ CTLs + FK506	ND	ND	611 ± 95	0 ± 0

Numbers are mean ± SD of interferonγ (IFNγ) spot-forming cells/10^5 cytotoxic T lymphocytes (CTLs).

EBV indicates Epstein-Barr virus; NT-CTLs, nontransduced cytotoxic T lymphocytes; siRNA, small interfering RNA; irr-siRNA, irrelevant si-RNA; and ND, not determined.

release assay. As shown in Figure 4B, EBV-CTLs expressing siRNA4 and cultured for 4 weeks in the presence of FK506 still retained major histocompatibility complex–restricted cytotoxic activity against EBV$^+$ targets (66% ± 22% lysis of autologous EBV-LCLs and 16% ± 12% of allogeneic EBV-LCLs, at a 20:1 E/T ratio). This was similar to irr-siRNA$^+$ EBV-CTLs (61% ± 12% lysis of autologous EBV-LCLs and 15% ± 10% of allogeneic EBV-LCLs, at a 20:1 E/T ratio). As expected, addition of FK506 during the 4-hour incubation did not impair CTL cytotoxic activity (data not shown).[13] To ensure that EBV-CTLs retained the broad EBV-specific reactivity necessary for effective control of EBV-PTLDs, we analyzed the specificities of 4 CTL lines with informative HLA typing, using their binding of EBV-specific HLA multimers and their IFNγ production in response to EBV-derived peptides in an ELIspot assay. Figure 4C shows a representative donor in whom siRNA4$^+$ EBV-CTLs grown in the presence of FK506 for 3 weeks maintained the same frequency of T cells recognizing EBV-associated antigen. EBV-specific T cells were also functional as they specifically released IFNγ in response to EBV-derived peptides (Figure 4D). In all 4 CTL lines, the broad repertoire of the EBV-CTLs was retained with detection of specific IFNγ production against lytic and latent EBV-associated proteins (Table 1).

siRNA4$^+$ EBV-CTLs have improved control of tumor growth in vivo in the presence of FK506

To assess whether siRNA4$^+$ EBV-CTLs could control the growth of EBV$^+$ lymphomas in the presence of FK506 in vivo, we used a SCID mouse xenograft model.[30] Eight-week-old sublethally irradiated SCID mice (8 mice/group) were implanted with FFLuc-labeled EBV$^+$ lymphomas in the peritoneal cavity. Light emission by tumor cells was monitored as an indication of tumor growth. Once progressive increase of bioluminescence occurred (usually 3-4 days after tumor injection) mice were treated intraperitoneally either with 2 doses of irr-siRNA$^+$ EBV-CTLs or siRNA4$^+$ EBV-CTLs, followed by intraperitoneal injection of IL-2 (1000 U/mice) and FK506 (10 mg/kg) 3 times a week.[30] Control groups received an equivalent amount of IL-2 but not FK506. As shown in Figure 5A and B, the tumor bioluminescence of mice treated with irr-siRNA$^+$ CTLs and FK506 progressively increased (from $6 \times 10^7 \pm 4 \times 10^7$ to $1.9 \times 10^9 \pm 1.6 \times 10^9$ p/s/cm^2/sr by day 33) compared with mice receiving siRNA4$^+$ CTLs and FK506 (from $5.3 \times 10^7 \pm 2 \times 10^7$ to $3.2 \times 10^8 \pm 3.6 \times 10^8$ p/s/cm^2/sr by day 33; $P = .02$). Control of tumor growth by siRNA4$^+$ CTLs in presence of FK506 was similar to that obtained in mice treated with irr-siRNA$^+$ EBV-CTLs or siRNA4$^+$ EBV-CTLs without FK506 (tumor bioluminescence $3.3 \times 10^8 \pm 2.8 \times 10^8$ and $4.4 \times 10^8 \pm 1.9 \times 10^8$, respectively, by day 33). The control of tumor growth in mice receiving siRNA4$^+$ EBV-CTLs in the presence of FK506 translated into an improved survival of these mice by day 40 after tumor injection ($P = .04$) compared with mice receiving irr-siRNA$^+$ CTLs and FK506 (Figure 5C). Hence, siRNA4$^+$ EBV-CTLs can control tumor growth in vivo in the presence of FK506.

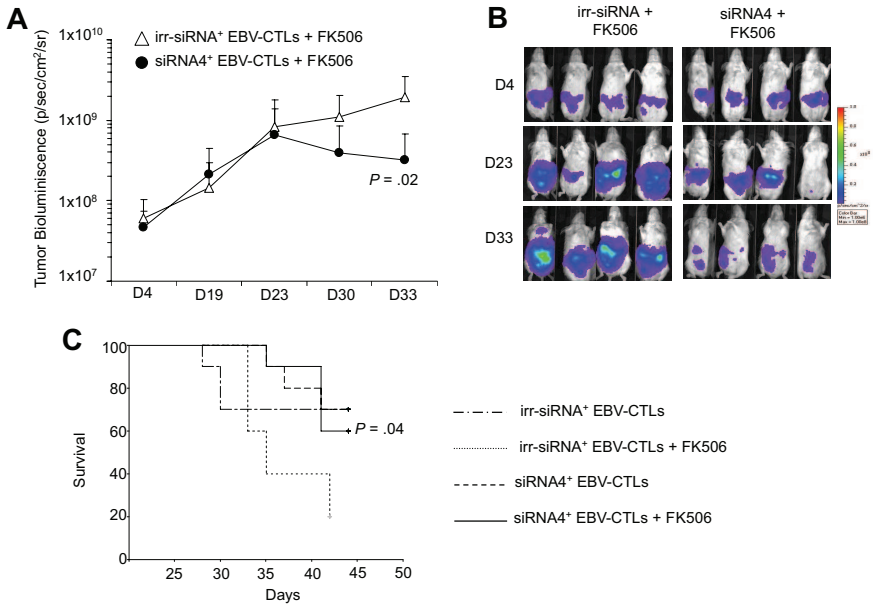

Figure 5. siRNA4$^+$ EBV-CTLs retain their function in vivo in the presence of FK506. To evaluate in vivo antitumor activity, irr-siRNA$^+$ and siRNA4$^+$ EBV-CTLs were injected intraperitoneally in SCID mice bearing EBV$^+$ lymphoma labeled with FFLuc. EBV-CTLs were transferred 4 and 11 days after intraperitoneal tumor implant. Tumor growth was monitored using the IVIS in vivo imaging system. IL-2 and FK506 were injected intraperitoneally 3 times per week. (A) By 33 days after CTL infusion, tumor growth, measured as maximum photon/sec/cm^2/steradian (p/s/cm^2/sr), was significantly greater in mice receiving irr-siRNA$^+$ EBV-CTLs and FK506 compared with mice (8 mice per group) receiving siRNA4$^+$ EBV-CTLs and FK506. Lines represent the average light emission ± SD. (B) Pictures of 4 representative mice per group. (C) The survival curve for SCID mice bearing EBV$^+$ lymphoma that received irr-siRNA$^+$ or siRNA4$^+$ EBV-CTLs and IL-2 and FK506 intraperitoneally 3 times/week. Control mice received irr-siRNA$^+$ or siRNA4$^+$ EBV-CTLs and IL-2 but not FK506.

Discussion

We have shown that EBV-CTLs can be made resistant to FK506, the most common immunosuppressive drug used for liver, heart, and renal transplant recipients.[14] This effect is obtained by a selective siRNA-mediated knockdown of FKBP12,[19] a key protein that, after FK506 biding, blocks the activation of the calcineurin pathway, which in turn inhibits NFAT activation.[18] As a consequence, even at doses of FK506 that inhibited EBV-CTLs with unmodified levels of FKBP12, gene-modified CTLs continue to proliferate and function as antitumor effector cells in vitro and in vivo in a xenograft model. This strategy can therefore preserve the function of desirable T cells, while maintaining suppression of alloreactive T cells. The approach could be adapted for the control of PTLDs or for other viral infections that cause morbidity and mortality in patients receiving solid organ transplantation.[11,33-35]

Recipients of SOT receive life-long immunosuppression to prevent rejection of the transplanted organ.[12] As a result, they have increased susceptibility to a range of viral infections,[11,33,35] and in particular EBV infection can induce the occurrence of often fatal lymphomas.[36] Although adoptive transfer of virus-specific T cells have proven safe in SOT as well as HSC transplant recipients,[11] the continuous immunosuppressive environment in SOT recipients limits proliferation and persistence of these cells in distinction to their expansion after HSC transplantation.[1,2] Although the short-term effects of adoptively transferred EBV-CTLs may control lymphoproliferative diseases in SOT recipients, they act imperfectly to control the high virus load in these patients,[7] and their lack of persistence means they cannot readily be used as prophylaxis to provide long-term control of EBV reactivation. The immunosuppressive drugs received by subject after SOT are designed specifically to inhibit T cells and reduce their ability to secrete and respond to cytokines upon stimulation.

We chose to block the function of FK506 by stably silencing the expression of FKBP12 using retroviral transduction with a specific siRNA vector, based on previous work in knockout mice showing that FK506-induced growth inhibition was abolished in FKBP12-deficient T cells and that these cells had normal function in response to antigen stimulation.[19] FK506 is an immunophilin-binding drug that specifically targets FKBP12.[19] Down-regulation of FKBP12 should prevent the formation of the FK506-FKBP12 complex that binds to calcineurins A and B and inhibits the dephosphorylation of cytoplasmic nuclear factor of activated T cells (NFAT), which translocates to the nucleus to initiate IL-2 transcription in activated T cells.[18] FKBP12, however, is an abundant protein and therefore it was not clear whether it would be susceptible to knockdown. Indeed of 17 siRNAs only 5 produced more than 50% inhibition and only 1 induced more than 80% inhibition, and was chosen for further studies. Our data demonstrate that silencing of FKBP12 in EBV-CTLs allows them to proliferate in the presence of the drug, so that their functionality should not be impaired in vivo when patients continue on their immunosuppressive regimen. Although other FKBPs (such as FKBP12.6 and FKBP51) are present in T cells, their role in mediating FK506-induced immunosuppression is dispensable, likely due to the their limited accessibility or lower binding affinity to the drug.[19] The substantial retained proliferation of our FKBP12-silenced CTLs in the presence of FK506 supports this interpretation.

Although previous studies showed that FKBP12-deficient murine T cells were not dysfunctional,[19] down-regulation of this protein in human EBV-CTLs may alter critical effector T-cell functions, such as cytotoxic activity, activation, and expansion after antigen-specific stimulation, or may alter phenotype or antigen specificity. Our data show that FKBP12-silenced EBV-CTLs have no such alterations. Hence, siRNA4$^+$ EBV-CTLs retain their major histocompatibility complex–restricted cytotoxic activity, produce IFNγ on exposure to EBV-associated antigens, and proliferate in the presence of FK506. As a result, the control of lymphoma growth in our in vivo xenogenic mouse model was significantly prolonged in mice receiving FK506.

FK506 is not an exclusive ligand for FKPB12. Rapamycin, another immunosuppressive agent used in SOT recipients,[37] also binds to the FKBP12 to produce T-cell inhibition.[18] Although rapamycin acts through the mammalian target of rapamycin rather than the calcineurin pathway,[18] the beneficial effects of FKBP12-silenced T cells may also be extended to patients receiving rapamycin immunosuppression (supplemental Figure 3).

We conclude that the down-regulation of FKBP12 in EBV-CTLs can be used to sustain their proliferative activity even in the presence of FK506, and provide efficient control of EBV-related lymphomas. A similar approach may be of value for protecting other pathogen-specific T cells such as cytomegalovirus- and adenovirus-specific CTLs[38] that could be infused in patients after solid organ transplantation, thereby helping reduce morbidity and mortality from infection in these patients,[33-35] while retaining organ engraftment. Combinations of pharmacologic immunosuppression, including mycophenolate and steroids in addition to calcineurin inhibitors, are often used and resistance to multiple immunosuppressive drugs may be explored. Obviously other obstacles to adoptive EBV-CTL therapy in solid organ transplantation would remain, including cytokine dependency of CTLs and the role and direct immunosuppressive effects of the tumor environment, and will need further elucidation. The combination of different strategies will help in designing the most successful approach.

Acknowledgments

This work was supported in part by P50CA126752 from the National Institutes of Health, and a Leukemia & Lymphoma Society Specialized Center of Research. B.S. is supported by National Institutes of Health RO1 R01CA131027 and by a Leukemia & Lymphoma Society Translational Research grant. G.D. is supported by the Doris Duke Charitable Foundation/Clinical Scientist development award and by a Leukemia & Lymphoma Society Translational Research grant. B.D.A. is the recipient of a fellowship from the Società Italiana di Ematologia Sperimentale.

Authorship

Contribution: B.D.A. designed the research, performed the majority of the experiments, analyzed the data, and wrote the manuscript; G.D. designed the research, supervised the generation of the retroviral vectors, analyzed the data, and wrote the manuscript; C.Q. and L.E.H. performed some in vitro experiments; L.Z. and M.Z. provided technical assistance for some of the in vitro experiments; F.P., H.E.H., M.K.B., and C.M.R. provided assistance in the design of the research and critically reviewed the manuscript; B.S. designed the research, analyzed the data, and wrote the

manuscript; and all authors approved the final version of the manuscript.

Conflict-of-interest disclosure: The authors declare no competing financial interests.

Correspondence: Barbara Savoldo, Center for Cell and Gene Therapy, Baylor College of Medicine, 6621 Fannin St, MC 3-3320, Houston, TX 77030; e-mail: bsavoldo@bcm.tmc.edu.

References

1. Heslop HE, Ng CY, Li C, et al. Long-term restoration of immunity against Epstein-Barr virus infection by adoptive transfer of gene-modified virus-specific T lymphocytes. *Nat Med*. 1996;2(5):551-555.
2. Rooney CM, Smith CA, Ng CY, et al. Infusion of cytotoxic T cells for the prevention and treatment of Epstein-Barr virus-induced lymphoma in allogeneic transplant recipients. *Blood*. 1998;92(5):1549-1555.
3. Khanna R, Bell S, Sherritt M, et al. Activation and adoptive transfer of Epstein-Barr virus-specific cytotoxic T cells in solid organ transplant patients with posttransplant lymphoproliferative disease. *Proc Natl Acad Sci U S A*. 1999;96(18):10391-10396.
4. Comoli P, Labirio M, Basso S, et al. Infusion of autologous Epstein-Barr virus (EBV)-specific cytotoxic T cells for prevention of EBV-related lymphoproliferative disorder in solid organ transplant recipients with evidence of active virus replication. *Blood*. 2002;99(7):2592-2598.
5. Haque T, Taylor C, Wilkie GM, et al. Complete regression of posttransplant lymphoproliferative disease using partially HLA-matched Epstein Barr virus-specific cytotoxic T cells. *Transplantation*. 2001;72(8):1399-1402.
6. Haque T, Wilkie GM, Taylor C, et al. Treatment of Epstein-Barr-virus-positive post-transplantation lymphoproliferative disease with partly HLA-matched allogeneic cytotoxic T cells. *Lancet*. 2002;360(9331):436-442.
7. Savoldo B, Goss JA, Hammer MM, et al. Treatment of solid organ transplant recipients with autologous Epstein Barr virus-specific cytotoxic T lymphocytes (CTLs). *Blood*. 2006;108(9):2942-2949.
8. Haque T, Wilkie GM, Jones MM, et al. Allogeneic cytotoxic T-cell therapy for EBV-positive post-transplantation lymphoproliferative disease: results of a phase 2 multicenter clinical trial. *Blood*. 2007;110(4):1123-1131.
9. Comoli P, Maccario R, Locatelli F, et al. Treatment of EBV-related post-renal transplant lymphoproliferative disease with a tailored regimen including EBV-specific T cells. *Am J Transplant*. 2005;5(6):1415-1422.
10. Haque T, Crawford DH. The role of adoptive immunotherapy in the prevention and treatment of lymphoproliferative disease following transplantation. *Br J Haematol*. 1999;106(2):309-316.
11. Straathof KC, Savoldo B, Heslop HE, Rooney CM. Immunotherapy for post-transplant lymphoproliferative disease. *Br J Haematol*. 2002;118(3):728-740.
12. Younes BS, McDiarmid SV, Martin MG, et al. The effect of immunosuppression on posttransplant lymphoproliferative disease in pediatric liver transplant patients. *Transplantation*. 2000;70(1):94-99.
13. Savoldo B, Goss J, Liu Z, et al. Generation of autologous Epstein-Barr virus-specific cytotoxic T cells for adoptive immunotherapy in solid organ transplant recipients. *Transplantation*. 2001;72(6):1078-1086.
14. First MR. Tacrolimus based immunosuppression. *J Nephrol*. 2004;17(suppl 8):S25-S31.
15. Vanrenterghem YF. Which calcineurin inhibitor is preferred in renal transplantation: tacrolimus or cyclosporine? *Curr Opin Nephrol Hypertens*. 1999;8(6):669-674.
16. Onsager DR, Canver CC, Jahania MS, et al. Efficacy of tacrolimus in the treatment of refractory rejection in heart and lung transplant recipients. *J Heart Lung Transplant*. 1999;18(5):448-455.
17. Busuttil RW, Holt CD. Tacrolimus (FK506) is superior to cyclosporine in liver transplantation. *Transplant Proc*. 1997;29(1-2):534-538.
18. Sharma VK, Li B, Khanna A, Sehajpal PK, Suthanthiran M. Which way for drug-mediated immunosuppression? *Curr Opin Immunol*. 1994;6(5):784-790.
19. Xu X, Su B, Barndt RJ, et al. FKBP12 is the only FK506 binding protein mediating T-cell inhibition by the immunosuppressant FK506. *Transplantation*. 2002;73(11):1835-1838.
20. Huai Q, Kim HY, Liu Y, et al. Crystal structure of calcineurin-cyclophilin-cyclosporin shows common but distinct recognition of immunophilin-drug complexes. *Proc Natl Acad Sci U S A*. 2002;99(19):12037-12042.
21. Ke H, Huai Q. Structures of calcineurin and its complexes with immunophilins-immunosuppressants. *Biochem Biophys Res Commun*. 2003;311(4):1095-1102.
22. Dotti G, Savoldo B, Pule M, et al. Human cytotoxic T lymphocytes with reduced sensitivity to Fas-induced apoptosis. *Blood*. 2005;105(12):4677-4684.
23. Schomber T, Kalberer CP, Wodnar-Filipowicz A, Skoda RC. Gene silencing by lentivirus-mediated delivery of siRNA in human CD34+ cells. *Blood*. 2004;103(12):4511-4513.
24. Vera J, Savoldo B, Vigouroux S, et al. T-lymphocytes redirected against the kappa light chain of human immunoglobulin efficiently kill mature B-lymphocyte derived malignant cells. *Blood*. 2006;108(12):3890-3897.
25. Kelly PF, Carrington J, Nathwani A, Vanin EF. RD114-pseudotyped oncoretroviral vectors: biological and physical properties. *Ann N Y Acad Sci*. 2001;938:262-276.
26. Di Stasi A, De Angelis B, Rooney CM, et al. T lymphocytes co-expressing CCR4 and a chimeric antigen receptor targeting CD30 have improved homing and anti-tumor activity in a Hodgkin's tumor model. *Blood*. 2009;113(25):6392-6402.
27. Savoldo B, Rooney CM, Di Stasi A, et al. Epstein Barr virus specific cytotoxic T lymphocytes expressing the anti-CD30zeta artificial chimeric T-cell receptor for immunotherapy of Hodgkin disease. *Blood*. 2007;110(7):2620-2630.
28. Khanna R, Burrows SR. Role of cytotoxic T lymphocytes in Epstein-Barr virus-associated diseases. *Annu Rev Microbiol*. 2000;54:19-48.
29. Houssaint E, Saulquin X, Scotet E, Bonneville M. Immunodominant CD8 T cell response to Epstein-Barr virus. *Biomed Pharmacother*. 2001;55(7):373-380.
30. Vera JF, Hoyos V, Savoldo B, et al. Genetic manipulation of tumor-specific cytotoxic T lymphocytes to restore responsiveness to IL-7. *Mol Ther*. 2009;17(5):880-888.
31. Loser K, Balkow S, Higuchi T, et al. FK506 controls CD40L-induced systemic autoimmunity in mice. *J Invest Dermatol*. 2006;126(6):1307-1315.
32. Quintarelli C, Vera JF, Savoldo B, et al. Co-expression of cytokine and suicide genes to enhance the activity and safety of tumor-specific cytotoxic T lymphocytes. *Blood*. 2007;110(8):2793-2802.
33. Fisher RA. Cytomegalovirus infection and disease in the new era of immunosuppression following solid organ transplantation. *Transpl Infect Dis*. 2009;11(3):195-202.
34. Leen AM, Rooney CM. Adenovirus as an emerging pathogen in immunocompromised patients. *Br J Haematol*. 2005;128(2):135-144.
35. Fischer SA. Emerging viruses in transplantation: there is more to infection after transplant than CMV and EBV. *Transplantation*. 2008;86(10):1327-1339.
36. Gottschalk S, Rooney CM, Heslop HE. Post-transplant lymphoproliferative disorders. *Annu Rev Med*. 2005;56:29-44.
37. Monaco AP. The role of mTOR inhibitors in the management of posttransplant malignancy. *Transplantation*. 2009;87(2):157-163.
38. Leen AM, Myers GD, Sili U, et al. Monoculture-derived T lymphocytes specific for multiple viruses expand and produce clinically relevant effects in immunocompromised individuals. *Nat Med*. 2006;12(10):1160-1166.

Chapter 7

Gene Therapy to Improve Migration of T Cells to the Tumor Site

Antonio Di Stasi, Biagio De Angelis, and Barbara Savoldo

Abstract

One requirement for anti-tumor T cells to be effective is their successful traffic to tumor sites. Trafficking of T cells to lymphoid organs and peripheral tissues is a multistage process. Soluble and tissue-bonded chemokines interacting with chemokine receptors expressed by T lymphocytes certainly play a pivotal role in determining migration under physiologic conditions and during inflammation. Therefore a match between the chemokines the tumor produces and the chemokine receptors the effector T cells express is required. Since chemokine produced by the targeted tumor may not match the subset of chemokine receptors expressed by T cells, gene therapy can be used to force the expression of the specific chemokine receptor by effector T cells so that the anti-tumor activity of adoptively transferred anti-tumor T cells is maximized.

Key words: Chemokine, chemokine receptor, T cells, migration assay.

1. Introduction

1.1. Chemokines and Migration

Chemokines are small proteins (8–10 kDa) with chemoattractant properties (1). They are divided into four groups (C, CC, CXC, and CX3C), according to the number and the spacing of the first two cysteine residues in the amino-terminal part of the protein. Their effects are exerted through the binding of seven-transmembrane domain G protein-coupled receptors (7TM-GPCR). Chemokines play critical role in regulating homeostatic trafficking and inflammatory responses of hematopoietic stem cells, lymphocytes, and dendritic cells (2). In addition, chemokines are implicated in promoting autocrine or paracrine

P. Yotnda (ed.), *Immunotherapy of Cancer*, Methods in Molecular Biology 651,
DOI 10.1007/978-1-60761-786-0_7, © Springer Science+Business Media, LLC 2010

growth of cancer cells, in regulating angiogenesis, cancer cell invasion, and metastasis, and in supporting immune cells infiltration into tumors (3).

1.1.1. Migration of Immune Cells from the Circulation

Cells circulating in the blood flow exit the vasculature at post-capillary venules, after an initially loose attach (tether) and roll on endothelial cells (recruitment stage, step 1). This first step is mediated through the interaction of homing receptors present on the surface of T cells (mostly selectins but also some integrins) with their respective ligands expressed on endothelial cells, and allows cells to be exposed to chemical signals (step 2, up-regulation of adhesive capabilities) consisting of chemokines, cytokines, inflammatory lipid mediators, complement proteins such as C3a and C5a, and microbial products. This interaction results in the activation-dependent up-regulation of integrin adhesive capabilities, with arrest (step 3, firm arrest) and then exit of the circulating cell from the vasculature into tissue(s) (step 4, transmigration) (4).

1.1.2. Migration of Immune Cells to Tumors

Tumors develop when transformed cells evade the surveillance of the immune system (5). Although the majority of tumors contain immune cells, their presence is not sufficient to control cancer cells growth and/or spread (6). Predominant cell types at tumor sites are macrophages and lymphocytes. In some cancers the presence of natural killer cells, eosinophils, granulocytes, and B cells has been reported (7). Chemokines are critical players in causing infiltration by immune cells. Their role can be dual, as they can favor the infiltration of effector T cells or induce migration of cells that create a favorable environment for the tumor. Chemokines that promote recruitment of Th1 cells are small inducible cytokine A4 (MIP-1-beta), interferon inducible protein 10 (IP-10), Rantes, MIP-1 alfa, and MCP-1 (8–11). However, many chemokines can be produced by the tumor itself to escape immune surveillance (12). For instance, the chemokine CCL2 attracts type II (or M2) polarized macrophages (tumor-associated macrophages, TAM) with primarily pro-tumor functions, as they produce factors promoting angiogenesis and impairing NF-kB inflammatory pathways, and inhibitory cytokines, such as IL-10 and PGE-2 (13, 14). In addition, TAMs produce other chemokines such as CCL18 (15), which recruit naïve T cells that become anergic because of the presence of M2 and immature dendritic cells (DC), and CCL17 and CCL22, which attract $CCR4^+$ expressed on Th2 and regulatory T cells (Treg cells), which provide another immunoevasion strategy (16). CCL17 and CCL22 can be produced by the tumor itself (for example, by Reed-Sternberg cells in Hodgkin lymphoma) to attract $CCR4^+$ Th2, Treg cells as well as monocytes (17).

1.2. Significance of Studying Migration and Chemoattraction

The development of in vitro and in vivo assays to study cell migration can help in better understanding the physiological mechanisms involved in cells migration and define the components implicated in the process. For oncological applications, characterizing the interactions between chemokines and chemokine receptors offers the opportunity to improve the homing of effector T cells to the tumor side, by chemokine receptor genetic modification. An example of this application is presented in this chapter where Hodgkin lymphoma (HL) is used as a model. Indeed, this tumor generates a chemokine milieu that significantly influences which T-cell subtypes traffic to and accumulate in the tumor (17, 18). For instance, Reed-Stemberg cells produce the chemokines TARC/CCL17 and MDC/CCL22 that attract Th2 cells and Tregs, which express CCR4, the receptor for these chemokines (17, 19–22). In contrast, $CD8^+$ effector T cells, which lack CCR4 expression, are rarely detected within HL tumors, a result likely attributable to an incompatible match between the chemokines secreted by the tumor cells and the chemokine receptors expressed by the effector T cells. The abundance of Tregs (and Th2 cells) in tumors including HL can create a hostile immune microenvironment by impairing the anti-tumor activity of the few cytotoxic-effector T lymphocytes able to reach the tumor site (23). Thus, increasing the number of cytototxic T cells that efficiently reach the tumor site should enhance anti-tumor responses. Here we describe how improved migration of T cells at the tumor site can be studied using in vitro and in vivo assays.

1.3. In Vitro Evaluation of Migration: Transwell Migration Assay

Available techniques to examine in vitro migration have been reviewed by Wilkinson et al. (24). Here we describe an in vitro transwell migration assay protocol based on radioactive labeling with ^{51}Cr(25) to evaluate migration of T cells genetically modified to overexpress CCR4, the specific chemokine receptor for TARC.

1.3.1. Filter-Based Assay

Filter assays have been widely used by various authors since they are of easy accessibility and execution (26). However, because the cells cannot be observed in real time, any evidence of chemotaxis is indirect. The single-well Boyden chamber was first introduced in 1962, but several modified versions have since been developed. In Boyden's initial experiments, a 150-μm thick, cellulose ester membrane containing pores of 3-μm diameter was used to separate two compartments (upper and lower) of a chamber. A solution containing a potential chemoattractant was placed in the lower compartment, and a leukocyte suspension was placed in the upper compartment of the chamber, on top of the filter membrane. Migration was measured by counting the leukocytes

that had moved through the filter pores to the underside of the membrane in response to presentation of the chemoattractant for 1–4 h at 37°C. This system required large volumes of chemoattractants and numbers of cells.

Polycarbonate filters are more commonly used today (27). Unlike the cellulose, ester polycarbonate filters are thinner (10 μm). The pores are holes punched by neutron bombardment and the migration is dependent on a 2-D surface, whereas in cellulose filters, the cells are moving through a 3-D matrix. Despite this, the polycarbonate filter assays are more popular because they are easy to run and automatized multi-well microplates are now available, increasing the throughput of this procedure (28). By precoating the filter with either monolayer of endothelial cells (29), or extracellular matrix protein, or migration across an endothelium into a fibrillar matrix, is possible to recreate more physiological conditions.

1.3.2. Estimation of Chemotaxis

To indirectly quantify the number of migrated cells through microscope evaluation, cells can be labeled with fluorescent dyes, such as BCECF-AM and calcein AM (30, 31). Migrated cells can be more accurately quantified by simple counting or using analytic techniques, such as radioactive labeling with ^{51}Cr (25), propidium-iodide-based laser scanning cytometry (32), fluorescent-beads-based flow cytometric cell counting (33), or firefly luciferase in a high-throughput assay (34).

1.4. In Vivo Evaluation of Migration

Some of the available techniques to examine cell trafficking are based on cell labeling with tracing dyes (fluorescent dyes such as CFSE (carboxyfluorescein diacetate), bromodeoxyuridine, or radioisotopes). The major drawbacks of these techniques are the cell toxicity mediated by the dye, and the labeling loss through dilution during cell division (35, 36). To overcome such limitations, reporter genes, such as green fluorescent proteins (GFP), have been introduced (37). These optical markers allow examination of labeled cells by fluorescence microscopy and flow cytometry. However for many of these techniques, tissue/cell isolation is required, with no temporal information about dynamic cellular processes. Optical imaging techniques can overcome this problem as mammalian tissues, while relatively opaque, permit transmission of light in the visible and near infrared region of the spectrum. The bioluminescence imaging (BI) (36) is an optical imaging modality that detect externally light emitted from internal biological sources using a light-tight chamber equipped with a cooled sensitive charge-coupled device (CCD) camera (for higher sensitivity) and appropriate lenses (38). Here we describe the use of BI to evaluate migration in vivo of T cells genetically modified to overexpress CCR4, to the site of a tumor producing TARC.

Other validated methods to study in vivo migration of cells have been reviewed by Mandl et al. (36).

1.4.1. Bioluminescence Imaging

Reporter genes that encode bioluminescent enzymes (e.g., Firefly luciferase and Renilla luciferase) have been used as internal biological light sources. Since using two different substrates, they can be used together to monitor two populations simultaneously (i.e., effector and tumor cells) (39). The most frequently used enzyme is Firefly luciferase (*Photinus*). This enzyme produces light by catalyzing the oxidation of its small molecule substrate luciferin D (luciferin (D-(−)-2-(60-hydroxy-20-benzo-thiazolyl) thiazone-4-carbozylic acid) in an ATP-dependent process, with the final release of oxyluciferin, AMP, and light. The reaction is very energetically efficient: nearly all of the energy input into the reaction is transformed into light. In the last few decades, many luciferase genes have been isolated and used to build DNA vectors (40). The advantages of genome integration of such reporter genes are the possibility to carry on long-term studies and the development of animal models of neoplastic diseases. A popular device to measure bioluminescence is the IVIS® Imaging System. Some of the characteristic of the IVIS system are tridimensional spatial localization and co-registration with other imaging modes (computerized tomography (CT), MRI, bioluminescence, and fluorescent data simultaneously collected), ability to detect as few as 50 cells in vivo (one cell in vitro), and combination of epi- and trans-illumination for both superficial and deep tissue visualization. A recent report described the molecular optimization of firefly luciferase retroviral system to detect fewer than ten mouse T cells in an immunocompetent mouse model of cancer using this device (41).

2. Materials

2.1. Cell Lines Culture

1. There are several HL-derived cell lines available that produce the chemokine TARC. Examples are HDLM-2 and L-428 (German Collection of Cell Cultures, DMSZ, Braunschweig, Germany). As negative control, an anaplastic large cell lymphoma (ALCL)-derived cell line, Karpas-299 (German Collection of Cell Cultures, DMSZ), that does not produce TARC can be used. For experimental purposes, this cell line has also been genetically engineered to stably produce TARC by retroviral vector transduction (42).
2. T25/T75 tissue culture-treated flasks (Corning Life Sciences, Lowell, MA).

3. RPMI-1640 medium (Hyclone, Logan, Utah) containing 10% fetal bovine serum (FBS, Hyclone) and 2 mM L-glutamine (GIBCO-BRL, Gaithersburg, MD). Store at 4°C. Warm at 37°C before use.
4. Serum-free medium: AIM-V (GIBCO-BRL, Gaithersburg, MD). Store at 4°C. Warm at 37°C before use.

2.2. Genetically Modified Activated T Cells

1. Peripheral blood mononuclear cells (PBMCs).
2. OKT3 (ortho-Biotech) 1 mg/ml (Bridgewater, NJ). Store at 4°C.
3. Purified Mouse Anti-Human CD28 1 mg/ml (BD Pharmingen, San Diego, CA). Store at 4°C.
4. Sterile water (Baxter Healthcare Corporation).
5. Recombinant human interleukin-2 (IL-2) (Chiron, Emeryville, CA). Reconstitute in medium at 200 IU/μl. Store at –80°C in aliquots that can be used 5 or 6 times.
6. 24-well non-tissue culture-treated plates (BD Biosciences, San Jose, CA).
7. 24-well tissue culture plate (BD Biosciences).
8. Recombinant fibronectin fragment (FN CH-296; Retronectin; Takara Shuzo, Otsu, Japan). Reconstitute in water at 1 mg/ml and store aliquots at –20°C.
9. SFG-CCR4 retroviral supernatant (Vector Production Facility, Baylor College, Houston, TX). Store at –80°C in appropriate aliquots (*see* **Note 1**).
10. T cells medium: 45% RPMI (Hyclone, Logan UT), 45% Click's (Irvine, Scientific, Santa Ana, CA), 10% FBS, and 2 mM Glutamine (Gibco-BRL, Gaithersburg MD). Store at 4°C. Warm at 37°C before use.
11. Cell dissociation solution (Sigma-Aldrich, St Louis, MO). Store at 4°C.
12. IgG1-PE, IgG1-PerCP, CCR4-PE, CD8-PerCP, CD4-APC antibodies (BD Bioscience, San Jose, CA).

2.3. Transwell Migration Assay

1. 0.5-μm pore 24-well transwell plates (Corning Life Sciences, Lowell, MA).
2. AIM V medium (Gibco-BRL). Store at 4°C. Warm at 37°C before use.
3. Anti-human CCL17/TARC Antibody (R&D system, Minneapolis, MN). Reconstitute in DPBS (Gibco-BRL) at a concentration of 0.1 mg/ml. Store aliquots at –20°C to –70°C for 6 months. Avoid repeated freeze–thaw cycles.

4. Mouse anti-human IgG1 (R&D system). Reconstitute in DPBS (Gibco-BRL) at a concentration of 0.1 mg/ml. Store aliquots at –20°C. Avoid repeated freeze–thaw cycles.

2.4. Effector Cells Radiolabeling

1. ^{51}Cr (100 μcurie) (MP Biomedical, Solon, OH).
2. 1%-Triton X solution (Sigma).
3. Gamma counter Packard cobra quantum (Packard Instrument Company, Downers Grove, IL).

2.5. In Vivo Imaging

1. SFG-eGFP-FFluciferase retroviral supernatant (Vector Production Facility, Baylor College, Houston, TX). Store at –80°C in appropriate aliquots
2. Matrigel (BD Biosciences, San Jose, CA). Store at –20°C. Thaw on ice and keep it on ice when in use.
3. CB17/SCID mice (Harlan-Sprague, Indianapolis, IN).
4. IVIS® Imaging System 100 Series equipment (Caliper Life Sciences, Hopkinton, MA).
5. rhIL-2 (Teceleukin, Fisher Bioservices, Rockville, MD). Reconstitute at 200 IU/μl and store at –80°C.
6. D-luciferin, firefly, potassium salt, 1.0 g/vial (Caliper Life Sciences, Hopkinton, MA). Reconstitute D-luciferin in PBS w/o Mg^{2+} and Ca^{2+} at a concentration of 15 mg/ml, filter sterilize through a 0.2–μm filter and store at –20°C.

3. Methods

3.1. Generation and Transduction of Activated T Cells

1. On day 0, coat the appropriate amount of wells of a 24-well non-tissue culture treated plate with 0.5 ml of water containing 1 μg/ml of OKT3 and 1 μg/ml of anti-CD28 and incubate for 3–4 h at 37°C.
2. Aspirate the antibody/solution and wash with 2 ml of complete medium.
3. Resuspend PBMC at 0.5 $\times 10^6$ ml^{-1} in T-cell medium, add 2 ml/well, and incubate at 37°C, 5% CO_2.
4. On day 1, remove 1 ml of medium and replace with fresh T-cell medium containing rhIL-2 (100 U/ml).
5. On day 1, also, coat the required number of wells of a non-tissue culture-treated 24-well plate, with retronectin at a concentration of 7 μg/ml/well. Incubate at 4°C for 16–24 h.

6. On day 2 remove the retronectin-coated plate from 4°C, aspirate retronectin, and wash with medium.
7. Add 0.5 ml of SFG-CCR4 retroviral supernatant and incubate for 20 min in the biosafety cabinet. Aspirate and add another 0.5 ml of retroviral sup for 20 min.
8. Aspirate, add 1.5 ml of retroviral sup and add 0.5 ml of T cells resuspended at the concentration of 1×10^6 ml^{-1} in complete medium containing rhIL-2 (100 IU/ml) (*see* **Note 2**).
9. Spin plate at 1000 g for 20 min and incubate at 37°C for at least 48 h.
10. Two days after transduction, remove 1 ml of medium/sup from each well.
11. Add 1 ml of eGFP-FFLuc supernatant to each well and IL-2 (100 U/ml).
12. Spin plate at 1000 g for 20 min and incubate at 37°C for 48 h.
13. After 48 h of incubation, collect cells from each well and remove eventual adherent cells by using cell dissociation medium.
14. Count cells (both transduced and NT), resuspend them at the concentration of 0.5×10^6 ml^{-1} in complete medium containing rhIL-2 (50 U/ ml), and aliquot 2 ml/well.
15. Feed cells every 3–4 days with medium containing rhIL-2 (50 U/ml). Once a week, collect cells, count them, and replate them as described in **Section 3.1**, Step 11 until the number of cells is sufficient to perform the assays described below (**Sections 3.2** and **3.3**) is achieved.

3.2. Immunophenotype

Assess transduction efficiency of T cells by FACS analysis.

1. Collect 1×10^6 of T cells and wash with PBS containing 1% FBS.
2. Aliquot 1×10^5 T cells/tube.
3. Add 5 μl (or as recommended by the manufacturer) of appropriate antibodies combination to each tube:
   control: isotype PE and isotype PerCP;
   test tube: CCR4-PE and CD3-PerCP (or CD4-PerCP or CD8-PerCP).
4. Incubate in the dark for 20 min (*see* **Note 3**).
5. Wash cells with PBS/1% FBS.
6. Analyze using FACScan (Becton Dickinson) equipped with the filter set for triple fluorescence signals and cell quest software (*see* **Note 4**).

The results of a representative transduction experiment are shown in **Fig. 7.1.**

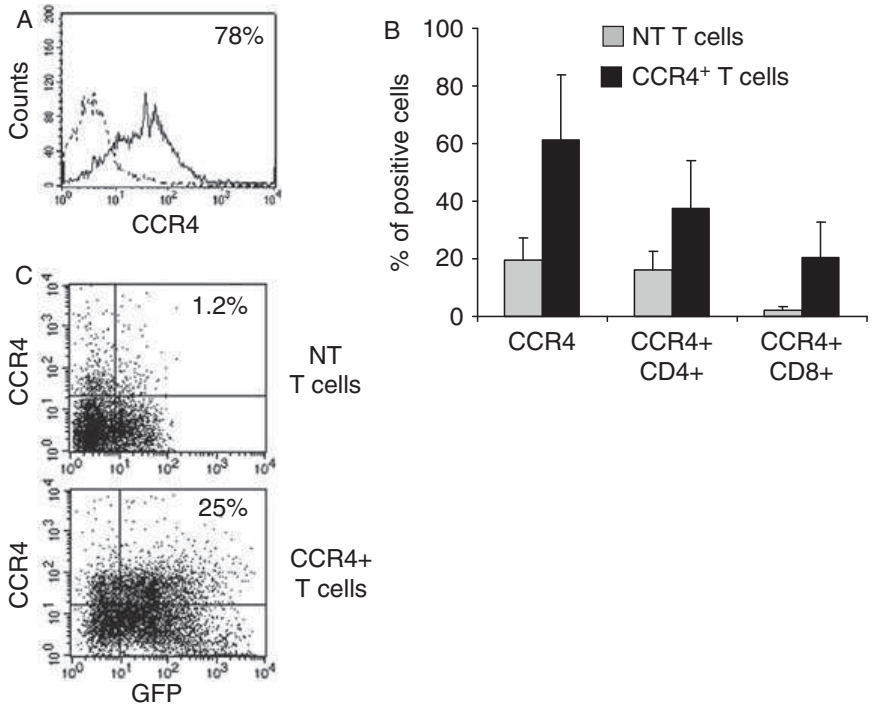

Fig. 7.1. Panel A shows phenotypic analysis of T cells generated from one healthy donor and transduced with CCR4 retroviral vector. The histogram shows the expression of CCR4 in control (Non-Transduced, NT; *dotted line*) T cells and in CCR4$^+$ T lymphocytes (*solid line*). Surface expression of CCR4 was evaluated by FACS analysis. Panel B shows the expression of CCR4, evaluated on CD4$^+$ and CD8$^+$ T cells, of NT T cells (gray bars) and CCR4$^+$ T cells (*black bars*). Bars represent the average $\pm$ standard deviation of T cells from 4 experiments. Panel C shows the expression of FF-lucifarese of NT (*upper plot*) and CCR4$^+$ (*lower plot*) T cells evaluated by FACS based on GFP expression.

3.3. Transwell Migration Assay

3.3.1. Preparation of Supernatant and of Effector T Lymphocytes

1. Cell lines producing the chemokine of interest are kept in culture in complete medium in T75 flasks. Cells should be fed at least twice weekly, by removing half of the medium and replacing it with fresh medium.
2. To perform the assay, culture the cell lines HDLM-2, L-428, Karpas, and Karpas/TARC for 16 h in serum-free medium (i.e., AIM V, to reduce the chemoattractant effect of protein contained in the medium) at a concentration of 10^6 ml^{-1} in T25 tissue culture-treated flasks (*see* **Note 5**).
3. Collect, count, and wash effector T cells in complete medium. Label at least 2–3 $\times$ 10^6 cells (*see* **Note 6**).
4. Resuspend pelleted T cells by finger-flicking and perform radiolabeling by adding 100 μCi of ^{51}Cr in a radioactive safety cabinet. Labeled cells are then incubated for 1 h at 37°C, gently resuspending cells by finger-flicking every 15 min (*see* **Note 7**).

3.3.2. Lower Chamber Preparation

1. Set up the same experimental condition for each set of effector cells, i.e., in this case NT – T cells and SFG-CCR4$^+$ transduced T cells (*see* **Note 8**).
2. Collect the supernatant, containing the chemokine of interest, from the T25 flasks in a conical tube and spin at 400 g for 5 min to remove residual cells.
3. Load the lower chamber with 500 μl of supernatant and incubate at 37°C while preparing effector cells. For example, for this particular setting add the following:
   a. HDLM-2 supernatant to two wells (one well for NT and one well for CCR4$^+$);
   b. L-428 supernatant to two wells (one well for NT and one well for CCR4$^+$);
   c. Karpas-299 supernatant to two wells (one well for NT and one well for CCR4$^+$),
   d. Karpas-299/TARC supernatant to six wells (one well for NT, one well for NT + isotype Ab, one well for NT + anti-TACR Ab; one well for CCR4$^+$, one well for CCR4$^+$ T cells + Isotype Ab, one well for CCR4$^+$ T cells + anti-TACR Ab) (*see* **Note 9**).
4. Place 500 μl of the serum-free medium in one well as negative control (to measure random migration).
5. Place 400 μl of the serum-free medium in one well where later T cells will be added (*see* **Section 3.3.3**, Step 3) (to measure maximal migration).

3.3.3. Upper Chamber Preparation

1. Wash ^{51}Cr-labeled T lymphocytes by centrifugation at 400 g for 5 min using 5 ml of complete medium; count cells after the third wash, and then resuspend them at the concentration of 1×10^6 ml^{-1} in AIM-V medium.
2. Add 100 μl of T cells into appropriate transwell inserts (upper compartment of the plate).
3. Add 100 μl of cells to the lower compartment of well containing the 400 μl of medium (*see* **Section 3.3.2**, Step 5, maximal migration).
4. Incubate the plates for 4–5 h at 37°C, 5% CO_2 (*see* **Note 10**).

3.3.4. Collection of Migrated Cells

1. After the incubation time, carefully remove the transwell inserts.
2. Add 100 μL of 1% Triton X solution to lyse cells to release the ^{51}Cr from migrated cells.
3. Collect the content of the lower chamber (migrated cells) and read using a gamma counter.

3.3.5. Measurements and Analysis of the Results (see Note 11)

1. Measure ^{51}Cr release for each specimen.
2. The chemotactic index is calculated by dividing the number of migrated cells by the random migration in the presence of medium only.
3. The percent of migration is calculated as follows: [cpm from experimental supernatant (cells migrated in the lower chamber) – cpm in the presence of medium only (random migration)]/[cpm of maximal migration – cpm of random migration] x 100.

The results of a representative migration experiment are shown in **Fig. 7.2**.

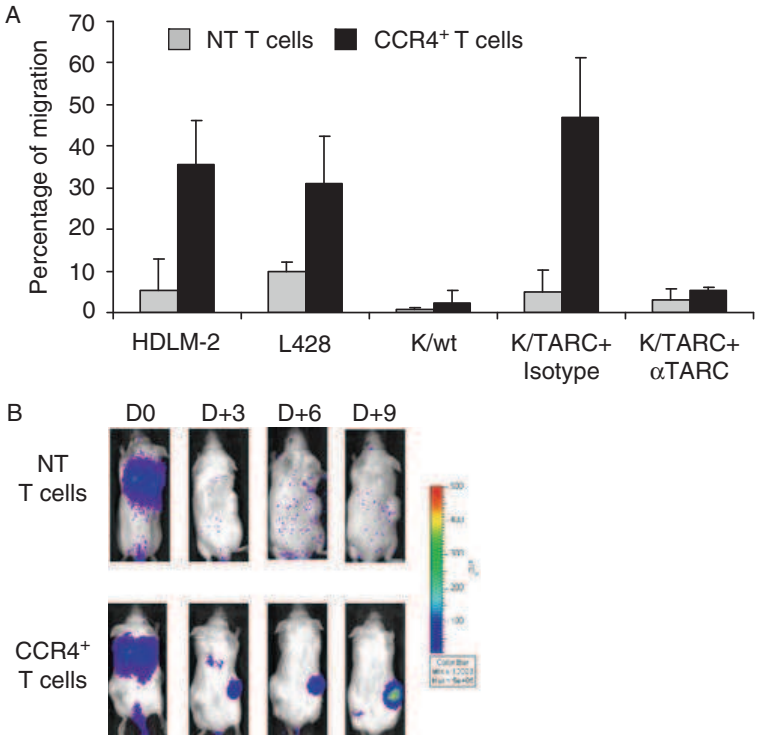

Fig. 7.2. Panel A shows the migration of NT (*gray bars*) and CCR4$^+$ (*black bars*) T cells toward TARC gradients, using the transwell migration assay in one representative donor (average $\pm$ standard deviation). T-cell migration was evaluated using culture supernatants collect from the two HL-derived cell lines (HDLM-2 and L428) that physiologically produce high amount of TARC, and from the Karpas-299 cell line genetically modified to produce TARC (K/TARC). Unmodified Karpas-299 (K/wt) was used as a control. The panel shows that migration toward TARC is significantly improved if T cells are genetically modified to overexpress CCR4 and that this improved migration of CCR4$^+$ T cells (*black bars*) is TARC-mediated as inhibited by addition of anti-TARC antibodies but not by the addition of isotype control. Panel B shows the bioluminescence signal from NT and CCR4$^+$ T cells in a SCID mouse engrafted with TARC$^-$ tumor (K/wt) on the left side and the TARC$^+$ tumor (K/TARC) on the right side. While no significant expansion of the bioluminescent signal was observed to either site of tumor in mice receiving NT T cells (*upper pictures*), increase of bioluminescence was observed in mice receiving CCR4$^+$ T cells (*lower pictures*) only at the site of tumor-producing TARC.

3.4. In Vivo Migration

3.4.1. In Vivo Tumor Model

1. Sublethally irradiate (230 cGy) 6- to 8-week-old CB17/SCID mice to oblate NK cells.
2. Inject subcutaneously (s.c.) 5×10^6 tumor cells resuspended in 200 μL of matrigel. Karpas-299 (tumor cell that does not produce TARC) can be injected on the left flank, while Karpas-299 genetically modified to express TARC can be injected on the right flank of the same animal (*see* **Note 12** and **Note 13**).
3. When tumor is palpable (0.5 cm; 5–7 days later), inject intravenously via tail vein 10×10^6 FFluciferase$^+$ T cells (control group) or CCR4$^+$FFluciferase$^+$ T cells (experimental group) (*see* **Note 14**).
4. Inject intraperitoneally (i.p.) IL-2 (500 U/mouse) three times a week to sustain T cells' expansion.

3.4.2. In Vivo Imaging Assessment System

1. Anesthetize mice in a clear Plexiglas chamber filled with 2.5% Isoflurane/air mixture (*see* **Notes 15** and **16**).
2. Inject D-luciferin intraperitoneally at a concentration of 150 mg/kg body weight (10 μl/g of body weight, i.e., for mouse 100μL of the 15 mg/ml solution to deliver 1.5 mg of D-luciferin) (*see* **Notes 17** and **18**).
3. Allow 10 min for D-luciferin distribution (*see* **Note 19**).
4. Place mice fully anesthetized in the light-tight chamber (ensure isoflurane/air deliver through the nose cones attached to the manifold).
5. Close the door of the chamber and begin acquisition using the living image program on the computer screen.
6. Expose mice for appropriate time (ranging from 5 min to <10 seconds, depending on the strength of signal). The mice position may be dorsal or ventral depending on the experiment. When the mice are turned from dorsal to ventral (or vice versa) attention must be paid to any sign of distress.
7. Select appropriate parameters, according to experimental conditions, including filters (f/stop), binning, photography (low f number and high diameter lens gives higher sensitivity and uniform light collection), and field of view (*see* **Note 20**).
8. After imaging is complete, mice are returned to their cages where they should wake up quickly. However, in this phase mice should be monitored for any possible sign of distress (rare).

9. Using the appropriate program analysis, draw a constant region of interest (ROI) over the tumor regions and measure the intensity of the signal as total photon/sec/cm^2/sr (p/s/cm^2/sr). The image data can be exported directly on an excel worksheet for further analysis (*see* **Notes 20** and **21**).

Results of a representative migration experiment are shown in **Fig. 7.2**.

4. Notes

1. Do not refreeze unused viral supernatant.
2. Keep some T cells as Non-Transduced (NT, control). These cells will need to be plated at the same concentration in complete medium containing IL-2 (100 U/ml) in a 24-well tissue culture-treated plate.
3. Room temperature is recommended when testing for CCR4 chemokine receptor.
4. Assess for GFP using the FL-1 channel.
5. The production of chemokines can be tested for each cell line to determine the types and amount of chemokine produced. Supernatant should be tested using commercially available ELISA kits (R&D System or Peprotech).
6. To estimate the required number of cells, consider that about 1×10^5 will be needed for each well of the transwell plate. However, cells will be lost during cell washes so it is recommended to start from $\sim5\times10^5$ T cells for every 1×10^5 required.
7. Wear appropriate radio-protection equipment and monitor the work area using a survey meter; label and dispose of radioactive waste according to approved guidelines; personnel monitoring with thermoluminescence dosimetry is recommended.
8. It is recommended that experiments are set in duplicate or triplicate for each condition.
9. For the wells containing supernatant and antibodies (isotype antibody or chemoattractant blocking antibody) incubate for at least 20 min prior the loading of the effector T cells in the upper transwell compartment.
10. A time-course evaluation before setting up experiment is required to evaluate the optimal period of incubation for a particular set of experimental conditions.

11. A different option to this protocol is to quantitate the migrated cells by direct counting. In this case, you will not need to label cells with ^{51}Cr. In addition, it is recommended to plate at least 1×10^6 cells in the upper compartment. Then follow the alternative step in **Section 3.3.4** Migrated cells collection: after incubation, carefully remove the transwell inserts and collect the content of the lower chamber making sure to collect all the migrated cells; count viable cells after dilution with trypan blue. The percent of migration is calculated as above (**Section 3.3.5**, Step 3) using the cell number as the parameter.
12. Using this approach each mouse acts as a "self-control" for unmodified and CCR4$^+$ T cells.
13. Ensure that the two cell lines have comparable in vivo growth.
14. Collect T cells and wash them with DPBS; then count and resuspend them in DPBS in 200 μl final volume.
15. In vivo imaging assessment can be performed starting from the day of lymphocyte injection and subsequently three times a week.
16. A clear chamber allows unimpeded visual monitoring of the animals, e.g., to easily determine if the animals are breathing.
17. A D-luciferin kinetic study should be performed for each animal model to determine peak signal time. Preferred site for injection is the animal's lower left abdominal quadrant. Mice can be manually restrained, dorsal recumbency (abdomen side up), with cranial (head) end of animal pointed down. Needle should be bevel-side up and slightly angled when entering the abdominal cavity. Penetrate just through abdominal wall (about 4–5 mm). The tip of the needle should just penetrate the abdominal wall of the animal's left lower abdominal quadrant.
18. Recommended needle size is 25 gauge (usually used with 1-cc syringe).
19. Ten minutes post-substrate administration, the D-luciferin has been shown to distribute in saturation levels broadly to tissues throughout the body and can cross the blood–brain barrier and placental barrier (38).
20. Refer to IVIS manual and software for further information.
21. When using photon/sec/cm^2/sr, measured signals are automatically corrected for these variables; autofluorescent background is automatically subtracted as well.

References

1. Mackay, C. R. (2001) Chemokines: Immunology's high impact factors. *Nat Immunol 2*, 95–101.
2. Mantovani, A., Allavena, P., Sozzani, S., Vecchi, A., Locati, M., and Sica, A. (2004) Chemokines in the recruitment and shaping of the leukocyte infiltrate of tumors. *Semin Cancer Biol 14*, 155–160.
3. Balkwill, F. (2004) Cancer and the chemokine network. *Nat Rev Cancer 4*, 540–550.
4. Sackstein, R. (2005) The lymphocyte homing receptors: gatekeepers of the multistep paradigm. *Curr Opin Hematol 12*, 444–450.
5. Liotta, L. A. and Kohn, E. C. (2001) The microenvironment of the tumour-host interface. *Nature 411*, 375–379.
6. Dunn, G. P., Old, L. J., and Schreiber, R. D. (2004) The immunobiology of cancer immunosurveillance and immunoediting. *Immunity 21*, 137–148.
7. Vicari, A. P. and Caux, C. (2002) Chemokines in cancer. *Cytokine Growth Factor Rev 13*, 143–154.
8. Moran, C. J., Arenberg, D. A., Huang, C. C., Giordano, T. J., Thomas, D. G., Misek, D. E., Chen, G., Iannettoni, M. D., Orringer, M. B., Hanash, S., and Beer, D. G. (2002) RANTES expression is a predictor of survival in stage I lung adenocarcinoma. *Clin Cancer Res 8*, 3803–3812.
9. Tang, K. F., Tan, S. Y., Chan, S. H., Chong, S. M., Loh, K. S., Tan, L. K., and Hu, H. (2001) A distinct expression of CC chemokines by macrophages in nasopharyngeal carcinoma: implication for the intense tumor infiltration by T lymphocytes and macrophages. *Hum Pathol 32*, 42–49.
10. Negus, R. P., Stamp, G. W., Hadley, J., and Balkwill, F. R. (1997) Quantitative assessment of the leukocyte infiltrate in ovarian cancer and its relationship to the expression of C-C chemokines. *Am J Pathol 150*, 1723–1734.
11. Monti, P., Leone, B. E., Marchesi, F., Balzano, G., Zerbi, A., Scaltrini, F., Pasquali, C., Calori, G., Pessi, F., Sperti, C., Di, C. V, Allavena, P., and Piemonti, L. (2003) The CC chemokine MCP-1/CCL2 in pancreatic cancer progression: regulation of expression and potential mechanisms of antimalignant activity. *Cancer Res 63*, 7451–7461.
12. Gabrilovich, D. (2004) Mechanisms and functional significance of tumour-induced dendritic-cell defects. *Nat Rev Immunol 4*, 941–952.
13. Elgert, K. D., Alleva, D. G., and Mullins, D. W. (1998) Tumor-induced immune dysfunction: the macrophage connection. *J Leukoc Biol 64*, 275–290.
14. Mantovani, A., Sozzani, S., Locati, M., Allavena, P., and Sica, A. (2002) Macrophage polarization: tumor-associated macrophages as a paradigm for polarized M2 mononuclear phagocytes. *Trends Immunol 23*, 549–555.
15. Adema, G. J., Hartgers, F., Verstraten, R., de, V. E., Marland, G., Menon, S., Foster, J., Xu, Y., Nooyen, P., McClanahan, T., Bacon, K. B., and Figdor, C. G. (1997) A dendritic-cell-derived C-C chemokine that preferentially attracts naive T cells. *Nature 387*, 713–717.
16. Balkwill, F. (2004) Cancer and the chemokine network. *Nat Rev Cancer 4*, 540–550.
17. van den, B. A., Visser, L., and Poppema, S. (1999) High expression of the CC chemokine TARC in Reed-Sternberg cells. A possible explanation for the characteristic T-cell infiltratein Hodgkin′s lymphoma. *Am J Pathol 154*, 1685–1691.
18. Maggio, E. M., van den, B. A., Visser, L., Diepstra, A., Kluiver, J., Emmens, R., and Poppema, S. (2002) Common and differential chemokine expression patterns in rs cells of NLP, EBV positive and negative classical Hodgkin lymphomas. *Int J Cancer 99*, 665–672.
19. Ishida, T., Ishii, T., Inagaki, A., Yano, H., Komatsu, H., Iida, S., Inagaki, H., and Ueda, R. (2006) Specific recruitment of CC chemokine receptor 4-positive regulatory T cells in Hodgkin lymphoma fosters immune privilege. *Cancer Res 66*, 5716–5722.
20. Iellem, A., Mariani, M., Lang, R., Recalde, H., Panina-Bordignon, P., Sinigaglia, F., and D'Ambrosio, D. (2001) Unique chemotactic response profile and specific expression of chemokine receptors CCR4 and CCR8 by CD4(+)CD25(+) regulatory T cells. *J Exp Med 194*, 847–853.
21. D′Ambrosio, D., Iellem, A., Bonecchi, R., Mazzeo, D., Sozzani, S., Mantovani, A., and Sinigaglia, F. (1998) Selective up-regulation of chemokine receptors CCR4 and CCR8 upon activation of polarized human type 2 Th cells. *J Immunol 161*, 5111–5115.
22. Marshall, N. A., Christie, L. E., Munro, L. R., Culligan, D. J., Johnston, P. W., Barker, R. N., and Vickers, M. A. (2004) Immunosuppressive regulatory T cells are abundant in the reactive lymphocytes of Hodgkin lymphoma. *Blood 103*, 1755–1762.

23. Curiel, T. J., Coukos, G., Zou, L., Alvarez, X., Cheng, P., Mottram, P., Evdemon-Hogan, M., Conejo-Garcia, J. R., Zhang, L., Burow, M., Zhu, Y., Wei, S., Kryczek, I., Daniel, B., Gordon, A., Myers, L., Lackner, A., Disis, M. L., Knutson, K. L., Chen, L., and Zou, W. (2004) Specific recruitment of regulatory T cells in ovarian carcinoma fosters immune privilege and predicts reduced survival. *Nat Med* ***10***, 942–949.
24. Wilkinson, P. C. (1998) Assays of leukocyte locomotion and chemotaxis. *J Immunol Methods* ***216***, 139–153.
25. Capsoni, F., Minonzio, F., Ongari, A. M., and Zanussi, C. (1989) A new simplified single-filter assay for ′in vitro′ evaluation of chemotaxis of 51Cr-labeled polymorphonuclear leukocytes. *J Immunol Methods* ***120***, 125–131.
26. Wilkinson, P. C. (1998) Assays of leukocyte locomotion and chemotaxis. *J Immunol Methods* ***216***, 139–153.
27. Horwitz, D. A. and Garrett, M. A. (1971) Use of leukocyte chemotaxis in vitro to assay mediators generated by immune reactions. I. Quantitation of mononuclear and polymorphonuclear leukocyte chemotaxis with polycarbonate (nuclepore) filters. *J Immunol* ***106***, 649–655.
28. Falk, W., Goodwin, R. H., Jr., and Leonard, E. J. (1980) A 48-well micro chemotaxis assembly for rapid and accurate measurement of leukocyte migration, *J Immunol Methods* ***33***, 239–247.
29. Roth, S. J., Carr, M. W., Rose, S. S., and Springer, T. A. (1995) Characterization of transendothelial chemotaxis of T lymphocytes. *J Immunol Methods* ***188***, 97–116.
30. De Clerck, L. S., Bridts, C. H., Mertens, A. M., Moens, M. M., and Stevens, W. J. (1994) Use of fluorescent dyes in the determination of adherence of human leucocytes to endothelial cells and the effect of fluorochromes on cellular function. *J Immunol Methods* ***172***, 115–124.
31. Frevert, C. W., Wong, V. A., Goodman, R. B., Goodwin, R., and Martin, T. R. (1998) Rapid fluorescence-based measurement of neutrophil migration in vitro. *J Immunol Methods* ***213***, 41–52.
32. Butt, O. I., Krishnan, P., Kulkarni, S. S., Moldovan, L., and Moldovan, N. I. (2005) Quantification and functional analysis of chemotaxis by laser scanning cytometry. *Cytometry A* ***64***, 10–15.
33. Molema, G., Mesander, G., Kroesen, B. J., Helfrich, W., Meijer, D. K., and de Leij, L. F. (1998) Analysis of in vitro lymphocyte adhesion and transendothelial migration by fluorescent-beads-based flow cytometric cell counting. *Cytometry* ***32***, 37–43.
34. Vishwanath, R. P., Brown, C. E., Wagner, J. R., Meechoovet, H. B., Naranjo, A., Wright, C. L., Olivares, S., Qian, D., Cooper, L. J., and Jensen, M. C. (2005) A quantitative high-throughput chemotaxis assay using bioluminescent reporter cells. *J Immunol. Methods* ***302***, 78–89.
35. Lyons, A. B. (2000) Analysing cell division in vivo and in vitro using flow cytometric measurement of CFSE dye dilution. *J Immunol Methods* ***243***, 147–154.
36. Mandl, S., Schimmelpfennig, C., Edinger, M., Negrin, R. S., and Contag, C. H. (2002) Understanding immune cell trafficking patterns via in vivo bioluminescence imaging. *J Cell Biochem. Suppl* ***39***, 239–248.
37. Okabe, M., Ikawa, M., Kominami, K., Nakanishi, T., and Nishimune, Y. (1997) 'Green mice' as a source of ubiquitous green cells. *FEBS Lett* ***407***, 313–319.
38. Edinger, M., Hoffmann, P., Contag, C. H., and Negrin, R. S. (2003) Evaluation of effector cell fate and function by in vivo bioluminescence imaging. *Methods* ***31***, 172–179.
39. Bhaumik, S. and Gambhir, S. S. (2002) Optical imaging of Renilla luciferase reporter gene expression in living mice. *Proc Natl Acad Sci. US A* ***99***, 377–382.
40. Greer, L. F., III and Szalay, A. A. (2002) Imaging of light emission from the expression of luciferases in living cells and organisms: A review. *Luminescence* ***17***, 43–74.
41. Rabinovich, B. A., Ye, Y., Etto, T., Chen, J. Q., Levitsky, H. I., Overwijk, W. W., Cooper, L. J., Gelovani, J., and Hwu, P. (2008) Visualizing fewer than 10 mouse T cells with an enhanced firefly luciferase in immunocompetent mouse models of cancer. *Proc Natl Acad Sci USA* ***105***, 14342–14346.
42. Di Stasi, A., De Angelis, B., Rooney, C. M., Zhang, L., Mahendravada, A., Foster, A. E., Heslop, H. E., Brenner, M. K., Dotti, G., and Savoldo, B. (2009) T lymphocytes coexpressing CCR4 and a chimeric antigen receptor targeting CD30 have improved homing and antitumor activity in a Hodgkin tumor model. *Blood* ***113***, 6392–6402.

blood

2011 117: 3353-3362
Prepublished online January 28, 2011;
doi:10.1182/blood-2010-08-300376

High-avidity cytotoxic T lymphocytes specific for a new PRAME-derived peptide can target leukemic and leukemic-precursor cells

Concetta Quintarelli, Gianpietro Dotti, Sayyeda T. Hasan, Biagio De Angelis, Valentina Hoyos, Santa Errichiello, Martha Mims, Luigia Luciano, Jessica Shafer, Ann M. Leen, Helen E. Heslop, Cliona M. Rooney, Fabrizio Pane, Malcolm K. Brenner and Barbara Savoldo

Blood (print ISSN 0006-4971, online ISSN 1528-0020), is published weekly by the American Society of Hematology, 2021 L St, NW, Suite 900, Washington DC 20036.

High-avidity cytotoxic T lymphocytes specific for a new PRAME-derived peptide can target leukemic and leukemic-precursor cells

Concetta Quintarelli,[1-3] Gianpietro Dotti,[1,4,5] Sayyeda T. Hasan,[1] Biagio De Angelis,[1-3] Valentina Hoyos,[1] Santa Errichiello,[2,3] Martha Mims,[4] Luigia Luciano,[2,3] Jessica Shafer,[1,6] Ann M. Leen,[1,6] Helen E. Heslop,[1,4,6,7] Cliona M. Rooney,[1,5,6,8] Fabrizio Pane,[2,3] Malcolm K. Brenner,[1,4,6,7] and Barbara Savoldo[1,6]

[1]Center for Cell and Gene Therapy, Baylor College of Medicine, Houston, TX; [2]CEINGE Biotecnologie Avanzate, Napoli, Italy; [3]Dipartimento di Biochimica e Biotecnologie Mediche, University of Naples Federico II, Naples Italy; [4]Department of Medicine, Baylor College of Medicine, Houston, TX; [5]Department of Immunology, Baylor College of Medicine, Houston, TX; [6]Department of Pediatrics, Texas Children's Hospital, Houston, TX; [7]The Methodist Hospital, Houston, TX; and [8]Department of Virology, Baylor College of Medicine, Houston, TX

The cancer testis antigen (CTA) preferentially expressed antigen of melanoma (PRAME) is overexpressed by many hematologic malignancies, but is absent on normal tissues, including hematopoietic progenitor cells, and may therefore be an appropriate candidate for T cell–mediated immunotherapy. Because it is likely that an effective antitumor response will require high-avidity, PRAME-specific cytotoxic T lymphocytes (CTLs), we attempted to generate such CTLs using professional and artificial antigen-presenting cells loaded with a peptide library spanning the entire PRAME protein and consisting of 125 synthetic pentadecapeptides overlapping by 11 amino acids. We successfully generated polyclonal, PRAME-specific CTL lines and elicited high-avidity CTLs, with a high proportion of cells recognizing a previously uninvestigated HLA-A*02–restricted epitope, P435-9mer (NLTHVLYPV). These PRAME-CTLs could be generated both from normal donors and from subjects with PRAME$^+$ hematologic malignancies. The cytotoxic activity of our PRAME-specific CTLs was directed not only against leukemic blasts, but also against leukemic progenitor cells as assessed by colony-forming–inhibition assays, which have been implicated in leukemia relapse. These PRAME-directed CTLs did not affect normal hematopoietic progenitors, indicating that this approach may be of value for immunotherapy of PRAME$^+$ hematologic malignancies. (*Blood*. 2011; 117(12):3353-3362)

Introduction

Cytotoxic T lymphocytes (CTLs) directed to tumor-associated antigens (TAAs) have the potential to eradicate malignant diseases.[1-4] These CTLs may be generated in vivo by peptide-based vaccination[5-7] or ex vivo for subsequent adoptive transfer.[2,3] Irrespective of the methodology used for generation, the therapeutic effectiveness of CTLs relies on both the nature of the antigen targeted and the potency and avidity of the specific CTLs elicited. Ideally, the target antigen should be uniquely or highly expressed by tumor cells compared with normal tissues to minimize the occurrence of autoimmunity and to be directly involved in maintaining the tumor phenotype to limit the emergence of tumor escape mutants.

The cancer testis antigen (CTA) preferentially expressed antigen of melanoma (PRAME)[8] is a potential target antigen for use in the treatment of tumors. First, PRAME is overexpressed by many hematologic malignancies, such as chronic myelogenous leukemia (CML), acute myeloid leukemia (AML),[9-12] and Hodgkin lymphoma (HL),[13] as well as by solid tumors,[8] but its expression is low or absent in normal tissues, including hematopoietic progenitor cells.[10] Secondly, PRAME may significantly contribute to maintaining the tumor phenotype, because its expression can strongly inhibit cell differentiation induced by the retinoic acid receptor-α ligand all-*trans* retinoic acid,[14] a crucial pathway for the proliferation and differentiation of both normal and malignant hematopoietic cells.[15] Indeed, it has recently been demonstrated that PRAME overexpression contributes to leukemogenesis by inhibiting myeloid differentiation through blockage of the retinoic acid receptor-α–signaling pathway.[14,16]

We[17] and others[18] have generated CTLs targeting PRAME-derived peptides from healthy donors and leukemic patients using antigen-presenting cells (APCs) loaded with specific peptides[17] selected by in vitro digestion of long peptides[8] or by mass spectrometry of acid elutes obtained from tumor cells.[19] Unfortunately, these approaches have produced PRAME epitopes that have preferentially expanded low-avidity CTLs, whose modest functional activity would likely be suboptimal for clinical benefit. Therefore, to exploit PRAME as a potential target antigen in patients with hematologic malignancies and other solid tumors and to induce effective antitumor activity, we sought a means of generating high-avidity, PRAME-specific CTLs.

We now describe natural and artificial APCs loaded directly with a peptide library consisting of 125 synthetic pentadecapeptides, overlapping by 11 amino acids, which span the entire PRAME protein and generate polyclonal, PRAME-specific CTL lines with high affinity for tumor targets. We also describe an immunodominant peptide within PRAME and demonstrate selective killing of putative leukemia-progenitor cells with sparing of normal hemopoietic precursor cells. Because we could generate

Submitted August 24, 2010; accepted January 1, 2011. Prepublished online as *Blood* First Edition paper, January 28, 2011; DOI 10.1182/blood-2010-08-300376.

The online version of this article contains a data supplement.

The publication costs of this article were defrayed in part by page charge payment. Therefore, and solely to indicate this fact, this article is hereby marked "advertisement" in accordance with 18 USC section 1734.

these PRAME-specific CTLs from normal donors and from subjects with PRAME$^+$ disease, our approach may be of value for immunotherapy of PRAME$^+$ malignancies.

Methods

Cell lines and samples from healthy donors and leukemic patients

The following tumor cell lines were used: KT1 (CML) kindly provided by Dr Fujita (First Department of Internal Medicine, School of Medicine, Ehime University, Japan); BV173 (CML) and L428 (HL) from the German Collection of Cell Cultures (DSMZ, Braunschweig, Germany); and U266B1 and ARH77 (multiple myeloma), K562 (erythroleukemia), and MRC-5 (normal human fetal lung fibroblasts) from the ATCC. Cells were maintained in culture with RPMI 1640 medium (HyClone) containing 10% fetal bovine serum (HyClone), 2mM L-glutamine (GIBCO-BRL), 25 IU/mL of penicillin, and 25 mg/mL of streptomycin (BioWhittaker) in a humidified atmosphere containing 5% CO_2 at 37°C. Peripheral blood and bone marrow samples were collected according to the local institutional review board–approved protocol (University of Naples Federico II, Naples, Italy, and Baylor College of Medicine, Houston, TX).

Generation and expansion of PRAME-CTLs

CTL lines were generated from peripheral blood mononuclear cells (PBMCs) as described previously.[17] Briefly, we selected CD8$^+$ cells using "magnetic antibodies," and primed them with autologous APCs (dendritic cells or CD40-activated B lymphocytes generated from autologous PBMCs at a ratio of 1:20 APCs:CD8$^+$ cells that we loaded with HLA-A*02–restricted peptides for 2 hours and then washed twice). The cells were cultured in complete medium (45% RPMI 1640, 45% Click medium [Irvine Scientific] that we supplemented with 5% human AB serum and 2 mmoL of L-glutamine) and IL-7 (10 ng/mL), IL-12 (1 ng/mL), and IL-15 (2 ng/mL; all from R&D Systems). We loaded APCs with: (1) a pool of 4 previously identified PRAME peptides (referred as P4, a peptide pool composed of P100 VLDGLDVLL, P142 SLYSFPEPEA, P300 ALYVDSLFFL, and P425 SLLQHLIGL at 10μM each[8,17]); (2) a newly identified PRAME-derived nonamer (referred to as P435, NLTHVLYPV at 5 μM); (3) a pool of 5 PRAME-peptides (referred as P5, consisting of a P4 pool supplemented with P435 peptide at 10μM each); or (4) a peptide library, PRAME-PepMix (0.6 nmol of each peptide; JPT Technologies) composed of 125 pentadeca-peptides spanning the entire PRAME protein and also containing the 4 nonadecamers (P100, P142, P300, and P425) previously identified. To exclude the possibility of antigenic competition between peptides mixed together in the P4 pool, we included control experiments using single peptides. Other controls used APCs loaded with the HLA-A*02–restricted, pp65-derived peptide NLVPMVATV or the HLA-A*02–restricted, MART-1-derived peptide ELAGIGILTV and an irrelevant PepMix. All peptides were obtained from Genemed Synthesis. After priming with APCs, T cells were collected and stimulated weekly with artificial APCs (aAPCs) derived from the K562 cell line[17] (PBMC:K562/aAPC ratio, 4:1) loaded with the respective peptides or PepMix. IL-7, IL-12, and IL-15 cytokines were also included in this second stimulation. Subsequently, cells were expanded in complete medium with fetal bovine serum (HyClone) using IL-2 alone (50 IU/mL).[17] In selected experiments, these CTL lines were generated from CD8$^+$CD45RO$^+$ or CD8$^+$CD45RA$^+$ T cells prepared by negative immunomagnetic sorting (Miltenyi Biotec).[17]

Immunophenotyping

We stained T cells with phycoerythrin (PE)–conjugated, fluorescein isothiocyanate (FITC)–conjugated, allophycocyanin and peridinin chlorophyll protein (PerCP)–conjugated CD3, CD4, CD8, CD56, CD45RA, CD45RO, CCR7, CD28, CD27, CD62L, and CD57 monoclonal antibodies (all Becton Dickinson). We also stained cells using the KLRG antibody (Santa Cruz Biotechnology) and PE-conjugated goat anti–rabbit antibody (Jackson ImmunoResearch). Finally the T-cell receptor-Vβ (TCR-Vβ) repertoire was analyzed by fluorescence-activated cell sorting (FACS; IOTest βMark kit; Immunotech). Control samples labeled with an appropriate isotype-matched antibody were included in each experiment. We analyzed these cells using a FACScan (Becton Dickinson) equipped with the filter set for 4 fluorescence signals. T-cell lines were also analyzed for binding of specific tetramers, prepared by the Baylor College of Medicine core facility, as described previously.[20] For each sample, a minimum of 100 000 cells were analyzed using a FACSCalibur with CellQuest software (BD Biosciences).

ELISpot assay

We used an IFNγ ELISpot assay, as described previously.[21] T cells were plated in triplicate, serially diluted from 1×10^5 to 1×10^4 cells/well, and then peptides (5μM) were added. In all experiments, T cells were also incubated with an irrelevant peptide to show the specificity of IFNγ release. Alternatively, either PRAME-PepMix or an irrelevant PepMix (pp65; 0.06 nmol) was added instead of the single peptide. As a positive control, T cells were stimulated with 25 ng/mL of phorbol myristate acetate and 1 μg/mL of ionomycin (Sigma-Aldrich). The IFNγ$^+$ spot-forming cells (SFCs) were enumerated (ZellNet).

Chromium-release assay

The cytotoxic specificity of T cells was evaluated using a standard 4-hour ^{51}Cr-release assay, as described previously.[20] We incubated target cells in medium alone or in 1% Triton X-100 (Sigma-Aldrich) to determine spontaneous and maximum ^{51}Cr release, respectively. The mean percentage of specific lysis of triplicate wells was calculated as follows: [(test counts − spontaneous counts)/(maximum counts − spontaneous counts)] × 100%.

Q-RT-PCR

PRAME and p210 mRNA were measured by quantitative real-time PCR (Q-RT-PCR) analysis, as described previously.[17,22] Total RNA was also isolated from single hematopoietic colonies as described previously.[23]

Colony-forming inhibition assay of leukemic and normal hematopoietic progenitors

We purified mononuclear cells (MNCs) from the bone morrow of 3 healthy HLA-A*02$^+$ donors and from 5 samples (3 bone marrow, 2 peripheral blood) of HLA-A*02$^+$ patients with CML and from bone marrow samples from 2 HLA-A*02$^-$ subjects with CML. MNCs ($0.5\text{-}2 \times 10^4$ cells) were then coincubated with PRAME-CTLs (P435-specific, PRAME-PepMix–specific, or P4-specific: P100, 142, 300, and 425) or CTLs specific for an irrelevant peptide (ELA) at an effector:target (E:T) ratio of 10:1 for 6 hours in 0.5 mL of complete medium at 37°C. After coincubation, cells were plated in triplicate in methylcellulose medium supplemented with recombinant cytokines (MethoCult; StemCell Technologies), and incubated at 37°C. Granulocyte-macrophage colony-forming units and erythrocyte colony-forming units (CFU) were scored using a high-quality inverted microscope after 2 weeks of culture. In selected experiments, colonies were collected to assess PRAME and p210 expression by Q-RT-PCR.[23]

HLA peptide–binding assay

The binding affinity of peptides for the HLA-A*02 molecule was assessed by an HLA stabilization assay, as described previously.[24] Briefly, the HLA-A*0201–positive cell line CEM-T2 was plated in 96-well plates at 10^5 cells per well and incubated overnight with the candidate peptides at concentrations between 0 and 100mM in serum-free RPMI 1640 medium. The CEM-T2 cells were washed twice with 1× phosphate-buffered saline (PBS), and then incubated with anti–HLA-A*02-FITC monoclonal antibody (Becton Dickinson) at 4°C for 20 minutes. The cells were washed and fixed with 0.5% paraformaldehyde before FACS analysis. The fluorescence index (FI) was calculated as FI = (MFI with the given peptide − MFI without peptide)/MFI without peptide). The FI at 6mM was determined as high if > 1.5, intermediate if 1-1.5, and low if < 1.[24] Hepatitis B virus core

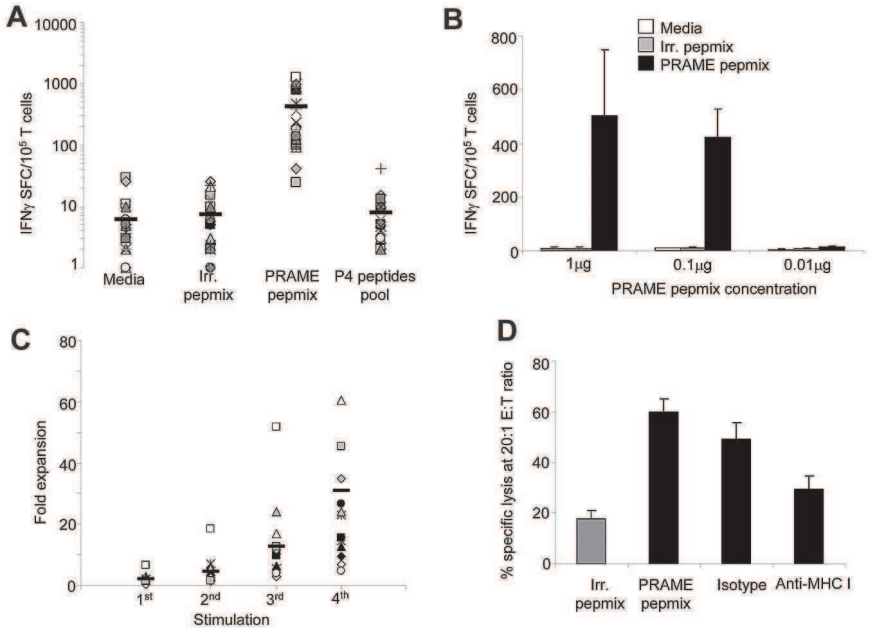

Figure 1. Generation of PRAME-specific CTLs using PepMix. We used a peptide library of 125 pentadecapeptides spanning the entire PRAME protein to load APCs for the generation of PRAME-specific CTLs. (A) Specificity of the generated CTL lines using PRAME-PepMix as assessed by INFγ ELISpot assay against control PepMix, PRAME PepMix, and a pool of the 4 previously identified HLA-A*02–restricted peptides (P4).[8,18] Medium was used to evaluate background production of IFNγ by nonstimulated CTL. Each symbol represents 1 of the 23 individual PRAME-CTLs; horizontal lines represent the mean group value. (B) IFNγ production of CTLs generated from 4 donors using the PRAME-PepMix at a concentration of 1, 0.1, or 0.01 μg (corresponding to 6, 0.6, and 0.06 nmol each of the 125 15-mer composing PRAME-PepMix, respectively) against medium, irrelevant PepMix, or PRAME-PepMix. (C) The fold expansion of PRAME-PepMix CTLs primed with autologous APCs and stimulated with aAPCs for 3 weeks. Each symbol represents one of the 15 individual PRAME-CTLs; horizontal lines represent the mean group value. (D) PRAME-CTLs expanded from healthy donors were evaluated for their cytotoxic activity using a standard 4-hour ^{51}Cr-release assay against autologous PHA blasts loaded with irrelevant (gray bar) or PRAME-PepMix (black bars). Data represent the means ± SD of PRAME-CTLs from 9 healthy donors. Shown is the killing at a 20:1 E:T ratio by PRAME-CTLs, which was significantly higher against PRAME PepMix–loaded targets compared with control PepMix targets. In addition, killing of PRAME PepMix–loaded autologous PHA blasts by CTLs was significantly inhibited by preincubation of the targets with an anti–HLA class I antibody, but not by an isotype control, indicating HLA-restricted killing.

antigen (FLPSDFPSV residues 18-27; referred as the FL peptide) was used as the positive standard for high HLA-A*0201–binding affinity.[24]

Immunofluorescence

PRAME expression was evaluated at the subcellular level with an immunofluorescence assay, as described previously[25] with some modifications. Briefly, 5×10^4 MNCs derived from 3 bone marrow and 2 peripheral blood samples from patients with CML were suspended in PBS and centrifuged on a glass slide using a Shandon CytoSpin 2 (ThermoFisher Scientific). In addition, CD34$^+$ cells obtained after immunomagnetic selection (Miltenyi Biotec) from bone marrow aspirates of 2 healthy donors were centrifuged on a glass slide using a Shandon CytoSpin 2. Cells were then fixed for 10 minutes at room temperature using 1% paraformaldehyde, permeabilized for 2.5 minutes with 0.1% Triton-X (Sigma-Aldrich), and incubated for 30 minutes with an Image-iT FX signal enhancer (Invitrogen) at room temperature. Finally, slides were incubated for 2 hours at room temperature in 0.5% bovine serum albumin with 5 μg/mL of rabbit anti–PRAME antibody (Abcam) and stained using an Alexa Fluor 555–conjugated anti–rabbit immunoglobulin G antibody (Invitrogen) for 45 minutes at room temperature. After counterstaining with 4′,6-diamidino-2-phenylindole, dihydrochloride (Boehringer), fluorescence was visualized using an Olympus BX61 microscope (Zeiss). After the acquisition of fluorescence images using CytoVision 6.5 software, slides were extensively washed in PBS and stained by Diff-Quik solution (Siemens Healthcare Diagnostics) before reexamination using a Genetics GSL10 microscope station.

Statistical analysis

All data are presented as means ± SD. Student *t* test was used to determine the statistical significant differences between samples, and $P < .05$ was accepted as indicating a significant difference.

Results

Generation of functional PRAME-CTLs from HLA-A*02$^+$ healthy donors using PRAME-PepMix

Using optimized culture conditions and 4 previously described HLA-A*02–restricted PRAME peptides (P100/VLD, P142/SLY, P300/ALY, and P425/SLL), we consistently generated PRAME-CTLs from 8 of 9 healthy donors and from 5 of 6 CML patients.[17] However, these T-cell lines were generally characterized by low TCR affinity based on titration of the specific peptides and tetramer staining. To evaluate whether this observation reflected the elimination of PRAME-CTLs with higher TCR affinity (and associated superior antitumor activity) from the circulation, with only low-avidity T cells remaining in the peripheral blood, we loaded APCs with a library of 125 pentadecapeptides spanning the entire PRAME protein (PRAME-PepMix).

We determined whether the immune responses obtained using our approach would merely recapitulate those obtained with peptide-loaded APCs or if new T-cell specificities with enhanced TCR affinity would be generated. After priming and expansion for 2 weeks using PRAME PepMix–loaded APCs and aAPCs, T-cell lines were characterized for their PRAME specificity using the IFNγ ELISpot assay. As shown in Figure 1A, 21 of 23 (91%) of the resulting T-cell lines specifically responded to PRAME-PepMix (IFNγ 416 ± 86 SFCs/10^5 cells), whereas T-cell lines generated using APCs loaded with an irrelevant PepMix did not (IFNγ 8 ± 2 SFCs/10^5 cells; $P < .001$). Surprisingly, CTLs generated using APCs loaded with PRAME-PepMix did not

Table 1. Description of PRAME subpool.

Subpool	Amino acids (Swiss Prot P78395)	Previously described eptide
1	1-51	
2	41-91	
3	81-131	P100 (VLDGLDVLL)
4	121-171	P142 (SLYSFPEPEA)
5	161-211	
6	201-251	
7	241-291	
8	281-331	P300 (ALYVDSLFFL)
9	321-371	
10	361-411	
11	401-451	P425 (SLLQHLIGL)
12	441-491	
13	481-509	

significantly respond to the P4 peptide pool containing the 4 previously identified immunodominant peptides[8,17] (IFNγ 6 ± 2 SFCs/10^5 cells). To evaluate if the response to the P4 peptide pool could be restored using different concentrations of the PepMix, we performed titration experiments. As shown in Figure 1B, similar frequencies of IFNγ spots were obtained when concentrations of 1 or 0.1 μg of PRAME-PepMix were used, whereas no IFNγ spots could be detected when the concentration was reduced to 0.01 μg. No response to the P4 peptide pool was observed (data not shown), suggesting that priming with PRAME-PepMix may determine the generation of CTLs skewed to different PRAME epitopes.

As shown in Figure 1C, T-cell lines expanded in culture by repeated stimulations with PRAME-PepMix–loaded APCs and aAPCs (median expansion, 23-fold; range, 5- to 124-fold after 4 stimulations). T-cell lines also had specific cytotoxic activity against PRAME-PepMix–loaded autologous phytohemagglutinin (PHA) blasts (specific lysis of 60% ± 5% at a 20:1 E:T ratio) compared with PHA blasts loaded with an irrelevant PepMix (18% ± 3%; $P < .01$), as assessed by a standard 4-hour ^{51}Cr-release assay. Cytotoxic activity was major histocompatibility complex (MHC) class I restricted because it was significantly inhibited by preincubation of target cells with anti–HLA class I antibody (30% ± 5% at a 20:1 E:T ratio), but not by preincubation with the appropriate isotype control antibody (50% ± 6%; $P < .01$; Figure 1D).

PRAME-CTLs generated using the PRAME-PepMix are polyclonal and preferentially recognize distinct HLA-A*02–restricted PRAME epitopes

Because the PRAME-CTLs we generated using APCs and aAPCs loaded with PRAME-PepMix failed to recognize HLA-A*02–restricted PRAME peptides previously identified as immunodominant,[8,17] we further characterized their epitope specificity against an array consisting of 13 subpools of overlapping peptides spanning the entire PRAME protein (Table 1). PRAME-CTLs generated from 14 HLA-A*02$^+$ healthy donors were incubated with each subpool, and IFNγ release was measured using ELISpot assays. Half of the T-cell lines (57%) were polyclonal, because they produced IFNγ$^+$ SFCs in response to at least 2 subpools (Table 2 and supplemental Figure 1, available on the *Blood* Web site; see the Supplemental Materials link at the top of the online article). The polyclonality of these PRAME PepMix-CTL lines was also confirmed by TCR-Vβ analysis (supplemental Table 1).

Table 2. Donor responses to the PRAME subpools.

	1 pool	2 pools	3 pools	4 pools	5 pools	9 pools
Number of responding donors	6	3	2	1	1	1

The majority (77% ± 21%) of the ex vivo–expanded CD8$^+$ T cells had an effector phenotype lacking CD62L, CD45RA, and CCR7, and some lines also had a small proportion (11% ± 13%) of CD45RO$^+$ and CD62L$^+$ effector-memory cells (supplemental Figure 2). A variable proportion of cells expressed CD27 (28% ± 26%) and/or CD28 (15% ± 21%). Our T cells lacked KLRG-1 (2.6% ± 1.2%), which identifies senescent effector cells with diminished replicative capacity. No natural killer cells (CD3$^-$CD56$^+$; < 0.1%) and few natural killer T cells (CD3$^+$CD57$^+$; 3% ± 2.2%) were observed.

Although the majority of CTLs responded to subpools 11 (57%; 755 ± 224 IFNγ$^+$ SFCs/10^5 cells) and 7 (43%; 265 ± 23 IFNγ$^+$ SFCs/10^5 cells for subpool 7; Figure 2A), the most robust IFNγ response was against subpool 11, which spans the C-terminal region of PRAME protein between amino acids 401 and 451 (Figure 2B). None of the CTL lines responded to subpool 4, which contains the epitope P142/SLY.[8] Although 3 of 14 CTL lines (21%) responded to subpools 3 and 8, which contain the epitopes P100/VLD and P300/ALY,[8] respectively, the production of IFNγ$^+$ spots in response to these subpools was significantly lower (116 ± 71 and 150 ± 44 IFNγ$^+$ SFCs/10^5 cells, respectively) compared with subpool 11 ($P = .03$; Figure 2B). Because subpool 11 contains the immunodominant epitope P425/SLL,[8] which failed to be recognized when it was tested as part of the P4 pool (Figure 1A), we further mapped this region by generating ten 15-mer overlapping peptides (amino acids 401-451) and found that the reactivity was predominantly directed against 2 peptides, P429 and P433 (651 ± 479 and 429 ± 319 IFNγ$^+$ SFCs/10^5 cells, respectively; Figure 3A). Two computational algorithms (SYFPEITHI and BIMAS) were used to predict possible HLA-A*02–binding peptide motifs in this region. Five minimal putative

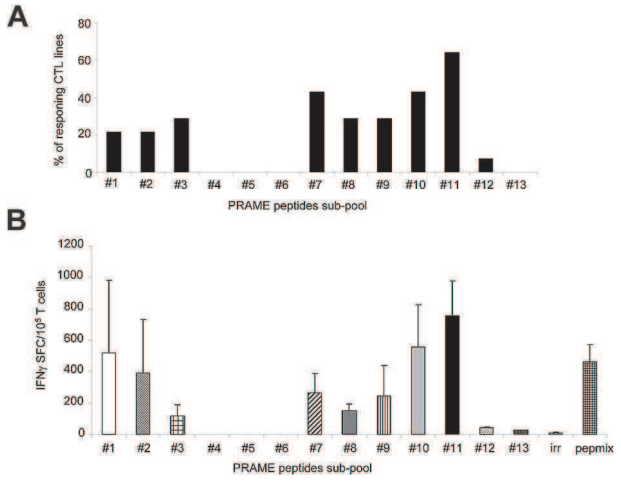

Figure 2. PRAME-CTLs generated using PRAME-PepMix are polyclonal. We evaluated the polyclonality of the expanded lines by assessing their reactivity against an array consisting of 13 subpools of overlapping 15-mers spanning the entire PRAME protein. (A) Percentage of CTL lines (generated from 14 donors) responding to each of the 13 subpools. The majority of the CTL lines reacted against subpools 7 and 11. (B) Frequency of these CTLs responding to the PRAME-PepMix and each subpool as assessed by IFNγ ELISpot assay. Shown are the means ± SD of the responding lines. The highest reactivity of PRAME-PepMix CTLs was observed for subpool 11.

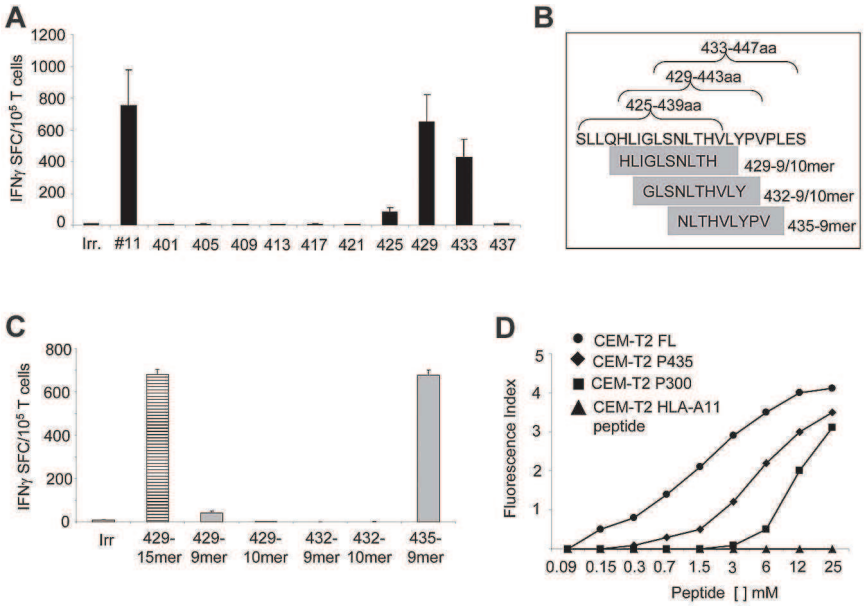

Figure 3. Identification of an immunodominant, HLA-A*02–restricted PRAME epitope. When we minimized subpool 11 in ten 15-mer overlapping peptides, IFNγ production by PRAME-CTL was directed against the P435/NLT peptide. (A) Reactivity of PRAME-CTLs was predominantly directed against two 15-mers, P429 and P433. (B) Five predicted HLA-A*02–binding peptide motifs in this region using 2 computational algorithms (SYFPEITHI and BIMAS; Table 3). (C) IFNγ production by 8 PRAME-CTL lines against the 5 minimized epitopes. Although some IFNγ production was observed against the P429-9mer (HLI), the most significant response was observed for the P435-9mer (NLT). (D) Stabilization assay of the new epitope P435/NLT for the HLA-A*02 molecule using a T2-binding assay. An HLA-A11–restricted peptide was used as a negative control. FL, a hepatitis B virus core antigen with high HLA-A*0201–binding affinity, was used as a positive control. The affinity of P435/NLT was superior to that of the previously described P300/ALY.

peptides with the highest predicted binding scores (Table 3), referred as P429-9mer, P429-10mer, P432-9mer, P432-10mer, and P435-9mer (Figure 3B), were then tested in vitro for their ability to elicit IFNγ production by PRAME-CTL lines using an ELISpot assay. Although the P429-9mer peptide (HLIGLSNLT) led to some IFNγ production (42 ± 8 SFCs/10^5 cells), the most significant response was observed for P435-9mer (NLTHVLYPV; amino acids 435-443; 677 ± 22 SFCs/10^5 cells; Figure 3C). We evaluated the binding affinity of the new epitope P435/NLT for the HLA-A*02 molecule using a T2-binding assay, and found that this epitope greatly enhanced the stabilization of the HLA-A*02 molecule (FI > 1.5) on T2 cells when used at 6mM compared with the previously described P300/ALY epitope[8] (FI > 1.5) when used at a 12mM peptide concentration (Figure 3D), indicating that HLA molecules recognizing P435/NLT have higher affinity compared with the P300/ALY epitope for which we previously detected the most robust CTL generation.[17]

Characterization of P435/NLT–specific CTLs generated from HLA-A*02$^+$ healthy donors

Having identified this highly immunogenic PRAME epitope (P435/NLT) within the PepMix, we then investigated whether it could be used directly to generate PRAME-CTLs in vitro.[17] We stimulated CD8$^+$ T cells obtained from 10 healthy HLA-A*02$^+$ donors with APCs and aAPCs loaded with either P435/NLT or the P4 pool. As shown in Figure 4A, APCs loaded with the P435/NLT peptide successfully expanded specific CTLs in 9 of 10 subjects. In particular, this peptide induced the generation of specific CTLs in samples obtained from 3 subjects in whom the P4 pool failed to elicit specific CTL responses. Furthermore, even in the P4-responder patients, the frequency of IFNγ$^+$ spots in response to P435/NLT was higher (521 ± 100 SFCs/10^5 cells) than for P4 (248 ± 101 SFCs/10^5 cells). Supplemental Figure 3 shows data confirming our previous observation[17] that there is a lower frequency of PRAME-specific CTLs to the P4 pool, and that this observation cannot simply be attributed to antigenic competition between peptides. The degree of expansion of P435/NLT–specific CTL lines after 3 rounds of stimulation with loaded aAPCs was similar to that observed for CTL lines obtained using stimulation with the P4 pool or PRAME-PepMix (range, 4- to 142-fold; Figure 4B). P435/NLT–specific CTLs also specifically bound a specific tetramer in 9 of 10 CTL lines tested (range, 0.4%-42%; Figure 4C).

As further evidence that P435/NLT–specific cells were consistently selected and expanded during PRAME-CTL generation, we expanded PRAME-specific T cells from 3 healthy donors using a mixture of P100/VLD, P142/SLY, P300/ALY, P425/SLL, and P435/NLT peptides (designated as the P5 pool), and analyzed the reactivity of the CTLs using the ELISpot assay. We found that these T-cell lines were mainly reactive against the P435/NTL peptide (439 ± 215 SFCs/10^5 cells), further suggesting that this peptide is indeed more immunogenic (supplemental Figure 4).

We next determined whether the P435/NLT–specific T-cell lines were of higher affinity because the responding cells were derived from the memory rather than the naive T-cell compartment. Using the same culture conditions, we generated P435/NLT–specific CTLs from the CD45RO$^+$ or CD45RA$^+$ T-cell fractions. In 4 healthy subjects, we detected P435/NLT-peptide–responsive T cells only in CTL lines originating from the naive (CD45RA$^+$) T-cell subset (Figure 4D). In contrast, virus-specific CTLs recognizing the NLVPMVATV peptide derived from the pp65 protein of cytomegalovirus were obtained exclusively from the CD45RO$^+$ memory T-cell fraction. The immunophenotype of the P435-specific CTL line was similar to that of the PepMix-specific CTLs (data not shown).

We then evaluated the cytotoxic activity of P435/NLT–specific CTLs against autologous PHA blasts loaded with the P435/NLT peptide using a standard 4-hour ^{51}Cr-release assay. As shown in Figure 5A, P435/NLT–specific CTLs specifically lysed P435/NLT–loaded PHA blasts (67% ± 11% at a 20:1 E:T ratio),

Table 3. Peptides prediction by computational algorithms.

Start position	Peptide sequence	SYFPEITHI	BIMAS
429-9mer	HLIGLSNLT	20	0.25
429-10mer	HLIGLSNLTH	17	0.003
432-9mer	GLSNLTHVL	25	8.759
432-10mer	GLSNLTHVLY	13	0.075
435-9mer	NLTHVLYPV	24	159.970
300-10mer	ALYVDSLFFL	27	1.312
FL-reference	FLPSDFPSV	24	607.884

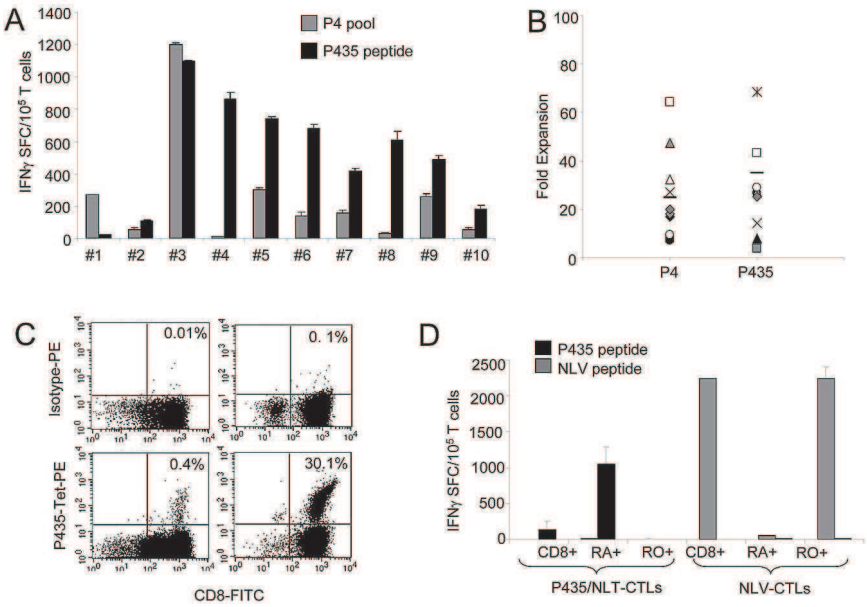

Figure 4. Functional P435/NLT–specific CTLs can be expanded from HLA-A*02⁺ healthy donors. P435/NLT could be used to generate PRAME-CTLs. (A) IFNγ response of P435/NLT–specific or P4-specific CTLs generated from 10 healthy HLA-A*02⁺ donors. P435/NLT–specific CTLs could be generated from 9 of 10 samples tested. (B) Expansion of P435/NLT–specific or P4-specific CTL lines after 3 rounds of stimulation. (C) Staining with the P435/NLT–specific tetramer of CTL lines generated from 2 representative healthy donors. (D) IFNγ⁺ SFCs in response to P435/NLT-peptide or NLV-pp65 (from the pp65 protein of CMV) peptide of P435/NLT–specific CTLs expanded from sorted naive (CD45RA⁺) and memory (CD45RO⁺) T-cell subsets. T cells producing IFNγ in response to the P435/NLT peptide were significantly higher in CTL lines that originated from the naive (CD45RA⁺) T-cell subset. In contrast, CTLs generated against the viral peptide NVL originated predominantly from the memory (CD45RO⁺) T-cell subset. Shown is 1 of 4 representative donors.

but not PHA blasts loaded with an irrelevant peptide ($P < .001$). The cytotoxic effect was MHC class I restricted, because it was significantly inhibited by preincubation of target cells with an anti–HLA class I antibody (30% ± 8% at a 20:1 E:T ratio), but not by preincubation with the appropriate isotype control antibody (50% ± 11%; $P = .004$; Figure 5B). We next assessed the capacity of P435/NLT–specific CTLs to recognize target cells naturally expressing the PRAME protein by measuring the cytotoxic activity of P435/NLT–specific CTLs against the PRAME⁺ HLA-A*02⁺ tumor cell lines U266, ARH77, KT1, and BV173.[17] As shown in Figure 5C, killing of U266, ARH77, KT1, and BV173 tumor cells by P435-specific CTL lines was superior (55% ± 17%, 43% ± 14%, 61% ± 7%, and 58% ± 14%, respectively) to that of L428 (12% ± 8%), which is PRAME⁺ but HLA-A*02⁻. We confirmed that killing was mediated through HLA class I by blocking cytotoxicity after preincubation of target cells with an anti–HLA class I antibody (range of killing at the 20:1 E:T ratio, 28%-44%), but not with the appropriate isotype control antibody (range of killing at the 20:1 E:T ratio, 40%-64%). Similarly, IFNγ production against the PRAME⁺ HLA-A*02⁺ tumor cell lines U266, HDLM-2, and ARH77 was increased compared with control CTLs or the PRAME⁻ HLA-A*02⁺ cell line (Figure 5D)

P435/NLT–specific CTLs selectively inhibit the growth of leukemic precursor cells

To measure the cytotoxic activity of P435/NLT–specific CTLs against leukemic precursor cells, we used clonogenic assays of 3 bone marrow and 2 peripheral blood samples from 5 HLA-A*02⁺ patients with untreated CML. All 5 patients had PRAME⁺ disease (as assessed by Q-RT-PCR; data not shown) and a high expression of PRAME protein in leukemic cells derived from both the bone marrow (supplemental Figure 5A) and the peripheral

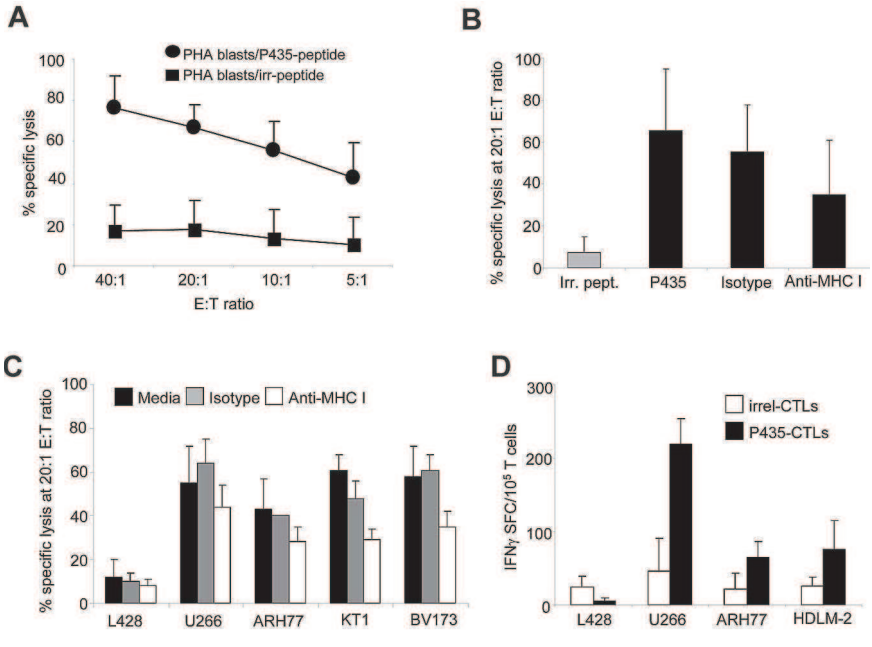

Figure 5. P435/NLT–specific CTLs are cytotoxic to PRAME+ tumor cell lines. (A) Cytotoxic activity of P435/NLT–specific CTLs toward autologous PHA blasts loaded with NLV-irrelevant peptide or loaded with the NLT peptide. Data represent the means ± SD of PRAME-CTLs from 7 healthy donors. (B) Data at a 20:1 E:T ratio of P435/NLT–specific CTLs against autologous PHA blasts loaded with NLV-irrelevant peptide or loaded with the NLT peptide preincubated with isotype control or an anti–HLA class I antibody to confirm MHC-restricted killing. (C) Cytotoxic activity of P435/NLT–specific CTLs toward PRAME⁺ HLA-A*02⁺ tumor cell lines evaluated using a standard ^{51}Cr-release assay. As negative controls, we used the L428 tumor cell line (PRAME⁺ but HLA-A*02⁻). Killing of PRAME⁺HLA-A*02⁺ cell lines was significantly higher than that of the PRAME⁺HLA-A*02⁻ L428, and was inhibited by preincubation with an anti–HLA class I antibody but not by an isotype control. (D) IFNγ ELISpot release of P435/NLT–specific CTLs or control/irrelevant CTLs against the indicated PRAME⁺ HLA-A*02⁺ cell lines or the control PRAME⁻ HLA-A*02⁺ cell line.

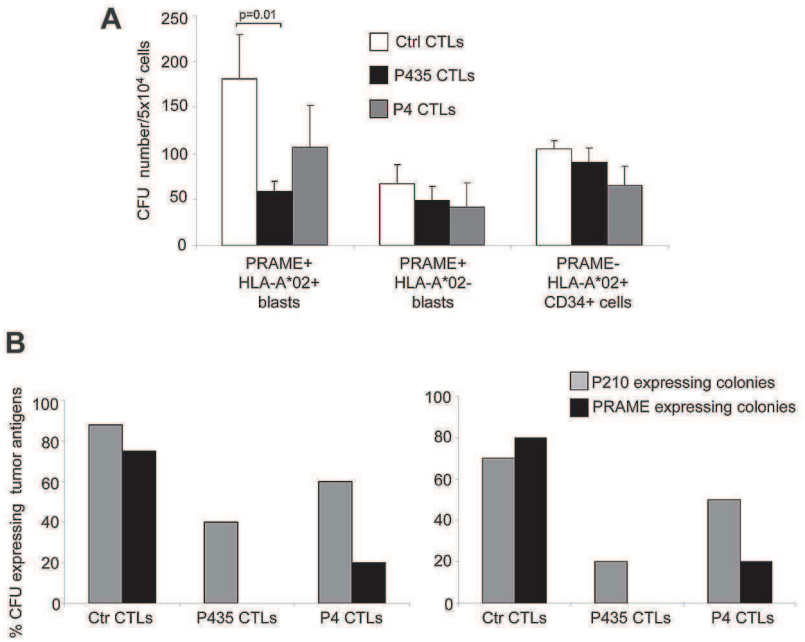

Figure 6. P435/NLT–specific CTLs target primary tumor cells and tumor progenitors. We performed clonogenic assays using peripheral and bone marrow MNCs from patients with CML to test antitumor activity by PRAME-CTLs against tumor progenitors. (A) CFUs generated from MNCs of PRAME$^+$HLA-A*02$^+$ and PRAME$^+$HLA-A*02$^-$ CML patients with active disease and HLA-A*02$^+$CD34$^+$ cells from healthy donors incubated with P435/NLT–specific CTLs, P4-specific CTLs, or control CTLs (targeting the MART1-derived ELA epitope or the pp65-derived NLV peptide). P435/NLT–specific CTLs had a specific cytotoxic activity against PRAME$^+$HLA-A*02$^+$ leukemic precursors, because the number of CFUs was significantly lower when MNCs were coincubated with P435/NLT–specific CTLs compared with control CTLs ($P = .01$). (B) Expression of PRAME and the oncogenic fusion BCR-ABL (p210) transcript using Q-RT-PCR in colonies collected from 2 independent experiments. P435/NLT–specific CTLs almost completely eliminated the growth of PRAME$^+$ CFUs and significantly reduced the growth of BCR/ABL$^+$ CFUs.

blood (supplemental Figure 5B). In contrast, patient T and B lymphocytes lacked discernible PRAME protein expression (data not shown). Similarly, CD34$^+$ cells obtained from the bone marrow of healthy donors lacked both PRAME transcripts and protein (supplemental Figure 6), confirming that PRAME expression was restricted to leukemic cells.

MNCs from these subjects were incubated with P435/NLT–specific CTLs, P4-specific CTLs, or control CTLs, and then placed in standard hematopoietic colony-forming cultures. As shown in Figure 6A, P435/NLT-CTLs had specific cytotoxic effects against PRAME$^+$HLA-A*02$^+$ leukemic precursors, which resulted in a consistent and significant reduction in CFUs when MNCs were coincubated with P435/NLT–specific CTLs (59 ± 11 CFUs/5×10^4 cells) compared with control CTLs (181 ± 48 CFUs/5×10^4 cells; $P = .01$). P4-specific CTLs showed a trend of inhibition (107 ± 45 CFUs/5×10^4 cells), although this was not statistically significant compared with control CTLs. Growth inhibition by P435/NLT–specific CTLs was highly specific for PRAME$^+$ precursors, because these CTLs had no effect on the growth of bone marrow–derived MNCs obtained from 3 HLA-A*02$^+$PRAME$^-$ normal donors or from 2 donors who had HLA-A*02$^-$PRAME$^+$ CML blasts. The CFUs that outgrew in the presence of the P435/NLT CTLs were profoundly depleted of PRAME expression and BCR/ABL p210 transcripts (as detected by Q-RT-PCR in single-cell colonies). Therefore, as shown in Figure 6B, P435/NLT–specific CTLs almost completely eliminated the growth of PRAME$^+$ CFUs and significantly reduced the growth of BCR/ABL$^+$ CFUs. We also collected and analyzed CFUs from 2 healthy donors, and neither PRAME$^+$ nor BCR/ABL$^+$ precursor cells were detected (data not shown), further indicating that PRAME is not expressed by normal progenitor cells.

Generation of PRAME-CTLs from patients with leukemia

We next obtained peripheral blood from 11 HLA-A*02$^+$ patients affected by PRAME$^+$ AML (3 patients), CML (5 patients), HL (2 patients), or follicular lymphoma (1 patient). PBMCs were primed with autologous dendritic cells loaded with PRAME-derived peptides (P435/NLT, PRAME-PepMix, or the P4 pool) in the presence of IL-7, IL-12, and IL-15, and then stimulated with peptide-loaded aAPCs and IL-2. As shown in Figure 7A, in all 11 patients, we were successful in expanding T cells that responded to the PRAME-PepMix. In 10 of 11 subjects, the CTLs responded to P435/NLT, and 4 of the 9 tested CTL lines responded to the P4 peptides, suggesting that the frequency of precursor specific for the P435 epitope is higher compared with the previously described epitopes. As in healthy donors, responses were more robust against PRAME-PepMix and P435/NLT (709 ± 371 and 306 ± 166 IFNγ^+ SFCs, respectively) than against the P4 peptides (200 ± 86 IFNγ^+ SFCs).

To confirm antitumor activity, we tested these patient-derived CTLs against autologous tumor blasts in patients with CML. As shown in Figure 7B, we found that P435/NLT–specific CTLs produced IFNγ in an ELISpot assay when incubated with autologous PRAME$^+$ CML blasts (57 ± 10 SFCs/10^5 T cells). In contrast, CTLs generated from the same patient against control peptide did not produce IFNγ when they were incubated with P435/NLT peptide or with autologous CML blasts (< 5 SFCs/10^5 T cells; data not shown); once again, T-cell specificity was HLA restricted, because it was inhibited by preincubation with an anti–HLA class I antibody. As observed for healthy donors, in 4 of 6 P435/NLT–specific T-cell lines tested, after the third stimulation, we could detect P435/NLT-tetramer$^+$ cells (range, 2%-88%; Figure 7C), whereas no P435/NLT-tetramer$^+$ T cells were detected in PBMCs derived from patients before ex vivo expansion.

Discussion

Leukemias such as CML and AML and lymphomas can be highly susceptible to control by the immune system, and effector T cells recognizing minor histocompatibility antigens and other TAAs overexpressed in tumor cells play an important role in this process.[26-31] Recently, the CTA PRAME, which is expressed by leukemic blasts[9,11,32] and HLs,[13] has been investigated as a potential

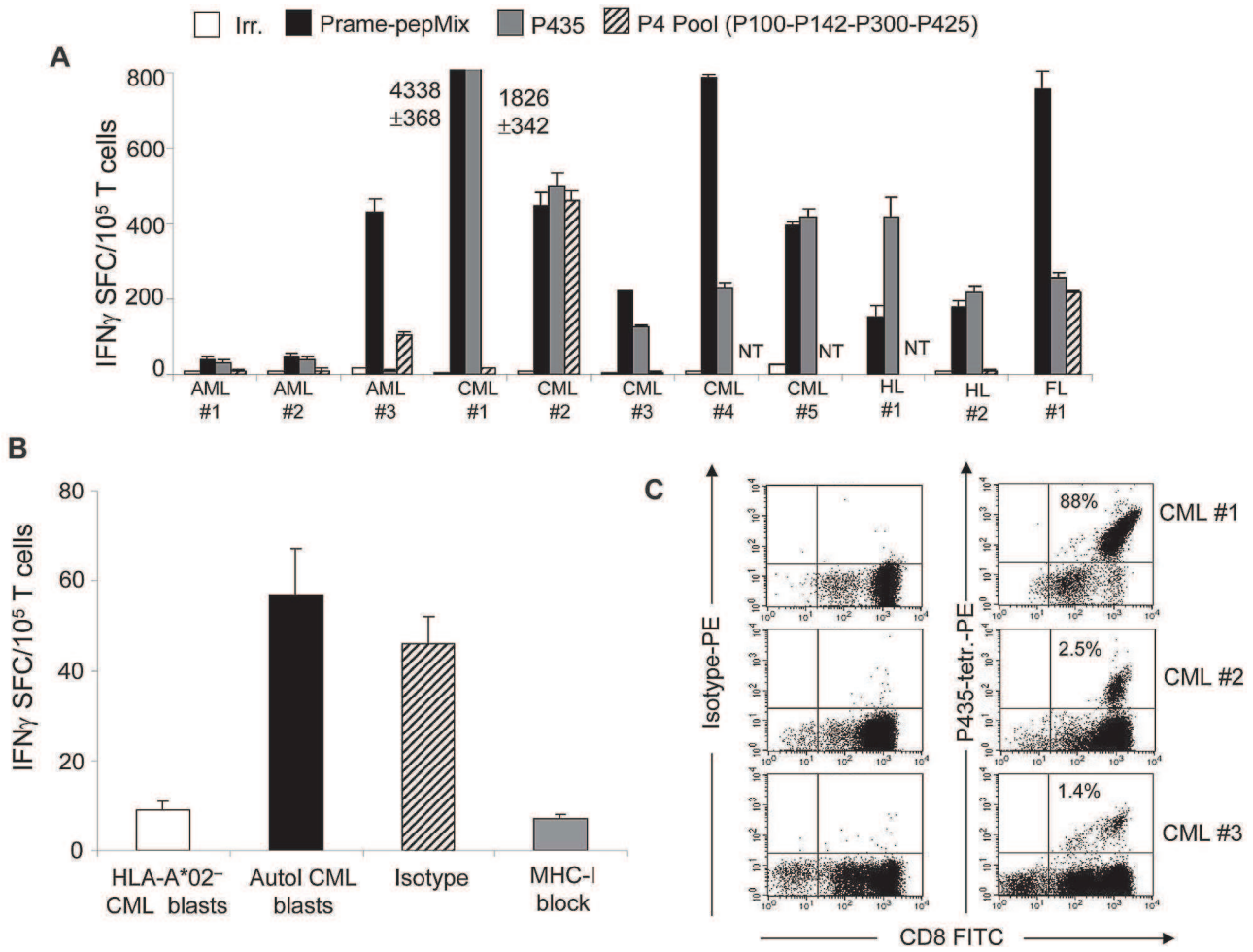

Figure 7. P435/NLT–specific CTLs can be generated from HLA-A*02⁺ patients. (A) Frequency of IFNγ⁺ CTLs specific for irrelevant (white bars), PRAME PepMix (black bars), P435 (gray bars) and P4 (striped bars) against specific peptides in 11 HLA-A*02⁺ patients with AML, CML, HL, or follicular lymphoma. NT indicates not tested. (B) PRAME-CTLs produced IFNγ⁺ SFCs in response to autologous CML blasts but not against HLA-A*02⁻ CML blasts, and this effect was HLA restricted because IFNγ⁺ SFCs were reduced when samples were preincubated with an anti–HLA class I antibody, but not with an isotype control. (C) Staining with the P435/NLT–specific tetramer of CTL lines generated from 3 representative patients.

target for immunotherapy of these malignancies.[17,18,33] Although we and others have previously been able to generate ex vivo PRAME-specific CTLs from both healthy donors and leukemic patients,[17] the low affinity of these cells for the target antigen has limited their suitability for clinical application.[17] We now show that loading professional and artificial APCs with a PRAME peptide library can generate high-avidity CTLs, and have identified a new immunodominant PRAME epitope. These high-affinity CTLs can be generated from both healthy donors and patients with CML, AML, and lymphomas, and have cytotoxic activity against both leukemic blasts and leukemic precursor cells while sparing normal hematopoietic precursors.

To effectively eliminate tumor cells, CTLs must recognize specific epitopes from tumor antigens in the context of the appropriate HLA molecules.[34] Therefore, for a tumor to be recognized by T cells, its TAAs must be degraded and processed by the tumor cells in vivo. Our understanding of the proteolytic process that leads to MHC peptide presentation remains incomplete, making it difficult to accurately predict which epitopes will be presented with the highest frequency by the tumor cells. Several strategies have been used to identify or predict antigen epitopes, including screening of cDNA libraries with clones derived from tumor-infiltrating lymphocytes and the use of specific algorithms (the so-called "reverse immunology" approach).[35,36] Kessler et al have identified HLA-A*02–restricted, PRAME-derived peptides by incorporating an in vitro, proteosome-mediated digestion of 27-mer polypeptides encompassing high-affinity binding peptides in the epitope prediction procedure.[8] Although we were able to generate PRAME-reactive CTLs using the 4 peptides described by Kessler et al, in our experience, the majority of T cells generated from both healthy donors and CML patients contain low-affinity TCRs,[17] and in only one report was it possible to detect high-avidity T cells—and then only with specificity for one of these peptides and only after allogeneic hemopoietic stem-cell transplantation.[37] Moreover, several high-affinity epitopes predicted by the algorithms were excluded from these earlier functional analyses based on the assumption that the correct C-termini would not be generated after the in vitro, proteasome-mediated digestion analysis.[8] However, peptidases that modify the C-termini of peptide precursors have subsequently been identified.[38] These more recent data suggest that the initial assumption about epitope suitability may have been incorrect, and this possibility is borne out by our observation that APCs loaded with a peptide library consisting of 125 synthetic pentadecapeptides, overlapping by 11 amino acids and spanning the entire PRAME protein, can indeed generate high-avidity CTLs that recognize the "incorrect" P435/NLT epitope. The high-avidity CTLs we made that recognized the P435/NLT epitope had antitumor activity against HLA-A*02⁺ PRAME⁺

tumor cell lines and primary leukemic blasts, and this activity was manifest in both cytotoxicity and IFNγ ELISpot assays, indicating that this peptide is efficiently processed and presented by tumor cells. Although the level of cytotoxicity was donor dependent, it was invariably present.

The level of expression of specific antigens in different tumor-cell subsets may influence their susceptibility to CTL recognition.[39,40] For many leukemias, including CML, there is evidence for an origin from a phenotypically distinct progenitor-cell compartment. Because these malignant progenitor cells may contribute to leukemia recurrence,[41] we evaluated whether they too were susceptible to recognition and elimination by high-avidity CTLs specific for the P435/NLT peptide. Using in vitro CFU assays as a surrogate assay for leukemic progenitors, we indeed found that high-avidity P435/NLT CTLs significantly reduced CFU formation from CML samples without affecting normal hematopoietic precursors.

Our ability to generate high-avidity CTLs recognizing the P435/NLT epitope even from subjects with PRAME$^+$ malignancy is striking, because the isolation and expansion of high-affinity T cells specific for self-antigens is impaired by both the physiologic deletion of these cells during thymic selection and by the tumor-specific induced T-cell apoptosis previously described for other antigens such proteinase 3[42] and for other PRAME-associated epitopes.[17] Because high-avidity P435/NLT-epitope–specific CTLs can be obtained in both healthy donors and leukemic patients, it seems unlikely that prior thymic deletion occurred, and it is possible that not all (normal and malignant) cells may be capable of processing and presenting this particular epitope.

Although we have used our approach only for subjects with an HLA-A*02 polymorphism, there is no reason why the methodology could not be applied to identify high-affinity epitopes for other common HLA phenotypes using the appropriate artificial APCs expressing the relevant HLA polymorphisms.[43] Unlike approaches using ex vivo digestion with immune proteasomes, PepMix libraries are readily available and standardized and could be useful for generating CTLs in vivo by vaccination and ex vivo for adoptive transfer to subjects with PRAME$^+$ hematologic malignancies.

Acknowledgments

We are grateful to Dr Marco Cosenza, Dr Ida Pisano, Dr Novella Pugliese, and Dr Raffaella Accetta for all of the advice and the data collection assistance in the immunofluorescence analysis. We also thank Linda Chapman of Golden Funds for the support.

This work was supported by National Institutes of Health grants P01CA094237, P50CA126752, and R21CA150109; by a Support of Competitive Research (SCOR) grant from the Leukemia & Lymphoma Society; and by grants from Regione Campania (DGRC 2326/07) and the Italian Ministry of Research (MIUR; PS 35-126/Ind). H.E.H. is supported by a Dan L. Duncan Chair and M.K.B. by a Fayez Sarofim Chair.

Authorship

Contribution: C.Q., G.D., and B.S. designed the research, performed experiments, analyzed the data, and wrote the manuscript; S.T.H., B.D.A., V.H., and S.E. performed some experiments; M.M., L.L., J.S., and F.P. provided patient samples; A.M.L., H.E.H., and C.M.R. provided expertise in T-cell generation and critically reviewed the manuscript; M.K.B. reviewed the experimental design and the manuscript; and all authors reviewed the manuscript.

Conflict-of-interest disclosure: The authors declare no competing financial interests.

Correspondence: Barbara Savoldo, MD, Center for Cell and Gene Therapy, Baylor College of Medicine, 6621 Fannin St, MC 3-3320, Houston, TX 77030; e-mail: bsavoldo@bcm.tmc.edu.

References

1. Rosenberg SA, Dudley ME. Adoptive cell therapy for the treatment of patients with metastatic melanoma. *Curr Opin Immunol.* 2009;21(2):233-240.
2. Bollard CM, Gottschalk S, Leen AM, et al. Complete responses of relapsed lymphoma following genetic modification of tumor-antigen presenting cells and T-lymphocyte transfer. *Blood.* 2007; 110(8):2838-2845.
3. Comoli P, Pedrazzoli P, Maccario R, et al. Cell therapy of stage IV nasopharyngeal carcinoma with autologous Epstein-Barr virus-targeted cytotoxic T lymphocytes. *J Clin Oncol.* 2005;23(35): 8942-8949.
4. Straathof KC, Bollard CM, Popat U, et al. Treatment of nasopharyngeal carcinoma with Epstein-Barr virus-specific T lymphocytes. *Blood.* 2005; 105(5):1898-1904.
5. Schmitt M, Schmitt A, Rojewski MT, et al. RHAMM-R3 peptide vaccination in patients with acute myeloid leukemia, myelodysplastic syndrome, and multiple myeloma elicits immunologic and clinical responses. *Blood.* 2008;111(3):1357-1365.
6. Bocchia M, Gentili S, Abruzzese E, et al. Effect of a p210 multipeptide vaccine associated with imatinib or interferon in patients with chronic myeloid leukaemia and persistent residual disease: a multicentre observational trial. *Lancet.* 2005; 365(9460):657-662.
7. Heslop HE, Stevenson FK, Molldrem JJ. Immunotherapy of hematologic malignancy. *Hematology Am Soc Hematol Educ Program.* 2003:331-349.
8. Kessler JH, Beekman NJ, Bres-Vloemans SA, et al. Efficient identification of novel HLA-A(*)0201-presented cytotoxic T lymphocyte epitopes in the widely expressed tumor antigen PRAME by proteasome-mediated digestion analysis. *J Exp Med.* 2001;193(1):73-88.
9. Paydas S, Tanriverdi K, Yavuz S, Seydaoglu G. PRAME mRNA levels in cases with chronic leukemia: clinical importance and review of the literature. *Leuk Res.* 2007;31(3):365-369.
10. Radich JP, Dai H, Mao M, et al. Gene expression changes associated with progression and response in chronic myeloid leukemia. *Proc Natl Acad Sci U S A.* 2006;103(8):2794-2799.
11. van Baren N, Chambost H, Ferrant A, et al. PRAME, a gene encoding an antigen recognized on a human melanoma by cytolytic T cells, is expressed in acute leukaemia cells. *Br J Haematol.* 1998;102(5):1376-1379.
12. Steinbach D, Viehmann S, Zintl F, Gruhn B. PRAME gene expression in childhood acute lymphoblastic leukemia. *Cancer Genet Cytogenet.* 2002;138(1):89-91.
13. Küppers R, Klein U, Schwering I, et al. Identification of Hodgkin and Reed-Sternberg cell-specific genes by gene expression profiling. *J Clin Invest.* 2003;111(4):529-537.
14. Epping MT, Wang L, Edel MJ, Carlee L, Hernandez M, Bernards R. The human tumor antigen PRAME is a dominant repressor of retinoic acid receptor signaling. *Cell.* 2005;122(6): 835-847.
15. Sakashita A, Kizaki M, Pakkala S, et al. 9-cis-retinoic acid: effects on normal and leukemic hematopoiesis in vitro. *Blood.* 1993;81(4):1009-1016.
16. Oehler VG, Guthrie KA, Cummings CL, et al. The preferentially expressed antigen in melanoma (PRAME) inhibits myeloid differentiation in normal hematopoietic and leukemic progenitor cells. *Blood.* 2009;114(15):3299-3308.
17. Quintarelli C, Dotti G, De AB, et al. Cytotoxic T lymphocytes directed to the preferentially expressed antigen of melanoma (PRAME) target chronic myeloid leukemia. *Blood.* 2008;112(5): 1876-1885.
18. Griffioen M, Kessler JH, Borghi M, et al. Detection and functional analysis of CD8+ T cells specific for PRAME: a target for T-cell therapy. *Clin Cancer Res.* 2006;12(10):3130-3136.
19. Pascolo S, Schirle M, Guckel B, et al. A MAGE-A1 HLA-A A*0201 epitope identified by mass spectrometry. *Cancer Res.* 2001;61(10): 4072-4077.
20. Savoldo B, Huls MH, Liu Z, et al. Autologous Epstein-Barr virus (EBV)-specific cytotoxic T cells for the treatment of persistent active EBV infection. *Blood.* 2002;100(12):4059-4066.
21. Savoldo B, Rooney CM, Quiros-Tejeira RE, et al. Cellular immunity to Epstein-Barr virus in liver transplant recipients treated with rituximab for

posttransplant lymphoproliferative disease. *Am J Transplant*. 2005;5(3):566-572.

22. Palandri F, Iacobucci I, Martinelli G, et al. Long-term outcome of complete cytogenetic responders after imatinib 400 mg in late chronic phase, philadelphia-positive chronic myeloid leukemia: the GIMEMA Working Party on CML. *J Clin Oncol*. 2008;26(1):106-111.
23. Savoldo B, Sammarelli G, Dotti G, et al. Reverse transcription polymerase chain reaction is a reliable assay for detecting leukemic colonies generated by chronic myelogenous leukemia cells. *Leukemia*. 1998;12(3):434-440.
24. Zhu B, Chen Z, Cheng X, et al. Identification of HLA-A*0201-restricted cytotoxic T lymphocyte epitope from TRAG-3 antigen. *Clin Cancer Res*. 2003;9(5):1850-1857.
25. Luetkens T, Schafhausen P, Uhlich F, et al. Expression, epigenetic regulation, and humoral immunogenicity of cancer-testis antigens in chronic myeloid leukemia. *Leuk Res*. 2010;34(12):1647-1655.
26. Luznik L, Fuchs EJ. Donor lymphocyte infusions to treat hematologic malignancies in relapse after allogeneic blood or marrow transplantation. *Cancer Control*. 2002;9(2):123-137.
27. Dazzi F, Szydlo RM, Goldman JM. Donor lymphocyte infusions for relapse of chronic myeloid leukemia after allogeneic stem cell transplant: where we now stand. *Exp Hematol*. 1999;27(10):1477-1486.
28. Giralt S, Hester J, Huh Y, et al. CD8-depleted donor lymphocyte infusion as treatment for relapsed chronic myelogenous leukemia after allogeneic bone marrow transplantation. *Blood*. 1995;86(11):4337-4343.
29. Bleakley M, Otterud BE, Richardt JL, et al. Leukemia-associated minor histocompatibility antigen discovery using T-cell clones isolated by in vitro stimulation of naive CD8+ T cells. *Blood*. 2010;115(23):4923-4933.
30. Biernacki MA, Marina O, Zhang W, et al. Efficacious immune therapy in chronic myelogenous leukemia (CML) recognizes antigens that are expressed on CML progenitor cells. *Cancer Res*. 2010;70(3):906-915.
31. Molldrem JJ, Lee PP, Wang C, Champlin RE, Davis MM. A PR1-human leukocyte antigen-A2 tetramer can be used to isolate low-frequency cytotoxic T lymphocytes from healthy donors that selectively lyse chronic myelogenous leukemia. *Cancer Res*. 1999;59(11):2675-2681.
32. Roman-Gomez J, Jimenez-Velasco A, Agirre X, et al. Epigenetic regulation of PRAME gene in chronic myeloid leukemia. *Leuk Res*. 2007;31(11):1521-1528.
33. Rezvani K, Yong AS, Tawab A, et al. Ex vivo characterization of polyclonal memory CD8+ T-cell responses to PRAME-specific peptides in patients with acute lymphoblastic leukemia and acute and chronic myeloid leukemia. *Blood*. 2009;113(10):2245-2255.
34. Rock KL, York IA, Goldberg AL. Post-proteasomal antigen processing for major histocompatibility complex class I presentation. *Nat Immunol*. 2004;5(7):670-677.
35. Bonini C, Ferrari G, Verzeletti S, et al. HSV-TK gene transfer into donor lymphocytes for control of allogeneic graft-versus-leukemia. *Science*. 1997;276(5319):1719-1724.
36. Kawashima I, Hudson SJ, Tsai V, et al. The multi-epitope approach for immunotherapy for cancer: identification of several CTL epitopes from various tumor-associated antigens expressed on solid epithelial tumors. *Hum Immunol*. 1998;59(1):1-14.
37. Amir AL, van der Steen D, Hagedoorn RS, Griffioen M, Falkenburg JH, Heemskerk MH. High avidity PRAME specific T cells derived from in vivo HLA mismatched transplantation setting potentially useful for immunotherapeutic strategies [Abstract]. *Blood*. 2009;114(22):1568.
38. Shen XZ, Lukacher AE, Billet S, Williams IR, Bernstein KE. Expression of angiotensin-converting enzyme changes major histocompatibility complex class I peptide presentation by modifying C termini of peptide precursors. *J Biol Chem*. 2008;283(15):9957-9965.
39. Disis ML, Smith JW, Murphy AE, Chen W, Cheever MA. In vitro generation of human cytolytic T-cells specific for peptides derived from the HER-2/neu protooncogene protein. *Cancer Res*. 1994;54(4):1071-1076.
40. Van Elsas A, Nijman HW, van der Minne CE, et al. Induction and characterization of cytotoxic T-lymphocytes recognizing a mutated p21ras peptide presented by HLA-A*0201. *Int J Cancer*. 1995;61(3):389-396.
41. Kavalerchik E, Goff D, Jamieson CH. Chronic myeloid leukemia stem cells. *J Clin Oncol*. 2008;26(17):2911-2915.
42. Molldrem JJ, Lee PP, Kant S, et al. Chronic myelogenous leukemia shapes host immunity by selective deletion of high-avidity leukemia-specific T cells. *J Clin Invest*. 2003;111(5):639-647.
43. Hasan AN, Selvakumar A, Doubrovina E, Riviere I, Sadelain MW, O'Reilly RJ. Artificial antigen presenting cells that express prevalent HLA alleles: A step toward the broad application of antigen-specific adoptive cell therapies. *Discov Med*. 2009;8(43):210-218.647.

Biochimica del

plasma e sistema ematopoietico

1

GIAMPAOLO MERLINI, FABRIZIO PANE

con la collaborazione di BIAGIO DE ANGELIS, FRANCESCA LAVATELLI, ANNA LUCIA PELUSO, CONCETTA QUINTARELLI

Sinossi

Il sangue è il tessuto fluido che, all'interno dei vasi dell'apparato circolatorio e del sistema linfatico, raggiunge tutti i tessuti consentendo il trasporto di ossigeno e sostanze fondamentali per la vita cellulare (grassi, aminoacidi, zuccheri, vitamine, sali e acqua) e l'allontanamento delle sostanze di rifiuto, ad esempio il diossido di carbonio e composti azotati solubili semplici, come l'urea. Il sangue inoltre permette la distribuzione degli ormoni e il trasporto delle cellule deputate alla difesa contro organismi o sostanze estranee. Nell'uomo sono presenti in media 4-6 litri di sangue, costituito da una componente liquida, il plasma sanguigno, che occupa circa il 55% del volume, e da una componente corpuscolare che comprende diversi tipi cellulari e ne rappresenta il 45%.

In questo capitolo, saranno caratterizzate le più importanti componenti proteiche che espletano le principali funzioni biochimiche a livello plasmatico e cellulare, con un particolare cenno alle classi proteiche che più frequentemente sono alterate nei processi neoplastici riguardanti il tessuto ematico.

Il plasma

Il plasma è la parte non corpuscolata del sangue e ne rappresenta circa il 55% in volume nei maschi e il 59% nelle femmine. Il volume totale del plasma è di 1300-1800 ml/m^2 di superficie corporea. Si ottiene centrifugando il sangue trattato con anticoagulanti (eparina o chelanti del calcio quali l'acido etilen-diamino-tetracetico, EDTA, ossalato o citrato). Quando il plasma è preparato per essere reinfuso, si utilizza il citrato come anticoagulante perché preserva i procoagulanti e il suo effetto è rapidamente reversibile dal calcio. Il plasma è costituito per il 90% da acqua (per un totale di circa 3.5 litri) e per il 10% circa di soluti inclusi gli elettroliti (10-12 g/L) vedi **Tabella 1.1**, composti organici di varia natura e origine e di grande rilevanza diagnostica (glucosio, urea, acido urico, acido lattico, lipidi) (10-15 g/L) e proteine (63-78 g/L).

Proteine plasmatiche

Nella sua classica serie di volumi intitolati "The Plasma Proteins", pubblicati fra il 1975 e il 1987, Frank Putnam ha definito come "vere" proteine plasmatiche quelle che svolgono la loro funzione nel circolo, escludendo quindi un ampio gruppo di proteine che mediano i segnali fra cellule e tessuti (come ad esempio gli ormoni peptidici) e le proteine strutturali che compaiono nel plasma a seguito di danno tissutale (ad esempio le troponine e la mioglobina a seguito di infarto del miocardio). Questa definizione è stata messa in discussione dal concetto di proteoma che origina dagli importanti avanzamenti analitici basati sulla spettrometria di massa che hanno permesso l'identificazione di uno spettro molto ampio di proteine e offerto nuove e formidabili opportunità diagnostiche (vedi il Capitolo 23). Ogni proteina identificata nel plasma, anche ai limiti inferiori delle nuove potenti tecnologie analitiche, può offrire straordinarie opportunità diagnostiche e prognostiche, come ad esempio le troponine cardiache, che sono presenti nel plasma in concentrazioni picomolari e che hanno rivoluzionato la gestione della sindrome coronarica acuta.

Tabella 1.1. Concentrazione degli elettroliti nel plasma.

Componente	Concentrazione (mEq/L)
Na+	142
K+	4 4
Ca2+	5
Mg2+	2
Elementi in tracce	1
Totale cationi	154.4
Cl-	103
HCO_3^-	27
Proteine-	16
Acidi organici-	5
HPO_4^{2-}	2
SO_4^{2-}	1
Totale anioni	154

Dal punto di vista funzionale le proteine possono essere classificate in:
- Proteine di trasporto
- Di difesa, comprendenti
  - Immunoglobuline
  - Proteine dell'emostasi
  - Proteine della fase acuta
- Recettori-ligandi, comprendenti quelli che agiscono a
  - *lunga distanza*, che includono ormoni peptidici e proteici le cui dimensioni sembrano correlare con la rapidità di azione: azioni rapide per ormoni di piccole dimensioni, come l'insulina, o lenti aggiustamenti con ormoni di maggiori dimensioni, come nel caso della eritropoietina;
  - *a breve distanza* nel microambiente, quali le citochine ed altri mediatori delle risposte cellulari. In generale, queste proteine hanno un peso molecolare sotto la soglia di filtrazione renale, e quindi hanno un breve tempo di residenza nel plasma, e sembrano disegnate per mediare le interazioni cellulari locali seguite poi da una diluizione nel plasma a concentrazioni inefficaci. Alte concentrazioni plasmatiche possono causare effetti deleteri in tessuti lontani dal sito di sintesi, come si osserva in corso di sepsi.
- Proteine in rapido transito che attraversano il compartimento plasmatico nel loro percorso verso il sito di funzione primaria, come nel caso delle proteine lisosomiali che sono prima secrete e poi catturate da un recettore e sequestrate nei lisosomi.
- Proteine rilasciate in circolo dai tessuti a seguito di danno o morte cellulare. Queste proteine includono potenti marcatori diagnostici, quali le troponine cardiache e gli enzimi epatici.
- Proteine aberranti, rilasciate da tumori o altri tessuti "ammalati", quali i biomarcatori neoplastici.
- Proteine eterologhe, prodotte ad esempio da microrganismi o parassiti, con notevoli potenziali diagnostici.

La distribuzione delle proteine nei vari compartimenti corporei è sotto stretto controllo fisiologico. La concentrazione plasmatica è dinamica e dipende dalla velocità di sintesi, catabolismo e distribuzione fra i compartimenti intra- ed extravascolari. Le proteine plasmatiche presentano una grande eterogeneità in struttura e funzione e presentano un range dinamico di circa 10^{10}. Dodici proteine costituiscono il 90% in massa delle proteine totali, e l'altro 10% è costituito essenzialmente dalle lipoproteine e dalle proteine della coagulazione (**Figura 1.1**). La maggior parte delle proteine plasmatiche sono glicoproteine con un contenuto in carboidrati tra il 10 e 25%, con l'eccezione importante dell'albumina che non è glicosilata.

Modificazioni post-traduzionali delle proteine

Sono note più di 200 modificazioni post-traduzionali delle proteine, le più importanti e frequenti sono la glicosilazione, la fosforilazione (di residui di serina, treonina, tirosina), l'ossidazione di residui di metionina, la deamidazione (asparagina), acetilazione e l'ubiquitinazione. Queste modificazioni svolgono un ruolo biologico fondamentale, ad esempio, nella regolazione della espressione genica (acetilazione delle proteine degli istoni) trasmissione del segnale (fosforilazione) o nel controllo della omeostasi proteica (ubiquitinazione). Il loro utilizzo in clinica, è solo agli

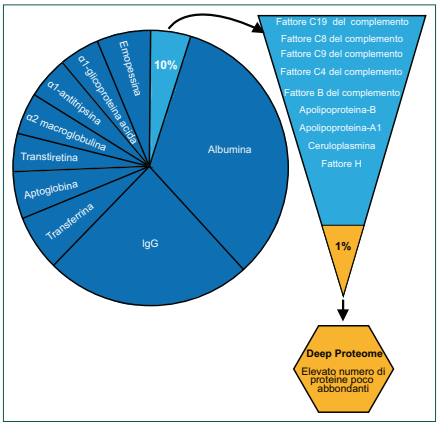

Figura 1.1. Abbondanza relativa delle principali proteine plasmatiche.

albori, ma già con importanti ricadute sulla cura dei pazienti. Un esempio paradigmatico è dato dalla glicazione che è il risultato della formazione di un legame covalente, non enzimatico, di una proteina o di un lipide con una molecola di carboidrato. La reazione avviene in più stadi, da quello reversibile (formazione della aldimmina) a quello lento, praticamente irreversibile (chetoammina) e successivamente alla formazione di prodotti finali di "glicazione avanzata". I prodotti di glicazione avanzata (AGE) sono responsabili di alcuni danni ai tessuti (complicanze neurologiche, renali, vascolari, oculari). Il primo stadio della glicazione (prodotto di Amadori) non provoca danni ed è possibile misurarne la quantità, potendo così essere impiegato come marcatore. La reazione di glicazione, essendo non enzimatica, dipende solamente dalla quantità di glucosio nel sangue, dalla quantità di proteine, dalla permeabilità delle cellule al glucosio e dai gruppi amminici liberi. I prodotti di glicazione formano ponti intermolecolari anomali ("cross links"), si legano a specifici recettori (RAGE) e si accumulano anche nelle cellule.

La glicazione proteica, in quanto dipendente dal contenuto di glucosio nel sangue, costituisce anche un marcatore del controllo metabolico. L'emoglobina glicata è ora un indispensabile strumento per la diagnosi e il monitoraggio dei soggetti diabetici. Da un punto di vista biochimico la reazione di glicazione dell'emoglobina è complessa, soprattutto per due motivi: (a) perché più residui aminoacidici sono in grado di reagire col glucosio, principalmente le valine terminali delle catene beta (Val1beta), ma anche diversi altri residui (Lys66beta, Lys17beta, Val1alfa); (b) perché la reazione ad ogni residuo avviene in più fasi, da quella reversibile (formazione della aldimmina) a quella lenta, praticamente irreversibile (chetoammina). La glicazione ai residui N-terminali delle catene beta rappresenta circa il 60% della glicazione totale della molecola, ma esistono significative differenze tra individui a seconda del grado di scompenso glicometabolico.

Biosintesi e turnover delle proteine plasmatiche

La concentrazione di una proteina nel plasma dipende dall'equilibrio di diversi fattori, la velocità di sintesi, la distribuzione fra il compartimento circolante ed extravascolare e il catabolismo (vedi **Figura 1.2**). La maggior parte delle proteine plasmatiche è di sintesi epatica, mentre le immunoglobuline sono sintetizzate dalle plasmacellule midollari. L'albumina è la principale proteina plasmatica. La sua sintesi è regolata sia a livello trascrizionale che post-trascrizionale da ormoni, (insulina, ormone della crescita, ormoni tiroidei e glucocorticoidi), e in maniera significativa, anche dall'apporto nutrizionale. L'albumina è responsabile per l'80% della pressione oncotica, quando quest'ultima si riduce, la sintesi dell'albumina, assieme a quella di transferrina, apolipoproteina A-1 e fibrinogeno aumenta a livello trascrizionale. La distribuzione fra i compartimenti intra ed extravascolare dipende principalmente dalla massa della proteina, dalla permeabilità vascolare (che può essere alterata in presenza di mediatori della infiammazione) e dal volume dei compartimenti. Studi condotti negli anni 60-70 hanno definito la percentuale del pool intravascolare catabolizzata giornalmente (fractional catabolic rate, FCR) per le principali proteine plasmatiche definendo tre fondamentali modalità:

1) Il FCR è direttamente proporzionale alla concentrazione plasmatica della proteina, come nel caso delle IgG e dell'albumina;
2) Il FCR è inversamente proporzionale alla concentrazione plasmatica della proteina, come nel caso dell'aptoglobina, della transferrina, delle IgD e delle IgE;
3) Il FCR è fisso e indipendente dalla concentrazione plasmatica della proteina, come nel caso del fibrinogeno, delle IgA e delle IgM (vedi **Figura 1.3**).

L'emivita delle principali proteine plasmatiche è in generale inferiore ai 7 giorni e per alcune proteine inferiore alle 24 ore, per esempio l'emivita della proteina legante il retinolo è di 12 ore. Fanno eccezione le IgG (tranne le IgG3 per il motivo che vedremo più avanti) con una emivita di circa 3 settimane e l'albumina con una emivita di circa 15-18 giorni. Questa eccezionalmente prolungata emivita delle IgG è mediata da un singolo recettore, il recettore Fc neonatale (FcRn) per le IgG. FcRn è un eterodimero composto da una specifica catena alfa della famiglia non classica MHC di classe I associata alla beta-2-microglobulina. Poiché l'affinità per le IgG è insignificante a pH fisiologico, l'FcRn lega le IgG solo dopo la pinocitosi nell'endosoma precoce dove il pH scende

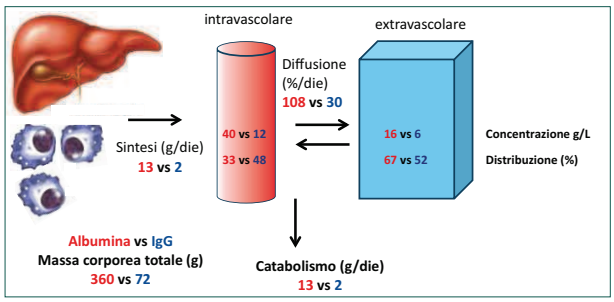

Figura 1.2. Metabolismo dell'albumina e delle IgG. Sintesi, distribuzione e catabolismo dell'albumina (i cui valori sono sempre indicati in rosso), sintetizzata dal fegato, rispetto alle IgG (indicate in blu), prodotte dalle plasmacellule.

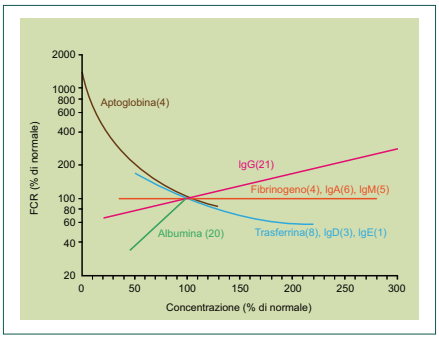

Figura 1.3. Percentuale del pool intravascolare catabolizzata giornalmente (fractional catabolic rate, FCR) in relazione alla concentrazione plasmatica di alcune proteine significative. In parentesi sono riportate le emivite, in giorni, delle proteine considerate.

a 6.5. Il complesso FcRn-IgG è poi trasportato fuori dalla via lisosomiale, proteggendo pertanto le IgG dalla degradazione, e viene riciclato sulla superficie cellulare o sul lato opposto della cellula, consentendo pertanto il movimento attraverso l'endotelio (vedi **Figura 1.4**). Al momento della fusione fra vescicole e membrana cellulare il pH ritorna fisiologico con rilascio delle IgG. È stato successivamente dimostrato che l'FcRn lega, su un sito di legame distinto rispetto alle IgG, e in maniera non-cooperativa, l'albumina che è pertanto protetta dal catabolismo lisosomiale attraverso lo stesso meccanismo. Molto recentemente è stato finalmente chiarito il meccanismo alla base della breve emivita (una settimana) delle IgG3. Anche le IgG3 si legano all'FcRn, ma il legame è inibito dalla presenza delle IgG1. È stato chiarito che questa inibizione dipende dalla differenza di un singolo aminoacido in posizione 435, una arginina nella IgG3 al posto dell'istidina presente nelle altre sottoclassi di IgG. L'arginina 435 determina un legame meno forte a pH acido all'FcRn rispetto alla istidina.

I siti di degradazione delle proteine sono l'endotelio e gli organi che presentano un endotelio fenestrato o discontinuo, come il fegato e la milza, ma praticamente tutte le cellule nucleate dell'organismo sono in grado di degradare le proteine attraverso il meccanismo della pinocitosi e della degradazione lisosomiale.

Le proteine del sangue coinvolte nel trasporto

La **Tabella 1.2** riporta le proteine di trasporto plasmatiche.

Albumina

L'albumina costituisce più del 50% delle proteine del plasma, con una concentrazione di circa 45 g/L (0.6 mmol/L). È una piccola proteina globulare composta da 585 amino acidi, con pochi residui di triptofano o metionina, ma con abbondanza di residui carichi, come la lisina e l'acido aspartico. Non è glicosilata e circa il 67% della struttura ha una conformazione ad alfa elica. La proteina è composta da tre domini omologhi (I-III), ciascuno con due sotto-domini (A e B) composti da 4 e 6 alfa eliche rispettivamente. I sottodomini sono incardinati su residui di prolina che facilitano l'accomodamento e il trasporto di un insieme

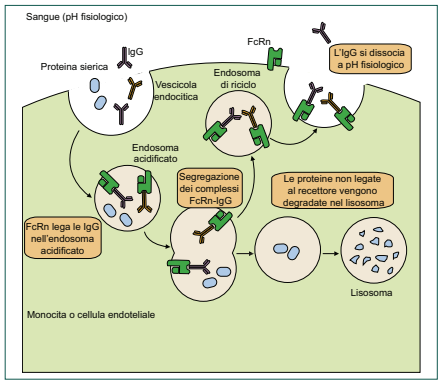

Figura 1.4. Protezione delle IgG dalla degradazione lisosomiale. Il recettore neonatale per l'Fc (FcRn) è espresso dalle cellule endoteliali e dai monociti circolanti. Queste cellule internalizzano le IgG del siero, che si legano all'FcRn in presenza di pH acido nell'endosoma proteggendole dalla degradazione. Il legame all'FcRn determina il riciclo delle IgG nel circolo, estendendone la emivita. L'albumina si lega pure, ma ad un sito distinto e non cooperativo, all'FcRn e segue la sorte delle IgG. Le proteine plasmatiche che non si legano al recettore/riciclante sono destinate alla degradazione lisosomiale.

di sostanze. La **Figura 1.5** illustra la struttura terziaria con legati acidi grassi. L'albumina contiene 35 residui di cisteina, la maggior parte dei quali è impegnata in 17 ponti disolfuro, che stabilizzano la struttura terziaria. Il gruppo tiolico della cisteina 34 è redox-attivo, e rappresenta l'80% (500 umol/L) dei gruppi tiolici nel plasma. Questo gruppo tiolico è reattivo e capace di tiolazione (albumina-S-R) e di nitrosilazione (albumina-S-NO). La forma di albumina predominante è quella ridotta, con il gruppo tiolico libero (albumina-SH), ed è nota come mercaptoalbumina. In teoria si potrebbero formare dimeri di albumina (albumina-S-S-albumina), ma in pratica è improbabile la loro formazione in vivo per interferenza sterica. Tuttavia questo processo è noto occorrere ex vivo durante la purificazione o lo stoccaggio e può avere implicazioni nell'uso terapeutico dell'albumina.

Sintesi e metabolismo

Il gene dell'albumina fa parte della superfamiglia dell'albumina sul braccio lungo del cromosoma 4 (4q11-q13) e include anche i geni per l'alfa-fetoproteina, la proteina legante la vitamina D e l'alfa-albumina (afamina). Sono note circa 80 varianti genetiche dell'albumina, la maggior parte delle mutazioni non causa

Tabella 1.2. Principali proteine plasmatiche di trasporto.

Proteina plasmatica	Ligando o molecola trasportata
Transtiretina (o prealbumina)	Tiroxina
Albumina	Bilirubina, acidi grassi liberi, alcuni ormoni steroidei e loro metaboliti, alcuni farmaci, ioni (Ca^{2+}, Cu^{2+}, Zn^{2+})
Apolipoproteine	Trigliceridi, colesterolo, colesterolo esterificato
Transferrina	Ferro
Aptoglobina	Emoglobina libera
Emopexina	Eme libero
Ceruloplasmina	Rame
Proteina legante il retinolo	Retinolo
Transcobalamina I, II, III	Vitamina B_{12}
Transcortina	Cortisolo
Globulina legante gli ormoni sessuali	Testosterone, estradiolo

conseguenze cliniche, e circa 65 mutazioni risultano in una modificazione della carica netta dell'albumina con sdoppiamento della sua banda elettroforetica (bisalbuminemia).

L'albumina è sintetizzata dagli epatociti (10-15 g/die) e rappresenta il 10% della attività protidosintetica del fegato. Una quantità relativamente piccola (circa 2 g) è immagazzinata nel fegato mentre la maggior parte è liberata nel torrente circolatorio. Circa il 30-40% dell'albumina sintetizzata è mantenuta nel compartimento plasmatico, il rimanente è localizzato nel liquido interstiziale tissutale soprattutto a livello muscolare e cutaneo. Studi con albumina radio marcata condotti su giovani maschi sani riportano una emivita variabile fra 12.7 e 18.2 giorni (media 14.8 giorni). Circa il 5% dell'albumina plasmatica passa nel liquido interstiziale ogni ora e una quantità equivalente ritorna nel compartimento intravascolare attraverso il sistema linfatico. La sintesi è un processo continuo regolato sia a livello trascrizionale che post-trascrizionale da stimoli specifici anche se le modifiche della pressione oncotica sembrano essere predominanti. L'omeostasi dell'albumina è mantenuta dal bilancio fra sintesi e catabolismo che avviene in tutti i tessuti e soprattutto (per il 40-60%) nel muscolo, fegato e rene. L'iperalbuminemia si osserva raramente ed è di solito dovuta a disidratazione. L'ipoalbuminemia si osserva in corso di numerosi processi patologici, inclusi i processi infiammatori acuti e cronici, epatopatie, nefropatie (in particolare la sindrome nefrosica), neoplasie, sepsi severa e deficit nutrizionale. È noto che in corso di sepsi la permeabilità del letto capillare aumenta significativamente con perdita di albumina verso il liquido interstiziale. È stato osservato che l'emivita dell'albumina infusa in pazienti con sepsi o malattie gravi è solo di 9 giorni. La formazione di ascite è una complicanza frequente della cirrosi e contribuisce, assieme alla ridotta sintesi epatica, alla riduzione della concentrazione intravascolare di albumina. La sindrome nefrosica è caratterizzata da proteinuria (> 3.5 g/die), ipoalbuminemia, edema e iperlipidemia. La proteinuria, costituita prevalentemente da albumina, è causata da una aumentata permeabilità dei capillari glomerulari alle proteine plasmatiche con importante perdita di albumina nelle urine con rilevanti alterazioni della composizione delle plasma proteine (aumento della alfa-2-macroglobulina e delle apolipoproteine). L'analbuminemia è una condizione ereditaria autosomica recessiva caratterizzata da una sintesi molto ridotta o assente di albumina. Nonostante la pressoché totale assenza di albumina i segni e sintomi sono modesti con facile faticabilità, dovuta alla bassa pressione arteriosa, e modesti edemi declivi. La concentrazione plasmatica di numerose proteine, inclusi i fattori della coagulazione, apolipoproteine e immunoglobuline, è aumentata, vicariando circa il 50% della perdita di pressione colloido-oncotica.

Proprietà dell'albumina

Trasporto

Le straordinarie capacità di legame della albumina riflettono la sua organizzazione strutturale in molti domini. L'albumina è nota trasportare pressoché ogni piccola molecola, rappresentando un cargo molecolare o un nano veicolo con potenziali applicazioni cliniche, biofisiche e industriali. In condizioni fisiologiche, l'albumina non solo lega composti di basso peso molecolare endogeni e esogeni, ma anche peptidi e proteine (vedi **Figura 1.5**). Almeno 35 proteine sono state trovate associate all'albumina comprese sia proteine presenti ad alta che a bassa concentrazione (apolipoproteine, emoglobina, plasminogeno, protrombina, transferrina, angiotensinogeno, clusterina, etc). La frazione dei peptidi e proteine legate all'albumina è definita come "albuminoma" nell'ambito degli studi di proteomica. L'albumina lega molti composti endogeni ed esogeni, inclusi gli acidi grassi, ioni metallici, farmaci e metaboliti con implicazioni per il rilascio e l'attività dei farmaci, la detossificazione, e la protezione antiossidante. Numerosi siti di legame a bassa ed alta affinità sono stati identificati sulla albumina, i primi (chiamati sito I e II) sono responsabili per il legame della maggior parte dei farmaci. I siti I e II sono localizzati in domini differenti e mostrano affinità di legame differenti, anche se non sempre esclusive. Il sito I tende a legare composti eterociclici relativamente grandi, o acidi dicarbossilici. Un diverso gruppo di composti, fra loro non correlati, lega con alta affinità a varie regioni del sito I, indicando una certa flessibilità del sito ad accomodare vari composti. Inoltre, questo sito è ampio e capace di legare sostanze endogene di grande ingombro sterico, inclusa la bilirubina e le porfirine. In contrasto, il sito II, noto come il sito dell'indolo-benzodiazepine, è più piccolo e meno flessibile perché il legame è più stereo-specifico. Sono inoltre presenti ulteriori regioni di legame ad alta affinità per alcuni farmaci e composti, mentre i siti di legame di alcuni composti come la digossina e gli acidi biliari rimangono indeterminati. Il residuo di cisteina in posizione 34 lega alcuni farmaci come il cisplatino, la D-penicillamina e la *N*-acetilcisteina. Interazioni covalenti (tiolazioni) avvengono con formazione di ponti disolfuro con sostanze endogene, di basso peso molecolare che contengono gruppi tiolici. La cisteina in posizione 34 può essere ossidata con formazione di residui di acido sulfenico, sulfinico o sulfonico. L'ossido nitrico sia esogeno che endogeno interagisce con la cisteina-34 attraverso l'addizione elettrofilica dello ione nitrosonio ($N{=}O^+$), tuttavia il ruolo dell'albumina nel metabolismo dell'ossido nitrico è ancora oggetto di studio. L'albumina trasporta inoltre numerosi cationi. La porzione amino terminale dell'albumina (NAsp-Ala-His-Lys-) lega gli ioni Cu, Ni, e Co con alta affinità, mentre gli ioni Au, Ag, e Hg si legano alla cisteina-34. L'albumina è inoltre la principale proteina che lega lo Zn nel plasma e possiede una debole capacità legante il ferro.

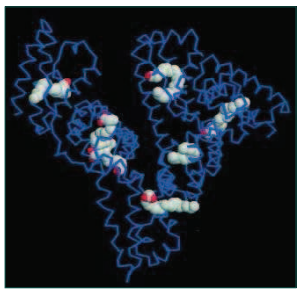

Figura 1.5. Struttura terziaria dell'albumina. È evidenziato il legame di sette molecole di acido arachidonico (dalla banca dati RCSB, PDB ID: 1gnj).

Azione antiossidante

L'albumina svolge un'azione anti-ossidante attraverso la cisteina-34 che è ossidata a residuo di acido sulfenico (albumina-SOH) poi convertito in gruppo disulfidico e quindi in mercaptoalbumina (albumina-SH) reintegrando pertanto la sua funzione antiossidante. L'albumina può fornire una efficace azione antiossidante anche attraverso il trasporto di composti con nota azione antiossidante, come la bilirubina. Il gruppo eme è considerato possedere proprietà pro-ossidanti attraverso le proprietà redox del ferro. L'albumina lega il gruppo eme efficientemente riducendone significativamente le proprietà pro-ossidanti, anche se in condizioni fisiologiche l'emopessina provvede la maggiore protezione anti-ossidante. Tuttavia, in condizioni di severa emolisi intravascolare o di sovraccarico di ferro, l'emopessina diviene insufficiente e l'albumina acquisisce un ruolo importante di protezione antiossidante. Anche il rame può manifestare importante effetto pro-ossidante. Grazie al suo sito che lega con alta affinità il rame, l'albumina limita il danno ossidativo catalizzato dal rame.

Mantenimento della pressione oncotica

L'albumina è una proteina di dimensioni relativamente piccole e rappresenta circa il 75% delle molecole proteiche nel plasma dei soggetti sani, ed è responsabile di circa il 75% della pressione colloido-oncotica. La pressione oncotica diviene pressione osmotica quando le cariche negative dell'albumina attraggono il sodio trattenendo quindi l'acqua. Il rimanente contributo alla pressione colloido-oncotica è dovuto all'effetto Donnan attribuibile alla sua complessiva carica negativa e ai cationi (Na^+ and K^+) che ne sono attratti. Inoltre, l'albumina può influenzare l'integrità vascolare direttamente, legandosi alla matrice interstiziale e al sub endotelio conferendo una carica negativa e riducendo la permeabilità alle macromolecole,

e indirettamente attraverso le sue proprietà di "scavenging".

Albumina glicata

È noto che la glicazione delle proteine è aumentata nei pazienti diabetici rispetto ai non-diabetici. La proteina glicata di riferimento è l'emoglobina, tuttavia l'emoglobina glicata (HbA1C) non riflette le modifiche della glicemia che avvengono in tempi relativamente brevi e presenta limitazioni in presenza di anemia e di alcune varianti emoglobiniche. Nei soggetti normali circa il 6-10% dell'albumina è glicata e i siti principali di legame del glucosio sono l'arginina 410 e la lisina 525. La misura della albumina glicata consente di rilevare più precocemente cambiamenti rapidi della glicemia che sono avvenuti negli ultimi 10-15 giorni. La sua misura può essere utile nei pazienti con varianti emoglobiniche (Hb S o Hb C che determinano ridotta emivita degli eritrociti) o con anemie emolitiche.

Transferrina

Le "transferrine" sono una ampia famiglia di proteine bilobate (chiamati lobi N e C) che legano il ferro e che sono presenti in tutti gli eucarioti. Il gene della transferrina è localizzato sul cromosoma 3 (3q21). La transferrina è una glicoproteina con massa di 79.6 kDa e presenta numerose isoforme. Si conoscono, infatti, almeno 38 varianti genetiche che differiscono per uno o più aminoacidi anche se tre sono i tipi di transferrina che si possono trovare con una prevalenza >1%. La transferrina C è la più comune nella popolazione caucasica: di questa si conoscono almeno 16 varianti (C1-C16). La variante C1 è la più diffusa (95%) ed il suo gene codificante, polimorfico, possiede due varianti alleliche che generano la transferrina C2 e la C3. Vi sono poi la transferrina B con migrazione più anodica e la transferrina D con migrazione più catodica delle quali a loro volta si conoscono numerose varianti. A queste si aggiungono le associazioni eterozigoti tra le varie C, B e D. La transferrina consiste di una singola catena polipeptidica di 679 aminoacidi con 19 ponti disolfuro ed è separata in due domini globulari (N-terminale aminoacidi 1-336 e C-terminale aminoacidi 337-679). Questi domini possono legare ciascuno uno ione Fe^{3+}, indipendentemente uno dall'altro (**Figura 1.6**). Il dominio C-terminale porta due catene glucidiche legate all'N delle asparagine 413 e 611 che costituiscono il 6% del peso molecolare. La transferrina è sintetizzata principalmente dal fegato ed in piccola quantità dal sistema reticolo endoteliale e dalle ghiandole endocrine (testicoli ed ovaie) con un'emivita di circa 10.5 giorni. L'intervallo di riferimento è di 2.0 - 3.6 g/L. La sintesi è aumentata in presenza di basse concentrazioni di ferro, dagli estrogeni e dai corticosteroidi. La transferrina trasporta il ferro nel plasma dal tratto gastrointestinale agli organi che l'utilizzano o l'immagazzinano, sistema emopoietico nel midollo osseo, fegato e milza. Meno dello 0.1% del ferro corporeo è legato alla transferrina attraverso i due domini che legano un atomo di ferro trivalente ciascuno. Vi sono quattro forme di transferrina: l'apotransferrina (punto isoelettrico (pI) Fe0 = 6.1), le transferrine monoferriche dove il ferro è legato nei domini N- o C-terminali

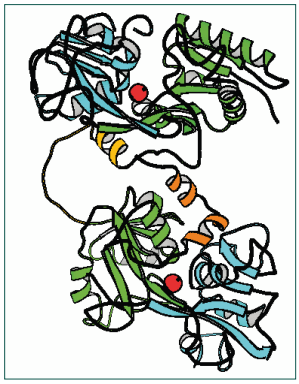

Figura 1.6. Modello della transferrina. Un atomo di ferro occupa ciascuno dei due lobi distinti (Figura prodotta con Molscript).

(pI Fe1N = 5.8 e pI Fe1C = 5.7) e la transferrina diferrica (pI Fe2 = 5.4). Negli individui normali il livello di saturazione del ferro è circa il 30%: per ogni ione ferrico si osserva una variazione approssimativa del pI di 0.3 unità. La concentrazione plasmatica della transferrina è utile per definire lo stato del ferro corporeo. In considerazione del preciso rapporto molare del legame del ferro alla transferrina, la misura della capacità totale di legame del ferro (total iron binding capacity, TIBC) è stata ampiamente sostituita dalla quantificazione della transferrina. La misura della saturazione della transferrina, il rapporto tra concentrazione di ferro e di transferrina, espresso in percentuale (TS) è un accurato indicatore dell'apporto di ferro al midollo osseo. Nella sideropenia, il valore della saturazione della transferrina è un indicatore sensibile della deplezione funzionale di ferro.

TIBC (µmol/L) = Transferrina (g/L) x 25.12 (µmol/g);
TS (%) = Sideremia (µmol/L) / TIBC (µmol/L) x 100 oppure
TS (%) = 3.98 x [Sideremia (µmol/L) / Transferrina (g/L)]

Le cellule con un elevato fabbisogno di ferro presentano sulla membrana numerosi recettori per il complesso transferrina-ferro. Il ferro è necessario per l'attività della ribonucleotide reduttasi che è essenziale per la divisione cellulare. Infatti questo enzima catalizza una delle prime reazioni che portano alla sintesi di DNA. La transferrina lega il ferro con una elevata affinità (Kd 10^{22} mol/L^{-1}) e il legame del Fe^{3+} richiede un anione (solitamente il carbonato) che serve da ponte tra il ferro e la proteina. L'abbassamento del pH sotto 7 protonizza lo ione carbonato con indebolimento del legame al ferro. I due oligosaccaridi "N-linked" sono costituiti da residui di N-acetilglicosammina, mannosio e galattosio e possono essere bi-, tri- e tetranntennati. Ciascuna antenna termina con una molecola di acido sialico che crea una carica negativa alla terminazione della catena. In linea teorica sono possibili transferrine con residui di acido sialico da 0 ad 8 (da 0 a 2 catene, cioè da 0 ad 8 antenne). Le forme asialo, monosialo e ottasialo non sono normalmente rilevabili nel siero. La tetrasialo-Fe_{1N}-transferrina, la glicoforma piu rappresentata nel siero umano, contiene due N-glicani biantennari per un totale di 4 residui di acido sialico (pI 5.4); sono inoltre presenti glicoforme a diverso contenuto di acido sialico quali la disialo-transferrina (pI 5.7), la trisialo-transferrina, (pI 5.6), la pentasialo-transferrina (pI 5.2) e la esasialo-transferrina, (pI 5.0). Per ogni residuo di acido sialico si osserva una variazione approssimativa del pI di 0.1 unità per molecola. L'etanolo inibisce la glicosilazione e l'assunzione di 50-80 gr di alcol al giorno per almeno 7 giorni determina un aumento delle forme carenti di carboidrati (carbohydrate-deficient transferrin, CDT). Sia l'asialo che la disialotransferrina sono chiaramente correlabili al consumo alcolico cronico, sebbene le due molecole mostrino differenti sensibilità e specificità. Il gruppo di studio della International Federation of Clinical Chemistry and Laboratory Medicine (IFCC) ha identificato nella disialotransferrina l'analita target per la CDT cui far riferimento per la standardizzazione della misurazione della molecola in qualità di biomarcatore dell'abuso alcolico. Infatti, pur essendo la asialoforma più specifica della disialotransferrina nell'identificare l'abuso alcolico, essa è rilevabile solo quando la forma disialo è già alta e pertanto al momento è quest'ultima forma ad avere la più elevata sensibilità diagnostica. L'esatto meccanismo mediante il quale l'uso eccessivo di alcol etilico determini l'aumento delle glicoforme carboidrato-carenti della transferrina non è ancora completamente compreso. È un processo complesso che coinvolge sia il trasporto intracellulare di proteine che l'attività enzimatica della glicosilazione. Vi sono inoltre evidenze secondo cui la concentrazione di CDT aumenta, pur rimanendo entro i comuni limiti di normalità, anche in caso di moderato consumo di bevande alcoliche. La concentrazione serica di CDT si riduce a seguito dell'astinenza da alcol etilico con un'emivita media di circa 14 giorni. Non è ancora chiarita la variabilità individuale dei meccanismi fisiopatologici che

sottendono all'incremento in ragione del consumo alcolico. Non risultano significative differenze nelle concentrazioni basali di CDT in differenti aree geografiche, includendo anche quelle aree (paesi orientali) in cui è noto un deficit dei sistemi ossidativi dell'alcol.

La transferrina può rilasciare il ferro all'interno delle cellule grazie al legame con un recettore di membrana specifico (recettore 1 della transferrina, TfR1) (**Figura 1.7**). Il gene che codifica questa proteina è localizzato sul cromosoma 3 (3q26.2-qter). Il recettore è un omodimero con ponte disolfuro e di peso molecolare 190 kDa. Ciascun recettore lega due molecole di transferrina diferrica. Virtualmente tutte le cellule, ad eccezione degli eritrociti maturi, presentano il recettore sulla membrana e in numero maggiore nell'eritrone, placenta e fegato. Nell'adulto circa l'80% dei TfR1 sono nel midollo eritroide. La carenza di ferro intracellulare determina un aumento della espressione dei recettori, mentre un sovraccarico di ferro causa una riduzione del numero di TfR1. Il complesso del recettore e le due transferrine legate è internalizzato nell'endosoma, assieme ad un'altra proteina, la "divalent-metal ion-transporter" (DMT-1). Il pH dell'endosoma si abbassa a circa 5.5, in queste condizioni di acidità l'affinità della transferrina per il ferro si riduce e questo viene rilasciato come ione Fe^{3+} che viene quindi ridotto a Fe^{2+}. La proteina DMT-1 trasporta il ferro dall'endosoma al citosol mentre il TfR1 e l'apo-transferrina sono riciclati sulla membrana dove l'apo-transferrina è rilasciata (**Figura 1.7**). Una forma troncata del TfR1, chiamata recettore solubile della transferrina (sTfR) è una glicopropteina di circa 85 kDa che può essere misurata nel plasma. Il sTfR è prodotto per proteolisi da parte di una proteasi serinica di membrana sulla superficie degli esosomi, nel corpo multi vescicolare, prima dell'esocitosi. La concentrazione plasmatica di sTfR è proporzionale alla quantità totale di cellule che esprimono il TfR1 e riflette pertanto lo stato dell'eritropoiesi e della carenza di ferro funzionale. Intervalli di riferimento <16 anni: 1.5 - 3.0 mg/L, adulti maschi: 2.2 - 5.0 mg/L; femmine (premenopausali): 1.9 - 4.4 mg/L.

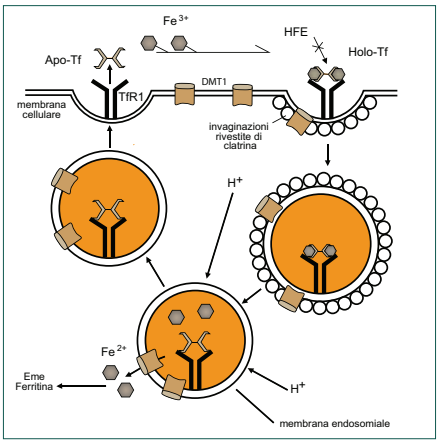

Figura 1.7. Ciclo della transferrina e del recettore 1 della transferrina (TfR1). La transferrina diferrica si lega al recettore 1 della transferrina e il complesso è internalizzato e acidificato per mezzo di una pompa protonica. Il ferro è quindi rilasciato dalla transferrina e trasportato fuori dagli endosomi attraverso il 'divalent metal transporter' (DMT1). La proteina dell'emocromatosi (HFE) sembra inibire l'endocitosi, probabilmente legandosi al TfR1. L'apotransferrina e TfR1 sono riciclati sulla superficie cellulare, dove a pH neutro si dissociano e sono resi disponibili per un secondo ciclo di cattura del ferro. Il ferro intracellulare è incorporato nell'eme o immagazzinato nella ferritina.

Alla fine degli anni 90 è stato clonato e sequenziato il recettore 2 per la transferrina (TfR2) il cui gene è sul cromosoma 7q22 e come il TfR1 è una glicoproteina transmembrana di tipo II con l'aminoterminale nel citoplasma, un singolo dominio trans membrana seguito da un grande ectodominio. TfR2 è espresso predominantemente sugli epatociti e il complesso HFE (proteina dell'emocromatosi)-TfR2 è un sensore della saturazione della transferrina e modula la trascrizione dell'epcidina, la molecola centrale dell'omeostasi del ferro.

Transtiretina (prealbumina)

La transtiretina è un omotetramero costituito da quattro subunità identiche di 127 aminoacidi ciascuna (**Figura 1.8**), e il suo gene è mappato sul cromosoma 18 (q11.2-q12.1). Il 95% della transtiretina è sintetizzato dal fegato, meno del 5% dai plessi coroidei dell'encefalo e dall'epitelio pigmentato della retina. La sintesi è stimolata dai glucocorticoidi, dagli androgeni ed è depressa dagli estrogeni. È catabolizzata principalmente dal rene e presenta una emivita di circa 2.5 giorni. La sua concentrazione nel plasma è compresa fra 0.20 e 0.40 g/L. Ha un elevato contenuto in triptofano e uno dei più alti rapporti di aminoacidi essenziali/non essenziali delle proteine plasmatiche e per questo la sua concentrazione offre una stima della qualità della nutrizione. Il nome della transtiretina deriva dalla sua capacità di trasportare la tiroxina e il retinolo (**trans**ports **thy**roxine and **retin**ol). La transtiretina è in grado di trasportare due molecole della proteina legante il retinolo (RBP), ma in media una molecola di transferrina lega 0.5 molecole di RBP. La tiroxina (T_4) è trasportata da tre proteine nel plasma, l'albumina, che ha la più alta concentrazione, 620 µM, la transtiretina, 5 µM e la globulina legante la tiroxina (thyroxine-binding globulin TBG), 0.3 µM. L'affinità per la tiroxina è più alta per la TBG (K_D 0.1 nM), seguita dalla transtiretina (K_D 15 nM) e dall'albumina (K_D 1.5 µM). In effetti, meno del 10% del T_4 è legato alla transtiretina che pertanto circola nel plasma prevalentemente nella forma non legata né al T_4 né alla RBP.

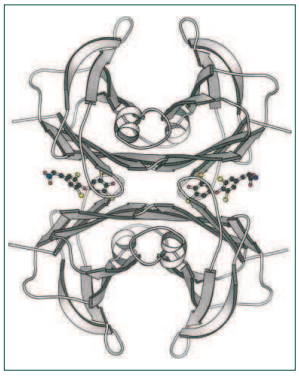

Figura 1.8. Modello della struttura della transtiretina umana. La molecola di tiroxina è mostrata nelle due possibili tasche tra i dimeri, anche se il legame presenta una negatività cooperativa. Sono stati proposti anche altri potenziali siti di legame (Figura prodotta con Molscript utilizzando il file 2ROX).

Sono note più di cento mutazioni della transtiretina che causano amiloidosi sistemiche (vedi **Scheda clinica 1**) con preponderante interessamento del sistema nervoso periferico con sviluppo di polineuropatia sensitivo motoria progressiva (polineuropatia amiloidotica familiare, FAP) e di cardiomiopatia restrittiva amiloidotica. Queste mutazioni, trasmesse con carattere autosomico dominante, destabilizzano il tetramero di transtiretina facilitando la dissociazione in monomero. Quest'ultimo può assumere una conformazione parzialmente alterata con esposizione di residui idrofobici che promuovono l'aggregazione in oligomeri che, con il concorso di glicosaminoglicani, quali l'eparansolfato, e della pentraxina siero amiloide P (SAP), si organizzano in fibrille con struttura a foglietti beta antiparalleli. Queste fibrille, del diametro di circa 10-12 nm, rigide, non ramificate, facilmente riconoscibili alla microscopia elettronica, costituiscono i depositi di amiloide

Scheda clinica 1: Le amiloidosi sistemiche

Le amiloidosi sistemiche *sono malattie rare causate da proteine con anomalie nel loro ripiegamento (protein misfolding diseases). Le alterazioni conformazionali rendono la proteina meno stabile e favoriscono la sua aggregazione in oligomeri che si organizzano in fibrille con conformazione a foglietti beta. L'aggregazione può essere favorita da un persistente aumento della concentrazione della proteina amiloidogenica, da una mutazione, o dai processi di invecchiamento. I glicosaminoglicani, e in particolare l'eparansolfato, facilitano la formazione degli oligomeri e costituiscono l'impalcatura per la formazione delle fibrille. Queste sono stabilizzate dal legame, attraverso il calcio, di una pentraxina, siero amiloide P (SAP), che è presente in tutti i depositi di amiloide. La formazione degli oligomeri e dei depositi di amiloide nei tessuti causa un progressivo danno funzionale, che in assenza di terapia, può condurre a morte il paziente. Sono note circa 30 diverse proteine che possono formare depositi di amiloide. La nomenclatura internazionale prevede che le proteine amiloidogeniche siano indicate con la lettera A, per amiloide, seguita dalla abbreviazione della proteina. Ad esempio, AL indica le catene leggere immunoglobuliniche monoclonali che formano amiloide e ATTR indica la transtiretina che causa depositi di amiloide. Questi possono essere localizzati, ad esempio nel cervello nella malattia di Alzheimer, o danneggiare numerosi organi e tessuti, come nel caso delle amiloidosi sistemiche. Le amiloidosi sistemiche sono circa una dozzina, e le forme più comuni in Italia, che costituiscono più del 95% dei casi, sono l'amiloidosi AL (circa 70% dei casi), l'amiloidosi reattiva (AA) (8%), l'amiloidosi ATTR (10%), causata sia dalla proteina mutata nelle forme familiari che dalla proteina "wild type" nella amiloidosi senile sistemica, e l'amiloidosi da apolipoproteina A1 (AApoA1) (8%). L'amiloidosi AL presenta una incidenza di circa 10 nuovi casi per milione per anno. È causata da un clone plasmacellulare midollare di solito di modeste dimensioni (l'infiltrato plasmacellulare midollare mediano è del 7%) che produce una catena leggera immunoglobulinica lambda nel 75% dei casi e kappa nel 25% dei casi. La catena leggera presenta anomalie del ripiegamento (misfolded) ed è in grado di esercitare un effetto tossico diretto su tessuti e organi bersaglio oltre che un danno strutturale causato dall'accumulo dei depositi di amiloide. L'amiloidosi AL coinvolge praticamente tutti gli organi con l'eccezione del sistema nervoso centrale: il cuore è il più coinvolto assieme al rene, seguito poi dal tratto gastroenterico, dai tessuti molli e dal sistema nervoso periferico e autonomico. L'amiloidosi cardiaca è il principale determinante della sopravvivenza e la sua gravità può essere valutata sia con tecniche di imaging, ecocardiografia, risonanza magnetica nucleare, e scintigrafia, sia con marcatori biochimici, quali il peptide natriuretico di tipo B e le troponine cardiache. I biomarcatori cardiaci sono alla base di un sistema di stadiazione molto efficiente. L'amiloidosi AA si associa a infiammazione cronica causata da malattie reumatologiche, infettive croniche, neoplastiche, da sindromi autoinfiammatorie, e in circa il 15% dei pazienti la causa non è identificabile. L'organo bersaglio è il rene con perdita di albumina nelle urine e progressivo danno della funzione fino alla fase terminale della insufficienza renale con necessità di trattamento dialitico. L'amiloidosi senile sistemica è causata dal deposito fibrillare di transtiretina "wild type" (vedi testo) nel cuore soprattutto in pazienti maschi dopo i 60 anni. Causa una cardiomiopatia restrittiva con sviluppo di insufficienza cardiaca congestizia. Sono note più di 100 mutazioni diverse della transtiretina che possono causare amiloidosi sistemica ereditaria di tipo autosomico dominante. Le manifestazioni cliniche variano da forme prevalentemente neuropatiche, come nel caso della variante "portoghese" Val30Met, con interessamento sia del tessuto nervoso periferico che di quello autonomico, a forme con preponderante coinvolgimento cardiaco. La amiloidosi da apolipoproteina A1 è sostenuta da circa 20 mutazioni che causano la formazione di depositi di amiloide in vari organi vitali, quali il cuore, fegato e rene. In generale i depositi sono costituiti da frammenti N-terminali comprendenti 80-100 residui della apolipoproteina A1, anche se il processo alla base della formazione di questi frammenti non è stato ancora definito.*

Segue Scheda clinica 1

La caratterizzazione della proteina che forma i depositi di amiloide è essenziale per definire una corretta strategia terapeutica. Il recente sviluppo di numerosi farmaci specifici per le varie forme di amiloidosi rende ancora più necessaria la corretta identificazione del precursore proteico. La metodica "gold standard" è ora rappresentata dalla proteomica con caratterizzazione inequivocabile della proteina amiloidogenica per mezzo di metodiche di spettrometria di massa.
Gli avanzamenti nella comprensione dei meccanismi molecolari coinvolti nella formazione dei depositi di amiloide e del danno tissutale hanno rivelato numerosi bersagli terapeutici e creato nuove opportunità per contrastare la progressione della malattia. Numerosi farmaci sono ora in sviluppo per inibire la sintesi del precursore amiloide, anche attraverso tecniche di "gene silencing" nella amiloidosi ATTR; per interferire con il legame fra glicosaminoglicani e proteina amiloide nella amiloidosi AA; per stabilizzare il precursore inibendone l'aggregazione e la formazione di fibrille sempre nella amiloidosi ATTR, o per promuovere il riassorbimento dei depositi attraverso piccole molecole o con immunizzazione passiva con anticorpi diretti contro le fibrille o loro costituenti come la SAP.

che si colorano con il colorante rosso Congo e assumono una patognomonica colorazione verde brillante quando osservate al microscopio in luce polarizzata (**Figura 1.9**). La mutazione più comune è Val30Met con cluster di migliaia di pazienti nel nord Portogallo, nel nord della Svezia e in Giappone. La variante Val122Ile è presente nel 3.9% degli afroamericani e in più del 5% della popolazione in alcune aree dell'Africa occidentale. Si associa al rischio di sviluppo di amiloidosi cardiaca in età avanzata in assenza di polineuropatia. In Italia sono state identificate più di 20 varianti, le più comuni sono Val30Met

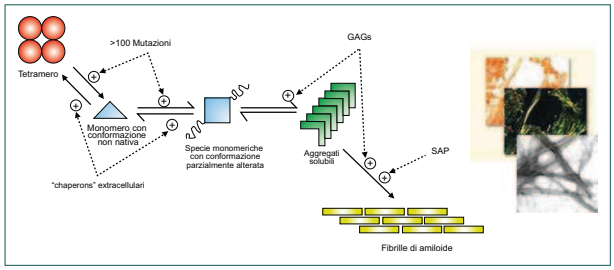

Figura 1.9. Cascata degli eventi che portano alla formazione delle fibrille di amiloide. La dissociazione del tetramero di transtiretina in monomero è facilitata da mutazioni che destabilizzano il tetramero e promuovono l'acquisizione di una conformazione anomala da parte del monomero. Questi effetti sono contrastati dai 'chaperones' extracellulari (come ad esempio la clusterina) che stabilizzano sia il tetramero che il monomero nella forma nativa. Il monomero con conformazione anomala espone sulla superficie aree idrofobiche che facilitano l'aggregazione in oligomeri solubili che si organizzano successivamente in fibrille con conformazione a foglietti beta. Il processo di aggregazione in oligomeri e di formazione delle fibrille di amiloide è facilitato dai glicosaminoglicani (GAGs), in particolare l'eparansolfato. Le fibrille di amiloide sono stabilizzate e protette dalla proteolisi dalla pentraxina siero amiloide P (SAP). Al microscopio elettronico le fibrille hanno un diametro di 10-12 nm. Si colorano intensamente con il rosso Congo e presentano una patognomonica colorazione verde brillante quando osservate in luce polarizzata.

(29%), Glu89Gln (26%), Phe64Leu (12%), Ile68Leu (7%). Sono ora disponibili farmaci che legandosi al tetramero di transtiretina lo stabilizzano riducendo la formazione di monomeri inibendo pertanto all'origine la cascata amiloidogenica. Sperimentazioni cliniche con questi farmaci hanno dimostrato la loro capacità di rallentare la progressione della polineuropatia.

Aptoglobina

L'aptoglobina è una glicoproteina tetramerica che lega l'emoglobina ed è costituita da catene alfa e beta legate da ponti disolfuro. Due forme alleliche della catena alfa determinano tre differenti fenotipi di aptoglobina. I geni sono stati mappati sul cromosoma 16q22. La catena alfa-1 è una proteina di 9 kDa e 83 aminoacidi, l'alfa-2 è di 17 kDa e 142 aminoacidi. La catena beta è circa 32-40 kDa (glicosilata) e contiene 245 aminoacidi. L'aptoglobina possiede otto siti di N-glicosilazione che formano glicani bi- e triantennari. L'aptoglobina tipo 1-1 è formata da due catene alfa-1 e due beta per un peso molecolare di circa 85 kDa. L'aptoglobina 1-2 comprende catene alfa-1 e alfa-2 e catene beta in varie proporzioni con massa molecolare compresa fra 100 e 200 kDa. L'aptoglobina tipo 2-2 è formata da oligomeri costituiti da una catena alfa-2 ed una beta con massa molecolare fino a 400 kDa (**Figura 1.10**). Questa eterogeneità strutturale è dovuta al numero differente di gruppi SH liberi disponibili per ponti disolfuro intercatena. Mentre la catena beta ha una cisteina libera in posizione 105, la catena alfa-1 ha due cisteine libere in posizione 15 (che lega l'altra catena alfa) e 72, che lega la catena beta in posizione 105. In aggiunta, la catena alfa-2 ha tre cisteine libere in posizione 15, 64 e 131 (che legano la catena beta in posizione 105). La catena alfa-2 pertanto consente la formazione di polimeri attraverso i ponti disolfuro. Il fegato è l'organo principale di sintesi, ma il gene per l'aptoglobina è espresso anche in altri tessuti: polmone, cute, milza, rene e tessuto adiposo. La sua sintesi è stimolata da: ormone della crescita, insulina, endotossine batteriche, prostaglandine e citochine come l'IL-6. L'aptoglobina è una proteina di fase acuta positiva. È sintetizzata come una singola catena polipeptidica che è poi clivata nelle due catene alfa e beta. La sua concentrazione plasmatica è più elevata nell'adulto che in età pediatrica. L'intervallo di riferimento è 0.3 - 2.0 g/L (30 -200 mg/dL). Le persone con aptoglobina 1-1 presentano le concentrazioni plasmatiche più elevate, la 2-2 le più basse e la 2-1 una concentrazione intermedia. L'emivita è di 3.5 giorni, ma il complesso aptoglobina-

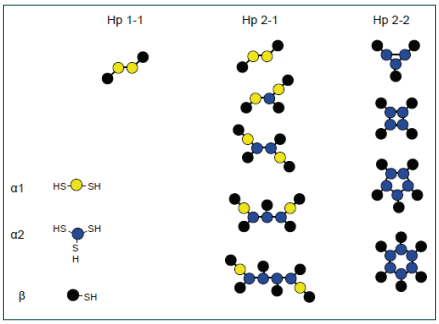

Figura 1.10. Struttura schematica dei sottotipi di aptoglobina (Hp).

emoglobina ha una emivita di soli 10 minuti. La sua funzione più nota è quella di rimuovere l'emoglobina libera dal circolo, l'aptoglobina lega l'emoglobina con altissima affinità (K_D 10^{-15} mol/L), probabilmente la più alta in natura. Il complesso aptoglobina-emoglobina è rapidamente rimosso dai macrofagi e monociti attraverso il legame con il recettore CD163. Legandosi all'emoglobina libera, l'aptoglobina ne limita i danni evitando la formazione di "reactive oxygen species" (ROS), la perossidazione degli acidi grassi delle membrane cellulari e l'ossidazione delle LDL. Inoltre l'aptoglobina esercita una potente azione immunosoppressiva e modula il bilancio fra T helper 1 e T helper 2. L'aptoglobina 1-1 è la più efficace nel legare l'emoglobina libera e nel sopprimere la risposta infiammatoria secondaria alla liberazione di emoglobina. L'aptoglobina 2-2 è biologicamente la meno attiva e l'aptoglobina 2-1 è moderatamente attiva.

La concentrazione plasmatica dell'aptoglobina aumenta in corso di infiammazione, ustioni, traumi e neoplasie. La concentrazione plasmatica aumenta 4-6 giorni dopo l'inizio dell'evento flogistico e ritorna alla concentrazione basale 2 settimane dopo lo spegnimento del processo infiammatorio. La sua concentrazione plasmatica si riduce in corso di emolisi intravascolare, malnutrizione, eritropoiesi inefficace, epatopatie, negli ultimi mesi di gravidanza e nei neonati. Nei soggetti con aptoglobina 1-1, con massa molecolare relativamente bassa, la concentrazione plasmatica si riduce in presenza di proteinuria. È stata studiata la possibile associazione dei polimorfismi allelici dell'aptoglobina con numerose condizioni patologiche come, ad esempio, le malattie cardiovascolari, diabete, alcune malattie infettive, eclampsia, e malattie neurologiche (epilessia, psicosi).

Emopessina

L'emopessina è una glicoproteina plasmatica costituita da una singola catena polipetidica di 439 aminoacidi di massa molecolare di 63 kDa. È glicosilata in cinque posizioni e contiene sei ponti disolfuro intracatena. Il gene è assegnato a 11p15.5-p15.4, lo stesso sito del gene del complesso della beta globina. Il gene presenta un elemento IL-6 responsivo che regola la risposta di fase acuta dell'emopessina. Elementi emopessina-simili fanno parte delle metalloproteasi di matrice e della vitronectina. La struttura dell'emopessina è caratterizzata da due domini omologhi a forma di elica a quattro pale composte da 35-45 residui, fra loro collegati da una regione cerniera ricca in istidina (**Figura 1.11**). I due domini derivano probabilmente da una duplicazione del gene. L'emopessina è espressa soprattutto nel fegato, e in minor misura nel sistema nervoso centrale e periferico e nella retina. È una proteina di fase acuta di tipo 2. L'intervallo di riferimento nell'adulto è: 0.4–1.5 g/L. La emopessina lega l'eme libero con alta affinità (K_D 10^{-9} mol/L) e lo trasporta al recettore LRP-1 (LDL receptor-related protein-1) noto anche come CD91, presente su numerosi tipi cellulari: epatociti, macrofagi, neuroni e sincizio trofoblasto. A seguito del legame del complesso eme-emopessina al LRP-1, il complesso è internalizzato per endocitosi nelle cellule, soprattutto epatociti e macrofagi splenici. Nel lisosoma l'eme viene catabolizzato dalle emeossigenasi in biliverdina, monossido di carbonio e ferro. Molto probabilmente anche l'emopessina viene degradata nel lisosoma. Grazie alla sua alta affinità per l'eme, l'emopessina è in grado di sottrarlo all'albumina, che rappresenta un'altra proteina che lega l'eme con alta capacità in virtù della sua elevata concentrazione plasmatica. L'emopessina lega anche l'eme liberato dalla mioglobina. Il legame dell'eme all'emopessina riduce la quantità di eme disponibile come catalizzatore della formazione di radicali in circolo, rende il ferro indisponibile ai microrganismi e contribuisce al recupero dei composti del ferro.

Recentemente è stato proposto lo studio del profilo degli N-glicani della emopessina per indagare l'insorgenza di carcinoma epatico nei pazienti cirrotici.

Ceruloplasmina

La ceruloplasmina è costituita da una singola catena polipeptidica di 1046 aminoacidi e tre catene oligosaccaridiche con un contenuto totale in carboidrati fra l'8 e il 9.5%, e una massa molecolare media di 132 kDa. La ceruloplasmina è una proteina multifunzionale sintetizzata dal fegato e che gioca un ruolo essenziale nel metabolismo del rame e del ferro (**Figura 1.12**). Trasporta il rame agli enzimi che lo contengono e partecipa alla ossidazione, trasporto e utilizzo del ferro. La ceruloplasmina esercita un'azione antiossidante prevenendo l'ossidazione dei lipidi delle membrane cellulari attraverso la sua attività ferro-ossidasica e può modulare la funzione della NO sintasi endoteliale e quindi controlla la vasodilatazione dipendente dall'NO. La ce-

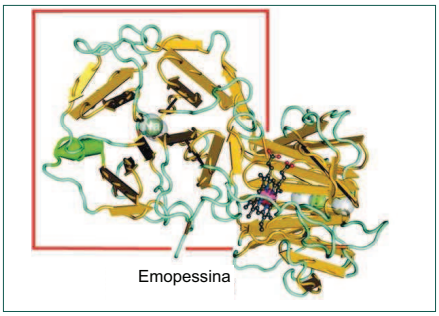

Figura 1.11. Struttura cristallina dei domini dell'emopessina. All'interno della cornice rossa si distingue la struttura ad elica a quattro pale.

ruloplasmina è ridotta nella malattia di Wilson nella quale vi è una ridotta capacità di incorporare il rame nella apoceruloplasmina. Ne deriva una aumentata concentrazione di rame libero nel plasma e nei tessuti, specialmente nel fegato e cervello. La concentrazione di ceruloplasmina è inoltre ridotta nella sindrome di Menkes, nella quale il difetto è secondario a uno scarso assorbimento e utilizzazione del rame della dieta, nella sindrome nefrosica, nelle enteropatie protido-disperdenti, nei malassorbimenti e nelle epatopatie avanzate. Alte concentrazioni di ceruloplasmina plasmatica si osservano in numerose neoplasie e malattie infiammatorie, nella colestasi, cirrosi biliare primitiva, nel lupus eritematoso sistemico, nell'artrite reumatoide e in gravidanza. La sintesi della ceruloplasmina è infatti stimolata dagli estrogeni e dai contraccettivi orali e dall'eccessiva assunzione di rame.

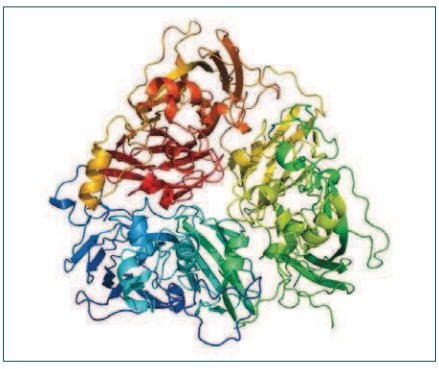

Figura 1.12. Struttura della ceruloplasmina (Elaborazione con PyMOL di PDB 1KCW).

Intervalli di riferimento: neonati <5 giorni: 0.05 - 0.40 g/L (5 - 40 mg/dL); adulti 0.20 - 0.60 g/L (20 - 60 mg/dL).

Proteine del sangue coinvolte nella coagulazione

La capacità dell'organismo di controllare il flusso sanguigno dopo una lesione dei vasi è essenziale per la sopravvivenza. Il processo della coagulazione del sangue e la successiva dissoluzione del coagulo che segue il riparo del tessuto danneggiato è definita emostasi. Questa è composta da 4 eventi principali che si susseguono dopo un danno vascolare:

1. Vasocostrizione, che riduce la perdita di sangue dall'area danneggiata (fase vascolare);
2. attivazione delle piastrine da parte della trombina e loro aggregazione in corrispondenza della lesione vascolare a formare il tappo piastrinico. Il fibrinogeno è il responsabile primario della adesione piastrinica che è favorita dalla esposizione del collagene che segue la rottura dell'endotelio vascolare. Le piastrine attivate liberano il nucleotide ADP e il trombossano 2 (che a loro volta attivano altre piastrine), serotonina, fosfolipidi, lipoproteine, e altre proteine importanti per la cascata coagulativa (fase piastrinica);
3. il tappo piastrinico è successivamente rinsaldato da un reticolo di fibrina per formare il coagulo (fase coagulativa);
4. al termine del processo il coagulo, svolta la sua funzione, è dissolto ad opera della plasmina (fase fibrinolitica).

La formazione del coagulo può avvenire attraverso due vie, intrinseca ed estrinseca, percorse dai fattori della coagulazione. Le due vie di attivazione della coagulazione non sono separate, ma interconnesse (**Figura 1.13**).

Sinossi della coagulazione

La formazione del coagulo avviene attraverso due vie interconnesse: intrinseca ed estrinseca.

- *La **via estrinseca**, evento emostatico più rilevante in condizioni fisiologiche, è iniziata dall'esposizione di fattore tessutale (TF) nel sito di lesione, cui consegue una serie di attivazioni a cascata dei fattori della coagulazione. Schematicamente, TF si lega al fattore VII, agendo come cofattore per l'attivazione, da parte di VIIa, del fattore X a fattoreXa e del fattore IX a fattore IXa. Il fattoreXa, in grado di attivare la protrombina a trombina, costituisce, insieme a IXa, il punto di unione tra via estrinseca ed intrinseca. Il fattore Xa, inoltre, amplifica la cascata attivandoil fattore VII a VIIa.*
- *La **via intrinseca** è meno importante per l'emostasi in condizioni fisiologiche rispetto alla via estrinseca; tuttavia, in alcune condizioni patologiche, diviene rilevante e conduce a processi trombotici. La via intrinseca è attivata quando la precallicreina ed il kininogeno ad elevato peso molecolare, i fattori XI e XII sono esposti ad una superficie caricata negativamente ("fase di contatto"). La conversione di precallicreina a callicreina attiva il fattore XII a fattore XIIa, cui consegue una cascata di attivazioni sequenziali, in cui ogni fattore attivato è in grado di attivare quello successivo, in presenza di ioni calcio e fosfolipidi (nell'ordine: attivazione di XI ad XIa, attivazione di IX a IXa, attivazione di X a Xa). L'attivazione del fattore Xa richiede l'assemblaggio del complesso tenasico formato dal calcio e dai fattori VIIIa, IXa e X sulla superficie delle piastrine attivate.*

Il fattore Xa, punto di unione fra via intrinseca ed estrinseca, attiva la protrombina a trombina, la quale, a sua volta, converte il fibrinogeno in fibrina.

La trombina modula la cascata coagulativa attivando i fattori VIII e V (i quali, a loro volta, contribuiscono all'attivazione di fattore X e protrombina), ed il fattore XI a XIa. La trombina, inoltre, attiva il fattore XIII, che stabilizza il coagulo creando legami crociati fra le molecole di fibrina.

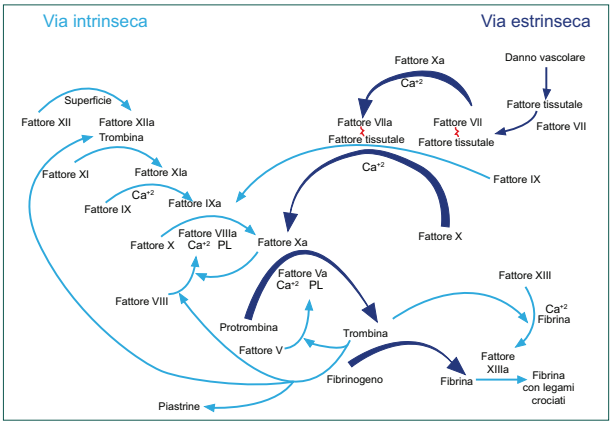

Figura 1.13. Schema generale della coagulazione. La via estrinseca è iniziata dal legame del fattore tissutale (TF) al fattore VII che produce l'attivazione a FVIIa e ad una serie successiva di attivazioni a cascata che conducono alla formazione di trombina. Questa attiva il fattore XI sulla superficie delle piastrine, il FXIa inizia la via intrinseca con generazione di ulteriore trombina accelerando la formazione di fibrina. Le due vie sono inoltre unite dalla attivazione del FIX a FIXa da parte del complesso FVIIa-TF.

Infatti, fattori generati nella via estrinseca attivano poi fattori e complessi della via intrinseca. Si ritiene che fisiologicamente la coagulazione all'interno del vaso non inizi con l'attivazione del sistema plasmatico attivabile da contatto, cioè attraverso quella che era definita la via intrinseca (questa via sarebbe importante nella generazione di mediatori chimici della flogosi di origine plasmatica, che non nell'attivazione della coagulazione), ma dal fattore tissutale (TF), attraverso la via estrinseca. Pertanto, la formazione di fibrina a seguito di un danno tissutale, con attivazione della via estrinseca, è l'evento emostatico più rilevante in condizioni fisiologiche. Affinché l'emostasi sia attivata è necessario che le piastrine aderiscano al collagene esposto, rilascino il contenuto dei loro granuli e aggreghino. L'adesione delle piastrine al collagene è mediata dal fattore di von Willebrand (vWF) che forma un ponte fra uno specifico complesso glicoproteico sulla superficie delle piastrine (GPIb-GPIX-GPV) e le fibre di collagene. La GPIb è composta da due proteine, GPIbα and GPIbβ codificate da due geni distinti. Oltre al suo ruolo come ponte fra le piastrine e il collagene esposto sulle superfici endoteliali, il vWF si lega e stabilizza il fattore VIII della coagulazione. Il legame del fattore VIII da parte del vWF è necessario per la normale sopravvivenza del fattore VIII in circolo. Il fattore di von Willebrand è una complessa glicoproteina contenuta nelle piastrine e stoccata nei granuli α. È sintetizzato dai megacariociti ed è presente nella matrice sub endoteliale. Il fattore di von Willebrand è stoccato anche nei granuli di Weibel-Palade delle cellule endoteliali sotto forma di ULMHMW (multimeri ad altissimo peso molecolare- Ultra Large), è liberato nel plasma dove per azione di ADAMTS 13 (una disintegrina e metalloproteinasi), attraverso tagli controllati, viene ridotto a MHMW vWF, in grado di svolgere il ruolo fisiologico. La permanenza in circolo

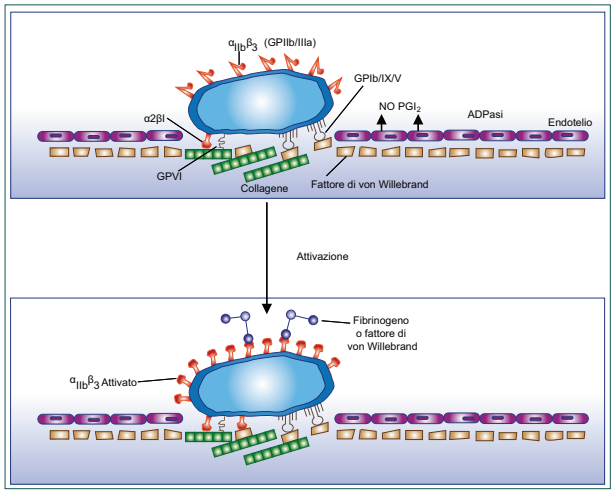

Figura 1.14. Adesione delle piastrine. Le cellule endoteliali limitano la adesione delle piastrine perché le separano dalle proteine adesive della regione subendoteliale, producono due inibitori della funzione piastrinica (l'ossido nitrico [NO] e la prostaciclina [PGI_2]) e contengono un potente enzima (CD39) che può degradare l'adenosina difosfato (ADP) rilasciato dalle piastrine. L'adesione piastrinica è iniziata dalla perdita di cellule endoteliali (o dalla rottura di una placca aterosclerotica) che espone glicoproteine (GP) adesive come il collagene e il fattore di von Willebrand del subendotelio assieme ad altre glicoproteine. Le piastrine aderiscono al subendotelio per mezzo di recettori che legano le GP adesive. Il legame della GP 1b al fattore di von Willebrand gioca un ruolo importante, ma anche il legame al collagene di α2β1 (GPIa/IIa) e GPVI e altri recettori piastrinici contribuiscono al legame. Dopo l'adesione, le piastrine vanno incontro ad un processo di attivazione che conduce a modificazioni conformazionali nei recettori $\alpha_{IIb}\beta 3$ che ne aumentano l'affinità per il fibrinogeno e il fattore di von Willebrand.

di ULMHMW per difetti di ADAMTS 13, su base genetica o immunologica, è responsabile della porpora trombotica trombocitopenica (PTT) in quanto i ULMHMW determinano la agglutinazione delle piastrine e la formazione di trombi piastrinici nel microcircolo.

La attivazione iniziale delle piastrine è indotta dal legame della trombina a recettori specifici sulla membrana delle piastrine che inizia una cascata di trasduzione del segnale (**Figura 1.14**). Il recettore della trombina è accoppiato ad una proteina-G, che a sua volta attiva la fosfolipasi C-γ (**Figura 1.15**). Quest'ultima idrolizza il fosfatidilinositolo-4,5-bifosfato (PIP_2) con formazione di inositolo trifosfato (IP_3) e diacilgliceorlo. IP_3 induce il rilascio di calcio dai depositi intracellulari e il diacilgliceorlo attiva la proteinkinasi C (PKC). Il collagene, al quale aderiscono le piastrine, e il rilascio di calcio intracellulare portano all'attivazione della fosfolipasi A_2 (PLA_2), che idrolizza i fosfolipidi di membrana con liberazione di acido arachidonico. Quest'ultimo causa un aumento della produzione e rilascio di trombossano A_2 (TXA_2), un potente vasocostrittore e induttore della aggregazione piastrinica attraverso il suo legame a re-

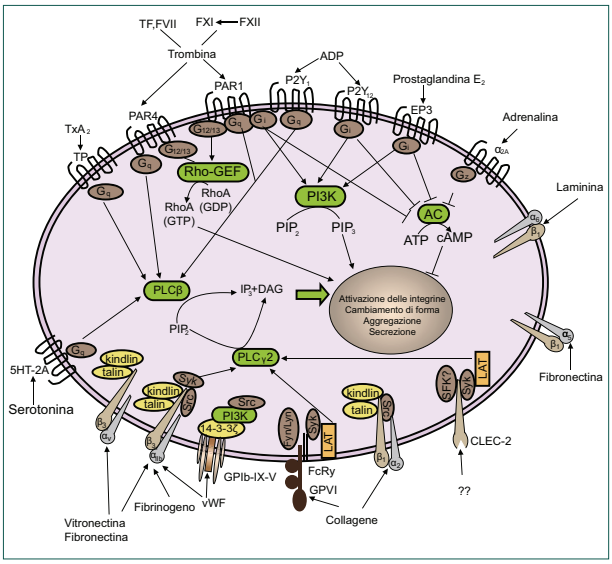

Figura 1.15. Recettori delle piastrine e vie di segnale più importanti che conducono alla attivazione piastrinica. Gli agonisti solubili stimolano i recettori accoppiati alle proteine G, innescando vie di segnale che coinvolgono le rispettive proteine G. Il legame crociato di GPVI o della "C-type lectin receptor" CLEC-2 risulta nella attivazione della fosfolipasi Cγ2 (PLCγ2). (TF, fattore tissutale; TxA_2, trombossano A_2; TP, recettore del TxA_2; PAR, protease-activated receptor; RhoGEF, Rho-specific guanine nucleotide exchange factor; PI3K, phosphoinositide-3-kinase; AC, adenylyl cyclase; PIP_2, phosphatidylinositol-4,5-bisphosphate; PIP_3, phosphatidylinositol-3,4,5-trisphosphate; IP_3, inositol-1,4,5-trisphosphate; DAG, diacylglycerol).

cettori che utilizzano la via della fosfolipasi C-β. Un altro enzima attivato dal rilascio del calcio intracellulare è la "myosin light chain kinase (MLCK)" che fosforila la catena leggera della miosina che quindi interagisce con l'actina alterando la morfologia e la motilità delle piastrine.

Uno dei molteplici effetti della PKC è la fosforilazione e l'attivazione di una proteina piastrinica specifica di 47 kDa. Questa proteina attivata induce il rilascio del contenuto dei granuli piastrinici incluso l'ADP che stimola ulteriormente le piastrine amplificando la cascata di attivazione piastrinica. L'importanza del ruolo dell'ADP nell'attivazione piastrinica è bene esemplificato dalla potente azione antitrombotica di un farmaco (clopidogrel) antagonista del recettore dell'ADP. L'ADP inoltre modifica la membrana piastrinica con esposizione del recettore glicoproteico complesso GPIIb-GPIIIa, al quale si legano il vWF e il fibrinogeno portando alla aggregazione piastrinica. Il complesso GPIIb-GPIIIa è un membro della famiglia delle integrine (ed è noto anche come integrin αIIb-β_3) ed intera-

gisce con la matrice extracellulare. Anomalie della proteina GPIIb e/o IIIa causano la forma più comune di piastrinopatia ereditaria, nota come tromboastenia di Glanzmann. Gli eterozigoti sono asintomatici e generalmente hanno risultati normali ai test di funzionalità piastrinica. Nei soggetti omozigoti, le più comuni manifestazioni cliniche sono epistassi, gengivorragia e menorragia. Sono disponibili per scopi terapeutici, come antiemostatici, anticorpi (come l'abciximab) che bloccano il recettore GPIIb-GPIIIa. Anche la proteina adesiva trombospondina (TSP) è importante nella adesione piastrinica, in quanto serve da collante per la interazione tra il collagene e la GPIV (precedentemente identificata come GPIIIb), presente sulla superficie delle piastrine. È importante sottolineare che le interazioni tra collagene, proteine adesive (vWF, TSP, fibrinogeno) e superficie piastrinica, vengono "stabilizzate" dal "cross-linking" operato dal fattore XIII della coagulazione. L'attivazione delle piastrine è richiesta per la loro successiva aggregazione a formare il tappo piastrinico, ma egualmente importante è il ruolo della attivazione della superficie piastrinica con esposizione di fosfolipidi che attivano la cascata della coagulazione.

Tutti gli antagonisti della aggregazione piastrinica possiedono recettori sulla superficie piastrinica associati a proteine G, con attività stimolatoria sulla adenilato-ciclasi (prostaciclì-

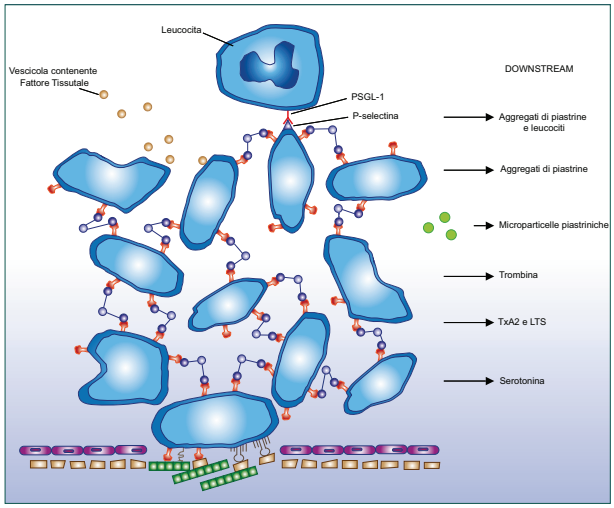

Figura 1.16. Aggregazione delle piastrine. L'aggregazione avviene quando le glicoproteine adesive multivalenti legano simultaneamente ai recettori $\alpha_{IIb}\beta_3$ di due differenti piastrine formando legami crociati fra i recettori. Le piastrine attivate rilasciano microparticelle procoagulanti ed esprimono la selectina-P sulla superficie che porta al reclutamento dei leucociti attraverso le interazioni fra la selectina-P piastrinica e il suo ligando (P-selectin glycoprotein ligand-1, PSGL-1) espresso sulla superficie dei leucociti.

na, prostaglandina D2, adenosina, adrenalina [recettori β]) o sulla guanilato-ciclasi (ossido nitrico, NO). Il più importante secondo messaggero inibitorio per l'aggregazione piastrinica è il cAMP, il cui livello intracellulare si innalza quando la adenilato ciclasi è attivata in risposta a segnali extracellulari inibitori (**Figura 1.15**). Il cAMP esercita effetti inibitori pleiotropici sulle piastrine, bloccando sia l'iniziazione sia il mantenimento delle risposte stimolatorie. Esso infatti blocca il legame degli agonisti ai loro recettori, inibisce la fosfolipasi C e la conseguente formazione di DAG e IP_3, inibisce la PKC ed antagonizza le risposte mediate dal calcio, inclusa la idrolisi dell'acido arachidonico dei fosfolipidi da parte della fosfolipasi A2. Il ruolo della attività inibitoria del cGMP (che si forma, per esempio, dalla stimolazione con l'antagonista NO), non è stato ben stabilito, ma sembra che venga inibita la attivazione della fosfolipasi C.

Riassumendo il ruolo delle piastrine, la lesione delle cellule endoteliali espone il tessuto connettivo sottoendoteliale altamente trombogenico (**Figura 1.14**), al quale le piastrine aderiscono entrando in uno stato di "attivazione" che comporta un cambiamento nella forma piastrinica e una reazione di esocitosi (**Figura 1.16**). I fattori che si liberano dai granuli piastrinici (ADP, TXA2, serotonina ed altri) reclutano ulteriori piastrine che aggregano sopra le prime, così da formare il tappo piastrinico. Tale reazione piastrinica avviene entro pochi minuti dalla lesione e, insieme alla vasocostrizione, costituisce la cosiddetta emostasi primaria. Se si tratta di lesioni capillari l'emostasi primaria è sufficiente a riparare il danno. Se si tratta di lesioni di vasi di calibro maggiore, l'esposizione di superficie negativa e di fattore tessutale nel sito di lesione, insieme ai fattori piastrinici, attiva il sistema della coagulazione, che porta alla formazione di trombina. La trombina converte il fibrinogeno a fibrina, formando il coagulo di fibrina e stimolando un ulteriore reclutamento di piastrine. Tutto ciò richiede più tempo ed il processo viene definito emostasi secondaria. Viene quindi prodotto il tappo emostatico secondario o permanente. La fibrina polimerizzata e le piastrine formano una massa solida che tampona l'emorragia nel sito della lesione.

La via intrinseca

Questa via, nota anche come via dell'attivazione per contatto è molto meno importante per l'emostasi in condizioni fisiologiche

Tabella 1.3. Principali fattori della coagulazione.

Fattore	Cromosoma	Massa molecolare kDa	Emivita giorni	Concentrazione Plasmatica mg/L (nM)
Precallicreina (PK)	4q34-q35	85-88	2	35-45 (400-510)
Chininogeno ad alto peso molecolare (HMWK)	3q26-qter	120	5	70-90 (580-750)
I Fibrinogeno	4q23-q32	340	3-5	3000 (8820)
II Protrombina	11	72	2.5-4.0	100 (1390)
III Fattore tissutale	1	45	-	-
IV Calcio		-	-	86-100 (2.15-2.5)*
V	1q21-25	330	0.5	7 (20)
VII	13	50	5 ore	0.5 (10)
VIII	Xq28	330	15 ore	0.1 (0.3)
IX	X	57	1	5 (90)
X	13q23-qter	56	1.25	10 (180)
XI	4q35	125	2.3-3.3	4-6 (30-50)
XII Hageman Factor	5q33-qter	76	2-3	29-40 (380-530)
XIII	6p24-25	320		10 (30)

*mmol/L

che la via estrinseca (**Figura 1.13**). Tuttavia, in alcune condizioni patologiche, come le dislipidemie o infezioni batteriche la via intrinseca diviene rilevante e conduce a processi trombotici. La via intrinseca richiede i fattori VIII, IX, XI e XII, la precallicreina (PK), il kininogeno ad elevato peso molecolare (HMWK), così come gli ioni calcio e i fosfolipidi liberati dalle piastrine per condurre alla attivazione del fattore X (vedi **Tabella 1.3**). La via intrinseca è attivata quando la PK e HMWK, i fattori XI e XII sono esposti ad una superficie caricata negativamente durante la cosiddetta "fase di contatto" con fosfolipidi (primariamente la fosfatidiletanolamina, PE) di lipoproteine circolanti, quali i chilomicroni, VLDL e LDL ossidate. Questa è la base del ruolo della iperlipidemia nella promozione di stati protrombotici e nello sviluppo della aterosclerosi. L'attivazione per contatto della via intrinseca può avvenire sulla superficie dei batteri, e attraverso l'interazione con cristalli di urato, acidi grassi, protoporfirine, amiloide beta, e altre proteine amiloidi con anomalie del ripiegamento (misfolded) e omocisteina. L'assemblaggio dei componenti della fase di contatto porta alla conversione della precallicreina a callicreina che a sua volta attiva il fattore XII in XIIa. Il fattore XIIa attiva il fattore XI ad XIa e idrolizza la precallicreina a callicreina creando una cascata di attivazione reciproca. La callicreina agisce sul HMWK portando al rilascio di bradichinina, che è un potente vasodilatatore. In presenza di calcio, il fattore XIa attiva il fattore IX a IXa. Il fattore IX è un proenzima che contiene residui di γ-carbossiglutammato vitamina K-dipendenti la cui attività di proteasi serinica è attivata a seguito del legame del calcio ai residui di γ-carbossiglutammato. Numerose proteasi seriniche della cascata coagulativa (II, VII, IX, and X) assieme alla proteina C ed S, sono proenzimi che contengono γ-carbossiglutammato e sono pertanto vitamina K-dipendenti (**Tabella 1.4**). La funzione della vitamina K è quella di mantenere concentrazioni normali di questi fattori che sono sintetizzati dal fegato come precursori inattivi. La loro conversione nelle forme attive richiede una modificazione post-traduzionale (carbossilazione) di specifici residui di glutammato, che divengono γ-carbossiglutammato, ad opera della carbossilasi che richiede la vitamina K come cofattore (**Figura 1.17**). I residui di γ-carbossiglutammato sono potenti chelanti del calcio che consente poi l'interazione con molecole cariche negativamente, quali i fosfolipidi e la successiva cascata di eventi proteolitici. Durante la reazione di carbossilazione la forma di idrochinone ridotto della vitamina K è convertito nella forma 2,3 epossidica. La rigenerazione della forma idrochinonica richiede una reduttasi e questa reazione è inibita dai cumarolici, che sono pertanto utilizzati in terapia come potenti anticoagulanti (**Figura 1.17**). Il fattore IXa taglia un legame interno arginina-isoleucina del fattore X attivandolo a fattore Xa. L'attivazione del fattore Xa richiede l'assemblaggio del complesso tenasico formato dal calcio e dai fattori VIIIa, IXa e X sulla superficie delle piastrine attivate che espongono fosfatidilserina e fosfatidilinositolo. L'esposizione di questi fosfolipidi consente la formazione del complesso tenasico. Il ruolo del fattore VIII nel processo è quello di un recettore per i fattori IXa e X. L'attivazione del fattore VIII avviene in presenza di minime quantità di trombina, e quando la concentrazione di quest'ultima aumenta il fattore VIIIa viene proteolizzato e inattivato dalla trombina stessa attraverso l'attivazione della proteina C da parte del complesso trombina-trombomodulina. Questa duplice azione della trombina sul fattore VIII, iniziale attivazione e successiva inattivazione modula la formazione del complesso tenasico e controlla la cascata coagulativa.

Tabella 1.4. Classificazione funzionale dei fattori della coagulazione.

Zimogeni di proteasi seriniche	Cofattori	Regolatori/altre proteine
Fattori II, VII, IX, X, XI, XII	Fattori III, V, VIII	Fattore di von Willebrand, proteina C, proteina S, trombomodulina, antitrombina

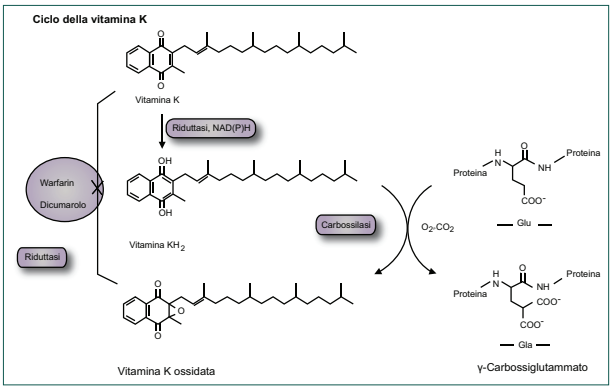

Figura 1.17. Meccanismo della gamma carbossilazione mediata dalla vitamina K.

La via estrinseca

Il fattore Xa è il punto di raccordo sul quale convergono le vie intrinseca ed estrinseca della cascata coagulativa (**Figura 1.13**). La via estrinseca inizia nella sede di un danno tissutale in risposta al rilascio del fattore tissutale (fattore III, TF), ed è pertanto nota anche come via del fattore tissutale. Quest'ultimo è un cofattore che agisce nella attivazione del fattore X catalizzata dal fattore VIIa il quale è una serina proteasi con residui di γ-carbossiglutammato che attiva il fattore X nello stesso modo del fattore IXa nella via intrinseca. L'attivazione del fattore VII avviene attraverso l'azione della trombina o del fattore Xa creando pertanto un ponte fra le due vie coagulative. Una ulteriore connessione fra le due vie è rappresentata dalla capacità del fattore tissutale e del fattore VIIa di attivare il fattore IX. La formazione del complesso fra fattore VIIa e il fattore tissutale è considerato il punto chiave della cascata coagulativa. Un inibitore principale della via estrinseca è rappresentato dall'inibitore della coagulazione associato alla lipoproteina (LACI, noto anche come "extrinsic pathway inhibitor, EPI" o, soprattutto nella letteratura recente, "tissue factor pathway inhibitor, TFPI") che lega in modo specifico il complesso fattore tissutale-fattore VIIa-Ca^{2+}-Xa. LACI è composto da tre domini inibitori delle proteasi in tandem. Il dominio 1 lega il fattore Xa e il dominio 2 lega il fattore VIIa solo in presenza del fattore Xa.

Attivazione della protrombina a trombina

Come detto, il punto in comune delle due vie è l'attivazione del fattore X a fattore Xa. Il fattore Xa attiva la protrombina (fattore II) a trombina (fattore IIa) che a sua volta converte il fibrinogeno in fibrina. L'attivazione della trombina avviene sulla superficie delle piastrine attivate e richiede la formazione del complesso protrombinasi formato da fosfolipidi piastrinici, fosfatidilinositolo e fosfatidilserina, Ca^{2+}, i fattori Va e Xa e la protrombina. Il fattore V è un cofattore nella formazione del complesso protrombinasi e svolge un ruolo simile al fattore VIII nella formazione del complesso tenasico. Come nel caso del fattore VIII, anche il fattore

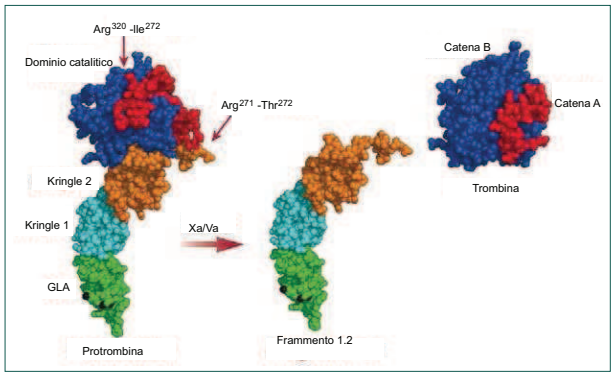

Figura 1.18. Attivazione della protrombina (modelli dalle strutture PDB 2PF2, 1HAG, 1A0H, e 1HAI). Sono mostrati i domini GLA, "kringle" e quello catalitico. Gli ioni calcio sono mostrati in nero. Il taglio da parte dei fattori X e V attivati rilascia la trombina formata da una piccola catena A unita da un ponte disolfuro alla catena B catalitica attiva, dal resto della molecola, frammento 1.2 (Modelli molecolari costruiti con il programma PyMol).

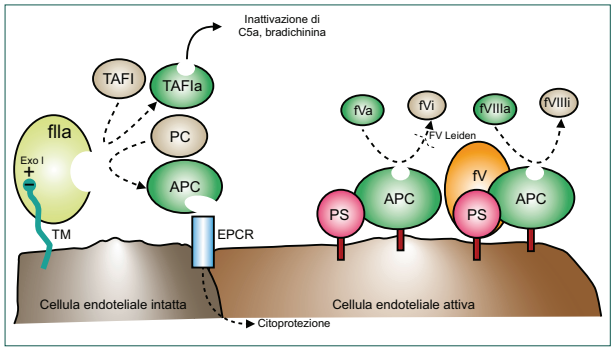

Figura 1.19. Azione anticoagulante della proteina C e della proteina S. La trombomodulina (TM) espressa sull'endotelio intatto, si lega velocemente alla trombina (fIIa) che taglia preferenzialmente la proteina C e l'inibitore della fibrinolisi attivabile dalla trombina (thrombin activatable fibrinolysis inhibitor, TAFI) attivandoli. La proteina C attivata (APC) svolge una azione anti-infiammatoria attraverso il recettore endoteliale della proteina C (EPCR), innescando segnali citoprotettivi intracellulari. Anche TAFIa esercita una azione anti-infiammatoria degradando il fattore del complemento C5a e la bradichinina. APC si lega alla proteina S (PS) e inattiva il fattore V attivato e il fattore VIII attivato. L'inattivazione del fattore Va è ritardata nel caso di presenza di una mutazione del fattore V (fattore V Leiden). L'inattivazione del fattore VIIIa è potenziata dal fattore V.

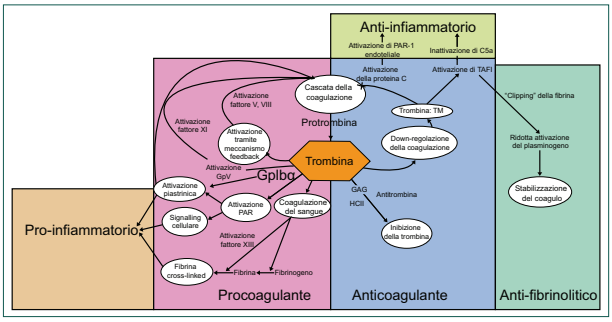

Figura 1.20. Ruoli molteplici della trombina. Questa proteasi serinica può svolgere azione procoagulante, anticoagulante, antifibrinolitica e sia pro- che anti-infiammatoria.

V è attivato a fattore Va da minime quantità ed è inattivato da alte concentrazioni di trombina. Il fattore Va si lega a recettori specifici sulla superficie di piastrine attivate e forma un complesso con la protrombina e il fattore Xa.

La protrombina è una proteina a singola catena di 72 kDa che contiene 10 residui di γ-carbossiglutammato nella regione amino terminale. All'interno del complesso protrombinasi, la protrombina è tagliata in corrispondenza dell'arginina 271 e dell'arginina 320 dal fattore Xa. Il dominio catalitico (trombina) di peso molecolare 36.6 kDa è rilasciato dal resto della molecola (frammento di protrombina 1.2) (**Figura 1.18**). Oltre al suo ruolo fondamentale nella formazione di fibrina nel coagulo la trombina svolge un ruolo importante nella regolazione della coagulazione. La trombina si combina alla trombomodulina presente sulla superficie delle cellule endoteliali a formare un complesso che converte la proteina C in proteina C attivata (Ca). Il cofattore proteina S e la proteina Ca degradano i fattori Va e VIIIa, limitandone l'attività nella cascata coagulativa (**Figura 1.19**). La trombina si lega anche a recettori associati alla proteina G, chiamati recettori attivati dalle proteasi (PARs) e specificamente PAR-1, -3 e -4 (**Figura 1.15**). I PARs utilizzano un meccanismo unico per convertire il risultato di un clivaggio proteolitico extracellulare nella trasmissione di segnale intracellulare. Le cascate di segnale attivate dai PARs dopo interazione con la trombina sono numerose e portano al rilascio di citochine (IL-1 e IL-6), aumentata secrezione della molecola di adesione intercellulare (ICAM-1) e della molecola di adesione vascolare-1, (VCAM-1). Il segnale indotto dalla trombina produce anche aumento della attivazione piastrinica e dell'adesione dei leucociti. La trombina attiva anche l'inibitore della fibrinolisi attivabile dalla trombina (thrombin-activatable fibrinolysis inhibitor,TAFI), modulando la fibrinolisi (**Figura 1.19**). TAFI è anche noto come carbossipeptidasi U che rimuove le lisine C-terminali dalla fibrina parzialmente degradata. Questo causa una ridotta attivazione del plasminogeno e la velocità di dissoluzione del coagulo.

La trombina è stata definita molecola camaleonte, svolgendo molteplici azioni, da procoagulante ad anticoagulante, antifibrinolitica e sia pro- che anti-infiammatoria (**Figura 1.20**).

Inibitori fisiologici della coagulazione

La coagulazione è un meccanismo finemente controllato che tende a localizzare il coagulo nel sito della lesione, prevenendo così una reazione a catena (questa potrebbe provocare un'estesa e mortale coagulazione, basti pensare che la coagulazione di 1 ml di sangue produce trombina in grado di far coagulare il fibrinogeno presente in 3 litri di sangue). Gli inibitori fisiologici più importanti sono la antitrombina, il cofattore eparinico II (HCII), le proteine C ed S ed il TFPI. Oltre a questi sono rilevanti la alfa 1-antitripsina, il C1 inattivatore e l'alfa2-macroglobulina.

L'attività della trombina, che svolge un ruolo centrale nella coagulazione è strettamente regolata da quattro inibitori specifici, l'antitrombina (nota anche come antitrombina III) è il più importante perché inibisce anche le attività dei fattori IXa, Xa, XIa e XIIa, plasmina, e callicreina. L'antitrombina è una glicoproteina di 58 kDa, sintetizzata a livello epatico. Appartiene alla famiglia delle cosiddette serpine (serine-protease inhibitors) e forma un complesso stechiometrico, equimolecolare ed irreversibile con la trombina ed alcune altre proteasi seriniche, rendendole inattive. L'interazione fra trombina e antitrombina avviene anche spontaneamente, ma l'attività dell'antitrombina è potenziata dalla presenza di eparano e eparansolfato sulla superficie delle cellule endoteliali (o da eparina somministrata terapeuticamente) che si legano ad un sito specifico della antitrombina modificandone la conformazione con conseguente aumento della affinità, di oltre tre ordini di grandezza, per la trombina e per gli altri substrati. Questo è il meccanismo di controllo principale dell'attivazione della via intrinseca. L'attività della

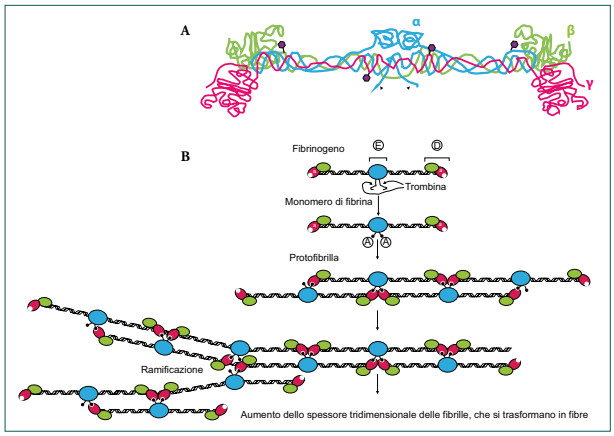

Figura 1.21. A) Struttura del fibrinogeno. La catena alfa è evidenziata in blu, la beta in verde e la gamma in rosa; le punte di freccia indicano i punti di clivaggio sulla catena alfa. Gli ioni calcio legati alle catene gamma sono rappresentati come sfere color porpora; B) Fasi iniziali della polimerizzazione della fibrina. I noduli centrali contengono le porzioni amino terminali delle sei catene (α, β, γ)2 e sono riferite come regioni "E" che sono fiancheggiate da due eliche che terminano con le regioni "D". Dopo il taglio del fibrinopeptide "A" da parte della trombina, i nuovi siti di polimerizzazione "A" si legano alle tasche di polimerizzazione "a" che appartiene alla catena gamma del fibrinogeno. Quindi i monomeri di fibrina si allineano in modo semi-sfasato a formare lunghe protofibrille con due filamenti e ponti con altre fibrille si formano sporadicamente e contribuiscono alla formazione della rete di fibrina.

trombina è anche inibita dal cofattore eparinico II, dalla α_2-macroglobulina, e dalla α1-antitripsina, quest'ultima è uno dei più potenti inibitori delle proteasi seriniche.

Formazione della fibrina

Il fibrinogeno (fattore I) è formato da tre paia di polipeptidi $([A\alpha][B\beta][\gamma])_2$ (**Figura 1.21**) Le 6 catene sono legate covalentemente vicino all'aminoterminale attraverso ponti disolfuro. Le porzioni A e B delle catena Aα e Bβ rappresentano i fibrinopeptidi A e B. Le regioni dei fibrinopeptidi del fibrinogeno contengono numerosi residui di glutammato e aspartato che conferiscono una carica altamente negativa a questa regione e facilitano la solubilità del fibrinogeno nel plasma. La trombina attivata è una proteasi serinica che idrolizza il fibrinogeno in corrispondenza dei 4 legami arginina-lisina tra il fibrinopeptide e le porzioni a e b della proteina. Il rilascio trombina-mediato dei fibrinopeptidi genera monomeri di fibrina con la struttura $(\alpha\beta\gamma)_2$. Questi monomeri aggregano spontaneamente in strutture regolari formando un debole coagulo di fibrina (**Figura 1.21**). La trombina converte il fattore XIII in XIIIa, una transglutaminasi altamente specifica che introduce legami crociati (cross-links) composti da legami covalenti tra l'azoto amidico delle glutamine e il gruppo ε-aminico delle lisine dei monomeri di fibrina. Questi legami crociati formano una robusta rete fibrinica che rinsalda il coagulo.

Fibrinolisi e dissoluzione del coagulo

La fibrinolisi è la dissoluzione del coagulo che si è formato dopo che questo ha svolto la sua funzione. La plasmina, una proteasi serinica che circola come proenzima inattivo, plasminogeno, degrada i coaguli di fibrina. Il plasminogeno è una glicoproteina a singola catena di peso molecolare 88 kDa, sintetizzata nel fegato. La forma nativa ha come amminoacido N-terminale l'acido glutammico (Glu-plasminogeno), e viene facilmente convertita (mediante limitata digestione plasminica) in Lys-plasminogeno (peso molecolare 83.000 Da), in cui l'ultimo aminoacido è rappresentato dalla lisina. Il plasminogeno contiene numerosi siti di legame che gli permettono di interagire con il fibrinogeno e la fibrina e viene pertanto incorporato nel coagulo durante la sua formazione. In condizioni normali, solo circa il 60% del plasminogeno circolante è disponibile per essere attivato. Il rimanente è legato, seppure reversibilmente, ad una glicoproteina circolante ricca di istidina, la cosidetta "glicoproteina ricca di istidina", che impedisce il legame alla fibrina. La plasmina circolante è rapidamente inibita dalla α_2-antiplasmina. Il plasminogeno si lega sia al fibrinogeno che alla fibrina. L'attivatore tissutale del plasminogeno (tPA) e, in grado minore, l'urochinasi, sono proteasi seriniche che convertono il plasminogeno in plasmina. Il tPA inattivo è rilasciato dalle cellule dell'endotelio vascolare a seguito di una lesione, si lega alla fibrina e quindi viene attivato. L'urochinasi è prodotta come precursore, pro-urochinasi, dalle cellule dei tubuli renali e da fibroblasti, e da cellule epiteliali e macrofagi. Il tPA attivato trasforma il plasminogeno in plasmina che poi digerisce la fibrina. Sono noti almeno quattro inibitori di tPA, i più importanti sono gli inibitori di tipo 1 e 2 (PAI-1 e PAI-2). PAI-1 (plasminogen activator inhibitor 1) è una glicoproteina a singola catena con peso molecolare di circa 52 kDa. Appartiene alla famiglia delle serpine. Forma complessi covalenti con tPA a singola e a doppia catena e con uPA a doppia catena (tcu-PA). La produzione di PAI-1 è modulata da vari fattori di crescita: trombina, IL-1, TNF, TGF-beta ne aumentano la sintesi. PAI-2 (plasminogen activator inhibitor 2) è glicosilato, ha un peso molecolare di circa 70 kDa. Non è presente normalmente nel plasma, ma compare durante la gravidanza ed è di derivazione placentare. È una serpina ed inibisce il t-PA e l'u-PA a doppia catena.

La plasmina è in grado di tagliare ponti peptidici arginina-lisina di molte proteine, compreso il fibrinogeno, la fibrina non stabilizzata e la fibrina insolubile, stabilizzata dal fattore XIII della coagulazione. La degradazione del fibrinogeno e della fibrina avviene

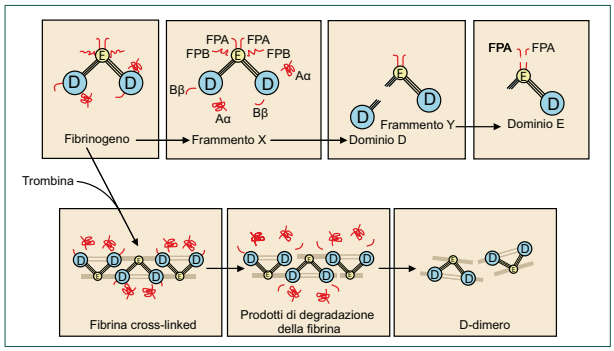

Figura 1.22. Degradazione del fibrinogeno e della fibrina "cross-linked" da parte della plasmina. La plasmina inizialmente taglia le regioni C terminali delle catene α e β all'interno del dominio D del fibrinogeno rilasciando i frammenti Aα e Bβ. Inoltre, un frammento contenente il fibrinopeptide B (FPB) dalla regione N-terminale della catena β viene rilasciato, dando luogo al frammento intermedio X. Successivamente, la plasmina taglia le tre catene polipeptidiche di connessione fra i domini D ed E dando origine ai frammenti D, E ed Y. Nel pannello inferiore è riportata la degradazione della fibrina "cross-linked" da parte della plasmina che inizialmente taglia la regione C-terminale delle catene a e b nel dominio D. Successivamente, alcuni dei polipeptidi di connessione tra i domini D ed E sono tagliati. La fibrina è solubilizzata attraverso l'idrolisi di ulteriori legami peptidici all'interno della porzione centrale dando origine ai D-dimeri.

a tappe (**Figura 1.22**). La degradazione del fibrinogeno comprende: 1- rimozione di parte delle catene laterali, con formazione di tre frammenti (frammenti α, β e un frammento grande X); 2 - degradazione asimmetrica del frammento X, a livello di una regione di connessione a un frammento D (100 kDa) ed un frammento Y (150 kDa); 3 - il frammento Y è un prodotto intermedio e viene successivamente degradato con formazione di un frammento D e frammento E (50 kDa), entrambi espressione delle singole regioni globulari del fibrinogeno. La degradazione della fibrina non stabilizzata è pressoché identica alla degradazione del fibrinogeno. La degradazione della fibrina stabilizzata dal fattore XIIIa è più lenta e difficile e non produce frammenti X ed Y. Si ha una iniziale rimozione delle catene laterali con la formazione di polimeri ad alto peso molecolare. Quindi, in seguito a digestione più prolungata, si formano dei polimeri intermedi, contenenti più domini globulari (fibrin degradation products). Infine, in seguito a tagli proteolitici successivi a livello delle regioni di connessione, si formano frammenti solubili DD/E (**Figura 1.18**). La misura del D-dimero è utilizzata nella pratica clinica nella diagnosi della malattia trombo embolica.

La componente corpuscolare del sangue

Le cellule del sistema ematopoietico hanno origine nel midollo osseo da un ristretto pool di cellule staminali attraverso progressive tappe di maturazione e proliferazione cellulare. Queste cellule quindi, passano nel torrente circolatorio dove svolgono la loro funzione fisiologica anche attraverso la migrazione nei tessuti periferici o la migrazione nel sistema specializzato di vasi linfatici.

Tutte le cellule del sangue, inclusi i globuli rossi che trasportano l'ossigeno, le piastrine

che favoriscono la formazione del coagulo ed i leucociti che costituiscono il sistema di difesa naturale ed immunitario, derivano da un'unica tipo cellulare, le cellule ematopoietiche staminali midollari, che hanno quindi caratteristiche di cellule staminali pluripotenti.

In base a specifiche caratteristiche morfofunzionali, le cellule del sangue possono quindi essere suddivise in tre gruppi principali: globuli rossi (o eritrociti), globuli bianchi (o leucociti) e piastrine (o trombociti).

Gli eritrociti, o globuli rossi, contengono grandi quantità di emoglobina e sono coinvolti principalmente nel trasporto di ossigeno e di anidride carbonica. Svolgono la loro funzione esclusivamente all'interno del sistema vascolare e sono presenti nella concentrazione di circa 4.5 milioni per mm^3 di sangue nella donna, e circa 5 milioni per mm^3 di sangue nell'uomo. I globuli rossi hanno forma di disco biconcavo, con diametro pari a circa 7µm, sono privi di nucleo e di organuli cellulari. Sulla loro membrana sono presenti particolari proteine antigeniche, che permettono di distinguere diversi gruppi sanguigni.

I leucociti, o globuli bianchi, responsabili della risposta immunitaria, sono presenti con diversi tipi che si distinguono per la forma del nucleo e l'affinità ai coloranti: granulociti (neutrofili, eosinofili e basofili), monociti, linfociti T e B. Svolgono un ruolo importante nel sistema di difesa e immunitario dell'organismo e, pertanto, agiscono principalmente al di fuori dei vasi ematici ovvero nei tessuti; hanno infatti la capacità di spostarsi negli spazi interstiziali e nei vasi del sistema linfatico. I leucociti sono presenti nella concentrazione di 4000-9000 cellule per mm^3 di sangue. I granulociti e i monociti, dotati di attività fagocitaria, possono eliminare particelle e microorganismi estranei e sono coinvolti nei meccanismi aspecifici di difesa (infiammazione). I linfociti sono i responsabili della risposta immunitaria specifica.

Le piastrine sono frammenti cellulari di forma irregolare e di diametro pari a 1-4µm, presenti nel sangue in una concentrazione che va da 150.000 a 400.000 per mm^3 di sangue. Svolgono un ruolo cruciale nel controllo della coagulazione (emostasi) tamponando le lesioni delle pareti dei vasi sanguigni e contribuendo all'attivazione della cascata della coagulazione.

Le alterazioni biochimiche della trasformazione neoplastica delle cellule del sangue

Le patologie neoplastiche del sistema emopoietico (leucemie e linfomi) costituiscono un gruppo piuttosto eterogeneo di malattie neoplastiche, che sono attualmente classificate dall'Organizzazione Mondiale della Sanità (World Health Organization; WHO), non più solo in base a parametri morfologici e clinici, ma anche in relazione ad alterazioni della struttura (o della quantità) di proteine di membrana o intracellulari, ad alterazioni della struttura di cromosomi o di specifici geni. Sono infatti state identificate, in un numero sempre crescente di leucemie e linfomi, specifiche aberrazioni cromosomiche e/o mutazioni geniche che alterano la normale funzione o espressione proteica, conferendo al clone neoplastico un vantaggio di crescita rispetto alle cellule emopoietiche normali. Appare quindi chiaro che la trasformazione neoplastica delle cellule del sistema emopoietico è legata da una parte all'accumulo di danno genotossico e dall'altra all'incapacità di riparare da parte di specifici sistemi proteici tale danno. È da notare, tuttavia, che alcune delle mutazioni riscontrate nei tumori emopoietici rendono intrinsecamente la cellula più resistente all'apoptosi, riducendo così le potenzialità di protezione verso il danno genotossico da parte di questi sistemi. Non è chiaro quale è la causa eziologica che induce i danni genomici nelle cellule emopoietiche, tuttavia, alcune di esse, ed in particolare quelle della serie linfocitaria, vanno fisiologicamente incontro, durante il differenziamento, a profondi rimaneggiamenti della struttura del DNA genomico necessari alla diversificazione del repertorio di immunoglobuline o di recettori delle cellule T (TCR). Questi processi sono molto complessi (si rimanda a testi specifici di immunologia per una trattazione completa) e comportano escissione

di porzioni piuttosto lunghe del genoma in corrispondenza dei geni delle immunoglobuline o del TCR con ricombinazione intracromosomica del DNA per la "maturazione" di questi geni o, nella fase di incremento dell'affinità di legame per l'antigene, consistono nell'aggiunta di nucleotidi "random" in corrispondenza delle sequenze di questi geni che codificano per il sito di legame dell'antigene. Le cellule linfocitarie, pertanto, durante tutte le fasi della maturazione antigene-dipendente o indipendente sono intrinsecamente esposte ad errori che procurano danni irreversibili del DNA.

La perdita dei meccanismi che normalmente controllano e riparano le mutazioni a carico del DNA possono condurre all'accumulo di mutazioni multiple stabili nel genoma delle cellule patologiche che determinano la trasformazione neoplastica quando il danno è a carico di una serie di geni che controllano le fasi critiche di omeostasi cellulare (proliferazione, apoptosi e differenziamento).

Le più semplici mutazioni sono date dalle **mutazioni puntiformi** che inducono il cambiamento di una singola base con un'altra e ne esistono di due tipi. Le *transizioni* consistono in sostituzioni di una pirimidina con l'altra pirimidina, o di una purina con l'altra purina, mentre le *transversioni* sono date da sostituzioni di pirimidine con purine oppure di purine con pirimidine. Altre mutazioni semplici consistono nell'inserimento o nella delezione di un singolo nucleotide o di un piccolo numero di nucleotidi. Generalmente, le mutazioni a carico di un singolo nucleotide, dette mutazioni puntiformi, non sempre inducono modifica funzionale nella proteina codificata dal gene. In particolare le mutazioni della terza base di un codone spesso non ne alterano la "cornice di lettura" della sequenza nucleotidica e non determinano modificazioni della struttura proteica (*mutazione silente*). Quando la mutazione porta ad una sostituzione amminoacidica nella proteina codificata si parla di *mutazione missenso*. Queste mutazioni possono alterare la funzione proteica quando ricadono in domini proteici funzionali, o quando alterano la struttura secondaria e terziaria delle proteine, modificando così la loro capacità di ripiegamento e di interazione proteina-proteina. Le mutazioni missenso possono dare origine ad una neoplasia con meccanismi differenti, ma quello più frequente è la riduzione della funzione di una proteina implicata nel controllo diretto o indiretto dell'integrità del genoma, come ad esempio la proteina p53, o nella modulazione in senso negativo della crescita cellulare, come ad esempio gli inibitori delle cicline come la CDKNA o CDKNB. Quando causa la comparsa di un codone di stop, la mutazione è detta *nonsenso*, poiché induce il rilascio da parte del ribosoma di un polipeptide incompleto, privo di uno o più domini funzionali, dovuto alla terminazione prematura della traduzione proteica. La mutazione nonsenso si verifica più spesso, però, in seguito alla comparsa di una mutazione di scivolamento della cornice di lettura (**mutazione frameshift**) indotto da inserzione o delezione di un numero di nucleotidi non multipli di tre. Le mutazioni frameshift possono dare origine ad alterazioni proteiche di tipo oncogenico come ad esempio la mutazione che determina nella proteina NPM la creazione di un addizionale segnale di esportazione nucleare che modifica la localizzazione subcellulare della proteina (dal nucleo al citoplasma). A tale mutazione consegue l'acquisizione di caratteristiche trasformanti per le cellule emopoietiche mieloidi.

Anche lunghe inserzioni o delezioni e grossi riarrangiamenti della struttura cromosomica possono causare alterazioni della sequenza o della struttura di alcune proteine intracellulari, che svolgono funzioni cruciali nel controllo della crescita cellullare e determinare la trasformazione neoplastica. Queste mutazioni sono causate da eventi di ricombinazione cromosomica alterata o, per esempio, dall'inserzione di un trasposone, che in genere introduce alcune migliaia di nucleotidi di DNA estraneo nella regione codificante o regolatrice di un gene (**Figura 1.23**).

In generale, la frequenza media con cui una nuova mutazione insorge spontaneamente in un qualunque sito del cromosoma ha un valore compreso tra 10^{-6} e 10^{-11} per ciclo di replicazione. Tuttavia alcuni siti del cromosoma rappresentano dei "punti caldi" caratterizzati da una più elevata frequenza di mutazione, mentre altri siti

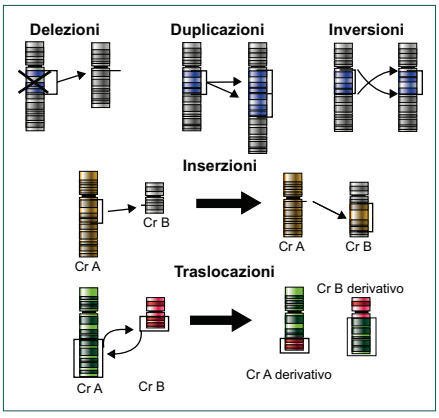

Figura 1.23. Alterazioni cromosomiche nelle patologie neoplastiche ematologiche.

sono caratterizzati da una frequenza di mutazione più bassa della media del restante genoma.

Le alterazioni grossolane dei cromosomi possono essere di tipo quantitativo, cioè acquisizione o perdita di un intero cromosoma, o qualitativo, cioè alterazioni strutturali cromosomiche che coinvolgono lo scambio di materiale tra due o più cromosomi (**Figura 1.23**). Le alterazioni strutturali più comuni sono le **traslocazioni** (indicate con la lettera t), che coinvolgono lo scambio di materiale tra due o più cromosomi. Per effetto della traslocazione quindi, la parte telomerica di uno dei bracci (p o q) di un cromosoma si congiunge con la parte centromerica di un altro (**Figura 1.23**). Le traslocazioni cromosomiche possono "attivare" la trasformazione neoplastica con almeno due meccanismi distinti. Il primo determina la modificazione della struttura del prodotto proteico di un gene importante per un processo cellulare come la trasduzione del segnale o la trascrizione genica. È il caso delle traslocazioni che determinano la fusione tra le sequenze codificanti di due geni disposti con lo stesso orientamento sui rispettivi cromosomi e, cioè, telomero/centromero o viceversa. Per effetto della traslocazione una serie di esoni posti nella parte 5' di un gene si fonde con gli esoni terminali posti, cioè, al 3' di un altro gene localizzato sulla porzione dell'altro cromosoma coinvolto nella traslocazione. Il punto di fusione tra le sequenze di DNA dei due geni è generalmente contenuto negli introni dei due geni, pertanto dopo lo splicing nel RNA messaggero maturo, le sequenze codificanti (esoniche) di un gene sono direttamente giustapposte a quelle terminali dell'altro gene. È importante notare che la cornice di lettura di entrambi i geni viene mantenuta nel gene di fusione e le proteine ibride prodotte contengono, quindi, alcuni dei domini proteici di entrambe le proteine. È questo il caso del primo gene di fusione scoperto nella storia della medicina derivato dalla traslocazione tra i cromosomi 9 e 22 [traslocazione t(9;22)], la quale determina la fusione tra i geni BCR ed ABL (quest'ultimo codificante per una proteina ad attività tirosino chinasica) con la produzione di una proteina ibrida BCR/ABL ad attività tirosino chinasica costitutivamente attivata e determinazione della Leucemia Mieloide Cronica (LMC). I meccanismi che determinano la trasformazione neoplastica da parte di questa

proteina ibrida sono stati studiati in dettaglio e costituiscono un importante modello per capire come la alterazione di una proteina possa avere conseguenze così "catastrofiche" sulla omeostasi cellullare da determinare la trasformazione leucemica e, pertanto, saranno descritti in dettaglio in questo capitolo. Un gene di fusione che codifica per una proteina ibrida può avere anche origine da **inversioni cromosomiche paracentriche** (indicate dalla sigla inv), che si verificano quando in un singolo cromosoma le due porzioni telomeriche si interrompono e la porzione centrale, che comprende il centromero, si inverte ruotando ed i due bracci cromosomici si riuniscono alle regioni telomeriche opposte; come esempio si può citare l'inversione paracentrica del cromosoma 16 [inv(16)], che genera la proteina di fusione CBFβ/SMMHC, la quale determina la trasformazione leucemica in un sottogruppo di pazienti con Leucemia Mieloide Acuta.

Le traslocazioni cromosomiche determinano trasformazione di cellule del sistema emopoietico anche senza alterare la struttura di specifiche proteine. È questo il caso in cui per effetto della traslocazione la sequenza di un intero proto-oncogene viene a trovarsi nelle vicinanze delle regioni regolative dei geni delle immunoglobuline o del TCR (**Figura 1.24**). Conseguentemente, le cellule emopoietiche durante il differenziamento linfoide inducono il programma di attivazione della trascrizione dei geni delle immunoglobuline aumentando i livelli nucleari di fattori di trascrizione che legano specificamente il promotore di questi geni. In tal modo si attiva in queste cellule anche la trascrizione sul cromosoma derivativo del gene che viene a trovarsi, per effetto della traslocazione, sotto il controllo del promotore delle immunoglobuline o del TCR. Si ha come conseguenza ultima la produzione in elevate quantità di una proteina normalmente non espressa nelle cellule linfoidi che determina la trasformazione leucemica. Un esempio ben conosciuto di questo meccanismo è costituito dalla traslocazione t(8;14), che pone il gene cMyc sotto il controllo trascrizionale del promotore del gene della catena pesante delle immunoglobuline. Il gene cMyc codifica per una proteina che promuove la divisione cellulare e, quando regolato dal promotore delle immunoglobuline, causa la cosiddetta leucemia/linfoma di Burkitt, caratterizzata da un'elevatissima frazione di crescita cellulare.

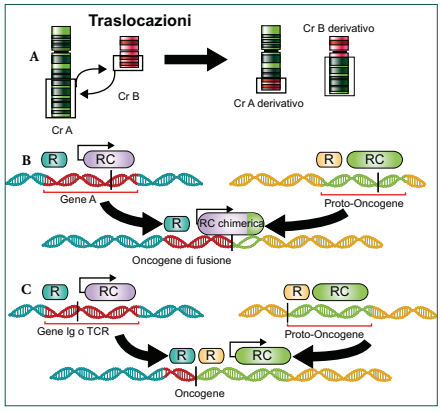

Figura 1.24. Le due tipologie di traslocazioni cromosomiche. A) Rappresentazione schematica di una traslocazione cromosomica bilanciata; B) Traslocazione con giunzione tra le sequenze codificanti di due geni e formazione di un gene di fusione; C) Traslocazione con fusione tra i loci genici e scambio delle regioni di regolazione della trascrizione senza alterazioni delle sequenze codificanti.(R, regione regolatoria; RC, regione codificante, Ig, geni codificanti per le immunoglibuline; TCR, geni codificanti per il recettore dei linfociti T).

Alterazioni grossolane della struttura genica possono essere costituite anche da **delezioni** (indicate con la sigla del), che determinano la perdita di lunghe sequenze del DNA cromosomico nelle cellule neoplastiche. In questo caso i meccanismi della trasformazione neoplastica possono essere vari. Si può verificare la formazione di un gene di fusione, quando vengono perse nel cromosoma derivativo le sequenze che separano due geni disposti nello stesso orientamento su di un braccio cromosomico. È questo il caso della delezione del braccio corto del cromosoma 4 (del4q12) che determina la formazione del gene di fusione FIP1L1/PDGFRA che codifica per una proteina ibrida in cui l'attività tirosino chinasica del recettore per il fattore di crescita PDGF-alfa (Platelet derived Growth Factor) è costitutivamente attivata determinando così la leucemia eosinofilica cronica. Alternativamente, la delezione cromosomica può determinare la perdita di uno o più geni contenuti sulla porzione del cromosoma che viene deleta; in questo caso si può determinare la riduzione nella quantità della proteina (o delle proteine) codificata dal gene (o dai geni) deleto/i. Questa situazione è definita **aploinsufficienza allelica** e consiste nell'incapacità dell'allele genico rimasto nel genoma cellulare di far fronte alle esigenze cellulari per una specifica proteina. Un esempio di questo meccanismo è fornito dalla delezione del braccio corto del cromosoma 5 (del5q-), che si associa con una specifica forma di sindrome mielodisplastica denominata, appunto, Sindrome del 5q-. In questi pazienti la aploinsufficienza di un gene che codifica per una proteina ribosomiale, la RPS14, determina la carenza nella funzione dei ribosomi con conseguente riduzione nella produzione di alcune proteine, come la MDM2 che regola la funzione di p53. Oltre alle delezioni di lunghe sequenze cromosomiche, evidenziabili direttamente al microscopio mediante citogenetica convenzionale, lo sviluppo di tecniche di genomica comparativa basata su ibridazione e genotipizzazione degli SNP (Polimorfismi di Singoli Nucleotidi), ha dimostrato la presenza di microdelezioni cromosomiche o, alternativamente, di microinserzioni in pazienti affetti da patologie onco-ematologiche. Queste alterazioni possono interessare anche le regioni codificanti di un gene portando alla produzione di proteine alterate per perdita di un dominio, o, più frequentemente, per inserzione di una sequenza anomala. È questo il caso della duplicazione di un segmento esonico del gene FLT3 che codifica per il recettore di un fattore di crescita dei progenitori mielopoietici, ovvero il ligando FLT3 (FLT3-L). Per effetto della duplicazione che coinvolge sequenze esoniche che codificano per il dominio juxtamembrana della proteina recettoriale si determina una modificazione della struttura tridimensionale della proteina ed una perdita dell'autoinibizione della funzione tirosino chinasica della parte intracellulare del recettore, che normalmente è presente nella proteina in assenza del ligando extracellulare. Pertanto l'inserzione intragenica di queste sequenze duplicate in tandem (**Internal Tandem Duplication**) determina l'attivazione costitutiva della proteina recettoriale che si associa a forme particolarmente aggressive di leucemia mieloide acuta. Nella **Tabella 1.5** sono riassunti i principali meccanismi che alterano il DNA genomico e che possono determinare una neoplasia del sistema emopoietico.

Oncogeni ed oncosoppressori nella patogenesi leucemica

Se i meccanismi che possono alterare il materiale genetico sono, come è stato descritto, molto vari, altrettanto numerose sono le categorie di geni la cui funzione è alterata dai meccanismi sovra descritti (vedi **Tabella 1.5**). È da notare che spesso non è sufficiente una sola alterazione e quindi la modificazione della funzione di una singola proteina per determinare la trasformazione neoplastica del sistema emopoietico, ma sono in genere necessarie più mutazioni, acquisite in sequenza in un clone cellulare, per avere il fenotipo neoplastico completo.

L'esaustiva conoscenza delle alterazioni della struttura delle proteine oncogeniche e della loro funzione è essenziale per ricostruire la patogenesi a livello molecolare delle principali categorie di neoplasie ematologiche. Le ricadute pratiche di ciò sono estremamente importanti: numerosi studi hanno dimostrato che la prognosi, e cioè il comportamento clinico della malattia, è correlata alla patogenesi molecolare ed è pertanto possibile

Tabella 1.5. Principali meccanismi che alterano il DNA genomico e che possono determinare una neoplasia del sistema emopoietico.

Mutazione genomica	Alterazioni nella proteina corrispondente	Meccanismo oncogenico	Proteina alterata	Esempi
Mutazioni puntiformi	Sostituzione di singolo aminoacido	Inattivazione oncosoppressore	p53	Linfomi Non Hodgkin Mielomi Leucemia Linfatica Cronica Sindromi Mielodisplastiche Leucemia Mieloide Acuta
			DNMT3A, CEBPα, AML-1, IDH1-2	Leucemia Mieloide Acuta
			NOTCH1	Leucemia Linfoide Acuta
	Sostituzione di singolo aminoacido	Attivazione Oncogene	K-Ras	Sindromi Mielodisplastiche Mielomi
			Jak-2	Trombocitemia essenziale Policitemia vera Mielofibrosi Idiopatica
			c-Kit	Leucemia Mieloide Acuta
	Riduzione della espressione intracellulare	Alterazione della funzione del promotore genico e della sua affinità per fattori di trascrizione	Bcl-6	Linfoma non Hodgkin diffuso a grandi cellule
Inserzioni nucleotidiche	Proteina troncata	Alterazione della posizione intracellulare	NPM	Leucemia Mieloide Acuta
Internal Tandem Duplication	Duplicazione di una sequenza aminoacidica	Modifica struttura terziaria	FLT-3	Leucemia Mieloide Acuta
Traslocazione Cromosomica con fusione genica	Fusione *in frame* tra due geni in corrispondenza di sequenze codificanti	Produzione di una proteina di fusione con attivazione del loro potenziale oncogenico	BCR/ABL	Leucemia Mieloide Cronica Leucemia Linfoide Acuta
			PML/RARa	Leucemia Promielocitica Acuta
			AML/ETO	Leucemia Mieloide Acuta
	Fusione tra due locus genici con sostituzione di promotore	Iperproduzione di una proteina normalmente non espressa nel tipo cellullare	BCL2	Linfoma non Hodgkin follicolare
			Ciclina D-2	Linfoma non Hodgkin mantellare
			c-Myc	Linfoma di Burkitt

stratificare i malati sulla base della caratterizzazione genetica adattando l'intensità della cura ad essa. La conoscenza della patogenesi molecolare, ed in particolare la struttura delle proteine oncogeniche, ha consentito lo sviluppo di una nuova generazione di farmaci antineoplastici che sono appunto denominati "a bersaglio molecolare" e che hanno mostrato elevata efficacia nella terapia dei tumori del tessuto emopoietico.

I geni implicati nello sviluppo di un tumore emopoietico appartengono a due principali categorie: oncogeni e oncosoppressori. Gli **onco-**

geni codificano per una proteina che, in seguito a mutazioni attivanti la funzione del prodotto genico (es. la funzione enzimatica per i geni che codificano per proteine ad attività tirosino chinasica), determinano o promuovono la crescita neoplastica; gli oncogeni sono quindi geni mutati che producono una proteina anomala capace di stimolare la divisione e la proliferazione cellulare, anche in assenza di stimoli che promuovono la crescita in condizioni normali. I **geni oncosoppressori** codificano per una proteina la cui mancanza di funzione, per effetto di una mutazione, o di una riduzione di espressione intracellulare, determina la trasformazione neoplastica. Si tratta, pertanto, di geni che in condizioni normali codificano per proteine che direttamente o indirettamente controllano in senso negativo il ciclo cellulare o attivano processi apoptotici ed altre funzioni chiave per la stabilità cellulare. Una più corretta classificazione delle proteine coinvolte nella trasformazione neoplastica delle cellule del sistema emopoietico prevede il loro raggruppamento in categorie funzionali. Pertanto, si riconoscono le seguenti categorie (**Tabella 1.6**):

- Recettori di fattori di crescita
- Proteine della trasduzione del segnale
- Proteine del ciclo cellulare
- Fattori di trascrizione
- Proteine che regolano l'apoptosi
- Proteine di regolazione della metilazione genomica
- Proteine dello splicing

I **recettori dei fattori di crescita** costituiscono l'esempio più conosciuto tra gli oncogeni coinvolti nella leucemogenesi. Nell'emopoiesi due classi di recettori per fattori di crescita hanno un ruolo importante: la prima è costituita da recettori che possiedono una intrinseca attività tirosino chinasica (TK). I recettori TK più studiati nelle cellule progenitrici ematopoietiche fanno parte della famiglia di recettori di classe III, caratterizzata da un dominio extracellulare costituito da 5 regioni Ig-like (immunoglobuline-simili) per il legame di un ligando specifico ed un dominio chinasico intracellulare nel quale, oltre ad essere presente una regione catalitica capace di trasferire un gruppo fosfato da una molecola di ATP alla tirosina di una proteina bersaglio, sono anche presenti delle regioni regolatorie. Il legame del ligando esterno al recettore TK regola l'attivazione intracellulare del recettore modificando la sua specificità di substrato, l'affinità e l'attività chinasica. In seguito al legame con il proprio ligando il recettore ad attività TK dimerizza e autofosforila i residui di tirosina. Queste modifiche inducono cambiamenti conformazionali nella regione intracellulare del recettore, che portano all'attivazione del dominio catalitico e il conseguente legame e/o la fosforilazione di proteine trasduttori del segnale. Fanno parte di questa categoria il recettore per il fattore di crescita piastrinico (PDGF) di tipo a e b (PDGFRa e PDGFRb), il recettore per il fattore di crescita delle cellule staminali (SCF) ovvero il recettore cKIT o il recettore FLT3 che interagisce con il ligando FLT3-L. A carico di tale classe proteica sono state descritte mutazioni che portano alla produzione di un prodotto proteico costitutivamente attivato. Esempi di mutazioni di recettori per fattori di crescita sono costituiti dalle mutazioni del gene cKIT descritte nei pazienti affetti da leucemia mieloide acuta, da mastocitosi sistemica e da leucemia mastocitica; in queste patologie la proteina cKIT può presentare mutazioni a livello di due domini, ovvero la regione juxtamembrana che normalmente regola negativamente l'attivazione del recettore e il dominio di attivazione.

La seconda classe di recettori per fattori di crescita che possono essere alterati nelle neoplasie del tessuto emopoietico non contengono una propria attività enzimatica. Questi recettori sono costituiti da eterodimeri di una catena alfa che riconosce un fattore di crescita specifico e una subunità beta che trasduce il segnale e che è frequentemente condivisa tra diversi sottotipi recettoriali. La subunità beta trasmette il segnale attraverso l'interazione con chinasi intracellulari della famiglia Src e della famiglia Jak che a loro volta attivano mediante fosforilazioni proteine bersaglio (target). Entrambe le classi recettoriali sono in grado di attivare una serie di proteine di trasduzione del segnale strettamente connesse tra loro ed in grado di indurre modifiche nell'espressione genica e nella trasduzione di altre proteine fondamentali per la proliferazione e la sopravvivenza cellulare.

Tabella 1.6. Esempi di oncogeni/oncosoppressori e forme leucemiche associate.

Oncogene	Funzione	Mutazione	Tumore associato
Geni per fattori di crescita e recettori dei fattori di crescita			
PDGFR	Recettore TK	del(4)q12 e formazione del gene di fusione FIP1L1/PDGFRA	Leucemia ipereosinofilica
FLT3	Recettore TK	ITD e mutazione puntiforme (D835) nella regione catalitica	Leucemia Mieloide Acuta
cKIT	Recettore TK	Mutazioni puntiformi e delezioni/inserzioni nucleotidiche	Mastocitosi e Leucemia Mieloide Acuta
Geni per proteine della trasduzione del segnale			
ABL	Tirosina chinasi non recettoriale	Traslocazione cromosomica con fusione genica	Leucemia mieloide cronica Leucemia linfatica acuta
RAS	Chinasi ad attività GTP-asica	Mutazioni puntiformi nei codoni 12,13, 59-61.	Leucemie Mieloidi Acute, Sindrome Mielodisplastica,
PTEN	Fosfatasi	Mutazioni Puntiformi Missenso che inducono la perdita di attività dell'oncosoppressore	Leucemia Linfoblastica Acuta
JAK2	Tirosina chinasi	Mutazione puntiforme V617F	Policitemia Vera, Trombocitemia Essenziale e Mielofibrosi
Geni per proteine coinvolte nella regolazione del ciclo cellulare			
CICLINA D1	Chinasi	t(11;14)(q13:q32) che induce la iperespressione della ciclina D1	Linfomi Mantellari
Geni per fattori di trascrizione			
AML1 o CBFa	Fattore trascrizionale	t(8;21) e formazione del gene di fusione AML1-ETO	Leucemia Mieloide Acuta
CBFb	Fattore trascrizionale	inv(16) e formazione del gene di fusione CBFb/MYH11	Leucemia Mieloide Acuta
RARa	Fattore trascrizionale	t(15;17) e formazione del gene di fusione PML-RARa; t(11;17) e formazione del gene di fusione PLZF-RARa	Leucemia Promielocitica
GATA-1	Fattore trascrizionale	Aumentata Espressione	Eritroleucemia
Geni per proteine coinvolte nel riparo al DNA			
RAD51	Catalizza la ricombinazione omologa	Aumentata attivazione da parte dell'oncogene BCR-ABL	Leucemia Mieloide Cronica
Geni per proteine che regolano l'apoptosi			
BCL-2	Inibitore del processo apoptotico	t(14;18) che induce l'aumentata espressione dell'oncogene BCL2	Linfomi Follicolari
P53	Fattore trascrizionale	Mutazioni e delezioni nucleotidiche che inducono la perdita di attività dell'oncosoppressore	Leucemia Linfoblastica Acuta, Leucemia Linfocitica Cronica, Linfomi
Geni per proteine che regolano i processi epigenetici			
TET2	Diossigenasi che catalizza l'ossidazione della 5-metilcitosina (5mC) a 5-idrossimetilcitosina	Mutazioni puntiformi inattivanti l'oncosoppressore	Leucemia Mieloide Acuta, Mielodisplasie
IDH1-IDH2	Isocitrato deidrogenasi che catalizza la decarbossilazione di isocitrato in alfa-chetoglutarato	Mutazioni puntiformi inattivanti l'oncosoppressore	Leucemia Linfoblastica Acuta e Leucemia Mieloide Acuta
DNMT3A	DNA metiltransferasi 3A	Mutazioni puntiformi	Leucemia Mieloide Acuta
ASXL1	Proteina legante la cromatina	Mutazioni puntiformi inattivanti	Leucemia Mieloide Acuta e Leucemia Mieloide Cronica
Geni per proteine dello splicing			
SF3B1	Proteina dello splisosoma	Mutazioni puntiformi inattivanti	Mielodisplasie, Leucemia linfatica cronica (10% dei casi)

Varie proteine della **trasduzione del segnale** sono coinvolte nella leucemogenesi. L'esempio più conosciuto e studiato è sicuramente costituito dalla proteina ABL che ha attività tirosino chinasi ed il cui potenziale oncogenico viene attivato attraverso una traslocazione cromosomica, la traslocazione t(9;22), nella leucemia mieloide cronica (vedi **Scheda clinica 2**). Il meccanismo

Scheda clinica 2: Patologie oncoematologiche

La **leucemia acuta** *è una patologia tumorale delle cellule del midollo osseo. In questa malattia si verifica una trasformazione e una proliferazione dei precursori dei globuli bianchi che si accumulano nel midollo osseo o nel sangue periferico e causano una riduzione delle altre cellule ematiche: globuli rossi (anemia) e piastrine (piastrinopenia). Si riconoscono due forme di leucemie acute: le forme mieloidi (leucemia acuta mieloide - LAM) e quelle linfoidi (leucemia acuta linfoide - LAL) in relazione alla morfologia ed ai determinanti antigeniici di membrana delle cellule leucemiche. Nella LAM i precursori mieloidi (midollari) si bloccano ad una tappa molto precoce del loro percorso di crescita per diventare globuli bianchi maturi (leucociti), cioè rimangono allo stato di "blasti" e iniziano a replicarsi in maniera rapida e incontrollata. La LAM è relativamente rara (3 nuovi casi su 100.000 persone all'anno) ma la sua frequenza aumenta con l'aumentare dell'età: l'età media di insorgenza è intorno ai sessant'anni. Essa può presentarsi come forma acuta fin dall'esordio o (soprattutto nella popolazione anziana) evolvere da una precedente sindrome mielodisplastica (LAM secondaria). Le leucemie acute secondarie presentano un decorso inizialmente meno aggressivo, ma anche una maggiore resistenza alle terapie. I sintomi con cui si manifesta derivano dall'anemia (debolezza, affaticabilità, mancanza di respiro anche per sforzi lievi), dalla carenza di piastrine (tendenza alle emorragie cutanee e mucose). Infine derivano dalla presenza di globuli bianchi che, in quanto patologici, sebbene spesso presenti in numero superiore alla norma, non svolgono la loro funzione di proteggerci dalle infezioni: si osservano quindi spesso episodi febbrili e infezioni ricorrenti. Tutti questi sono sintomi relativamente poco specifici, ma la loro contemporanea presenza induce di solito il sospetto e porta ad eseguire esami di controllo. L'esame più indicativo è l'emocromo (esame emocromocitometrico), che fornisce una valutazione quantitativa delle varie cellule del sangue: spesso mostra un quadro di leucocitosi (aumento del numero dei globuli bianchi) associato a calo dei globuli rossi e delle piastrine. Talora invece anche il numero dei globuli bianchi nel sangue periferico (ma non nel midollo) risulta basso. L'esame diagnostico rimane comunque l'aspirato midollare. Osservando il sangue midollare al microscopio si può avere un quadro della condizione del midollo, che nel caso della leucemia acuta sarà in parte o completamente invaso dalle cellule immature caratteristiche della malattia (blasti leucemici). Oltre all'osservazione al microscopio vi sono altri esami più approfonditi che permettono di identificare vari sottotipi di malattia, come l'esame immunofenotipico e quello citogenetico. Inoltre, il capitolo fornisce una serie di esempi di oncogeni che caratterizzano sottotipi leucemici a migliore o peggiore prognosi, che sono correntemente identificati e caratterizzati mediante approcci molecolari.*

La **leucemia mieloide cronica** *(LMC) è una neoplasia maligna, causata da un'alterazione acquisita della cellula staminale totipotente del midollo osseo. Questa alterazione causa una proliferazione incontrollata del midollo osseo stesso con produzione di un numero elevato di globuli bianchi. I globuli bianchi in eccesso perdono la loro capacità di ritenzione nel midollo osseo e vanno a colonizzare il sangue periferico e la milza. Il termine cronica indica che la malattia ha inizialmente un decorso lento, con pochi sintomi, anche se dopo un periodo variabile di alcuni anni si trasforma inevitabilmente in una leucemia acuta. La malattia è caratterizzata dalla presenza del cromosoma Philadelphia (Ph), che prende il nome dalla città nella quale fu scoperto dal dottor Peter Nowell e dal dottor David Hungerford nel 1960. Questo unico marcatore cromosomico rappresenta l'anomalia genetica specifica della LMC, ed è il risultato di una traslocazione tra i cromosomi 9 e 22: tale scambio dà luogo a un cromosoma 22 più corto, detto appunto Philadelphia. Tale cromosoma oltre che nella LMC è presente anche nel 5% dei bambini e nel 30% degli adulti affetti da leucemia linfoblastica acuta. In seguito alla traslocazione, si produce una proteina anomala definita* **BCR-ABL**, *caratterizzata nel capitolo.*

Le **neoplasie mieloproliferative croniche BCR/ABL negative**, *sono un gruppo di malattie del sangue di tipo neoplastico che originano da cellule staminali mutate. Tali cellule neoplastiche causano una produzione e crescita incontrollata di globuli rossi, globuli bianchi e piastrine. Le neoplasie mieloproliferative BCR/ABL- principali sono tre: la Policitemia vera (PV), caratterizzata da una produzione eccessiva di globuli rossi; la Trombocitemia essenziale (TE), caratterizzata da una produzione eccessiva di piastrine; la Mielofibrosi idiopatica (ossia senza causa nota, MFI), caratterizzata da un deposito eccessivo di fibre nel Midollo osseo. In particolare, la PV è una neoplasia caratterizzata clinicamente, dall'incremento assoluto della massa eritrocitaria, spesso accompagnata da leucocitosi, trombocitosi e splenomegalia; istologicamente, da un quadro di panmielosi con iperplasia eritroide, granulocitaria e megacariocitaria; biologicamente, dall'indipendenza dell'iperplasia eritroide dal fisiologico fattore di crescita, eritropoietina (EPO). La mutazione somatica del gene JAK2 (V617F), caratterizzata nel capitolo, è presente in circa il 95% dei pazienti affetti da PV e non è mai stata rilevata in soggetti sani. La TE è una neoplasia caratterizzata clinicamente da un persistente aumento della conta piastrinica (>450.000/mmc) ed istologicamente da un quadro midollare di spiccata iperplasia megacariocitaria. La diagnosi di trombocitemia essenziale deve essere presa in considerazione in presenza di un valore di piastrine stabilmente superiore al valore normale (piastrine superiori a 450.000/µl, trombocitosi o piastrinosi) e viene formulata dopo aver escluso le altre patologie o condizioni che possono dare una trombocitosi reattiva e le altre malattie mieloproliferative croniche o mielodisplastiche associate a trombocitosi. Nella storia naturale della malattia è possibile, seppur con una bassa incidenza, l'evoluzione tardiva in mielofibrosi o in leucemia acuta. La mutazione somatica del gene JAK2 (V617F) è presente in circa la metà dei pazienti affetti da TE e non è mai stata rilevata in pazienti con trombocitosi secondaria. La MFI è clinicamente caratterizzata da gradi variabili di fibrosi midollare, emopoiesi extramidollare, anemia, leucoeritroblastosi e splenomegalia. I sintomi della MFI possono essere classificati in tre categorie principali: mieloproliferativi, citopenici e costituzionali. Il primo gruppo comprende l'epatosplenomegalia, spesso assai marcata e che può rappresentare il sintomo più importante per il paziente. Citopenie di varia severità sono caratteristiche della MFI e sono multifattoriali. L'anemia è la citopenia più comune ed è provocata da diverse cause che includono l'emopoiesi inefficace, il sequestro splenico, l'emolisi ed eventuali perdite emorragiche dal tratto gastrointestinale, per es. da varici esofagee. La piastrinopenia può peggiorare il rischio emorragico, mentre la leucopenia è più rara e raramente severa. Più frequentemente si osserva una leucocitosi con un tipico quadro leuco-eritroblastico, caratterizzato da elementi immaturi della serie granuloblastica nel sangue periferico e da anisopoichilocitosi eritrocitaria con cellule "a goccia", o dacriociti. L'elevato turn-over cellulare e l'ematopoiesi extramidollare tipici della malattia possonno inoltre indurre uno stato ipercatabolico con sintomi costituzionali, anche severi, quali perdita di peso, astenia, febbre e cachessia. La mutazione JAK2V617F trovata nel 20-40% dei casi di MFI comporta ipersensibilità cellulare alle citochine e nella sua espressione omozigote si associa più frequentemente ad anomalie citogenetiche peggiorando la prognosi.*

molecolare che attiva il potenziale oncogenico di questa proteina è stato esaustivamente studiato e gran parte delle interazione coinvolte sono oggi note; inoltre, la proteina ABL oncogenica è stata il primo bersaglio di una terapia antineoplastica a bersaglio molecolare intracellulare e, di conseguenza, è interessante presentare in maggior dettaglio i meccanismi molecolari della sua attivazione oncogenetica. In seguito alla traslocazione cromosomica si ha la formazione di un gene ibrido che presenta al 5' un numero variabile di esoni del gene BCR, normalmente situato sul cromosoma 22, ed al 3' i 10 esoni terminali, degli 11 totali, del gene ABL. In tal modo, la quasi totalità delle sequenze geniche, e conseguentemente dei domini proteici, di ABL sono inseriti nel gene di fusione (**Figura 1.25**) e, di conseguenza, la proteina BCR-ABL esplica le funzioni di ABL, ma sotto il controllo della proteina BCR. L'oncogene ABL è stato isolato negli anni 60 da un retrovirus responsabile di un tipo aggressivo di leucemia murina, ma solo nel 1980 è stato chiarito che il suo prodotto proteico, analogo a quello delle cellule dei vertebrati superiori e dell'uomo, è una proteina ad attività tirosino chinasi di tipo non re-

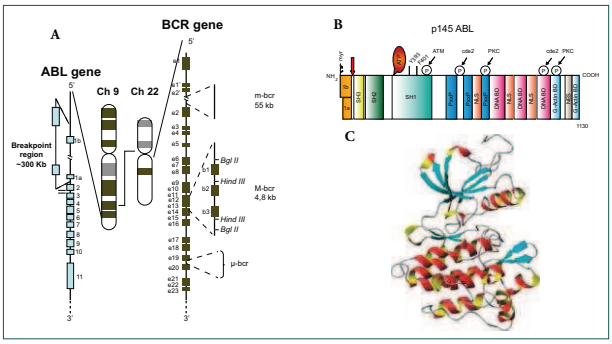

Figura 1.25. A) Traslocazione t(9;22) causante la leucemia mieloide cronica e localizzazione dei punti di rottura ai loci BCR ed ABL; B) Struttura della proteina ABL non traslocata. L'isoforma Ia è leggermente più corta dell'isoforma Ib, che contiene un sito di miristilazione per l'attacco alla membrana plasmatica. Il C-terminale contiene i domini leganti il DNA e la G- ed F-actina. I tre domini omologhi a SRC (SH) sono localizzati verso l'N-terminale (SH1, tirosin-chinasica; SH2, attivazione di ABL; SH3, repressione di ABL; Y393, sito di auto fosforilazione; PxxP, regione ricca in prolina capace di legare i domini SH3; NLS, segnale di localizzazione nucleare; NES, sequenza di esporto nucleare; ATM - cdc2 e PKC, siti di fosforilazione da Atm, cdc2 e PKC). La freccia rossa indica la posizione del punto di rottura nella proteina ABL coinvolta nella traslocazione t(9;22); C) Struttura quaternaria del sito catalitico di ABL determinata in base ad analisi di cristallografia ai raggi X. Porzione N-terminale (costituita da 6 foglietti β e da un'α elica), porzione contenente i residui di tirosina che fosforilati attivano ABL, dal dominio TK e dalla porzione C-terminale (costituita da un numero variabile di α eliche di varia lunghezza).

cettoriale. Per questo motivo la proteina è stata considerata un componente citoplasmatico del grande gruppo di proteine che trasferiscono al nucleo i segnali che arrivano ai recettori di membrana. Attualmente, però, è chiaro che le funzioni di questa proteina sono più complesse. La proteina ABL è una proteina di 145 kD che è presente nelle cellule in due isoforme derivanti dallo *splicing* alternativo del primo esone (Ia e Ib) (**Figura 1.25**). La struttura del dominio SH1 (dove SH sta per *Src Homology*, per l'omologia di sequenza nucleotidica con i geni Src), che codifica per il sito catalitico ad attività tirosino chinasi, è stata da poco determinata mediante studi cristallografici. Tali studi sono stati anche di fondamentale importanza per l'industria farmaceutica e lo sviluppo di terapie molecolari. ABL ha una struttura grossolanamente bilobare con un lobo N-terminale costituito da 6 strutture a beta-foglietto ed una serie di residui ad alfa-elica ed un lobo C-terminale costituiti da una serie di residui aminoacidici ad alfa-elica ripiegati su se stessi (**Figura 1.26**). Nel solco intramolecolare tra i due lobi vi è il sito catalitico, la cui accessibilità per i substrati è regolata da un'ansa aminoacidica detta "loop di attivazione" che, con i suoi spostamenti conformazionali, rende accessibile o non accessibile ai substrati il sito catalitico (**Figura 1.26**). La struttura del sito catalitico e la sua accessibilità è condizionata anche da altri domini intramolecolari; il dominio SH3 e le sequenze del "cap" N-terminale, ad esempio, si ripiegano sul sito catalitico nella proteina ABL inattiva stabilizzandone la conformazione. L'attivazione è invece dovuta all'interazione del dominio SH2 di ABL con i residui SH2 di altre proteine intracellulari con conseguente fosforilazione delle tirosine a valle. Si può quindi comprendere come la attività di ABL sia, in condizioni fisiologiche, strettamente regolata e come la proteina sia per lo più in conformazione inattiva. Servono in-

fatti tre modificazioni conformazionali per ottenere la sua attivazione: il dispiegamento del "cap" N-terminale, il dispiegamento del dominio SH3 ed l'apertura del loop di attivazione (**Figura 1.26**). In condizioni fisiologiche, ABL è localizzata prevalentemente a livello nucleare, in quanto contiene tre sequenze di localizzazione nucleare (NLS), una nella porzione N-terminale e due nella porzione centrale della proteina, mentre è presente una sola sequenza di esporto dal nucleo (NES) nella porzione C-terminale. In questo modo ABL può transitare dal citoplasma al nucleo e viceversa ed è in grado di regolare nel nucleo, attraverso l'interazione con la proteina p73, la funzione di alcuni geni coinvolti nell'arresto della proliferazione cellulare a seguito di un danno genotossico. In tal senso, la proteina ABL è unica tra le proteine ad attività tirosino chinasica che presenta un dislocazione nucleare. Una delle due isoforme di ABL, la forma Ib, contiene un sito di miristilazione, modifica stabile mediante l'aggiunta dell'acido grasso saturo tetradecanoico $CH_3(CH_2)_{12}COOH$, che ne consente l'ancoraggio a strutture del citoscheletro e della membrana; di conseguenza, sembra che altre funzioni della proteina ABL siano legate alla maturazione cellulare mediante la regolazione delle modificazioni del citoscheletro. Nei tre principali tipi di proteine di fusione BCR/ABL che si trovano nelle cellule leucemiche umane, e che si differenziano tra di loro per il punto di rottura sul cromosoma 22 a livello del gene BCR, sono inseriti praticamente tutti i domini proteici di ABL (con eccezione del sito di miristilazione) e pertanto la proteina oncogenica conserva l'attività tirosino chinasica (**Figura 1.25**). Al contrario della proteina non traslocata, ABL è costitutivamente attivata nelle cellule leucemiche per la presenza dei domini aminoterminali della protiena BCR. Quest'ultima è una proteina a localizzazione citoplasmatica probabilmente implicata nella trasduzione del segnale. Tra i domini aminoterminali di BCR, il dominio di omodimerizzazione è conservato nella proteina oncogenica BCR/ABL. La proteina oncogenica di fusione BCR/ABL, pertanto, si trova sempre nelle cellule leucemiche come un omodi-

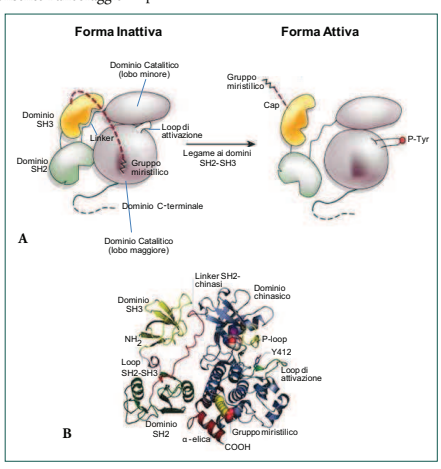

Figura 1.26. A) La proteina Abl è bloccata nello stato inattivo mediante il legame del gruppo miristilico del dominio SH3 con il dominio catalitico (lobo maggiore), localizzato al C-terminale. Il dominio SH2 lega il dominio catalitico bloccando il sito di legame delle fosfotirosine presenti nel dominio SH2. La regione di legame al substrato del dominio SH3 interagisce con il linker. Tali meccanismi causano l'inattivazione del dominio catalitico di ABL. L'attivazione di ABL avviene quando ligandi ad alta affinità per i domini SH3 e/o SH2 interrompono tali contatti intramolecolari; B) Struttura cristallografica della proteina c-ABL: il gruppo miristilico di c.ABL lega la tasca idrofobica del dominio chinasico e induce una modifica conformazionale (elica rosso scuro) che consente il blocco del dominio SH2.

mero in cui il ripiegamento del dominio SH3 sul sito catalitico è impedito per motivi sterici e l'attivazione dei due domini SH2 di ABL è mantenuto dall'autotransfosforilazione dei due monomeri. Da quanto detto si comprende che le cellule leucemiche contengono, per effetto della traslocazione cromosomica, una molecola proteica BCR/ABL con attività tirosino chinasica costitutivamente attivata. La proteina oncogenica di fusione ha inoltre una localizzazione esclusivamente citoplasmatica, fosforilando in modo incongruo ed attivando una serie di proteine citoplasmatiche, così da indurre la trasformazione cellulare. È interessante notare che la struttura della proteina oncogenica correla con il suo potenziale trasformante: infatti sono note tre tipologie di proteine di fusione BCR/ABL che differiscono tra di loro per la quantità di sequenze proteiche codificate dal gene BCR incluse in esse. Ciò dipende dalla variabilità del sito di rottura nel gene BCR. È stato dimostrato che la proteina BCR/ABL più corta, che si origina quando il breakpoint nel gene BCR va a cadere nel primo introne (ed è quindi conservato solo il primo esone nella proteina di fusione), ha un potere trasformante maggiore (P190) che caratterizza molecolarmente pazienti affetti da una leucemia a fenotipo acuto, come la leucemia acuta linfoide. Quando il punto di rottura nel gene BCR è contenuto nel 13° o 14° introne, e quasi la metà dei domini proteici BCR sono inclusi nel gene di fusione oncogenico, la proteina di fusione che ne deriva (P210) ha un potere trasformante più ridotto e si trova prevalentemente nella leucemia mieloide cronica. Quando, infine, il punto di rottura si trova nel 19° introne la proteina di fusione (P230) include praticamente quasi tutti i domini proteici di BCR oltre a quelli di ABL ed il potere trasformante della proteina è più ridotto causando una forma di leucemia cronica detta leucemia mieloide cronica a neutrofili, caratterizzata da un comportamento clinico poco aggressivo.

Oltre ai numerosi studi in sistemi cellulari indicanti il potere trasformante diretto della proteina di fusione BCR/ABL, nel 1990 è stato dimostrato in un modello sperimentale animale che la presenza della proteina BCR/ABL nelle cellule emopoietiche era di per sé sufficiente a determinare l'insorgenza di una leucemia ed aveva, quindi, una posizione centrale e cruciale nella patogenesi di questa neoplasia. Questa proteina e la sua attività enzimatica rappresentano un bersaglio ideale per lo sviluppo di molecole di sintesi ad attività farmacologica da utilizzare nella terapia delle leucemie associate alla traslocazione cromosomica t(9;22) e contenenti la proteina di fusione BCR/ABL. A tal scopo sono state testate una serie di molecole con analogia di struttura all'ATP che, occupando il sito catalitico tirosino chinasico di ABL, inattivano la proteina oncogenica (**Figura 1.26**). Tra queste, quella che si è rivelata la più efficace è un derivato pirimidinico, la 2-fenilalaninopirimidina, che è stata poi immessa in commercio con il nome di Imatinib. Questo composto, facilmente assorbibile quando somministrato per via orale, è stato brevettato nel 1993, e ha dimostrato inibire la proteina oncogenica sia nei modelli sperimentali animali sia nei pazienti, permettendo il controllo della malattia leucemica. Alla luce di ciò, l'Imatinib è considerato il precursore dei farmaci a bersaglio molecolare che sono progressivamente stati introdotti nella pratica clinica.

Un altro esempio particolarmente importante di alterazioni funzionali causanti stati patogenetici è costituito dalle alterazione delle proteine della famiglia Jak (denominazione derivata da Janus Kinase, **Figura 1.27**). La proteina Jak-2, componente di tale famiglia proteica, è mutata in tutti i casi di Policitemia Vera, una malattia mieloproliferativa di cui costituisce ora un marcatore molecolare utilizzato nella pratica clinica per la conferma diagnostica (vedi **Scheda clinica 2**). Mutazioni della proteina Jak-2 sono state riscontrate anche in più della metà dei casi dei pazienti affetti da altre due frequenti forme di neoplasie mieloproliferative croniche: la trombocitemia essenziale e la mielofibrosi idiopatica (vedi **Scheda clinica 2**). Nella stragrande maggioranza dei casi, il gene Jak-2 presenta una singola mutazione a livello del codone 617 con sostituzione di una valina con una fenilalanina (V617F) con conseguente modificazione

della struttura tridimensionale del dominio JH2 della proteina, denominato dominio pseudochinasico. Tale dominio, pur avendo una struttura aminoacidica simile a quella del dominio catalitico della proteina Jak-2, non ha alcuna attività enzimatica ma svolge una funzione regolatoria sull'attività tirosino chinasica della proteina Jak-2 che si esplica attraverso il ripiegamento e contatto intramolecolare tra i due domini proteici. La sostituzione aminoacidica fenilalanina/valina determina una variazione nella conformazione della proteina con la perdita del contatto tra i due domini e la conseguente attivazione costitutiva di quest'ultima (**Figura 1.27**). La proteina Jak-2, pur non essendo di per sé un recettore, si associa a recettori di membrana espressi sulla superficie dei progenitori emopoietici e trasduce il segnale derivante dal legame recettore/ligando ad altre proteine intracellulari. È stato dimostrato che tra i recettori con i quali Jak-2 interagisce vi sono quelli dell'eritropoietina e del G-CSF. Il segnale proveniente da questi recettori, anche in assenza del legame di questi due fattori di crescita, è trasferito alle proteine STAT, le quali hanno attività di fattori trascrizionali (trasduttori del segnale e attivatori della trascrizione), ed in particolare a STAT3 e STAT5 che hanno grande importanza nel supportare la sopravvivenza e la differenziazione in senso mielo-eritroide dei precursori emopoietici. Di fatto, le proteine STAT sono costitutivamente attivate nel citoplasma e nel nucleo delle cellule mieloidi dei pazienti affetti da neoplasie mieloproliferative.

Tra le altre proteine implicate nella trasduzione del segnale e che possono dare origine alle neoplasie del sistema emopoietico, sono sicuramente da menzionare le proteine della famiglia RAS *ad attività GTP-asica*. In condizioni fisiologiche le proteine RAS sono ancorate alla membrana cellulare in vicinanza di recettori di fattori di crescita, mediante ponti costituiti da gruppi prenilici (gruppo chimico composto da multipli dell'unità isoprenica), come ad esempio i gruppi farnesilici

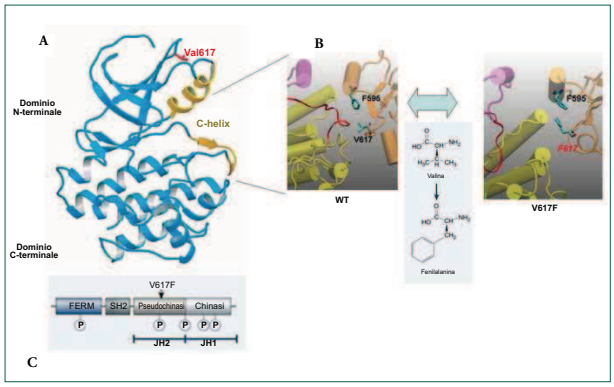

Figura 1.27. A) Modello tridimensionale dei domini JH1 (sito catalitico) e JH2 (sito pseudocatalitico) della proteina Jak-2; B) Il loop rosso è parte del loop di attivazione di JH1 (residui 995-1005); C) In dettaglio l'interfaccia JH1/JH2 e le strutture degli amminoacidi valina e fenilalanina. La posizione 617, sito della mutazione attivante è mostrata nel dettaglio.

(a 15 atomi di carbonio) aggiunti nelle tappe di modifica post-traduzionale, e rivestono grande importanza per la loro localizzazione subcellulare e, conseguentemente, per la loro funzione. Le proteine RAS sono attivate da recettori di membrana e trasmettono, a loro volta, il segnale ad una serie di proteine ad attività *serina/treonina chinasica* intracitoplasmatica, tra cui la proteina RAF. A sua volta, la proteina serina/treonina chinasi RAF fosforila ed attiva MEK, anch'essa una proteina ad attività serina/treonina chinasi, che trasduce il segnale attivando le proteine della famiglia MAPK (protein kinasi ad attività mitogenica), tra le quali ricordiamo la proteina ERK. Le MAPK una volta attivate, traslocano a livello nucleare e regolano l'attivazione di una serie di fattori trascrizionali e di proteine ribosomiali, che favoriscono la trascrizione e la traduzione di proteine coinvolte nella duplicazione cellulare. Il meccanismo fisiologico di attivazione coinvolge il legame e l'idrolisi del GTP. Una serie di mutazioni puntiformi attivanti sono state descritte nei geni RAS (N-RAS e K-RAS) in pazienti affetti da leucemia mieloide acuta (vedi **Scheda clinica 2**) e melodisplasia. La frequenza più elevata di mutazioni è stata riportata nel gene N-RAS (10-27%), più raramente nel gene K-RAS (4-10%) e sporadicamente nel gene H-RAS. Le mutazioni sono ristrette ai codoni 12, 13 e da 59 a 61; queste alterazioni riducono la capacità di RAS di idrolizzare il GTP, con la conseguente permanenza in fase attivata della proteina anche in assenza della stimolazione da parte di un recettore attivato. L'ancoraggio della proteina RAS alla membrana nelle vicinanze di un recettore attraverso l'aggiunta del ponte costituito dal gruppo farnesilico o prenilico rappresenta un possibile bersaglio terapeutico. Infatti, una serie di farmaci di nuova generazione sono diretti ad inibire le reazioni di farnesilazione o di prenilazione.

Tra le proteine che regolano il **ciclo cellulare**, e che possono essere coinvolte nelle neoplasie emopoietiche, la più studiata è la ciclina D1, proteina che svolge la sua funzione regolando la transizione delle cellule dalla fase G1 a quella S del ciclo cellulare, ed è stata recentemente identificata come proto-oncogene poiché la sua alterazione può sostenere la trasformazione cellulare neoplastica. Infatti, la traslocazione cromosomica t(11;14)(q13:q32), che interessa il gene che codifica la ciclina D1 e il gene che codifica per il recettore delle cellule T (TCR), è patogeneticamente associata ad uno specifico tipo di linfoma a decorso molto aggressivo che prende il nome di linfoma mantellare perché costituito da linfociti che derivano dalla zona mantellare del linfonodo. Il gene che codifica per la ciclina D1 in seguito alla traslocazione t(11;14), viene posto sotto il controllo trascrizionale del promotore del TCR, e viene pertanto costitutivamente iperespresso, inducendo la permanenza in ciclo dei linfociti neoplastici del linfoma mantellare (**Figura 1.28**). La ciclina D1 infatti interagisce, attivandone la funzione con le Chinasi ciclina dipendenti CDK4 e CDK6; queste ultime, una volta attivate, iniziano il rilascio del "freno" dipendente dall'attività della proteina RB sul ciclo cellulare.

Molte proteine con attività di **fattori trascrizionali** possono essere alterate nei tumori ematologici. I fattori trascrizionali, legandosi a sequenze geniche di tipo regolatorio, modulano l'espressione di una serie di geni bersaglio e di conseguenza controllano tutti i processi cellulari, tra cui crescita e differenziamento. Nelle neoplasie ematologiche possono essere alterate due classi principali di fattori trascrizionali. Il primo gruppo è costituito dai fattori trascrizionali che sono coinvolti nello sviluppo di quasi tutte le linee differenziative ematopoietiche, come il fattore trascrizionale AML-1 (o CBF-alfa). AML-1 è la proteina che controlla la prima fase dell'ematopoiesi e la costituzione di un pool di cellule ematopoietiche staminali. Per tale motivo, AML-1 è coinvolto nello sviluppo di tutte le linee differenziative ematopoietiche e la sua alterazione funzionale porta alla completa mancanza di sviluppo della componente ematica nell'embrione. Il fattore trascrizionale AML1 funziona nelle cellule come eterodimero attraverso il legame con la subunità beta (CBF-beta).

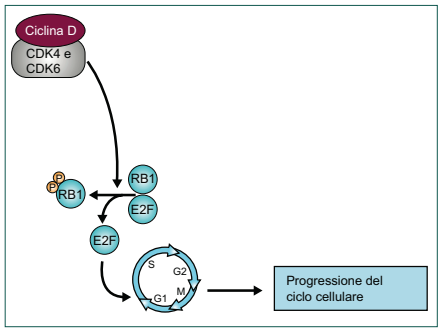

Figura 1.28. La ciclina D1 interagisce, attivandone la funzione, con le chinasi ciclina-dipendenti CDK4 e CDK6; queste ultime, una volta attivate, iniziano il rilascio del "freno" dipendente dall'attività della proteina RB sul ciclo cellulare.

Entrambe le subunità possono essere coinvolte da mutazioni in pazienti affetti da leucemie mieloidi acute. In particolare, la funzione del fattore trascrizionale CBF può essere alterata mediante due meccanismi differenti: una traslocazione cromosomica o mutazioni puntiformi della subunità alfa. Quattro differenti traslocazioni cromosomiche che interessano il fattore trascrizionale CBF sono state descritte nelle leucemie acute: la traslocazione t(8;21), l'inv(16), la più rara t(3;21) nelle forme di tipo mieloide e la t(12;21) che è la traslocazione cromosomica più frequente nella leucemia linfoide acuta dei bambini (**Figura 1.29**). In tutti i casi si ha la formazione di proteine di fusione in cui il fattore trascrizionale CBF conserva il dominio di legame al DNA, ma perde o altera i domini di legame con i complessi proteici di regolazione trascrizionale (i corepressori). Tutte queste proteine di fusione si comportano come dominanti negative sulla funzione della proteina CBF normale; i livelli di quest'ultimo sono infatti molto bassi all'interno delle cellule con la traslocazione poiché le proteine oncogeniche di fusione si comportano come repressori della trascrizione di CBF normale. Ciò determina in ultima analisi il blocco differenziativo nelle cellule emopoietiche. Inoltre i domini proteici addizionali a quelli di CBF che si trovano nelle proteine di fusione descritte in **figura 1.29**, possono ridirigere il fattore trascrizionale CBF anche a ridurre la trascrizione di altre proteine che sono importanti nel differenziamento emopoietico. È interessante notare che il potenziale oncogenico della proteina AML può essere attivato da mutazioni puntiformi che possono insorgere nel dominio di legame al DNA o di eterodimerizzazione con CBF-beta.

Il secondo gruppo di fattori trascrizionali che possono essere coinvolti in traslocazioni cromosomiche sono invece definiti lineage-specifici, perché controllano tappe precise del differenziamento emopoietico. Anche in questi casi, il meccanismo che altera il fattore trascrizionale è costituito da una traslocazione cromosomica con la formazione di un gene ibrido che codifica una proteina di fusione. Questa conserva il dominio di legame al DNA, ma sostituisce i domini di legame con i complessi proteici di regolazione trascrizionale e, attraverso il legame aberrante con un complesso di corepressione su di uno specifico promotore, la proteina di fusione altera l'espressione di geni target indispensabili per la corretta

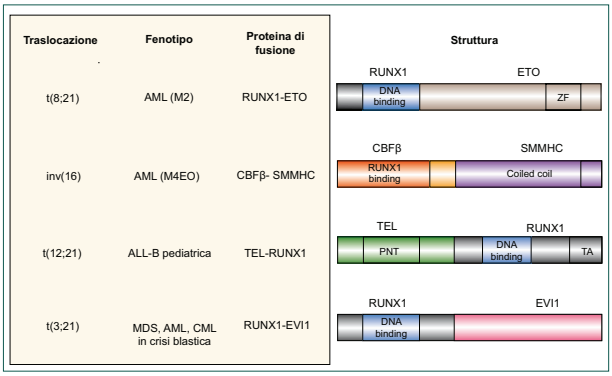

Figura 1.29. Struttura delle proteine di fusione che derivano dalle traslocazioni cromosomiche che interessano i geni che codificano le due subunità del fattore trascrizionale CBF.

differenziazione della cellula ematopoietica. Un esempio paradigmatico, è costituito dal fattore trascrizionale RARalfa (localizzato sul cromosoma 17) coinvolto in almeno cinque tipi di traslocazioni cromosomiche nonrandom (X-RARα) in pazienti affetti da leucemia acuta promielocitica (LAP), il cui tema comune è costituito sempre dall'alterazione della funzione della proteina RARalfa. Tra le cinque traslocazioni, la t(15;17) che genera la fusione tra il gene RARalfa e il gene PML, è di gran lunga la più frequente (**Figura 1.30**). Il gene RARalfa codifica per il recettore dell'acido retinoico e fa parte della famiglia dei recettori ormonali nucleari che includono il recettore retinoico X (RXR). In assenza di acido retinoico (RA), l'eterodimero RAR/RXR lega il complesso co-repressoriale contenente le istoni deacetilasi HDAC. La deacetilazione istonica induce la condensazione della cromatina e la conseguente repressione trascrizionale. La presenza di RA induce la dissociazione di questo complesso e promuove l'associazione di un complesso co-attivatore contenente l'acetil trasferasi CBP/p300. L'acetilazione istonica induce l'apertura della cromatina, l'esposizione del promotore e l'attivazione della trascrizione. Il gene PML codifica per una proteina oncosoppressore che non possiede di per se capacità di legare il DNA ed ha una caratteristica co-localizzazione nucleare in strutture definite POD (Dominio Oncogenico della proteina PML), nelle quali PML forma complessi tetramerici. Il suo ruolo biochimico non è ancora ben chiaro, ma è stato recentemente dimostrata la sua attività nella regolazione epigenetica, come mediatore dell'attività dell'interferone, come fattore pro-apoptotico e come proteina oncosoppressore. La proteina X-RARa conserva una identica sequenza di legame al DNA negli elementi RARE (retinoic acid response elements) cosi come è conservata la sua capacità di formare un complesso eterodimerico con RXR e di legare RA. È stato però dimostrato che la proteina di fusione PML-RARalfa interagisce con elevata affinità ai complessi corepressori sia in assenza che in presenza di concentrazioni fisiologiche di

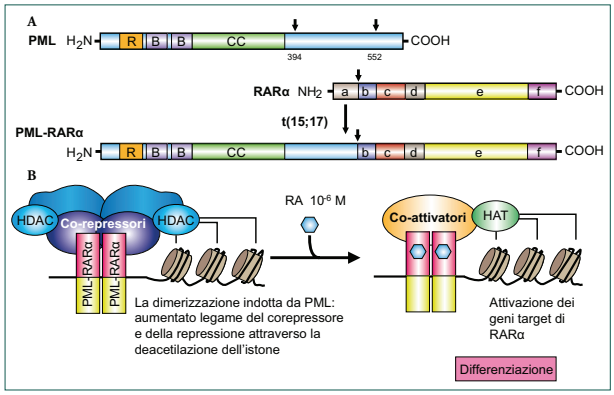

Figura 1.30. Modello di patogenesi APL. A) Struttura delle proteine PML e del recettore a dell'acido retinoico (RARα), e della proteina di fusione PML-RARα. I domini Ring (R), B boxes (B), coiled-coil (CC) di PML sono indicati. Il dominio che lega il DNA di RARα (c) e il dominio di legame l'ormone (e) sono mostrati. a, b, d e f sono altri domini regolatori. PML-RARα mantiene i domini funzionali di entrambe le proteine, permettendo l'attività di dominante negativo su PML e RARα; B) Gli omodimeri PML- RARα legano e reprimono i bersagli di RARα attraverso il reclutamento aumentato dei corepressori. L'acido retinoico (RA) converte PML- RARα in un attivatore e fa sì che la differenziazione cellulare possa avvenire, inducendo la remissione clinica (HAT, istone acetyl-transferasi; HDAC, istone deacetilasi).

RA (10^{-9} - 10^{-8} M). Invece, concentrazioni farmacologiche di vitamina (da 10^{-7} a 10^{-6} M) sono in grado di distaccare tali complessi proteici dalla proteina di fusione PML-RARalfa e favorire il legame con i complessi leganti le istone acetil trasferasi (HAT). È molto interessante sottolineare che questo fenomeno è attualmente utilizzato nella pratica clinica, con l'inclusione nella terapia di questo tipo di leucemia dell'acido retinoico ad elevate dosi.

Un'altra categoria di proteine le cui alterazioni recentemente sono state identificate nelle neoplasie ematologiche è costituita dalle proteine che regolano le **modificazioni epigenetiche del genoma**. I processi epigenetici regolano l'espressione genica e la funzionalità genomica mediante la regolazione della struttura dinamica della cromatina, andando primariamente a regolare in siti specifici la sua compattezza e quindi la sua accessibilità ai fattori trascrizionali. In tal modo, questi meccanismi svolgono un ruolo cruciale nella regolazione del differenziamento cellulare. Molte delle conoscenze su questi meccanismi derivano dagli studi che sono stati effettuati nei tumori e nelle neoplasie ematologiche. Infatti, le alterazioni epigenetiche sono oggi riconosciute come meccanismi fondamentali delle neoplasie ematologiche ed anche come marcatori molecolari della neoplasia. In particolare, sembra che l'alterazione di questi meccanismi possa costituire uno degli eventi iniziali nella trasformazione neoplastica. I meccanismi epigenetici regolano la trascrizione genica e la trasduzione proteica mediante una serie processi come la metilazione del DNA, le modifiche degli istoni, il posizionamento dei nucleosomi e la presenza di RNA non codificanti come i microRNA. La cro-

matina è infatti strutturata in unità ripetute di nucleosomi, costituiti da 146 paia di basi di DNA avvolte intorno ad un complesso proteico ottamerico costituito da quattro tipi di proteine istoniche (H3, H4, H2A e H2B). Per tanto i meccanismi epigenetici che modificano tale struttura cromatinica possono essere divisi in quattro categorie principali:

- la metilazione del DNA nelle isole CpG ad opera delle metiltrasferasi;
- le modifiche covalenti degli istoni comprendenti metilazioni, acetilazioni ad opera delle acetil-trasferasi, ubiquitinazioni e fosforilazioni;
- modifiche non-covalenti del nucleosoma mediante l'incorporazione di varianti istoniche;
- la presenza di RNA non codificanti, come i microRNA che legano gli mRNA bersaglio e ne favoriscono la degradazione.

L'interazione tra questi differenti processi è estremamente delicata e crea nell'insieme uno "scenario epigenetico" dinamico in cui le modificazioni plastiche della conformazione cromatinica rendono accessibili per la trascrizione soli i geni necessari alle varie specifiche fasi differenziative cellullari. Nelle neoplasie ematologiche, ed in particolare nelle sindromi mielodisplastiche e nella leucemia mieloide acuta, sono frequenti le alterazioni epigenetiche. In queste patologie, sono state identificate mutazioni puntiformi ricorrenti che portano alla riduzione della normale funzione di proteine con funzione di regolazione epigenetica, quali TET2, IDH1, IDH2, DNMT3A, UTX, e ASXL1. Ad esempio, TET2 converte enzimaticamente la 5-metil-citosina a 5-idrossimetil-citosina, possibilmente determinando la perdita nella metilazione del DNA. Mutazioni in TET2 sono comuni ed estremamente precoci nelle mielodisplasie e nelle neoplasie mieloproliferative croniche come la policitemia vera e la mielofibrosi idiopatica, oltre che nella leucemia mieloide acuta. Le mutazioni della isocitrato deidrogenasi-1 e -2 (IDH1 e IDH2) determinano una alterazione del metabolismo dall'alfa-chetoglutarato con il conseguente accumulo di 2-idrossiglutarato. Questo metabolita, accumulandosi nelle cellule determina una modificazione della metilazione istonica, con il conseguente blocco della differenziazione. Queste mutazioni sono state identificate con elevata frequenza (circa 10%) nei pazienti con leucemia mieloide acuta, e questa alterazione si associa a cattiva prognosi e ridotta risposta alla terapia.

Uno dei meccanismi di difesa cellulare dall'accumulo di mutazioni da danno genotossico è costituito dalle proteine che regolano i **processi apoptotici**. Non è quindi sorprendente che alcune di esse sono alterate in neoplasie ematologiche, conferendo così instabilità genomica alle cellule neoplastiche. Nelle cellule i processi apoptotici sono regolati attraverso meccanismi intrinseci o estrinseci, innescati questi ultimi da stimoli provenienti dall'esterno della cellula attraverso recettori specifici, e che entrano a far parte dei meccanismi omeostatici di controllo tissutale. La via intrinseca dell'apoptosi è regolata dalla famiglia di proteine Bcl-2 che agiscono sulla membrana mitocondriale esterna e dalla proteina p53. La famiglia Bcl-2 consiste di circa 20 proteine che possono essere divise in due gruppi con funzioni opposte: un gruppo di proteine Bcl-2 che inibisce l'apoptosi (ad esempio Bcl-2, Bcl-xl, Bcl-w, ecc.) e un altro gruppo che la promuove (ad esempio Bax, Bad, Bim/Bod, ecc.). Il locus del gene Bcl-2 può essere alterato nelle neoplasie ematologiche per effetto di una traslocazione che non determina fusione genica, la t(14;18) che è tipica dei linfomi follicolari. Nella t(14;18) il locus del gene Bcl-2 traslocato è giustapposto all'enhancer della catena pesante delle immunoglobuline. Come conseguenza il suo riposizionamento vicino a un promotore forte porta alla sovraespressione della proteina antiapoptotica Bcl-2 riducendo la possibilità di apoptosi delle cellule linfocitarie B con la traslocazione a livello dei follicoli linfatici secondari. Pertanto queste si accumulano nei follicoli degli organi linfatici determinando la comparsa della sintomatologia clinica del linfoma. La proteina p53 si trova normalmente in quantità piccolissime nella cellula, ma la

presenza di uno stress cellulare da danno genotossico o altre situazioni stressanti di tipo non genotossico, come ad esempio la ipossia con accumulo di radicali liberi, sono in grado di indurre l'aumento della concentrazione di questa proteina sia attraverso l'aumento della sua sintesi che mediante la riduzione della sua degradazione dipendente dall'interazione con la proteina MDM2; a questo punto una serie di altre proteine modulatrici (chinasi, acetilasi) attivano poi il potenziale transattivante della proteina p53, che attiva una serie di programmi intracellulari che in ultima analisi portano all'arresto del ciclo cellulare ed al riparo del danno del DNA o, se quest'ultimo non è possibile, all'apoptosi. In tal senso la proteina p53 ha una funzione cruciale nel mantenere l'integrità del genoma e viene spesso per tale motivo considerata "guardiano del genoma". In molte neoplasie ematologiche (ma anche nei tumori solidi), la funzione di p53 è abolita o ridotta mediante due meccanismi distinti che spesso coesistono; il locus genico sul cromosoma 17 può essere deleto determinando una situazione di emizigosi ed aploinsufficienza, o la proteina può presentare mutazioni puntiformi inattivanti. Queste forme mutanti di p53 si comportano come dominanti negative e si associano paradossalmente ad uno spiccato aumento della concentrazione intracellulare di p53, che da un lato non può essere degradata perché le modifiche nella struttura ne impediscono il legame ai complessi di degradazione e dall'altro sequestra le proteine p53 non mutate rendendole non funzionanti. Ne risulta quindi che queste mutazioni rendono estremamente instabili le cellule neoplastiche e conferiscono un carattere di estrema aggressività clinica alla neoplasia. Molte neoplasie ematologiche, come i mielomi, le leucemie acute (vedi **Scheda clinica 2**), i linfomi non Hodgkin's, acquisiscono come evento terminale mutazioni e/o delezioni di p53.

Infine, le proteine che regolano i **processi di splicing** (maturazione del RNA messaggero) sono state recentemente identificate come una importante classe di proteine implicate nella trasformazione neoplastica delle cellule emopoietiche. Almeno 8 differenti proteine che fanno parte dello "splisosoma", le proteine SF3B1, SRSF2, U2AF35, ZRSR2, SF3A1, PRP40B, SF1 e U2AF65, presentano mutazioni puntiformi con sostituzione aminoacidica in pazienti con sindromi mielodisplastiche e, complessivamente, le mutazioni di queste proteine rappresentano l'evento genetico più frequentemente dimostrabile in queste patologie neoplastiche (dal 45 all'85% dei casi di mielodisplasie o di leucemia mielomonocitica cronica). Ad esempio la proteina SF3B1 è mutata nel 25-45% dei casi di sindromi mielodisplastica e se si considerano separatamente le anemia refrattarie con sideroblasti ad anello. Le mutazioni di questo gene arrivano ad essere presenti nel 85% dei casi di cui rappresentano quindi un meccanismo patogenetico centrale. È da tenere presente che le mutazioni di questi geni non sono però esclusive delle sindromi mielodisplastiche. Infatti il 10-15% dei pazienti con leucemia linfatica cronica presentano mutazioni di SF3B1. In questo caso la mutazione si associa a prognosi sfavorevole.

Bibliografia essenziale

1. Peters T. All about albumin: biochemistry, genetics, and medical applications. San Diego: Academic Press; 1996.
2. Cote HC, Lord ST, Pratt KP. gamma-Chain dysfibrinogenemias: molecular structure-function relationships of naturally occurring mutations in the gamma chain of human fibrinogen. Blood 1998;92(7):2195-212.
3. Davie EW. A brief historical review of the waterfall/cascade of blood coagulation. J Biol Chem 2003;278(51):50819-32.
4. Anderson NL, Polanski M, Pieper R, et al. The human plasma proteome: a nonredundant list developed by combination of four separate sources. Mol Cell Proteomics 2004;3(4):311-26.
5. Sadrzadeh SM, Bozorgmehr J. Haptoglobin phenotypes in health and disorders. Am J Clin Pathol 2004;121 Suppl:S97-104.
6. Schenone M, Furie BC, Furie B. The blood coagulation cascade. Curr Opin Hematol 2004;11(4):272-7. Anderson CL, Chaudhury C, Kim J, Bronson CL, Wani MA, Mohanty S. Perspective-- FcRn transports albumin: relevance to immunology and medicine. Trends Immunol 2006;27(7):343-8.
8. Crawley JT, Zanardelli S, Chion CK, Lane DA. The central role of thrombin in hemostasis. J Thromb Haemost 2007;5 Suppl 1:95-101.
9. Dunn LL, Suryo Rahmanto Y, Richardson DR. Iron uptake and metabolism in the new millennium. Trends Cell Biol 2007;17(2):93-100.
10. Gailani D, Renne T. Intrinsic pathway of coagulation and arterial thrombosis. Arterioscler Thromb Vasc Biol 2007;27(12):2507-13.
11. Tanaka KA, Key NS, Levy JH. Blood coagulation: hemostasis and thrombin regulation. Anesth Analg 2009;108(5):1433-46.
12. Garrick MD. Human iron transporters. Genes Nutr 2011;6(1):45-54.
13. Stegner D, Nieswandt B. Platelet receptor signaling in thrombus formation. J Mol Med (Berl) 2011;89(2):109-21.
14. Vardiman JW, Thiele J, Arber DA, Brunning RD, Borowitz MJ, Porwit A, Harris NL, Le Beau MM, Hellström-Lindberg E, Tefferi A, Bloomfield CD. The 2008 revision of the World Health Organization (WHO) classification of myeloid neoplasms and acute leukemia: rationale and important changes. Blood 2009; 114(5):937-51.
15. Crans HN, Sakamoto KM. Transcription factors and translocations in lymphoid and myeloid leukemia. Leukemia 2001; 15(3): 313-331.
16. Gabert J, Beillard E, van der Velden VH, Bi W, Grimwade D, Pallisgaard N, Barbany G, Cazzaniga G, Cayuela JM, Cavé H, Pane F, Aerts JL, De Micheli D, Thirion X, Pradel V, González M, Viehmann S, Malec M, Saglio G, van Dongen JJ. Standardization and quality control studies of 'real-time' quantitative reverse transcriptase polymerase chain reaction of fusion gene transcripts for residual disease detection in leukemia – A Europe Against Cancer Program. Leukemia 2003;17(12):2318-57.
17. Pane F, Intrieri M, Quintarelli C, Izzo B, Muccioli GC, Salvatore F. BCR/ABL genes and leukemic phenotype: from molecular mechanisms to clinical correlations. Oncogene 2002; 21(56):8652-67.
18. Levine RL, Pardanani A, Tefferi A, Gilliland DG. Role of JAK2 in the pathogenesis and therapy of myeloproliferative disorders. Nat Rev Cancer 2007; 7(9):673-83.
19. Takahashi S. Current findings for recurring mutations in acute myeloid leukemia. J Hematol Oncol 2011; 14(4):36.
20. Saeed S, Logie C, Stunnenberg HG, Martens JH. Genome-wide functions of PML-RARα in acute promyelocytic leukaemia. Br J Cancer 2011;104(4):554-8.
21. Asai T, Liu Y, Bae N, Nimer SD. The p53 tumor suppressor protein regulates hematopoietic stem cell fate. J Cell Physiol 2011; 226(9):2215-21.
22. Cheung N, So CW. Transcriptional and epigenetic networks in hematological malignancy. FEBS Lett 2011; 585(13):2100-11.

Domande di verifica

1. L'albumina:
   a. Ha una emivita di 48 ore
   b. È responsabile di circa il 75-80% della pressione oncotica
   c. Ha una concentrazione plasmatica di 12-14 g/L
   d. Ha un peso molecolare di 18 kDa

2. La transferrina:
   a. È sintetizzata principalmente dagli eritroblasti
   b. Lega il ferro con la stessa affinità del rame
   c. Non è glicosilata
   d. È formata da una singola catena polipeptidica di 679 aminoacidi

3. L'applicazione clinica più importante della misura dell'aptoglobina nel siero è:
   a. Verificare la presenza di emolisi intravascolare
   b. Valutare la fase acuta
   c. Valutare la gravità di una epatite acuta
   d. Escludere intossicazione cronica da alcol

4. Il punto chiave della cascata emocoagulativa è
   a. L'attivazione del fattore XI
   b. La formazione del complesso fra fattore VIIa e il fattore tissutale
   c. L'attivazione del fattore XII
   d. L'attivazione del fattore VIII

5. La trombina ha azione:
   a. Procoagulante,
   b. Anticoagulante,
   c. Antifibrinolitica
   d. Tutte le precedenti

6. Il D-dimero è utile in clinica per:
   a. Valutare il rischio emorragico
   b. Valutare la via intrinseca della coagulazione
   c. Escludere la presenza di malattia trombo-embolica
   d. Tutte le precedenti

7. Quali sono le classi di mutazioni geniche che più frequentemente sono associate a patologie oncoematologiche?
   a. Traslocazioni cromosomiche
   b. Mutazioni Puntiformi
   c. Inversioni cromosomiche
   d. Tutte le precedenti

8. Quali alterazioni funzionali sono state riscontrate a carico dei recettori per fattori di crescita nel campo onco-ematologico?
   a. Mutazioni puntiformi inattivanti
   b. Modifica del riconoscimento del ligando
   c. Attivazione della via del segnale associata al recettore mutato, indipendente dalla presenza del ligando
   d. Formazione di eterodimeri recettoriali in cui la catena mutata funziona da dominante negativo

9. Quali sono le proteine della trasduzione del segnale più frequentemente alterate nelle patologie onco-ematologiche?
   a. Tyrosino chinasi e serina/treonina chinasi
   b. Fattori trascrizionali
   c. Proteine ad attività GTP-asica
   d. Tutte le precedenti

10. Quale terapia molecolare è oggi utilizzata nella pratica clinica di pazienti affetti da Leucemia Mieloide Cronica?
    a. Inibitori della Farnesil Trasferasi
    b. Inibitori delle Tirosino chinasi
    c. Inibitori delle deacetilasi Istoniche
    d. Tutte le precedenti

Clinical Cancer Research

Interleukin 15 provides relief to cytotoxic T lymphocytes from regulatory T cell-mediated inhibition: implications for adoptive T-cell based therapies of lymphoma

Serena K Perna, Biagio De Angelis, Daria Pagliara, et al.

Clin Cancer Res Published OnlineFirst November 13, 2012.

Author Manuscript Published OnlineFirst on November 13, 2012; DOI:10.1158/1078-0432.CCR-12-2143
Author manuscripts have been peer reviewed and accepted for publication but have not yet been edited.

Interleukin 15 provides relief to cytotoxic T lymphocytes from regulatory T cell-mediated inhibition: implications for adoptive T-cell based therapies of lymphoma

Running title: HL-derived Treg suppression on CTLs countered by IL15

Serena K Perna, MD[1], Biagio De Angelis, PhD[1], Daria Pagliara, MD[1], Sayyeda T Hasan[1], Lan Zhang[1], Aruna Mahendravada[1], Helen E Heslop, MD[1,2,3], Malcolm K Brenner, MD, PhD[1,2,3], Cliona M Rooney, PhD[1,3,4,5], Gianpietro Dotti, MD[1,2,4] and Barbara Savoldo, MD, PhD[1,3]

[1]Center for Cell and Gene Therapy, Departments of [2]Medicine, [3]Pediatrics, [4]Immunology, [5]Molecular Virology and Microbiology, Baylor College of Medicine, The Methodist Hospital and Texas Children's Hospital, Houston TX 77030, USA.

Corresponding authors: Barbara Savoldo, MD, PhD

Center for Cell and Gene Therapy

Baylor College of Medicine

6621 Fannin St, MC 3-3320

Houston, TX 77030

Phone: 832-824-4725

Fax: 832-825-4732

Email: bsavoldo@bcm.edu

Author Manuscript Published OnlineFirst on November 13, 2012; DOI:10.1158/1078-0432.CCR-12-2143
Author manuscripts have been peer reviewed and accepted for publication but have not yet been edited.

STATEMENT OF TRANSLATIONAL RELEVANCE

Adoptive transfer of antigen-specific cytotoxic T lymphocytes (CTLs) represents a promising therapy for cancer patients and IL-2 is frequently administered to sustain *in-vivo* their expansion and persistence. However, IL-2 also induces systemic toxicities and boosts the proliferation and function of regulatory T cells (Tregs), known to suppress the antitumor activity of CTLs. Therefore, IL-2 administration can be detrimental in cancer patients with abundant Tregs. In view of these challenges, we studies the benefits of IL-15, another cytokines now available for clinical use to promote the engraftment of *ex-vivo* expanded CTLs in supporting their antitumor effects despite the presence of Tregs. We studied the effects of IL-15 in our model of Epstein Barr Virus (EBV)-associated Hodgkin Lymphomas that can be successfully treated with infusions of EBV-specific CTLs. Our study provides preclinical data suggesting that IL-15 should be preferred for clinical use when circulating or tumor-infiltrating Tregs are increased in cancer patients.

Author Manuscript Published OnlineFirst on November 13, 2012; DOI:10.1158/1078-0432.CCR-12-2143
Author manuscripts have been peer reviewed and accepted for publication but have not yet been edited.

ABSTRACT

Purpose: Systemic administration of recombinant IL-2 is used to support the expansion and persistence of adoptively transferred antigen-specific cytotoxic T lymphocytes (CTLs) in cancer patients. However, IL-2 also expands regulatory T cells (Tregs) that in turn impair the antitumor activity of CTLs. As recombinant IL-15 is approaching clinical applications, we assessed the effects of this cytokine on the proliferation and antitumor activity of CTLs in the presence of Tregs. We used the model of adoptive transfer of Epstein-Barr-Virus (EBV)-CTLs, as these cells induce responses in patients with EBV-associated Hodgkin Lymphoma (HL), and Tregs are frequently abundant in these patients.

Experimental design: Tregs were isolated from the peripheral blood of healthy donors and HL patients or from HL tumors and assessed for their ability to inhibit the proliferation and antitumor activity of EBV-CTLs in the presence of IL-15 or IL-2. Specific molecular pathways activated by IL-15 were also explored.

Results: We found that in the presence of Tregs, IL-15, but not IL-2, promoted the proliferation, effector function and resistance to apoptosis of effectors T cells and EBV-CTLs. IL-15 did not reverse or block Tregs, but instead preferentially supported the proliferation of CTLs and effector T cells as compared to Tregs.

Conclusions: IL-15 selectively favours the survival, proliferation and effector function of antigen-specific CTLs in the presence of Tregs and thus IL-15, unlike IL-2, would have a significant impact in sustaining expansion and persistence of adoptively transferred CTLs in cancer patients including those infused with EBV-CTLs for treatment of EBV-associated malignancies.

KEYWORDS: Tregs, IL-15, Hodgkin Lymphoma

INTRODUCTION

Adoptive transfer of antigen-specific cytotoxic T lymphocytes (CTLs) is a promising therapy for cancer patients(1-3). Specifically, we have previously shown that the adoptive transfer of Epstein-Barr virus-specific cytotoxic T lymphocytes (EBV-CTLs) in patients with EBV-associated Hodgkin Lymphoma (HL) is well tolerated and induces objective clinical responses(4, 5). However, several clinical trials have demonstrated significant correlation between the *in-vivo* persistence of adoptively transferred CTLs and the achievement of sustained tumor regression(6, 7), indicating that strategies aimed at enhancing CTL persistence *in-vivo* should translate in better clinical outcomes.

Growth factors play a crucial role in sustaining survival and proliferation of different T-cell subsets. In particular, CTLs expanded *ex-vivo* are highly dependent on cytokines such as interleukin(IL)-2 or IL-15 for their growth(8). However, these cytokines are frequently unavailable in the tumor environment, rendering CTLs short living, as they are immediately starved from these crucial survival factors. In order to overcome this limitation, recombinant human IL-2 is frequently administered to patients to support the expansion of adoptively transferred CTLs (9, 10). Although high doses of IL-2 may be effective, their benefits are frequently hampered by severe systemic toxicities(11-13). Moreover, IL-2 also facilitates the expansion of $CD4^+$ T lymphocytes with regulatory activity(14-17). These regulatory T cells (Tregs), characterized by the constitutive expression of the high affinity IL-2 receptor alpha (IL-2Rα, CD25) and of the forkhead box P3 (FoxP3) protein, actively inhibit the proliferation and function of effector T lymphocytes(18). Tregs are particularly relevant in cancer patients, since these cells are frequently increased in the peripheral blood and in tumor biopsies(19-21). In addition, their presence often correlates with poor clinical outcome(20, 21). In the specific case of HL, Tregs are found particularly abundant both in the circulation and at the tumor site(22-24), so that the

use of IL-2 to sustain *in-vivo* the expansion of adoptively transferred EBV-CTLs is highly discouraged.

IL-15 is another γ-chain cytokine that supports the proliferation and maintenance of effector T lymphocytes(25). Previous studies in mice have shown that the administration of IL-15 or the transgenic expression of IL-15 by effector T cells(26-28) enhance their anti-tumor effects. Recently IL-15 has been tested in nonhuman primates, showing a favorable toxicity profile, with a preferential increase in $CD8^+$ T lymphocyte counts and minimal effects on the absolute numbers of circulating Tregs(29, 30).

The effects of IL-15 on human Tregs remain largely unclear, due to differences in the doses used and in the origin of effector T cells and Treg subpopulations tested between studies(31-41) . Here we modeled *ex-vivo* culture conditions to assess the impact of IL-2 and IL-15 on the effector function of a specific subset of clinically relevant antigen-specific CTLs (EBV-CTLs), in the presence of Tregs isolated from both healthy donors and HL patients. In addition, in our experimental conditions we used doses of IL-2 and IL-15 that correspond to *in-vivo* measured cytokine trough levels(29, 30, 42) which makes the observed effects physiologically relevant.

Author Manuscript Published OnlineFirst on November 13, 2012; DOI:10.1158/1078-0432.CCR-12-2143
Author manuscripts have been peer reviewed and accepted for publication but have not yet been edited.

MATERIALS AND METHODS

Isolation of Tregs from healthy donors. We isolated PB mononuclear cells (PBMC) from the buffy coats of 10 healthy volunteers (Gulf Coast Regional Blood Center – Houston, Texas) by centrifugation on a density gradient (Ficoll, Axis-shield PoC AS, Oslo, Norway). Naturally occurring Tregs were enriched based on CD4 and bright expression of CD25 using immuno-magnetic selection, as previously described(43). Briefly, the $CD25^{bright}$ fraction was positively selected using non-saturating concentrations (2 µl/1x10^7 PBMC) of anti-human CD25 magnetic beads (Miltenyi Biotech, Germany) and further selected using anti-human CD4 magnetic beads (Miltenyi) following the manufacturer's instructions. The selection process resulted in a significant enrichment in cells coexpressing CD4, CD25 and FoxP3 (**Supplementary Fig. 1A**). As control we used cells obtained from the $CD4^+$ population after depletion of the $CD25^{bright}$ subset ($CD4^+CD25^{depleted}$) (defined as "control cells" throughout the manuscript), which lacked substantial FoxP3 expression (**Supplementary Fig. 1B**). In selected experiments, Tregs were isolated using a MoFLo sorter (Beckman Coulter Inc., Brea, CA) based on CD4, CD25 and CD45RA expression to obtain $CD4^+CD25^{++}CD45RA^+$, $CD4^+CD25^+CD45RA^+$ or $CD4^+CD25^+CD45RA^-$ cells as previously described(44) (**Supplementary Fig. 2**). To evaluate the effects of Tregs on specific T-cell subsets, we used immunomagnetic selection to enrich $CD45RO^+CD62L^+$, $CD45RO^+CD62L^-$ or $CD45RA^+CD62L^-$ cells from PBMC. Purity of isolated cells was >95% and the re-analysis included CCR7 expression (**Supplementary Fig. 1C**).

Isolation of Tregs from Hodgkin Lymphoma (HL) samples. PB and/or tumor biopsies from 21 patients with HL were provided by the lymphoma bank of an NCI-funded lymphoma SPORE (Baylor College of Medicine, Houston, TX). PBMC were isolated by centrifugation on a density gradient, while biopsies were gently smashed. Because of the limited number of cells usually obtained from these samples, Tregs were selected based on their $CD25^{bright}$ expression without any further enrichment (**Suppl. Table 1**).

Author Manuscript Published OnlineFirst on November 13, 2012; DOI:10.1158/1078-0432.CCR-12-2143
Author manuscripts have been peer reviewed and accepted for publication but have not yet been edited.

Activation of $CD4^+CD25^{bright}$ cells. $CD4^+CD25^{bright}$ cells were used directly in experiments or cultured for 7 days in RPMI 1640 medium (HyClone, Thermo Scientific) supplemented with 5% human AB-serum (Valley Biomedical, Winchester, VA), 1% penicillin/streptomycin (Sigma, St Louis, MO), 1% Glutamine (BioWhittaker Inc., Walkersville, MD), 0.1% 2β-Mercaptoethanol (Invitrogen, Carlsbad, CA), anti-CD3 antibody (OKT3, Orthoclone, Zug, Switzerland) (0.5 μg/ml) and γ-irradiated (40 Gy) allogeneic PBMC as feeders (at a PBMC:feeder ratio of 2:1). We added recombinant human IL-2 (25 IU/ml) (Teceleukin, Hoffmann-LaRoche, Rockville) or recombinant human IL-15 (2.5 ng/ml) (PeproTech Inc, Rocky Hill, NJ) in experiments, as indicated.

Single cell cloning of Tregs. In selected experiments, Tregs isolated from healthy donors and HL samples were single-cell cloned by limiting dilution. Briefly, $1x10^3$ Tregs were resuspended in RPMI 1640 medium supplemented with 5% human AB-serum, 1% penicillin/streptomycin, 2 mmol/L L-Glutamine, 0.1% 2β-Mercaptoethanol, OKT3 (50 ng/ml), γ-irradiated (40 Gy) allogeneic feeders and IL-2 (100 IU/ml). Tregs were plated in 96-wells plates at the concentration of 1 Treg/well with the described activation mixture and incubated for 3-4 weeks. Cells were fed weekly with IL-2. Growing cells were then screened for inhibitory activity using the Cell Lab Quanta™ SC MPL (Beckman Coulter Inc, Brea, CA). Inhibitory clones were further re-expanded using allogeneic γ-irradiated feeders, irradiated EBV-immortalized lymphoblastoid cell lines (LCL), OKT3 and IL-2 (100 U/mL) to reach sufficient numbers for further experiments, including suppression and antitumor assays in the presence of cytokines. Clonality was confirmed by Vβ-repertoire phenotype (data not shown). As control for experiments using Treg-derived clones, we expanded in parallel clones that lacked suppression activity when screened by the Cell Lab Quanta™ SC MPL.

Author Manuscript Published OnlineFirst on November 13, 2012; DOI:10.1158/1078-0432.CCR-12-2143
Author manuscripts have been peer reviewed and accepted for publication but have not yet been edited.

Generation of EBV-CTLs. EBV-CTLs were generated from the PBMCs obtained from EBV-seropositive healthy donors and HL patients (PB collected according to the local IRB approved protocol, Baylor College of Medicine) by weekly stimulation with γ-irradiated (40 Gy) autologous LCL with the addition of IL-2 (50 UI/mL) as previously described(1, 2, 4, 5).

Immunophenotyping. Cells were stained with fluorescein isothiocyanate (FITC)-, phycoerythrin (PE)-, peridinin-chlorophyll-protein complex (PerCP)-, or allophycocyanin (APC)-conjugated monoclonal antibodies (mAbs). We used CD3, CD4, CD8, CD19, CD45RA, CD45RO, CD62L and CD25 from Becton Dickinson (BD Bioscience, Mountain View, CA), CCR7 from R&D System (Minneapolis, MN, USA) and FoxP3 from eBioscience Inc (San Diego, CA, USA). IL-15Rα expression was detected using an anti-IL-15Rα mAb (R&D Systems) in conjunction with a FITC-goat anti-mouse IgG1 (SouthernBiotech, AL, USA). Control samples were labeled with appropriate isotype-matched Abs. TCR Vβ-repertoire was studied using a specific kit for flow cytometry analysis (IOTest® Beta Mark TCR-Vβ Repertoire Kit, Beckman Coulter). We analyzed STAT5 phosphorylation after stimulation with IL-15 for 15 minutes using the anti-phospho-STAT5 (Y694) mAb-Alexa-Fluor-647-Conjugate (BD Phosflow Reagents, San Jose, CA). We measured BCL-2 expression in the presence of IL-15 in EBV-CTLs after stimulation with autologous LCLs, as well as in T cells and Tregs after activation with OKT3 and irradiated feeders, using the PE-conjugated-hamster anti-human BCL-2 (6C8) (BD Bioscience). Phosphorylation of S6K1 after T-cell activation in the presence of IL-15 was assessed using Phospho-S6-Ribosomal protein (Ser235/236) rabbit mAb-Alexa-Fluor-647-conjugate (Cell Signaling Technologies, Danvers, MA), according to manufacturer's instruction. Cells were analyzed using a BD FACScalibur system equipped with the filter set for quadruple fluorescence signals and the CellQuest software (BD Biosciences). For each sample we analyzed a minimum of 10,000 events.

Author Manuscript Published OnlineFirst on November 13, 2012; DOI:10.1158/1078-0432.CCR-12-2143
Author manuscripts have been peer reviewed and accepted for publication but have not yet been edited.

Carboxyfluorescein diacetate succinimidyl ester (CFSE)–based assays. Proliferation of EBV-CTLs, T cells and Tregs was assessed by CFSE dilution. Cells were labeled with 1.5 μM CFSE (Invitrogen) and activated with LCLs, or OKT3 (0.5 μg/ml) and irradiated feeders (ratio 2:1) in the absence or in the presence of IL-2 (25 U/ml) or IL-15 (2.5 ng/ml). CFSE dilution was measured by flow cytometry after 7 days of culture. To evaluate suppressive activity of Tregs and Treg-clones, PBMC were labeled with 1.5 μM CFSE and activated with OKT3 (0.5 μg/ml) and feeders (ratio Tregs: feeders of 2:1), in the presence of Tregs/Treg-clones or control cells at a 1:1 (T cells: Tregs) ratio, and IL-2 (25 IU/ml or at the indicated doses for the titration experiment) or IL-15 (2.5 ng/ml or at the indicated doses) or of the IL-15/IL-15Rα complex. In selected experiments, the ratio of T cells and Tregs was titrated to 2:1 and 4:1. After 7 days, cells were labeled with CD8 and CD4, analyzed by FACS and cell division assessed by CSFE dilution. In selected experiments, the suppressive activity of $CD4^+CD25^{++}CD45RA^+$, $CD4^+CD25^+CD45RA^+$ or $CD4^+CD25^+CD45RA^-$ cells was evaluated.

Evaluation of antitumor activity. EBV-CTLs generated from 6 healthy donors were cultured in the presence of autologous LCLs with control cells or activated Tregs freshly isolated from healthy donors (at the EBV-CTLs:LCLs:Tregs ratio of 1:2:1) and in the absence or presence of IL-2 (25 IU/ml) or IL-15 (2.5 ng/ml). Similarly, EBV-CTLs generated from 3 patients with HL were cultured in the presence of autologous LCLs with control cells or activated HL-derived Treg-clones. After 7 days, cells were collected, stained with CD8, CD4 and CD3 to identify T cells, and CD19 to quantify residual tumor cells, and analyzed by FACS. To define Tumor cells, we considered only $CD19^+$ cells and not $CD3^+CD19^+$ cells, as the latter likely represent T cells that had acquired positivity for the CD19 through trogocytosis(45).

Evaluation of apoptosis. EBV-CTLs, T cells and Tregs were activated with LCLs or OKT3 (0.5 μg/ml) and irradiated feeders (ratio 2:1) in the absence or presence of IL-2 (25 U/ml) or IL-15

Author Manuscript Published OnlineFirst on November 13, 2012; DOI:10.1158/1078-0432.CCR-12-2143
Author manuscripts have been peer reviewed and accepted for publication but have not yet been edited.

(2.5 ng/ml) and, after 7 days, collected, washed and labeled with Annexin-V-PE-conjugated and 7AAD (BD Bioscience) according to manufacture's instruction. The percentage of Annexin-V^+7AAD^- cells was measured by FACS analysis. For each sample, at least 100,000 events were analyzed.

Enzyme-linked immunosorbent assay

The presence of the complex IL-15/IL-15Rα in our culture supernatant were quantified using a commercially available specific-ELISA kit (R&D Systems). PBMC (1 $x10^6$/well) were activated with OKT3, feeders and IL-15 (2.5 ng/ml), supernatants harvested every 24h for 7 days and analyzed for the presence of the IL-15/IL-15Rα complex. As positive control, we pre-incubated IL-15 (2.5ng/ml or 0.6 ng/ml) with recombinant human IL-15Rα/Fc Chimera (R&D System) for 30 min at room temperature (46).

Statistical analysis. Unless otherwise noted, data were summarized by means and standard errors of the mean. Student *t*-test was used to determine the statistical significant differences between samples, with *P* value <0.05 indicating a significant difference.

Author Manuscript Published OnlineFirst on November 13, 2012; DOI:10.1158/1078-0432.CCR-12-2143
Author manuscripts have been peer reviewed and accepted for publication but have not yet been edited.

RESULTS

Putative Tregs are increased in PB and tumor samples from patients with HL

We first analyzed PB samples and/or lymphonode biopsies from 21 patients with HL for the presence of putative Tregs based on the expression of CD4, CD25 and FoxP3 markers, and compared it with that of PB samples obtained from healthy donors. We observed a significant increase in the frequency of circulating and tumor infiltrating $CD4^+CD25^{bright}$ cells (7.4% ± 1.7% and 8.7% ± 0.9%, respectively) and $CD4^+FoxP3^+$ cells (5.3% ± 1.6% and 6.2% ± 1.2%, respectively) in samples from HL patients as compared to those detected in the PB of healthy donors (2.5% ± 1.1% for $CD4^+CD25^{bright}$ and 2.4% ± 0.96% for $CD4^+FoxP3^+$ cells, respectively) (**Fig. 1A**). To ensure that $CD4^+CD25^{bright}$ cells detected in PB and tumor biopsies were indeed functional Tregs, we isolated these cells by immuno-magnetic selection and performed suppression assays to assess their inhibitory properties. Although limited by the starting amount of blood/tissues from patient's samples (**Suppl. Table 1**), we isolated sufficient numbers of enriched putative Tregs from the majority of samples for further functional characterization. When tested in a CFSE-based suppression assay, $CD4^+CD25^{bright}$ cells from both healthy donors (**Fig. 1B**) and HL patients (**Fig. 1C**) showed inhibitory activity. Specifically for healthy donors, the addition of Tregs to the cultures inhibited the proliferation of $CD8^+$ and $CD4^+$ cells by 68% ± 6% and 71% ± 7%, respectively, as compared to the addition of control cells ($p<0.001$ for both) (**Fig. 1B**). Similarly, the addition of Tregs isolated from HL patients inhibited the proliferation of $CD8^+$ and $CD4^+$ cells by 43% ± 14% and 50% ± 11%, respectively, as compared to control cells ($p<0.05$ for both) (**Fig. 1C**). Although not statistically significantly, we attributed the relatively less efficient T-cell inhibition by Tregs isolated from HL patients the isolation procedures utilized when starting from patients *vs*. healthy donors samples, which lacked the CD4 selection step due to the limited size of the samples (**Suppl. Table 1**).

IL-15 but not IL-2 sustains the proliferation of T cells in the presence of Tregs

As the γ-chain cytokines IL-2 and IL-15 can be used to sustain the *in-vivo* persistence of adoptively transferred CTLs (9, 10), we compared the effects of these cytokines on effector T cells in the presence of Tregs. We selected doses of IL-2 and IL-15 of 25U/ml and of 2.5 ng/ml, respectively, as they correspond to *in-vivo* measured cytokine trough levels (29, 30, 42). For these experiments we first used Tregs isolated from healthy donors and then validated the results using Treg-clones generated from HL patients. The establishment of Treg-clones allowed us to overcome the difficulties in performing these experiments using the limited amount of Tregs isolated from patient's samples. As shown in **Fig. 2A**, we found 30% ± 2% inhibition of $CD8^+$ cell proliferation and 33% ± 4% inhibition of $CD4^+$ cell proliferation in the presence of IL-2 and Tregs isolated from healthy donors as compared to the addition of IL-2 and control cells ($p<0.01$ for both). In contrast, inhibition was negligible for both $CD8^+$ and $CD4^+$ cells in the presence of IL-15 and Tregs as compared to the addition of IL-15 and control cells (7% ± 4% and 10% ± 6% respectively, p=0.1 and p=0.2, respectively) (**Fig. 2A**).

Since the percentage of $CD4^+$ at the beginning of our culture conditions was 47% ± 3%, in our suppression assay, the ratio CD4 cell:Tregs was approximately 1:2. Although this excess of Tregs better reflect the unfavorable setting likely present *in-vivo*, to ensure that the limited ability of IL-2 to drive T-cell proliferation in the presence of Tregs was not related to the consumption of the cytokine by Tregs, we titrated the number of Tregs in the suppression assays and tested increased PBMC:Tregs ratios in the presence of IL-2. As shown in **Suppl Fig. 2A**, Tregs maintained their ability to inhibit the proliferation of both CD4 and CD8, despite the presence of IL-2, thus confirming the limited ability of IL-2 to support T cells proliferation in the presence of Tregs. In addition, because previous studies have shown that freshly isolated $CD4^+CD25^+FoxP3^+$ cells are functionally heterogeneous, as they may contain a subpopulation lacking suppressive activity ($CD25^+CD45RA^-$ cells), in selected experiments we isolated Tregs

by flow sorting based on the expression of CD25 and CD45RA as previously described(44) (**Suppl. Fig. 2B and C**). Using these cell subsets, proliferation of activated T cells remained impaired when $CD25^{+}CD45RA^{+}$ or $CD25^{++}CD45RA^{-}$ cells (also referred as resting Tregs and activated Tregs, respectively)(44) were added to the culture in the presence of IL-2 but not of IL-15, suggesting that the latter cytokine protects T cells from Treg-inhibition rather than preferentially favors the effects mediated by $CD25^{+}CD45RA^{-}$ cells, known to lack suppressive activity despite the expression of FoxP3(44).

Based on the protective effects of IL-15 using polyclonal Tregs isolated from healthy donors, we repeated the experiments using single cell cloned Tregs generated from the PB of healthy donors and HL patients. Since Treg-clones from healthy donors and from HL patients and polyclonal Tregs were equally effective in suppressing T-cell proliferation (**Fig. 2B**), we validated the effects of IL-2 and IL-15 using Treg-clones. Similarly to polyclonal Tregs, both Treg-clones from healthy donors and HL patients significantly inhibited T-cell proliferation either in the absence of cytokine (73% ± 6% and 64% ± 8%, respectively) or in the presence of IL-2 (46% ± 12% and 32% ± 7%, respectively) as compared to control cells (**Fig. 2C and D**). In sharp contrast, the addition of IL-15 sustained T-cell proliferation in the presence of Treg-clones from HD and from HL (19% ± 10% inhibition and 5% ± 6%, respectively) as compared to control cells (**Fig. 2C and 2D**), indicating that IL-15, but not IL-2, significantly protects T cells from Treg-clone mediated inhibition ($p<0.01$).

Interestingly, when we titrated the amount of IL-15 in the culture system, we confirmed that low doses of IL-15 (in the range of 1.25 – 2.5 ng/ml, similar to that observed *in-vivo*)(29, 30) were sufficient to preserve the proliferation of T cells in the presence of Tregs (**Suppl. Fig. 3A**). In contrast, T cells could proliferate despite the presence of Tregs only in the presence of very high doses (>50U/ml) of IL-2, which corresponds to through levels associated with sever toxic events *in-vivo*(12, 13, 42). More importantly, we found that T-cell proliferation was preserved in

the presence of Tregs even when a very low dose of IL-15 (0.6 ng/ml) was added to the culture as heterodimeric complex with the IL-15Rα (**Suppl. Fig. 3B and C**) which is the bioactive form of IL-15 detected in the serum of patients(47). This suggests that in the presence of the IL-15/IL-15Rα complex very low doses of recombinant IL-15 may be sufficient in providing the expected relief from Treg-mediated inhibition *in-vivo* (**Suppl. Fig. 3**), while minimizing the systemic toxicity associated with high doses of cytokines(30).

IL-15 specifically preserves the antitumor effects of EBV-CTLs in the presence of Tregs

Since *ex-vivo* expanded EBV-CTLs used for adoptive T-cell therapy in HL(4, 5) and antigen-specific CTLs in general used for antitumor therapy are mainly composed of $CD45RO^+$ effector cells, with a majority of T_{EM} cells and a lower and variable proportion of the T_{CM} (23% ± 8%)(48-50), we first investigated if IL-15 protects the $CD45RO^+$ T-cell subset from Treg-mediated inhibition, in an antigen-independent manner. Therefore we measured the suppressive activity of Tregs against $CD45RO^+CD62L^+$, $CD45RO^+CD62L^-$ or $CD45RA^+CD62L^-$cells, as a source of central-memory, effector-memory and terminally differentiated T cells, respectively. We found that Tregs significantly inhibited the proliferation of T_{CM} cells, irrespective of whether we added IL-2 (42% ± 6%) or IL-15 (40% ± 7%) (**Fig. 3A**). In contrast, IL-15 more effectively sustained the proliferation of T_{EM} cells and T_{EMRA} cells in the presence of Tregs, as the percentage of inhibition was 35% ± 5% and 58% ± 8% in the presence of IL-2, but only 27% ± 5% and 36% ± 10% in the presence of IL-15 ($p<0.05$) (**Fig. 3B and C**). Hence, IL-15 seems to preferentially protect effector T cells (T_{EM} and T_{EMRA}) from the inhibitory effects of Tregs.

Then, IL-15 mediated protection was confirmed in our model of EBV-CTLs. As illustrated in **Fig. 4A**, when EBV-CTLs generated from healthy donors were cocultured with autologous LCL (1:2 CTL:LCL ratio to ensure an excess of target cells), the percentage of residual $CD19^+$ tumor cells, as assessed by flow cytometry by day 5-7, was 67% ± 11% in the cocultures containing Tregs

versus 36% ± 12% in control cultures ($p<0.01$), indicating that Tregs significantly impair the elimination of target cells by effector CTLs. We next assessed the effects of adding IL-2 or IL-15 to these cultures. As shown in **Fig. 4A**, the effector function of EBV-CTLs generated from healthy donors remained impaired by Tregs in the presence of IL-2, as the percentage of residual tumor cells increased from 22% ± 9% in the cocultures containing IL-2 and control cells to 42% ± 13% in cocultures containing IL-2 and Tregs isolated from healthy donors ($p<0.01$). In contrast, in the presence of IL-15, the effector function of EBV-CTLs was sustained with or without Tregs (residual tumor cells 11% ± 6% in IL-15 cultures with control cells versus 13% ± 5% in IL-15 with Tregs, p=NS) (**Fig. 4A**). Similar results were observed when EBV-CTLs generated from HL patients were cocultured with autologous LCL in the presence of HL-derived Treg-clones. As shown in **Fig. 4B**, residual tumor cells increased from 11% ± 1% in cocultures containing IL-2 and control cells, to 56% ± 9% in co-cultures containing IL-2 and Treg-clones ($p<0.01$). In contrast, in the presence of IL-15, the effector function of EBV-CTLs generated from HL patients was sustained with or without Tregs (residual tumor cells 4% ± 1% in IL-15 cultures with control cells versus 10% ± 1% in IL-15 with Tregs). Hence, IL-15 can preserve the effector function of antigen-specific CTLs in the presence of Tregs.

IL-15-mediated protection is due to a preferential increased proliferation and reduced cell death of effector T cells as compared to Tregs

To discover the mechanisms responsible for the protective effects of IL-15, we dissected the effects of this cytokine on Tregs and on effector T cells. First, we found that the protective effects of IL-15 were not determined by a reversal of Treg-inhibitory properties. Indeed, freshly isolated Tregs that had been activated and cultured for 7 days in the presence of IL-15, when tested in the suppression assay in the absence of cytokines, retained their inhibitory functions and blocked the proliferation of activated T cells (from 61% ± 7% to 34% ± 5%, in the presence of Tregs previously expanded in IL-15) ($p<0.01$) (**Fig. 5A**).

Author Manuscript Published OnlineFirst on November 13, 2012; DOI:10.1158/1078-0432.CCR-12-2143
Author manuscripts have been peer reviewed and accepted for publication but have not yet been edited.

When we looked at T-cell proliferation and expression of anti-apoptotic molecules accompanying the exposure to IL-15 (8, 25), we found a differential effect of this cytokine on effector T cells and Tregs, which were also different form the effects that IL-2 had on these populations. First, IL-15 significantly increased the division rate of $T_{EM/EMRA}$ cells (82% ± 3%), and EBV-CTLs (87% ± 2%) as compared to Tregs (58% ± 9%) (p=0.02 and p=0.01, respectively) (**Fig. 5B**). IL-2, instead, induced proliferation of Tregs (73% ± 7%) comparable to that of $T_{EM/EMRA}$ cells (76% ± 5%) and EBV-CTLs (77% ± 5%) (p=NS).

Second, in the presence of IL-15, apoptotic cells (Annexin-V^+7AAD^-) were significantly lower in $T_{EM/EMRA}$ cells (7% ± 2%) and EBV-CTLs (5% ± 1%) as compared to Tregs (14% ± 3%) (p=0.04 and p=0.03, respectively) (**Fig.5C**). In contrast, in the presence of IL-2 the percentage of apoptotic cells was similar in $CD45RO^+CD62L^-$ effector cells (11% ± 4%), EBV-CTLs (7% ± 1%) and Tregs (10% ± 3%) (p=NS). Hence, our data suggest that IL-15, unlike IL-2 has a differential effect on proliferation and apoptosis in effector and regulatory T cells.

Upon further investigation, we observed that IL-15 activates different pathways in Tregs and effector T cells, despite the expression of the IL-15Rα was similar in all subsets (**Fig. 6A**), and STAT5 phosphorylation was comparable in Tregs (63% ± 19%) and effector T cells ($T_{EM/EMRA}$, 48% ± 6%, EBV-CTLs, 76% ± 11%) following exposure to IL-15 (**Fig. 6B**). We found that in response to IL-15, phosphorylation of S6K1, a downstream target associated with a proliferative signature, was significantly higher in effector cells ($T_{EM/EMRA}$ = 16% ± 7%; EBV-CTLs = 48% ± 9%) as compared to Tregs (2% ± 0.4%) (**Fig 6C**). A similar pattern was, however, observed also in response to IL-2, with higher phosphorylation of S6K1 in effector T cells ($T_{EM/EMRA}$ = 31% ± 13%; EBV-CTLs = 37% ± 10%) as compared to Tregs (2% ± 1%) (**Fig 6C**). This prompted us to focus on potential differential effects of IL-2 and IL-15 in the apoptotic pathway.

Indeed, effector T cells significantly upregulated BCL-2 in response to IL-15 (MFI from 17 ± 3 to 24 ± 3 for $T_{EM/EMRA}$, and from 23 ± 2 to 37 ± 4 for EBV-CTLs), which was significantly better as

compared to IL-2 (15 ± 2 for $T_{EM/EMRA}$, and 26 ± 4 for EBV-CTLs), while both cytokines induced no equivalent BCL-2 upregulation in Tregs (MFI from 10 ± 1 to 9 ± 1 for IL-15 and to 8 ± 2 for IL-2) (**Fig. 5D**). Overall, these data suggest that the simultaneous preferential proliferation and resistance to apoptosis in effector T cells than in Tregs mediated by IL-15, but not by IL-2, may provide better resilience of effector T cells to Treg-inhibitory activity.

Discussion

The toxicity associated with the systemic administration of γ-chain cytokines, used to support the *in-vivo* persistence of adoptively transferred tumor-specific CTLs(12, 13), and the effects that these cytokines exert on the host inhibitory Tregs(14-17) remain obstacles to improve the clinical benefits of adoptive immunotherapy-based approaches. To address the specific issue of γ-chain cytokines and Tregs, we have analyzed the effects of IL-2 and IL-15 in our model of EBV-CTLs. We show that IL-15, but not IL-2, supports EBV-CTL effector function and proliferation in the presence of Tregs isolated from healthy donors or patients with HL. This protection from Treg-suppressive effects can be related to the enhanced proliferation and reduced activation induced cell death that IL-15 provides to effectors T cells but not to Tregs, likely through the activation of different pathways in effector T cells as compared to Tregs.

The infusion of tumor infiltrating T lymphocytes (TIL) and EBV-CTLs that have been expanded *in vitro* has shown clinical benefits in patients with melanoma and EBV-associated malignancies, including HL, respectively(2-5). Yet, IL-2 is often required to sustain CTL persistence and expansion *in-vivo*(9, 10). On the other hand, the administration of IL-2 induces systemic toxicities and enhances proliferation and function of Tregs, a subset of lymphocytes that suppress CTL proliferation and function(14-17). As a result of these dual properties, the administration of IL-2 can be particularly detrimental when EBV-CTLs are adoptively transferred in HL patients. The expansion of the transferred T cells would indeed be offset by an equivalent or superior expansion of Tregs that are particularly abundant in the peripheral blood and at the tumor site of HL patients(19, 22-24).

Efforts have been made to identify alternative growth factors that can promote robust engraftment of *ex-vivo* expanded antigen-specific CTLs without concomitant enhancement of Treg activity. IL-15, that is now entering clinical trials(29, 30), has the potential to be less toxic

than IL-2(8). However, previous pre-clinical models have produced somewhat contradictory results regarding the specific effects of IL-15 on Tregs. For example, short pre-incubation of human T lymphocytes with IL-15 protects their proliferation and IFNγ production in the presence of Tregs(39). Moreover, studies in nonhuman primates, have shown that IL-15 produces excellent expansion of T cells but limited effects on Tregs(29, 30). These beneficial effects of IL-15 on T lymphocytes concur with the observation that human autoimmune disorders, including rheumatoid arthritis, psoriasis and celiac diseases, are associated with the local overexpression of IL-15, which may favor a pro-inflammatory environment allowing autoreactive T cells to overcome the inhibition of functional Tregs(33-35). By contrast, other studies suggest that IL-15 can amplify both Treg number and suppressive function(37, 38), and contributes to their *de novo* generation(18, 32, 36-39, 51, 52). Finally, *IL-2*$^{-/-}$ *X IL-15*$^{-/-}$ mice show significantly decreased numbers of Tregs(31), and treatment with IL-15 promotes Treg activity sufficiently to protect NK-depleted NOG mice against developing diabete (38). These apparently disparate results may be in part attributable to differences in the distribution of the expression of the IL-15 private receptor (IL-15Rα). Unlike the IL-2α chain (CD25), which is constitutively expressed on Tregs, expression of IL-15Rα is more heterogeneous(53), so that the net effects produced on effector T cells and Tregs may be dependent on the precise target population, cytokine concentration and read-out used.

Our study has focused on the influence of IL-15 and Tregs specifically on EBV-CTLs and CD4 and CD8 effector subsets in general, when present in a complex cellular mixture, rather than on the selected $CD4^{+}CD25^{depleted}$ population, since the latter may not take into account the effects that each subset provides to the whole population(39, 54). In addition, testing the effect of the cytokines on the CD4/CD8 effector population should better predict the consequences of administering IL-15 as part of clinical studies since the majority of adoptively transferred CTLs

are CD4/CD8 effector/cytotoxic T cells(2, 4, 5). In addition, to ensure that our *ex-vivo* studies would better predict clinical relevance, we used a dose of IL-15 that is safely obtained *in-vivo* in nonhuman primates (29, 30). Although lower than concentrations used by many other studies, this is more likely to reflect concentrations that will be obtained in humans. Moreover, we used a CFSE-based assay to measure Treg-mediated inhibition rather than thymidine-incorporation assays that may fail to discriminate between proliferation of Tregs and effector T cells.

We found that IL-15, but not IL-2, supports T-cell effector function in *ex-vivo* coculture experiments that, similarly to tumor environment, put them simultaneously and for a prolonged period of time in contact with tumor cells and Tregs. IL-15, but not IL-2, preserves the proliferation and effector function of T cells and CTLs in the presence of Tregs either isolated from healthy donors or patients with HL. IL-15 also protects CTLs from apoptosis. Hence, by providing IL-15 it may be possible to sustain protection of CTLs against Tregs *in-vivo*.

Why does IL15 produce these differential effects in antigen-specific CTLs and effector T cells in general as compared to Tregs? Although our experiments illustrate that IL-15 is functional in Tregs, this cytokine does not modify their inhibitory function. However, the proliferation and resistance to apoptosis mediated by IL-15 is greater in effector T cells than in Tregs, so that the net activity of effector T cells is increased, both in term of proliferative potential and cytotoxic activity. We and others(37) have shown that the IL-15 private receptor (IL-15Rα) is expressed at low level both on Tregs and effector T cells, so that the differential effects of IL-15 on each subset likely lies in differences in downstream signaling and not on different expression levels of the receptor. IL-15 is also active when antigen presenting cells trans-present the IL-15Rα thus by-passing the need for IL-15Rα expression by target cells(53). However, this mechanism should be equally available to both effector T cells and Tregs, and again cannot explain the differential effects of IL-15 in these two cell subsets. When tested specifically, we found that IL-

15 supports T-cell proliferation in the presence of Tregs, regardless of its presence in a soluble form or in a complex with IL-15Rα. This may have additional important implications *in-vivo,* as the complex IL-15/IL-15Rα not only is more stable, has enhanced activity, and is the preferential form of IL-15 present in the serum of patients(47), but can further reduce the dose of IL-15 required to overcome the inhibitory effect of Tregs, thus further reducing the potential toxicity of this cytokine.

Exploring the down stream signaling of IL-15, we found that STAT5 was equally phosphorylated in effector T cells and Tregs after IL-15 exposure. By contrast, there was divergence in PI-3 kinase mediated signaling between effector T cells and Tregs in response to IL-15, with the former showing greater and simultaneous $p70^{S6Kinase}$ phosphorylation and BCL-2 expression, effects that are respectively consistent with their superior proliferation and resistance to apoptosis. It will be of future interest to analyze interactions with other modulatory pathways to provide a more detailed underpinning for the differential effects on PI-3 Kinase mediated signaling we report.

We conclude that since IL-15 benefits both the proliferative and antitumor activity of EBV-CTLs and effector T cells in general, without an equivalent increase in the inhibitory activity of Tregs, this cytokine could be of clinical value for patients with HL and other patients receiving T-cell therapies for their disease, and should be preferred when circulating or tumor-infiltrating Tregs are increased.

COMPETING FINANCIAL INTEREST

The authors have no competing financial interest.

All authors reviewed the manuscript and approved the final version of the manuscript.

AUTHORSHIP

S.K.P., G.D. and B.S. designed the research, analyzed the data and wrote the manuscript

S.K.P., B.DA. and D.P performed the experiments

S.T.H., L.Z. and A.M. provided technical assistance for some of the experiments

H.E.H., M.K.B and C.M.R. provided assistance in the design of the research and critically reviewed the manuscript.

ACKNOWLEDGEMENTS

This work was supported by grants: P50CA126752 (H.E.H.) and R01 CA131027 (B.S.).

S.K.P. is supported by a fellowship from the EHA-ASH Translational Research Training in Hematology; H.E.H. is supported by a Dan L Duncan Chair; M.K.B is supported by a Fayez Sarofim Chair; G.D. is supported by NIH R01 CA142636, a Leukemia and Lymphoma Society Translational Research grant and W81XWH-10-10425 Department of Defense, Technology/Therapeutic Development Award; B.S. is supported by NIH R01CA131027 and a Leukemia and Lymphoma Society Translational Research grant.

Reference List

(1) Rooney CM, Smith CA, Ng CY, Loftin SK, Sixbey JW, Gan Y, et al. Infusion of cytotoxic T cells for the prevention and treatment of Epstein-Barr virus-induced lymphoma in allogeneic transplant recipients. Blood 1998;92:1549-55.

(2) Savoldo B, Goss JA, Hammer MM, Zhang L, Lopez T, Gee AP, et al. Treatment of solid organ transplant recipients with autologous Epstein Barr virus-specific cytotoxic T lymphocytes (CTLs). Blood 2006;108:2942-9.

(3) Rosenberg SA, Restifo NP, Yang JC, Morgan RA, Dudley ME. Adoptive cell transfer: a clinical path to effective cancer immunotherapy. Nat Rev Cancer 2008;8:299-308.

(4) Bollard CM, Aguilar L, Straathof KC, Gahn B, Huls MH, Rousseau A, et al. Cytotoxic T lymphocyte therapy for Epstein-Barr virus+ Hodgkin's disease. J Exp Med 2004;200:1623-33.

(5) Roskrow MA, Suzuki N, Gan Y, Sixbey JW, Ng CY, Kimbrough S, et al. Epstein-Barr virus (EBV)-specific cytotoxic T lymphocytes for the treatment of patients with EBV-positive relapsed Hodgkin's disease. Blood 1998;91:2925-34.

(6) Rosenberg SA, Packard BS, Aebersold PM, Solomon D, Topalian SL, Toy ST, et al. Use of tumor-infiltrating lymphocytes and interleukin-2 in the immunotherapy of patients with metastatic melanoma. A preliminary report. N Engl J Med 1988;319:1676-80.

(7) Dudley ME, Rosenberg SA. Adoptive-cell-transfer therapy for the treatment of patients with cancer. Nat Rev Cancer 2003;3:666-75.

(8) Waldmann TA, Dubois S, Tagaya Y. Contrasting roles of IL-2 and IL-15 in the life and death of lymphocytes: implications for immunotherapy. Immunity 2001;14:105-10.

(9) Yee C, Thompson JA, Byrd D, Riddell SR, Roche P, Celis E, et al. Adoptive T cell therapy using antigen-specific CD8+ T cell clones for the treatment of patients with metastatic melanoma: in vivo persistence, migration, and antitumor effect of transferred T cells. Proc Natl Acad Sci U S A 2002;99:16168-73.

(10) Dudley ME, Wunderlich JR, Robbins PF, Yang JC, Hwu P, Schwartzentruber DJ, et al. Cancer regression and autoimmunity in patients after clonal repopulation with antitumor lymphocytes. Science 2002;298:850-4.

(11) Lotze MT, Matory YL, Ettinghausen SE, Rayner AA, Sharrow SO, Seipp CA, et al. In vivo administration of purified human interleukin 2. II. Half life, immunologic effects, and expansion of peripheral lymphoid cells in vivo with recombinant IL 2. J Immunol 1985;135:2865-75.

(12) Atkins MB. Interleukin-2: clinical applications. Semin Oncol 2002;29:12-7.

(13) Siegel JP, Puri RK. Interleukin-2 toxicity. J Clin Oncol 1991;9:694-704.

(14) Zorn E, Mohseni M, Kim H, Porcheray F, Lynch A, Bellucci R, et al. Combined CD4+ donor lymphocyte infusion and low-dose recombinant IL-2 expand FOXP3+ regulatory T cells following allogeneic hematopoietic stem cell transplantation. Biol Blood Marrow Transplant 2009;15:382-8.

(15) Weiss L, Letimier FA, Carriere M, Maiella S, Donkova-Petrini V, Targat B, et al. In vivo expansion of naive and activated CD4+CD25+FOXP3+ regulatory T cell populations in interleukin-2-treated HIV patients. Proc Natl Acad Sci U S A 2010;107:10632-7.

(16) Sereti I, Imamichi H, Natarajan V, Imamichi T, Ramchandani MS, Badralmaa Y, et al. In vivo expansion of CD4CD45RO-CD25 T cells expressing foxP3 in IL-2-treated HIV-infected patients. J Clin Invest 2005;115:1839-47.

(17) Malek TR. The main function of IL-2 is to promote the development of T regulatory cells. J Leukoc Biol 2003;74:961-5.

(18) Dieckmann D, Plottner H, Berchtold S, Berger T, Schuler G. Ex vivo isolation and characterization of CD4(+)CD25(+) T cells with regulatory properties from human blood. J Exp Med 2001;193:1303-10.

(19) Li J, Qian CN, Zeng YX. Regulatory T cells and EBV associated malignancies. Int Immunopharmacol 2009;9:590-2.

(20) Curiel TJ, Coukos G, Zou L, Alvarez X, Cheng P, Mottram P, et al. Specific recruitment of regulatory T cells in ovarian carcinoma fosters immune privilege and predicts reduced survival. Nat Med 2004;10:942-9.

(21) Wolf AM, Wolf D, Steurer M, Gastl G, Gunsilius E, Grubeck-Loebenstein B. Increase of regulatory T cells in the peripheral blood of cancer patients. Clin Cancer Res 2003;9:606-12.

(22) Schreck S, Friebel D, Buettner M, Distel L, Grabenbauer G, Young LS, et al. Prognostic impact of tumour-infiltrating Th2 and regulatory T cells in classical Hodgkin lymphoma. Hematol Oncol 2008.

(23) Marshall NA, Christie LE, Munro LR, Culligan DJ, Johnston PW, Barker RN, et al. Immunosuppressive regulatory T cells are abundant in the reactive lymphocytes of Hodgkin lymphoma. Blood 2004;103:1755-62.

(24) Baumforth KR, Birgersdotter A, Reynolds GM, Wei W, Kapatai G, Flavell JR, et al. Expression of the Epstein-Barr virus-encoded Epstein-Barr virus nuclear antigen 1 in Hodgkin's lymphoma cells mediates Up-regulation of CCL20 and the migration of regulatory T cells. Am J Pathol 2008;173:195-204.

(25) Waldmann TA. IL-15 in the life and death of lymphocytes: immunotherapeutic implications. Trends Mol Med 2003;9:517-21.

(26) Klebanoff CA, Finkelstein SE, Surman DR, Lichtman MK, Gattinoni L, Theoret MR, et al. IL-15 enhances the in vivo antitumor activity of tumor-reactive CD8+ T cells. Proc Natl Acad Sci U S A 2004;101:1969-74.

(27) Quintarelli C, Vera JF, Savoldo B, Giordano Attianese GM, Pule M, Foster AE, et al. Co-expression of cytokine and suicide genes to enhance the activity and safety of tumor-specific cytotoxic T lymphocytes. Blood 2007;110:2793-802.

(28) Hoyos V, Savoldo B, Quintarelli C, Mahendravada A, Zhang M, Vera J, et al. Engineering CD19-specific T lymphocytes with interleukin-15 and a suicide gene to enhance their anti-lymphoma/leukemia effects and safety. Leukemia 2010;24:1160-70.

(29) Berger C, Berger M, Hackman RC, Gough M, Elliott C, Jensen MC, et al. Safety and immunologic effects of IL-15 administration in nonhuman primates. Blood 2009;114:2417-26.

(30) Waldmann TA, Lugli E, Roederer M, Perera LP, Smedley JV, Macallister RP, et al. Safety (toxicity), pharmacokinetics, immunogenicity, and impact on elements of the normal immune system of recombinant human IL-15 in rhesus macaques. Blood 2011;117:4787-95.

(31) Soper DM, Kasprowicz DJ, Ziegler SF. IL-2Rbeta links IL-2R signaling with Foxp3 expression. Eur J Immunol 2007;37:1817-26.

(32) Wuest TY, Willette-Brown J, Durum SK, Hurwitz AA. The influence of IL-2 family cytokines on activation and function of naturally occurring regulatory T cells. J Leukoc Biol 2008;84:973-80.

(33) Ruprecht CR, Gattorno M, Ferlito F, Gregorio A, Martini A, Lanzavecchia A, et al. Coexpression of CD25 and CD27 identifies FoxP3+ regulatory T cells in inflamed synovia. J Exp Med 2005;201:1793-803.

(34) Zanzi D, Stefanile R, Santagata S, Iaffaldano L, Iaquinto G, Giardullo N, et al. IL-15 Interferes With Suppressive Activity of Intestinal Regulatory T Cells Expanded in Celiac Disease. Am J Gastroenterol 2011;106:1308-17.

(35) Benito-Miguel M, Garcia-Carmona Y, Balsa A, Perez de AC, Cobo-Ibanez T, Martin-Mola E, et al. A dual action of rheumatoid arthritis synovial fibroblast IL-15 expression on the equilibrium between CD4+CD25+ regulatory T cells and CD4+CD25- responder T cells. J Immunol 2009;183:8268-79.

(36) Imamichi H, Sereti I, Lane HC. IL-15 acts as a potent inducer of CD4(+)CD25(hi) cells expressing FOXP3. Eur J Immunol 2008;38:1621-30.

(37) Xu S, Sun Z, Sun Y, Zhu J, Li X, Zhang X, et al. IL-15 and dendritic cells induce proliferation of CD4(+)CD25(+) regulatory T cells from peripheral blood. Immunol Lett 2011.

(38) Xia J, Liu W, Hu B, Tian Z, Yang Y. IL-15 promotes regulatory T cell function and protects against diabetes development in NK-depleted NOD mice. Clin Immunol 2010;134:130-9.

(39) Ben AM, Belhadj HN, Moes N, Buyse S, Abdeladhim M, Louzir H, et al. IL-15 renders conventional lymphocytes resistant to suppressive functions of regulatory T cells through activation of the phosphatidylinositol 3-kinase pathway. J Immunol 2009;182:6763-70.

(40) Burchill MA, Yang J, Vogtenhuber C, Blazar BR, Farrar MA. IL-2 receptor beta-dependent STAT5 activation is required for the development of Foxp3+ regulatory T cells. J Immunol 2007;178:280-90.

(41) Bensinger SJ, Walsh PT, Zhang J, Carroll M, Parsons R, Rathmell JC, et al. Distinct IL-2 receptor signaling pattern in CD4+CD25+ regulatory T cells. J Immunol 2004;172:5287-96.

(42) Piscitelli SC, Forrest A, Vogel S, Chaitt D, Metcalf J, Stevens R, et al. Pharmacokinetic modeling of recombinant interleukin-2 in patients with human immunodeficiency virus infection. Clin Pharmacol Ther 1998;64:492-8.

(43) Godfrey WR, Ge YG, Spoden DJ, Levine BL, June CH, Blazar BR, et al. In vitro-expanded human CD4(+)CD25(+) T-regulatory cells can markedly inhibit allogeneic dendritic cell-stimulated MLR cultures. Blood 2004;104:453-61.

(44) Miyara M, Yoshioka Y, Kitoh A, Shima T, Wing K, Niwa A, et al. Functional delineation and differentiation dynamics of human CD4+ T cells expressing the FoxP3 transcription factor. Immunity 2009;30:899-911.

(45) Joly E, Hudrisier D. What is trogocytosis and what is its purpose? Nat Immunol 2003;4:815.

(46) Epardaud M, Elpek KG, Rubinstein MP, Yonekura AR, Bellemare-Pelletier A, Bronson R, et al. Interleukin-15/interleukin-15R alpha complexes promote destruction of established tumors by reviving tumor-resident CD8+ T cells. Cancer Res 2008;68:2972-83.

(47) Bergamaschi C, Bear J, Rosati M, Beach RK, Alicea C, Sowder R, et al. Circulating IL-15 exists as heterodimeric complex with soluble IL-15Ralpha in human and mouse serum. Blood 2012;120:e1-e8.

(48) Pule MA, Savoldo B, Myers GD, Rossig C, Russell HV, Dotti G, et al. Virus-specific T cells engineered to coexpress tumor-specific receptors: persistence

and antitumor activity in individuals with neuroblastoma. Nat Med 2008;14:1264-70.

(49) Dotti G, Savoldo B, Pule M, Straathof KC, Biagi E, Yvon E, et al. Human cytotoxic T lymphocytes with reduced sensitivity to Fas-induced apoptosis. Blood 2005;105:4677-84.

(50) Dunne PJ, Faint JM, Gudgeon NH, Fletcher JM, Plunkett FJ, Soares MV, et al. Epstein-Barr virus-specific CD8(+) T cells that re-express CD45RA are apoptosis-resistant memory cells that retain replicative potential. Blood 2002;100:933-40.

(51) Burchill MA, Yang J, Vang KB, Farrar MA. Interleukin-2 receptor signaling in regulatory T cell development and homeostasis. Immunol Lett 2007;114:1-8.

(52) Yates J, Rovis F, Mitchell P, Afzali B, Tsang JY, Garin M, et al. The maintenance of human CD4+ CD25+ regulatory T cell function: IL-2, IL-4, IL-7 and IL-15 preserve optimal suppressive potency in vitro. Int Immunol 2007;19:785-99.

(53) Dubois S, Mariner J, Waldmann TA, Tagaya Y. IL-15Ralpha recycles and presents IL-15 In trans to neighboring cells. Immunity 2002;17:537-47.

(54) Waldmann TA. The biology of interleukin-2 and interleukin-15: implications for cancer therapy and vaccine design. Nat Rev Immunol 2006;6:595-601.

Author Manuscript Published OnlineFirst on November 13, 2012; DOI:10.1158/1078-0432.CCR-12-2143
Author manuscripts have been peer reviewed and accepted for publication but have not yet been edited.

FIGURE LEGENDS

Fig. 1. Phenotypical and functional characterization of Tregs isolated from healthy donors and patients affected by HL. Phenotype and inhibitory function of Tregs freshly isolated from the PB of 10 healthy donors, 21 biopsies collected from HL patients and PB from 7 HL patients were assessed by FACS. **Panel A** shows plots for CD4 vs. CD25, CD4 vs. FoxP3 and CD25 vs. FoxP3 of circulating Tregs from a representative healthy donor and a patient with HL. The graph shows the summary of percentages of Tregs quantified by FACS. * p = 0.05. **Panel B** shows the proliferation of $CD8^+$ or $CD4^+$ cells in the presence of control or Tregs freshly isolated from one representative healthy donor. The graph shows the percentage of inhibition (mean ± SEM) for 10 independent experiments. **Panel C** shows the proliferation of $CD8^+$ or $CD4^+$ cells in the presence of control cells or Tregs freshly isolated from one representative patient with HL. The graph shows the percentage of inhibition for 4 independent experiments.

Fig. 2. IL-15 sustains T-cell proliferation in the presence of Tregs or Treg-clones derived from healthy donors or HL patients. Tregs were tested for their ability to inhibit T-cell proliferation using a CFSE-based suppression assay with or without IL-2 or IL-15. **Panel A** illustrates the proliferation of T cells in the absence of cytokines or in the presence of IL-2 or IL-15 with control cells or Tregs in one representative healthy donor. The graph summarize the inhibition mediated by Tregs for $CD8^+$ and $CD4^+$ cells (mean ± SD) for the 10 donors. *p<0.01. **Panel B** shows representative histograms for the proliferation of activated PBMC in the presence of freshly isolated Tregs, or in the presence of a healthy donor-derived Treg-clone or a HL-derived Treg-clone. Graph summarizes mean ± SEM of 4 donors/each. **Panel C** shows representative histograms for the proliferation of activated PBMC in the presence of control cells or a healthy donor-derived Treg clone with or without cytokines. The graph summarizes the inhibition mediated by Treg-clones from 4 donors. *p<0.05. **Panel D** shows representative histograms for the proliferation of activated PBMC in the presence of control cells or a HL-

derived Treg clone with or without cytokines. The graph summarizes the inhibition mediated by Treg-clones from 4 donors. *p<0.05.

Fig. 3. IL-15 protects the proliferation of effector T cells in the presence of Tregs. Tregs were tested for their ability to inhibit proliferation of different T-cell subsets using a CFSE-based suppression assay. **Panel A** shows T-cell proliferation of $CD45RO^{+}CD62L^{+}$ cells (T_{CM}), **Panel B** of $CD45RO^{+}CD62L^{-}$ cells (T_{EM}) and **Panel C** of $CD45RA^{+}CD62L^{-}$ cells (T_{EMRA}). Histograms show the proliferation in the absence or in the presence of IL-2 or IL-15 and of control cells or Tregs in one representative of 6 experiments. Graphs show the inhibition mediated by Tregs on each T-cell subset in the presence of IL-2 or IL-15. Shown is the average ± SEM of the 6 donors. *p<0.01.

Fig. 4. IL-15 sustains the antitumor effects of EBV-CTLs in the presence of Tregs. Tregs were tested for their ability to inhibit EBV-CTL antitumor activity in the presence or absence of cytokines in coculture experiments. **Panel A** illustrates a representative coculture experiment in which EBV-CTLs generated from a healthy donor were incubated with autologous LCL with or without Tregs freshly isolated from healthy donors and cytokines. Residual tumor cells were enumerated by flow cytometry based on the expression of CD19 by day 7 of culture. The graph summarizes the percentage of residual tumor cells (mean ± SEM) for the 6 independent experiments. *p<0.01. **Panel B** illustrates a representative coculture experiment in which EBV-CTLs generated from a HL patient were incubated with autologous LCL with or without Treg-clones and cytokines. The graph summarizes the percentage of residual tumor cells (mean ± SD) for 3 independent experiments. *p<0.01.

Fig. 5. IL-15 does not directly affect Treg-inhibitory function but preferentially supports the proliferation and survival of effector T cells. Panel A illustrates the ability of Tregs to

maintain inhibitory properties after expansion for 7 days in the presence of IL-15, before being tested in a classical CFSE-suppression assay. Histograms from this representative experiment shows the CFSE dilution of T cells in the presence of control cells or Tregs previously expanded in IL-15. The graph summarizes the percentage of inhibition (mean ± SEM) of 5 donors. **Panel B** illustrates the percent of proliferating Tregs, $T_{EM/EMRA}$ cells and EBV-CTLs activated in the absence or in the presence of IL-2 or IL-15 as assessed by CFSE dilution. Data are mean ± SEM of 5 independent experiments. *p<0.05. **Panel C** shows the percentage of apoptotic cells for Tregs, $T_{EM/EMRA}$ cells and EBV-CTLs assessed by Annexin-V and 7AAD staining in the absence or in the presence of IL-2 or IL-15. The graph summarizes mean ± SEM of 5 independent experiments. *p<0.05.

Fig. 6. IL-15 upregulates pS6K1 and BCL-2 in effector T cells as compared to Tregs. Panel A illustrates the expression of IL-15Rα by Tregs, $T_{EM/EMRA}$ and EBV-CTLs in one representative donor of 5 studied. **Panel B** illustrates STAT5 phosphorylation of Tregs, $T_{EM/EMRA}$ cells and EBV-CTLs in the presence of IL-15, as assessed by FACS. The graph summarizes means ± SD for 4 independent experiments. **Panel C** illustrates the phosphorylation of S6K1 (pS6K1), assessed by FACS, in Tregs, $T_{EM/EMRA}$ cells and EBV-CTLs in the absence or in the presence of IL-2 or IL-15. The graph summarizes data (means ± SD) from 4 experiments. **Panel D** shows BCL-2 expression by Tregs, $T_{EM/EMRA}$ cells and EBV-CTLs after stimulation with IL-15. The histograms show BCL-2 expression in one representative donor after activation in the absence (dotted line) or in the presence of IL-2 (thin line) or IL-15 (bold line). The graph summarizes the mean ± SEM of 6 independent experiments. *p<0.05.

Fig. 1

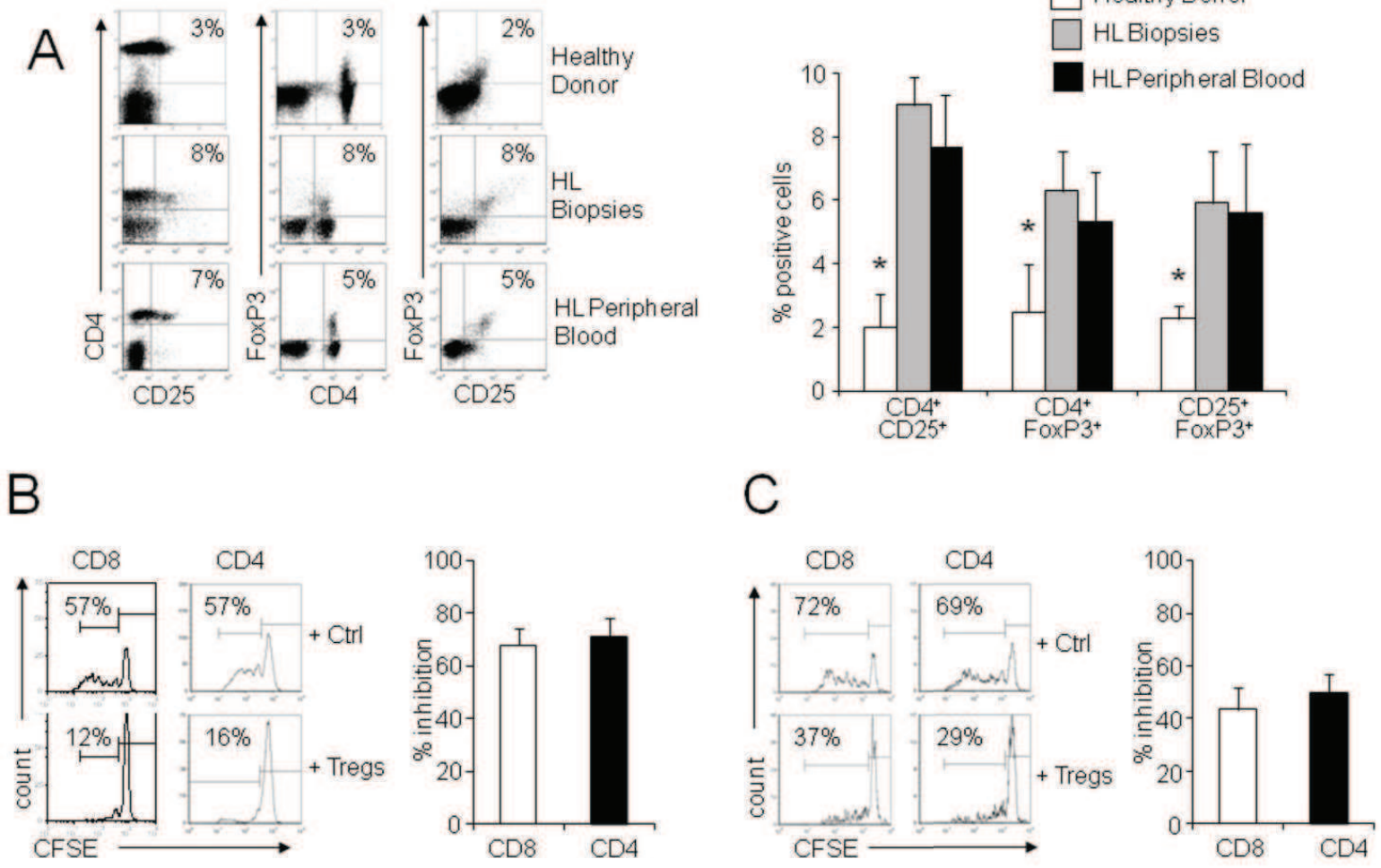

Fig. 2

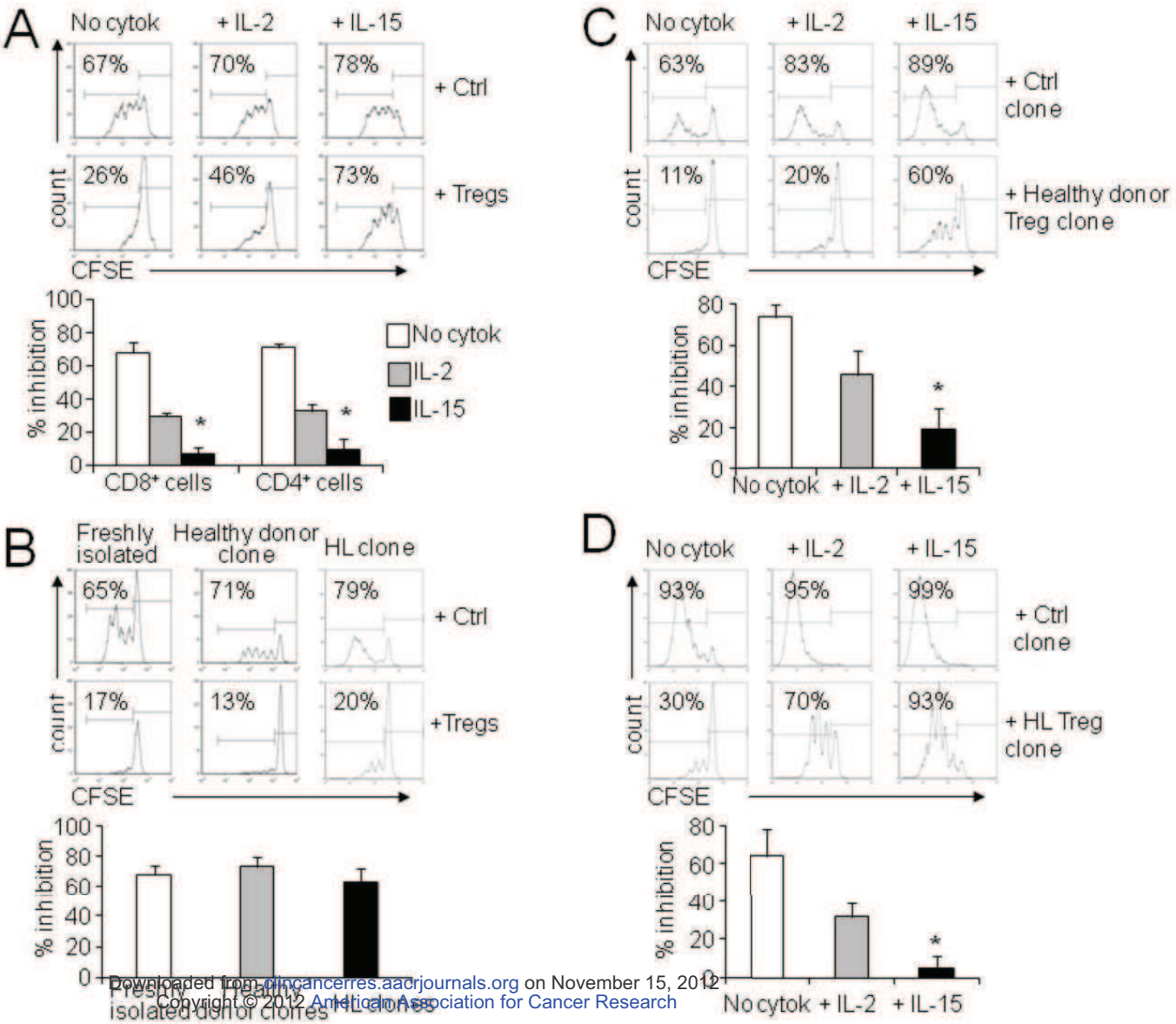

Fig. 3

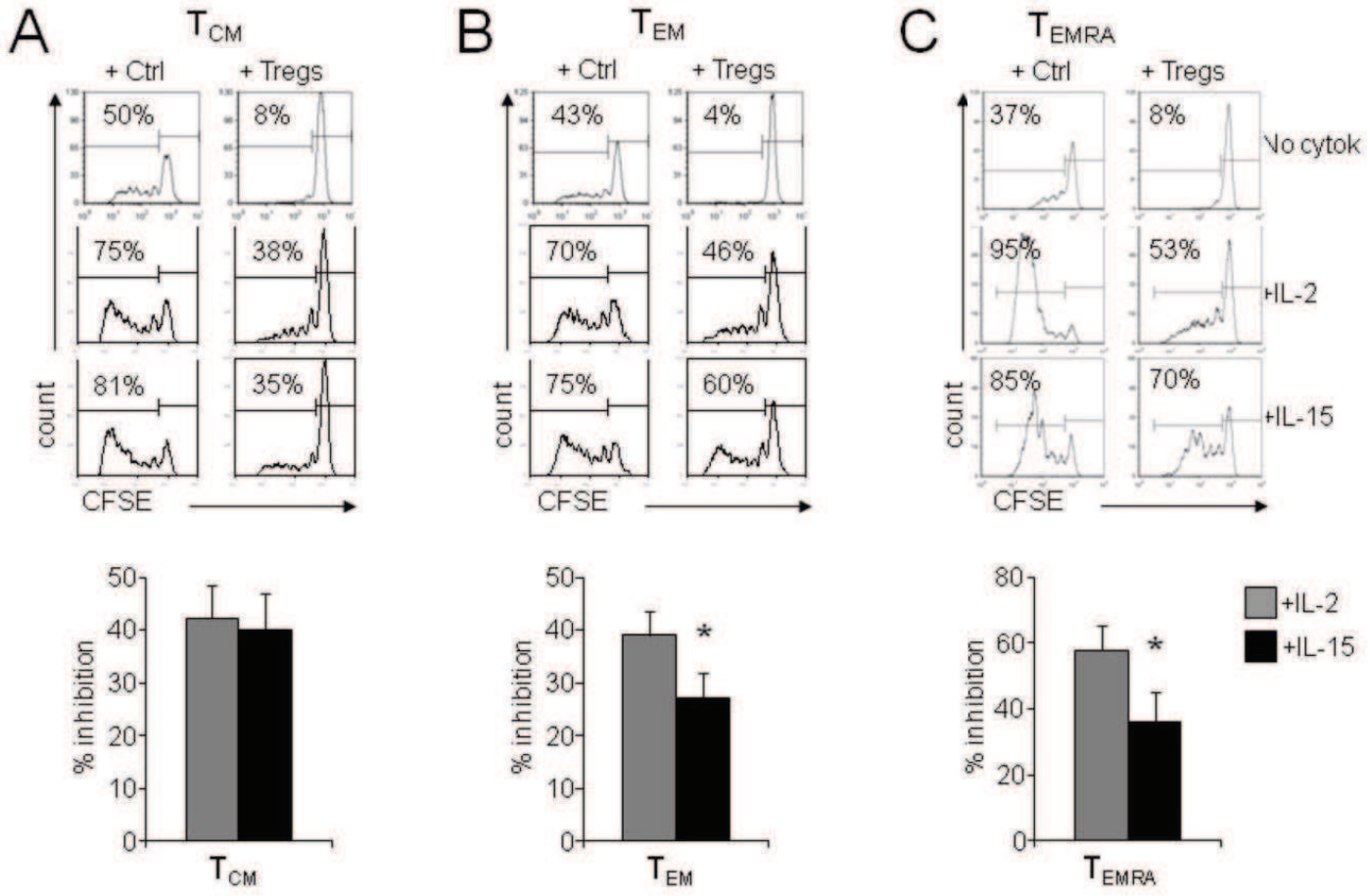

Fig. 4

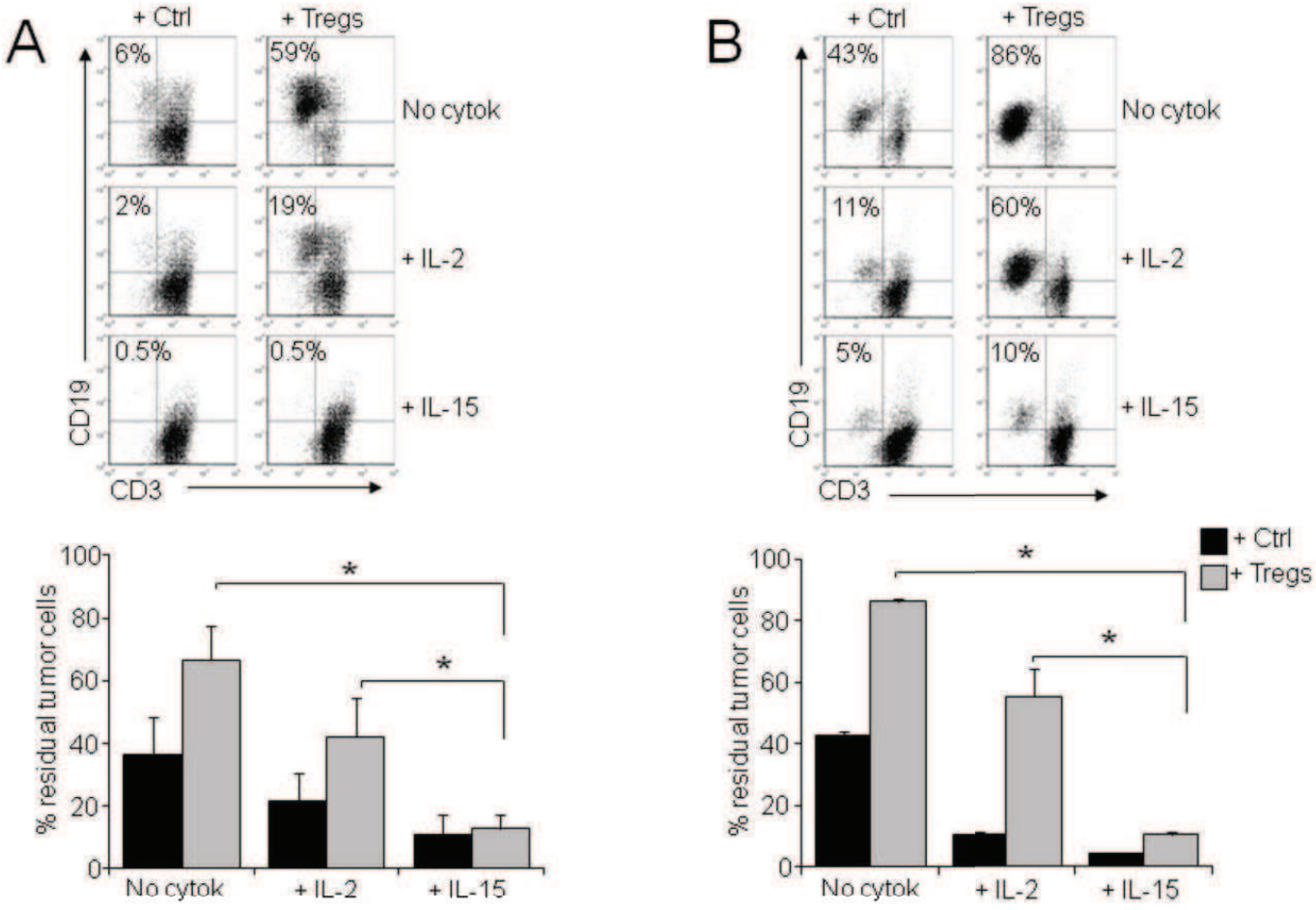

Fig. 5

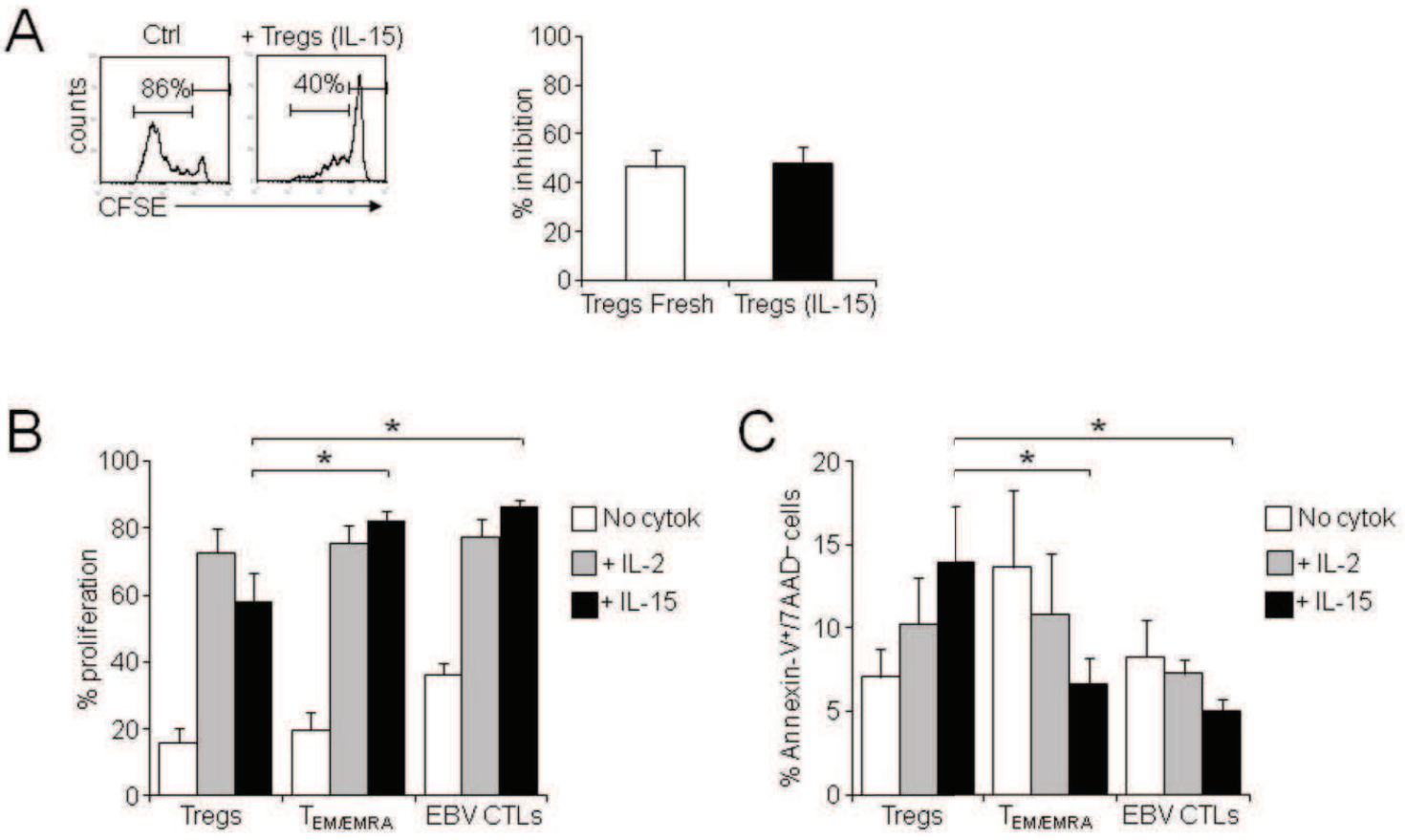

Fig. 6